AD-A062 507 NAVAL ACADEMY ANNAPOLIS MD F/G 5/11
PROCEEDINGS OF THE GENERAL MEETING (18TH) OF THE AMERICAN TOWIN--ETC(U)
1977 B JOHNSON, B NEHRLING

UNCLASSIFIED NL

1 OF 3

AD
AD 062507

LEVEL II

PROCEEDINGS OF

THE EIGHTEENTH GENERAL MEETING OF THE

AMERICAN TOWING TANK CONFERENCE

VOLUME TWO

CAVITATION SESSION

SEAKEEPING SESSION

23–25 AUGUST 1977

ANNAPOLIS, MARYLAND

SPONSORED BY:

ONR NAVSEA USNAMB

BRUCE JOHNSON

BRUCE NEHRLING

EDITORS

(1)

(6) PROCEEDINGS OF (18th)
THE ~~EIGHTEENTH~~ GENERAL MEETING OF THE
AMERICAN TOWING TANK CONFERENCE, 23-25 August 1977,
Annapolis, Maryland

Volume II

CAVITATION SESSION,
SEAKEEPING SESSION,

(11) 1977

(12) 275 p.

23 - 25 August 1977

Annapolis, Maryland

(10) Bruce/Johnson
Bruce/Nehrling
Editors

Sponsored by

U. S. Naval Academy

Office of Naval Research

Naval Sea Systems Command

~~78 04 24 007~~

406 245 600

CONTENTS

VOLUME II

18th

AMERICAN TOWING TANK CONFERENCE

Annapolis, Maryland, U.S.A.

REPORT OF
CAVITATION COMMITTEE

August 1977

United States Naval Academy

SUMMARY OF THE STATE-OF-THE-ART
prepared by
THE CAVITATION COMMITTEE, 18 ATTC

Cavitation Inception:

A steady progress in the understanding of cavitation-inception was made since the 17th ATTC Report (1974). Inception on smooth surfaces is influenced by Reynolds number, free-stream turbulence, the size and distribution of free-nuclei, the boundary-layer properties of the body and, its pressure-distribution. Depending on the above influences, inception occurs in the vicinity of the location of laminar flow separation, or behind the region where laminar to turbulent flow transition takes place. The distance between the locations of laminar boundary layer separation and inception is Reynolds number dependent.

Both trip-wires and polymers supress cavitation-inception. Trip-wires produce early transition and prevent (or reduce the chance of) laminar separation, while polymer solutions reduce the magnitude of pressure fluctuations at the reattachment region after laminar separation. Polymers also can cause early transition to turbulent flow, at much lower Reynolds number than in pure water. Increased turbulence moves the inception point forward, this effect naturally depends on the body pressure distribution. More work needs to be done on the effect of nuclei population. Relatively large micro-bubbles are important in the inception process, their effect depends on the body boundary layer characteristics.

Bubble dynamics continues to be of interest to workers in the field of cavitation inception. Our reviewers cite analytical and experimental investigations which study the influence of various physical effects on nucleus growth. For example, it has been found that the growth-rate of individual bubbles is not affected by polymer solutions. A large magnetic field however, does increase the growth-rate of bubbles.

Slow progress was made in Vortex Cavitation Inception Scaling, since the review of Acoasta and Parkin (1974). It appears that the critical cavitation number for propellers, varies as the term: (pitch/diameter ratio - less - advance coefficient) squared.

Body-oscillation tends to delay cavitation inception. This effect could conceivably be analogous to that caused by a high level of free-stream turbulence.

There is still a considerable discrepancy, when correlation is attempted between various flow facilities, with regard to different types of cavitation.

Reviewing the above summary, it appears to the Committee that some guidelines may be provided to the experimenter who wishes to predict cavitation inception for surface-ship components. They may be as follows:

Hydrodynamic bodies operating in the open sea environment will likely to be exposed to fully turbulent flow and saturated sea-water, having a large population of nuclei. It is clear from the foregoing that each of these three properties have a significant effect on inception and on the type of cavitation being present. It is thus suggested that the experimental facility should have a relatively high level of free-stream turbulence. The test model should be large enough so that it may operate with a fully turbulent boundary layer, or,

turbulent boundary layer should be induced by artificial devices (trip-wire, or polymer solution). The water in the facility should be close to saturation, and the nuclei-population should also be high.

It appears to the Committee, that controlled full-scale experiments should be promoted so that an assessment of model full-scale correlation may be made.

While the Committee feels that the foregoing guidelines and recomendations for correlation tests offer help for practically useful progress at an early date, we observe that much of the work cited concerns fundamental studies of basic inception mechanisms. Until these basic factors are more clearly understood and related to the various forms of noncavitating flows, the prediction of inception on full scale vessels will remain a black art. Indeed, the design of laboratory experiments which best apply to a given full scale situation is not free of controversy. Therefore the Committee applauds the continued emphasis on fundamental work by many investigators and laboratories. A balance between fundamental investigations and practical correlation experiments and trials seems to offer the best hope for future progress.

Wall Effects on Fully Developed Cavity Flows:

This is the first ATTC survey on this subject. Because of the difficulty of the problem, most of the analytical predictions are restricted to two-dimensional flow, in a closed-jet test section. No analytical treatment of this problem exists for fully cavitating propellers, although a simple momentum theory has been carried out by Tulin.

The author of this review concludes that the effect of tunnel walls is very small on the force coefficients of struts, hydrofoils and propellers, in fully cavitating flow, at a constant cavitation number. The largest relative wall effects occur when the body force coefficients are small (i.e.: a flat plate at amall angle of attack).

The tunnel wall effect is large with regard to two aspects: minimum achievable cavitation number in the test section, and the length of the body cavity relative to its open water value. Analytical prediction of the force coefficients and of the choking cavitation number on fully cavitating two-dimensional profiles in the pressence of tunnel walls is well developed. However, the predicted cavity shape (both cavity thickness and length) depends on the particular wake model used in the analysis. No techniques beyond those based on momentum theory are available for the three-dimensional hydrofoil and the propeller case.

The Committee feels that clearly, the wall effect problem has to be viewed with a eye toward full scale performance prediction. In this respect, the prediction of the correct cavity dimensions (cavity thickness over the body and cavity length) is critical for a successful design. A rigorous analytical approach in this critical area is needed both for three-dimensional hydrofoils and for supercavitating propellers.

Two currently ongoing experimental efforts should be mentioned. Tunnel effects on three-dimensional supercavitating hydrofoils are explored at M.I.T. (see LT. M.R. Maixner's paper in this report), while the investigation of tunnel effects on supercavitating propellers is underway at DTNSRDC. Hopefully, these efforts will provide the experimenter with some additional guidelines on tunnel effects for some three-dimensional flows.

Another investigation dealing with partial cavitation on two and three-dimensional wings is reviewed in these pages by Tulin and Hsu. Although their work does not apply directly to the wall-effects problem as such, it does illustrate the important effects of hydrofoil nose curvature and aspect ratio on the development of partial cavity flows. Their theoretical findings should be very helpful to experimentalists who must interpret their data for both fully cavitating and partially cavitating regimes.

Another important aspect concerning laboratory work is that two-dimensional force measurements in cavitation tunnels presently lack the precision required to assess the small theoretical differences due to tunnel wall effects. This situation is particularly true of drag measurements. The Committee does not know whether or not this difficiency can be remedied. However, efforts to refine water tunnel two-dimensional force measuring techniques are recommended.

Carriage VI, the 100 knot high speed towing carriage of DTNSRDC (described in the 17th ATTC Report) will be operational this fall. It will allow us to evaluate model behaviour at full scale speeds. A direct comparison of data obtained with this facility and in variable pressure tunnels will increase our confidence in making full scale performance prediction of ship subsystem components.

Scale Effects in Models with Forced or Natural Ventilation Near the Free Surface:

The following scale effects appear to exist for surface piercing ship components:

-The prototype appears to ventilate at a much lower angle of attack then observed in model scale.
-Fully ventilated cavities have not been observed full scale. Laboratory tests that reproduce the visual appearance of partial full scale cavities were achieved in highly turbulent flow, with roughness applied to the strut surface.
-It appears that full scale ventilation is a more gradual process than is indicated by the abrupt force changes caused by ventilation in model scale.
-Effect of anti-ventilation fences: only large tail fences appear to be useful for this purpose at model scale, while at full scale, even small, leading edge fences seem to work.

According to the author, the causes of these scale effects may be traced to the difference between laboratory conditions and full scale conditions, which are:

-rough surface full scale, smooth surface, model scale
-highly turbulent flow full scale
-although the full scale boundary layer is relatively thinner than on the model, it may be that the absolute thickness of the boundary layer is the controlling factor for the ability of the surface seal to maintain its integrity
-the apparent greater mixing of air and water in the full scale surface seal encourages earlier inception. The model requirement for a region of separation or cavitation prior to ventilation inception may not be there for full scale
-due to turbulence and roughness, ventilation inception (the breaking of the surface seal) starts close to the leading edge of the full scale struts (while mostly tail ventilation is ovserved on the model).

It seems to the Committee that there is a common trend in scale effects for both cavitation and ventilation inception. It appears that the same guidelines suggested for cavitation inception work are also applicable for ventilation inception work in the laboratory, if closer correlation with full scale observation is to be achieved. The lack of quantitative full scale data is most serious for ventilation inception, however.

As a result of differing behavior reported for ventilation forces in model and full-scale trials the Committee suggests that perhaps the effect of the boundary layer on ventilation should be judged with respect to its actual

thickness rather than its relative thickness with respect to strut or foil size. The characteristics and influence of the boundary layer upon ventilation inception requires further investigation. The measures required to simulate full-scale conditions need to be quantified. Closure angle appears to be more subject to scale effects than inception angle and therefore should not be used as a criterion for inception resistance. The interaction of ventilation and nonsteady phenomena such as waves, turbulence, or hydroelastic oscillations are important. They have hardly been investigated.

Another factor associated with the interaction of the free surface with surface-piercing struts on foils is that in the vicinity of the free surface, the medium is a bubbly mixture. The aggregate properties of this mixture differ from those of water and this difference should be accounted for in the planning and interpretation of laboratory work.

Cavitation Erosion Scaling:

In updating the 17th ATTC report on the same subject, the authors note one recently conducted study and one ongoing work.

The first work classifies the over-riding importance of the flow velocity on the cavitation damage rate. It appears that the absolute flow speed is the primary parameter that effects damage rate. The cavitation-bubble collapse-energy (per unit area and per unit time) increases as the 11th power of the fluid velocity (incubation zone).

In an ongoing study at DTNSRDC, the effect of propeller design and ship operating conditions on the collapse pressure of individual cavitation bubbles is being determined (inferring from crater-size and from the rate of crater formation. The model tests are correlated with full scale propeller tests.

Another fundamental study attempts to modify propeller design, to eliminate cavitation. Information on where and how should the propeller be modified is obtained from studying the effect of the wake encountered, in simulated operating condition, on cavitation bubble formation and on erosion damage ratio.

ABSTRACT

~~In summary, the Committee sees that~~ steady progress has been made in our understanding of the effect of laboratory environment on the prediction of full scale cavitation, ventilation and cavitation erosion. Tentative guidelines may be provided as how to minimize these scale effects in each subject area. However, in most cases, quantitative values for the level of turbulence, the proper roughness of the model surface, the proper size and distribution of nuclei can not be provided. Further fundamental studies on these and other matters are still needed and careful full scale measurements are required in most of the four areas in order to quantify the differences between laboratory and full scale environment.

ABSTRACT

CAVITATION INCEPTION

A Review - Progress Since 17th ATTC

by

Wm. B. Morgan and Frank B. Peterson
David W. Taylor Naval Ship Research and Development Center

INTRODUCTION

For the 17th ATTC Cavitation Committee Report, Acosta and Parkin (1974)* gave a review of certain selective topics on cavitation inception. This review was very comprehensive on three subject areas: (1) cavitation inception on smooth surfaces, (2) vortex cavitation inception and scaling, and (3) effects of polymer additives on inception. The present review starts chronologically where the previous review left off and generally covers the same topic areas. Although there has been an extensive literature on cavitation inception since the last ATTC, only a few papers advance our basic understanding of this complex problem.

Since the 17th ATTC, in addition to the usual number of reports and papers in technical journals, there have been two symposia on cavitation. These have been the Institute of Mechanical Engineers Conference on Cavitation held in Edinburgh, Scotland in September 1974 and the IAHR Symposium on Two-Phase Flow and Cavitation in Power Generating Systems held in Grenoble, France in April 1976. Also, in addition to the review by Acosta and Parkin previously mentioned, one should refer to the review papers by Acosta (1974), Holl, et al (1974), and Takahashi (1975).

This survey does not include a discussion of noise associated with cavitation inception nor of thermodynamic effects such as might be found in liquid metals, etc.

* See references at end of paper.

The discussion is restricted to cavitation inception in water or water with dilute solutions of additives. Any omissions of papers and reports published in the subject area since the Acosta and Parkin review are unintentional.

CAVITATION INCEPTION ON SMOOTH SURFACES

Since the review by Acosta and Parkin (1974) at the last ATTC, the major emphasis of reported research appears to lie in two areas: (1) correlation of viscous flow properties with inception, and (2) correlation of "nuclei" measurements with inception. The results have, in general, shown steady progress in understanding inception. An encouraging indication is that many initial results appear to have been supported by later independent research efforts. To demonstrate this point, the research progress in understanding the role of viscous effects will be reviewed in the chronological order in which the results were published.

Alexander (1974) postulated the importance of a "short" laminar separation bubble on a surface - which has very little influence on the overall pressure distribution, and a long bubble - which will reduce the magnitude of the $C_{p_{min}}$. Thus, the overall pressure distribution, which is calculated by neglecting viscosity, could be considerably in error when compared to that actually present.

Casey (1974) extended previous axisymmetric body results reported by others to show that when laminar separation is present on a two-dimensional foil, inception can also occur preferentially at the laminar separation location and not at the location of $C_{p_{min}}$.

Arakeri (1975), with experimental results obtained by schlieren flow visualization techniques demonstrated the strong Reynolds number dependence of the distance between the locations of laminar boundary layer separation and the cavitation leading edge.

Huang and Hannan (1976), with wind tunnel experiments, verified and extended previous results (see Acosta and Parkin - 1974) by showing that (1) wall pressure fluctuations in the reattachment region following laminar separation are one order of magnitude higher than those in a fully-turbulent boundary layer, (2) wall pressure fluctuations in a region of natural transition were 2 to 3 times higher than those in a fully-turbulent boundary layer, and (3) trip wires of appropriate size will reduce the high pressure fluctuations in regions of separation triggered transition.

Arakeri and Acosta (1976) extended the preliminary results of Acosta and Parkin (1974) by detailing the significant influence a boundary layer trip can have in suppressing laminar boundary layer separation with its attendant inception. In this work, boundary layers with artificially tripped transition produced a very significant delay in inception even though high tensions were inferred to be present on the body surface. In the course of these experiments, it was also

discovered that "spot" cavitation (see Acosta and Parkin - 1974) was suppressed when the trip produced boundary layer transition ahead of the $C_{p_{min}}$ location. The authors concluded that the "spot" cavitation they observed was not due to a surface source of nucleation.*

Huang and Peterson (1976) summarized pertinent experimental and analytical results to show how boundary layer properties can grossly change the inception characteristics and new experimental results previously unexplained can now be better understood. The conclusions were then used to demonstrate, numerically, the problems associated with scaling inception from model results to full-scale performance for a typical propeller blade section. The results dramatically point out the inherent difficulty in scaling blade surface types of cavitation inception when small model sizes are used at low Reynolds numbers.

Van der Meulen (1976b) studied the influence of boundary layer properties on inception by means of high-speed holography. These results also demonstrate that when very little free gas is present in the water, then inception occurs in the reattachment region of a laminar separated boundary layer. Furthermore, when polymer additives were injected into the boundary layer upstream of the laminar separation point, the boundary layer transition was promoted, thereby suppressing the separation. This result is the same as was found with a solid trip, i.e., a significant suppression of inception.

Blake, et al (1976) presented experimental results on a two-dimensional foil which reenforced previous conclusions that boundary layer trips can have a significant effect on inception when laminar separation would normally be present.

Effect of Turbulence and Nuclei

From the above summary of the chronologically occurring reports and papers, one can readily see the progress in understanding the importance of boundary layer characteristics in the inception process.

When the inception results from various facilities are compared, an obvious question arises. To what extent have free stream turbulence and nuclei influenced the various results subjected to comparison? The complete answer is not now available; however, some useful related information has been reported. Numachi (1975) has shown that for foils at small angles of attack, an increase in free stream turbulence from 0.52 percent to 3.96 percent moved the inception point forward. This result was obtained with a high total gas content in the water. Inception had the

* This point should be considered further since spot cavitation occurs in other situations where it may be due to roughness. It may be that if a fully-developed turbulent boundary layer were present at $C_{p_{min}}$, a significant suppression of inception would occur on surfaces normally having roughness induced cavitation.

form of bubble cavitation occurring near $C_{p_{min}}$ and ahead of the calculated laminar separation and transition points. The increased turbulence was also found to promote the inception.

A related study by Gates (1977) has considered both the free stream "nuclei" and turbulence as variables influencing inception on axisymmetric bodies. The results indicate that for the turbulence range from 0.04 percent to 3.75 percent, the sensitivity of laminar separation to changes in free stream turbulence is dependent on the overall body pressure distribution. Although the associated cavitation experiments were performed at turbulent levels of only 0.04 percent and 0.65 percent, the laminar separation induced inception did not change within this range. However, when large amounts of free gas were present in the water, these bubbles could initiate travelling bubble cavitation (vapor or gaseous) near $C_{p_{min}}$ and so disrupt the boundary layer that laminar separation was prevented. This study has also clearly pointed out the interrelationship between viscous flow characteristics, free stream gas bubbles, and inception. When inception did occur in a laminar separation region, free stream gas bubble populations (measured holographically) had little influence. However, when travelling bubble-type cavitation inception occurred first, then the free stream gas bubble populations had a significant influence.

It has recently become apparent that in a free surface tunnel, Albrecht and Bjørheden (1975), and in a vacuum towing tank, Noordzij (1976), inception was erratic and was being suppressed by the lack of sufficient nuclei in the water. Microbubble seeding of the water was employed with what appears to be favorable results. This approach certainly merits further consideration by members of the ATTC.

Methods of Nuclei Measurement

In the intervening 3 years since the previous cavitation inception review for the ATTC, attempts to measure cavitation nuclei have been dominated by optical methods already reported (Acosta and Parkin - 1974). Data have been obtained holographically by Peterson, et al (1975), Gates (1977), and Gates and Bacon (1977); by laser light scattering by Keller (1974), Arndt and Keller (1976), and Keller, et al (1976), Keller and Weitendorf (1976), Yilmaz, et al (1976), Weitendorf (1977); and photographically by Danel and Lecoffre (1976). The holographic and photographic methods have the potential to differentiate between bubbles and solid particles. However, at the present time, this differentiation is very time-consuming and is most likely not practical for scatterers below 25 μm in diameter. Results from all these studies collectively indicate that when relatively large microbubbles are present, they are important to inception. If microbubbles are suspected to be essentially absent during a test, then the particulate will nucleate cavitation. As already stated previously, the importance of "nuclei" populations appear to be dependent

on the boundary layer characteristics present on a body subject to cavitation. If, in the case of travelling bubble-type cavitation, standard definitions are not adopted, then this inception data will always be subject to ambiguity. The inception data should be based on the number of events in a given time interval over a given surface area and standard means for counting these events should be established. In the situation where many microbubbles are present, some means to differentiate between vaporous and gaseous cavitation would be very desirable.

Other methods to assess the susceptability of water to cavitate include the Coulter Counter, Hammitt (1975) and Pyun, et al (1976); a cavitating by-pass venturi Oldenziel (1975); and graduated filters, Takagawa, et al (1975).

At the present time, the authors of this review do not feel justified to recommend one method of "nuclei" measurement over another. Each method has certain areas of demonstrated usefulness when applied to appropriately configured experimental arrangements. Until more information is available on the "nuclei" present in an actual prototype operational environment and on how various hydrodynamic aspects scale with, for example, Reynolds number, many questions related to "nuclei" population will be unanswered.

Bubble Growth

Bubble growth and instability has been a continuing topic of research with the objective to give a better understanding of the role that bubble dynamics has on the inception process. However, it is not clear how these studies have contributed to the understanding of cavitation inception of interest to the ATTC. In the hope of obtaining a better understanding of the role that dilute polymer solutions have on cavitation, Ting and Ellis (1974) studied bubble growth in such solutions. They found that the bubbles grow at fairly constant rates which were low enough to suggest the growth mechanism involved in their experiments was dominated by thermal aspects. Moreover, they found that, in general, there was no significant change in the growth rates of individual bubbles caused by polymer additives. This leads to the conclusion that the effect of polymers on individual bubble growth plays a very minor role (if any) in inhibiting cavitation.

Theoretical studies of bubble growth were made by Persson (1974), Bonnin, et al (1976), and Raabe (1976). Persson made numerical computations of the maximum attainable radius for a bubble exposed to a transient pressure pulse to assess the validity of a scaling law for cavitation bubble growth proposed by Strasberg in 1957. His comparison between the analytical and the numerical results shows that the scaling law of Strasberg predicts the maximum radius adequately in most practical cases, except where the amplitude of the pressure pulse is large compared to the difference between the initial ambient pressure and the vapor pressure.

Bonnin, et al (1976) also made numerical computations and used an asymptotical solution for a growing bubble. They expressed the growth and collapse of a

spherical bubble, gaseous or vaporous, when it is unstable in an ambient liquid and in terms of generalized parameters taking into account either mass or heat diffusion. They found that the experimental results match with a unique instability parameter analogous to the Jacob number. However, the asymptotical solution was in some cases not satisfactory, and taking into account convection due to bubble translation will require a more sophisticated numerical computation than was used.

Raabe (1976) assumes the incipient cavitation number is proportional to the bubble growth ratio in the zone where evaporation starts. He developed a formula based on test results using the critical pressure, mass conservation, equation of motion, energy conservation and gas diffusion. There are a number of terms in his formulation. All terms depend on nuclei diameter, some on a polytropic power for the state variation of the bubble, the initial bubble growth velocity, and its deviation from its maximum. Verification of the formula will require additional experiments.

Other very useful results have been reported by Lauterborn (1976) where he has shown very clearly by high-speed holography the growth and collapse process of individual vapor bubbles. In a related work, Chen et al (1976) have presented additional data on the growth of bubbles in a superheated liquid at a solid surface. Both of these efforts have demonstrated the complexity of bubble dynamics associated with single bubble-type inception.

Hammitt, et al (1975) investigated the effects of a 6kG magnetic field upon cavitation inception in tap water, in water with 0.3 percent by mass salt addition, and in mercury in a vibratory cavitation facility. They found that cavitation inception was not changed beyond a range of ±1 percent. On the other hand, although they did not specifically measure cavitation inception, Shalobasov, et al (1974) found that a 7kG magnetic field substantially increased the bubble size, growth rate and collapse rate in tap water. Considerably more experimentation will be required before it will be determined whether or not these results are in conflict.

Weitendorf (1977) attempted to explain differences he obtained in propeller experiments of the extent of cavitation and of the pressure amplitudes by means of a theoretical analysis of the dynamic expansion of single bubbles in a flow with pressure gradients. He followed the theoretical work of Lederer (1976) for steady hydrofoil flow in incompressible water where single bubble growth was calculated as it passed over a hydrofoil. Weitendorf (1977) concludes from the theoretical investigations on bubble dynamics that the theoretical model of the bubble and its behaviour in pressure fields should be checked by geosim tests.

VORTEX CAVITATION INCEPTION AND SCALING

Acosta and Parkin (1974) gave a very adequate review of this subject so no extensive discussion is required (see also Holl, et al, 1974). Although this is an important subject for noise and vibration and considerable work is underway,

only two references subsequent to the Acosta and Parkin, and Holl, et al reviews discuss the inception and scaling of vortex cavitation inception to any extent. Van Oossanen (1975) presented tip and hub vortex cavitation inception results from a round-robin test on two foils. The tests made in a number of establishments and facilities show a large discrepancy in the results. He was unable to resolve these discrepancies.

Chandrashekhara (1976) reported on the results of a theoretical analysis and experiments on a number of hydrofoils with different aspect ratios and planforms and, also, on a number of propellers. His analysis gives a reasonable estimate of the critical cavitation number for the range of variables he investigated. The roles of the circulation distribution and of the Reynolds number, which have been found to be important, were not clearly defined by the theory or the experiments.

EFFECTS OF POLYMER ADDITIVES ON INCEPTION

As pointed out byAcosta and Parkin (1974), it has been known for some time that polymer additives tend to inhibit the inception of cavitation. The work on this area reported by Acosta and Parkin has continued and an extensive literature on this subject is accumulating. Some of the work has been very detailed; it appears that our basic understanding of the physical phenomena causing the change in cavitation inception with the addition of polymers is becoming better understood. From the studies which have been made to date, one can conclude that the delay in cavitation inception is most probably related to the effect the polymer has on the fluid dynamics (damping of the turbulence and eddies in the fluid) rather than the fluid physical properties or bubble growth, Ting and Ellis (1974). This conclusion is in general agreement with Hoyt (1976) who in reporting a study on jet cavitation considered a large number of physical properties in the fluid, such as viscosity, air content, nuclei number, surface tension and tensile strength. He could find none of these physical properties for polymer solutions and pure water that would cause the cavitation inception differences observed.

Other work on the effect of polymer solutions on jet cavitation has been carried out by Vyaz'menskii (1975) and Baker, et al (1976). The work of Vyaz'-menskii on slot cavitation generally agreed with that of Hoyt except for some quantitative differences. In addition, Vyaz'menskii also investigated the effect of an aqueous solution of butyl alcohol at a concentration of 4.7×10^{-3}. The addition of butyl alcohol to the water decreased the cavitation inception number to about one-half that for the polymer solution, i.e., 6 to 8 percent as compared to 15 percent. Baker, et al (1976) found about the same decrease in inception cavitation number with polymer additives as Vyaz'menskii (1975) and also noted quantitative differences. Both Baker, et al, and Vyaz'menskii feel that the quantitative differences of their work compared with Hoyt's are due to the experimental setups.

The most extensive investigation of the effect of polymer on cavitation

inception on bodies has been by Van der Muelen (1974, 1976a and 1976b) and Gates (1977). These extensive investigations carried out by different investigators in different facilities are very supportive. For bodies without separation, it is felt that the intense fluctuations in the transition region, see Figures 1 and 2 from Huang and Peterson (1976) and Figure 3 from Van der Muelen (1976b), may be damped by the polymer additives and thus influence the cavitation inception. And for bodies which separate in pure water, it is felt that the effect of polymer additives is to cause transition to turbulence at much lower Reynolds number than in pure water, see Figure 4 from Gates (1977), or reorientation of the flow field near the laminar separation bubble. This was also suggested by Holl, et al (1974) and Arndt, et al (1976).

MISCELLANEOUS

This section is devoted to miscellaneous topics on inception which do not fall under previous categories. The references cited are generally disconnected but offer considerable insight into the various phenomena of cavitation inception.

Palanichamy, et al (1974) investigated visual cavitation inception in a venturi with transverse cylinders of two sizes, 10mm and 20mm. Four types were used: smooth and rough circular cylinders, wedges and flat plates. They showed, as one would expect, that streamlining of the cylinders delays inception and roughening of the cylinders make inception occur at a higher cavitation number.

Radhi (1975) investigated theoretically and experimentally the cavitation inception on an oscillating two-dimensional hydrofoil. He found a considerable effect of reduced frequency. Increasing the reduced frequency tended to delay cavitation inception with the maximum suppression occurring at a nominal reduced frequency of 0.5.

Arndt (1976) carried out a semi-empirical analysis of cavitation in the wake of a sharp-edged disk. He found by his analysis that the characteristics of the unsteady pressure field in the wake of a sharp-edged disk are governed by the boundary-layer characteristics at the face of the disk. His analysis correlates reasonably well with experimental cavitation inception data.

Van Oossanen (1975) compared results of a round-robin series of inception experiments on two hydrofoils for the ITTC. He found that there was a wide variance between the various facilities in the results. For tip-vortex cavitation, the variance was the order of two; for sheet cavitation, the variance was the order of three; and for hub-vortex cavitation, the variance was the order of three to four. Analysis of the results, in regard to the effect of various facilities was not really possible.

Van Oossanen (1974, 1977a and 1977b) developed a procedure for analytically assessing the cavitation inception of blade surface cavitation on propellers. His analysis is based on boundary layer analysis and inception is assumed to occur at

the location of transition from a laminar to a turbulent boundary layer if no laminar separation exists. The procedure is as good as one could use, with the state of the present understanding of cavitation inception.

REFERENCES

Acosta, A.J. and Parkin, B.R. (1974), "Cavitation Inception - a Selective Review," 17th American Towing Tank Conference, Pasadena, California; also see Journal of Ship Research, Vol. 19, No. 4, Dec 1975, pp. 193-205.

Acosta, A.J. (1974), "Cavitation and Fluid Machinery," Proceedings Conference on Cavitation, Institute of Mechanical Engineers, Edinburgh, Scotland, pp. 383-396.

Albrecht, K. and Bjørheden, O. (1975), "Cavitation Testing of Propellers in a Free Surface Tunnel Utilizing Micro Air Bubble Control," Journal Fluids Engineering, Vol. 97, Series I, No. 4, pp. 523-530.

Alexander, A.J. (1974), "An Investigation of the Relationship between Flow Separation and Cavitation," Proceedings Conference on Cavitation, Institute of Mechanical Engineers, Edinburgh, Scotland, pp. 1-7.

Arakeri, V.H. (1975), "Viscous Effects on the Position of Cavitation Separation from Smooth Bodies," Journal Fluid Mechanics, Vol. 68, Part 4, pp. 779-799.

Arakeri, V.H. and Acosta, A.J. (1976), "Cavitation Inception Observations on Axisymmetric Bodies at Supercritical Reynolds Numbers," Journal of Ship Research, Vol. 20, No. 1, pp. 40-50.

Arndt, R.E.A. (1976), "Semiempirical Analysis of Cavitation in the Wake of a Sharp-Edged Disk," Journal of Fluids Engineering, Vol. 98, Series I, No. 3, pp. 560-562.

Arndt, R.E.A., Billet, M.L., Holl, J.W., and Baker, C.B. (1976), "A Note on the Inhibition of Cavitation in Dilute Polymer Solutions," ASME Cavitation and Polyphase Flow Forum - 1976, pp. 1-3.

Arndt, R.E.A. and Keller, A.P. (1976), "Free Gas Content Effects on Cavitation Inception and Noise in a Free Shear Flow," Proceedings IAHR - Symposium, Two-Phase Flow and Cavitation in Power Generation Systems, Grenoble, France, pp. 3-16.

Baker, C.B., Holl, J.W., and Arndt, R.E.A. (1976), "The Influence of Gas Content and Polyethelene Oxide upon Confined Jet Cavitation in Water," ASME Cavitation and Polyphase Flow Forum - 1976, pp. 6-8.

Blake, W.K., Wolpert, M.J. III, Geib, F.E., Jr., and Wang. H.T. (1976), "Effects of Boundary-Layer Development on Cavitation Noise and Inception on a Hydrofoil," David Taylor Naval Ship R&D Center Report 76-0051.

Bonnin, J., Reali, M., and Sardella, L. (1976), "Variation de volume d'une bulle de gaz ou de vapeur," Proceedings IAHR - Symposium Two-Phase Flow and Cavitation in Power Generating Systems, Grenoble, France, pp. 17-28.

Casey, M.V. (1974), "The Inception of Attached Cavitation from Laminar Separation Bubbles on Hydrofoils," Proceedings Conference on Cavitation, Institute of Mechanical Engineers, Edinburgh, Scotland, pp. 9-16.

Chandrashekhara, N. (1976), "Analysis of Tip Vortex Cavitation Inception at Hydrofoils and Propellers," Schiffstechnik, Vol. 23, No. 112, pp. 47-62.

Chen, M., Patel, P.D., and Theofanous, T.G. (1976), "Nucleation and Growth of Vapor Bubbles at a Solid/Liquid Interface," Proceedings IAHR - Symposium, Two-Phase Flow and Cavitation in Power Generating Systems, Grenoble, France, pp. 29-38.

Danel, F. and Lecoffre, Y. (1976), "Influence des germes contenus dans l'eau sur la cavitation developpée á bulles separées," Proceedings IAHR - Symposium, Two-Phase Flow and Cavitation in Power Generating Systems, Grenoble, France, pp. 39-52.

Gates, E.M. and Bacon, J. (1977), "Determination of Cavitation Nuclei Distributions by Holography," CalTech; submitted to the Journal of Ship Research.

Gates, E.M. (1977), "The Influence of Freestream Turbulence, Freestream Nuclei Populations and Drag-Reducing Polymer on Cavitation Inception on Two Axisymmetric Bodies," Ph.D. Thesis, California Institute of Technology, Pasadena, Calif.

Hammitt, F.G., Yilmaz, E., Ahmed, O., Bhatt, N.R., and Mikieewicz, J. (1975), "Effects of Magnetic and Electric Fields upon Cavitation in Conducting and Non-Conducting Liquids," ASME Cavitation and Polyphase Flow Forum - 1975, pp. 26-28.

Hammitt, F.G. (1975), "Effects of Entrained Particle Spectrum on Bubble Nucleation," Proceedings 6th International Symposium on Non-Linear Acoustics, Moscow, USSR.

Holl, J.W., Arndt, R.E.A., Billet, M.L., and Baker, C.B. (1974), "Cavitation Research at the Garfield Thomas Water Tunnel," Proceedings Conference on Cavitation, Institute of Mechanical Engineers, Edinburg, Scotland, pp. 81-87.

Hoyt, J.W. (1976), "Effect of Polymer Additives on Jet Cavitation," Journal of Fluids Engineering, Vol. 98, Series I, No. 1, pp. 106-112.

Huang, T.T. and Peterson, F.B. (1976), "Influence of Viscous Effects on Model/Full-Scale Cavitation Scaling," Journal of Ship Research, Vol. 20, No. 4, pp. 215-223.

Huang, T.T. and Hannan, D.E. (1976), "Pressure Fluctuation in the Regions of Flow Transition;" David Taylor Naval Ship R&D Center Report 4723.

Keller, A.P. (1974), "Investigations Concerning Scale Effects of the Inception of Cavitation," Proceedings Conference on Cavitation, Institute of Mechanical Engineers, Edinburgh, Scotland, pp. 109-119.

Keller, A., Yilmaz, E., and Hammitt, F.G. (1976), "Comparative Investigations of the Scattered Light Counting Method and the Coulter Counter for the Registration of Cavitation Nuclei," La Houille Blanche, Vol. 31, No. 1, pp. 59.

Keller, A.P. and Weitendorf, E.A. (1976), "Influence of Undissolved Air Content on Cavitation Phenomena at the Propeller Blades and on Induced Hull Pressure Amplitudes," Proceedings IAHR - Symposium, Two-Phase Flow and Cavitation in Power Generating Systems, Grenoble, France, pp. 65-76.

Lauterborn, W. (1976), "Optische Kavitation," Physikalische Blatter, Vol. 32, No. 12, pp. 553-563.

Lederer, L. (1976), "Profilströmungen unter Berücksichtigung der Dynamik von Kavitationblasen," (Hydrofoil Flow with Regard to Bubble Dynamics) Report No. 341, Institute für Schiffbau der Universität Hamburg.

Meulen, J.H.J. van der (1974), "The Influence of Polymer Injection on Cavitation," Proceedings Conference on Cavitation, Institute of Mechanical Engineers, Edinburgh, Scotland, pp. 17-25.

Meulen, J.H.J. van der (1976a), "Holographic Study of Polymer Effects on Cavitation," ASME Cavitation and Polyphase Flow Forum - 1976, pp. 4-5.

Meulen, J.H.J. van der (1976b), "A Holographic Study of Cavitation on Axisymmetric Bodies and the Influence of Polymer Additives," Ph.D Thesis, Technische Hogeschool Twente.

Noordzij, L. (1976), "Some Experiments on Cavitation Inception with Propellers in the NSMB Depressurized Towing Tank," International Shipbuilding Progress, Vol. 23, No. 265, pp. 300-306.

Numachi, F. (1975), "Effect of Turbulence in Free Stream and Cavitation Incipience of Hydrofoil," Journal of Fluids Engineering, Ser. I, Vol. 93, pp. 180-190.

Oldenziel, D.M. (1975), "Measurements on the Cavitation Susceptibility of Water," Proceedings 5th Conference on Fluid Machinery, Budapest.

Oossanen, P. van (1974), "Calculation of Performance and Cavitation Characteristics of Propellers Including Effects of Non-uniform Flow and Viscosity," Publication No. 457 of the Netherlands Ship Model Basin.

Oossanen, P. van (1975), "Comparative Hydrofoil Experiments and Development of a Standard Cavitator," Appendix 3, Report of Cavitation Committee, Proceedings of 14th International Towing Tank Conference, Vol. 2, Ottawa, pp. 76-93.

Oossanen, P. van (1977a), "Theoretical Prediction of Cavitation on Propellers," Presented at the Chesapeake Section of the Society of Naval Architects and Marine Engineers.

Oossanen, P. van (1977b), "The Choice of Propeller Design Parameters with Respect to Cavitation Control," Det Norske Veritas Symposium on Hydrodynamics of Ship and Offshore Propulsion Systems, Høvik outside Oslo.

Palanichamy, K., Syamala-Rao, C., and Lakshmann-Kao, N.S. (1974), "Investigation on Cavitation Inception in a Venturi with Transverse Pins," Proceedings Conference on Cavitation, Institute of Mechanical Engineers, Edinburgh, Scotland., pp. 145-152.

Persson, B. (1974), "On the Scaling of Cavitation Bubble Growth," Proceedings Conference on Cavitation, Institute of Mechanical Engineers, Edinburgh, Scotland, pp. 229-232.

Peterson, F.B., Danel, F., Keller, A., and Lecoffre, Y. (1975), "Comparative Measurements of Bubble and Particulate Spectra by Three Optical Methods," Appendix I, Report of Cavitation Committee, Proceedings of 14th International Towing Tank Conference, Vol. 2, Ottawa, pp. 27-52.

Pyun, J.J., Hammitt, F.G., and Keller, A. (1976), "Microbubble Spectra and Superheat in Water and Sodium, Including Effect of Fast Neutron Irradiation," Journal of Fluids Engineering, Vol. 98, Series I, No. 1, pp. 87-97.

Raabe, J. (1976), "The Scale Effect of Cavitation Inception Due to Tensile Stress, Heat Conduction and Gas Diffusion," Proceedings IAHR - Symposium, Two-Phase Flow and Cavitation in Power Generating Systems, Grenoble, France., pp. 101-110.

Radhi, M.H. (1975), "Theoretische und experimentelle Untersuchung über den Kavitationseinsatz an schwingenden Tragflugelprofilen," Doctor of Engineering Thesis, Technischen Universität Berlin.

Shalobasov, I.A., Shal'nev, K.K., Zvragincev, Yu. S., Kozyrev, S.P., Haldeev, E.V. (1974), "Remarks Concerning Magnetic Fields in Liquid," Electronic Machining of Materials Akad. Nauk Moldasky CCR, No. 3 (57), pp. 56-59.

Takagawa, S., Taniya, S., and Kato, H. (1975), "Effect of Size of Stream Nuclei on Inception of Cavitation," Journal Society of Naval Architects of Japan, Vol. 138, pp. 87-92.

Takahashi, H. (1975), "Basic Mechanisms of Cavitation Inception," Appendix 2, Report of Cavitation Committee, Proceedings of 14th International Towing Tank Conference, Vol. 2, Ottawa, pp. 53-75.

Ting, R.Y. and Ellis, A.T. (1974), "Bubble Growth in Dilute Polymer Solutions," The Physics of Fluids, Vol. 17, No. 7, pp. 1461-1462.

Vyaz'menskii, B.E. (1975), "Effect of Polymer Additives in Cavitation," Journal of Engineering Physics, Vol. 25, No. 6, pp. 1536-1538.

Weitendorf, E.A. (1977), "Cavitation and its Influence on Induced Hull Pressure Amplitudes," Det Norske Veritas Symposium on Hydrodynamics of Ship and Offshore Propulsion Systems, Høvik outside Oslo.

Yilmaz, E., Hammitt, F.G., Keller, A. (1976), "Cavitation Inception Thresholds in Water and Nuclei Spectra by Light-Scattering Technique," Journal Acoustical Society of America, Vol. 59, No. 9, pp. 329-338.

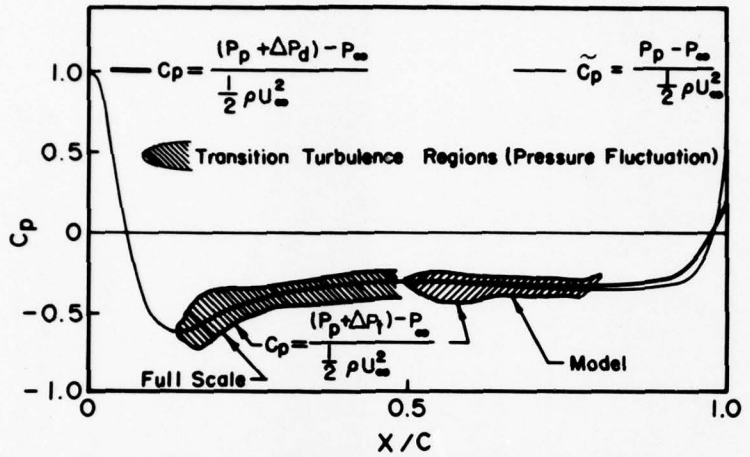

Fig. 1. Viscous Effect on Pressure Distributions of a Typical Hydrofoil Section Without Laminar Separation

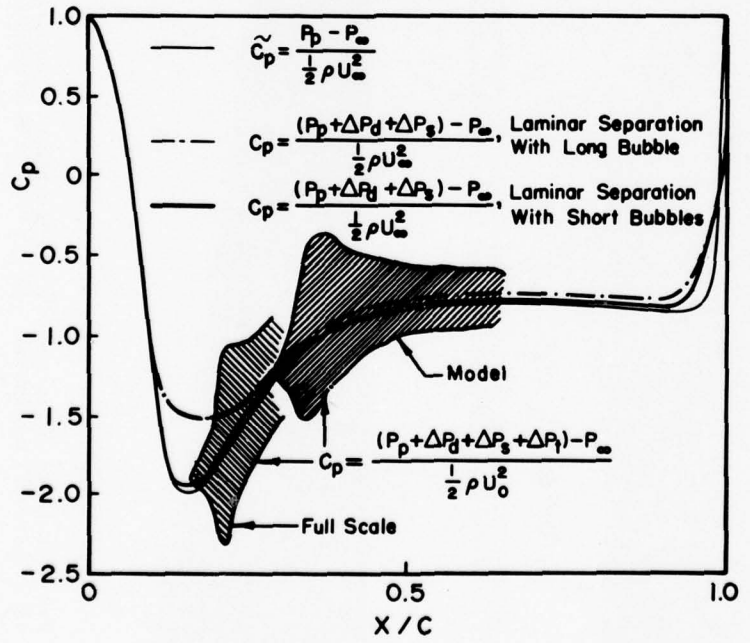

Fig 2. Viscous Effect on Pressure Distributions of a Typical Hydrofoil Section With Laminar Separation

Plate 14. Photograph of holographic reconstruction showing transition from laminar to turbulent boundary layer flow on blunt nose (s_T D 1.68). The flow is visualized by the injection of a 2 percent NaCl solution. The flow is from left to right. Re 0.81 10^5(V_∞ 7.95 m/s).

Plate 15. Photograph of holographic reconstruction showing transition from laminar to turbulent boundary layer flow on blunt nose (s_T/D 0.715). Injection of a 2 percent NaCl + 500 ppm Polyox WSR-301 solution. The flow is from left to right. Re 0.83 10^5 (V_∞ 8.0 m/s).

Figure 3 - Photographs of holographic reconstruction showing affect of a polymer transition region (Note: S_T is distance along body surface and D is maximum diameter of body).

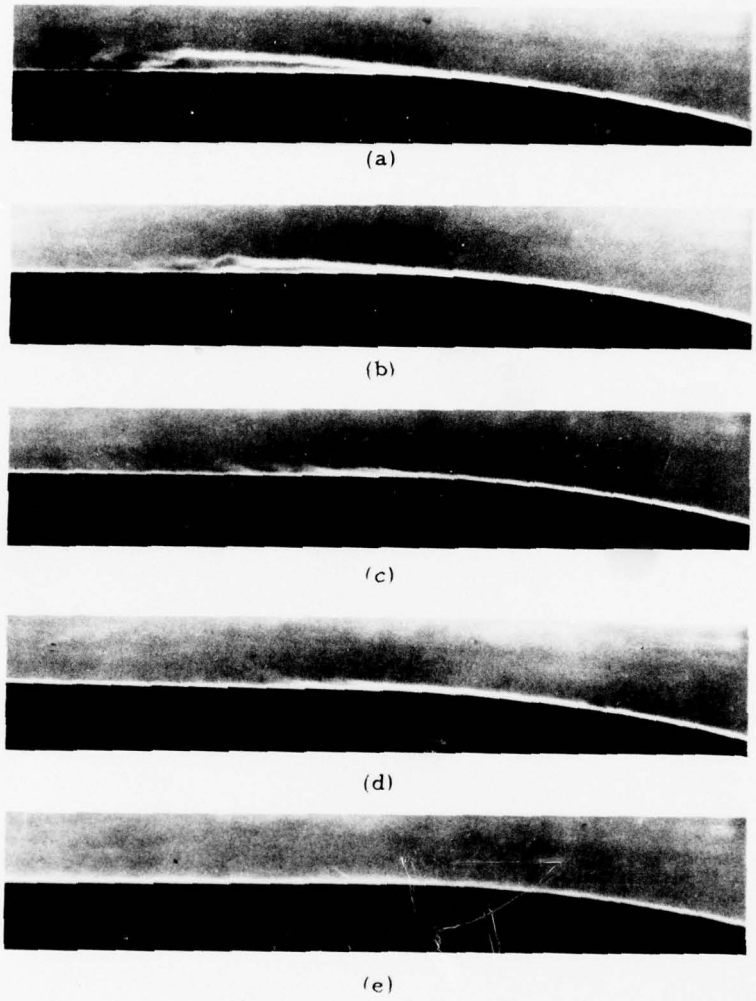

Fig. 4 - Effect of injection of Polyox (WSR 301) on the laminar separation on the hemisphere nose body. Flow is from right to left. $Re_0 = 4.2 \times 10^6$. Concentration = 500 wppm.
(a) $\dot{Q}$ (injection rate) = 0.0, G = 0.0
(b) $\dot{Q}$ = 0.1 ml/sec, $G = 0.47 \times 10^{-6}$
(c) $\dot{Q}$ = 0.3 ml/sec, $G = 1.40 \times 10^{-6}$
(d) $\dot{Q}$ = 0.5 ml/sec, $G = 2.34 \times 10^{-6}$
(e) $\dot{Q}$ = 2.0 ml/sec, $G = 9.35 \times 10^{-6}$

REVIEW OF WALL EFFECTS ON FULLY DEVELOPED CAVITY FLOWS

by

Elwyn S. Baker
David W. Taylor Naval Ship Research and Development Center

ABSTRACT

A review of the literature and a summary of current progress in the field of tunnel wall effects upon supercavitating hydrofoils and propellers is made primarily for the steady state operation. Both experimental and analytical results are considered. Bracketed fields are the forces on pure drag strut sections in two-dimensional flow tunnel test sections, lifting fully cavitating hydrofoil sections in cavitation tunnels, free surface channels, and open-jet test sections, and supercavitating propellers in closed-jet test sections. The tunnel wall effect upon the unsteady forces and upon the cavity length is also discussed. The general result is found that the tunnel wall effect is quite small on the force coefficients at a given cavitation number, but that the tunnel walls significantly raise the minimum cavitation number for testing and have a very large effect on the cavity length.

INTRODUCTION

When speed over 60 knots are required, the flow pattern over most underwater bodies and appendages is accompanied by attached cavitation. The cavity springs from sharp edges or curvatures of the body and trails into the wake, ending in a region of turbulent cavity collapse. These fully-developed cavity flows in incompressible fluids are dependent on the geometry of the solid body, where the incidence angle α for lifting surfaces or a deflection angle β for wedge or cone flows are considered to be the geometric variables, while the state of cavitation, itself of unknown geometry, is characterized by the dimensionless cavitation number

$$\sigma = \frac{P_\infty - P_c}{1/2\ \rho\ U_\infty^2}$$

Here P_c is the gaseous vapor pressure inside the cavity, while P_∞ and U_∞ are the pressure and velocity conditions far upstream ahead of the body, along the fluid streamline which passes over it. To a much lesser extent for cavity flows the dimensionless Froude number

$$Fr = \frac{U_\infty}{\sqrt{g\ell}}$$

where ℓ is some representative length dimension of the body, and the Reynolds number

$$Re = \frac{\rho U_\infty \ell}{\mu}$$

are used to scale the gravity and viscous effects of the fluid. The pressure in the cavity P_c is ordinarily taken to be the fluid vapor pressure at the ambient temperature. Occasionally this pressure will be artificially increased by providing an air path to the cavity from the atmosphere, such as that behind a ventilated strut, or by forcing air into the cavity through passages in the body or appendage itself.

A common experiment with cavity flow is to place a small model of the body in a section of a closed flow loop or tunnel. The pressure P_∞ in the loop is reduced so that the same value of cavitation number σ as for the prototype is created at a much reduced velocity U_∞. The test section of the loop may have the model mounted in the center of a large dead-water plenum while the fluid flows against it from an inlet pipe of larger diameter than the model. This is called an open jet test section. Alternatively, the test section may have the model mounted in a circular or rectangular pipe, called a closed jet or solid wall section. The model itself is attached to a balance arrangement which permits the total forces on it to be measured.

This paper is a review of reports concerned mainly with the effect of the closed jet test section on the forces and cavitating flow over the model. Because of this cavitation modelling, the primary emphasis is on the effects of the tunnel constriction, characterized by H/ℓ where H is the section height or diameter, on the flow over the body at constant cavitation number σ.

The solid wall section, which leads to the term "wall effects", is associated with the difficult concept of blockage. Each test facility, in the absence of a model, has some minimum cavitation number which can be achieved. The pressure P_∞ is limited by the quality of tunnel sealing and the strength of the evacuation pumps to the range of about 2 psia (14 kPa), while P_v for water is typically 1/2 psia (3 kPa). There is some maximum speed of fluid U_∞ which can be attained by the tunnel drive impeller through the test section. This limit

may range from 20 feet/sec (6 m/s) to 40 feet/sec (12 m/s) or higher. Speed is usually measured by calibrating the pressure drop across the upstream converging section (venturi). The static pressure P_∞ is often measured by a wall tap on the parallel part of the test section. This tap must be both downstream far enough from the venturi exit that the wall potential pressure distribution is indeed flat, and yet far enough upstream that the pressure field from the model is negligibly small. Space is desired in the test section for the model and a long trailing cavity, so the tap may be located upstream from the venturi in the pipe bend, and its reading related to the test section pressure by using Bernoulli's equation through the converging section. The use of a static pressure tap downstream from the model is not recommended for cavity flows since cavity length is not known beforehand.

Placing the model in the tunnel test section blocks the flow, limiting the maximum velocity which can be attained in the section, at a given cavitation number σ. The downstream pressure cannot be reduced below P_v as the cavity grows infinitely long, and the upstream pressure P_∞ is a component of the cavitation number calculation. For the given maximum pressure difference across the body, $P_\infty - P_v$, only a certain velocity U_∞ over the body and cavity can be developed, and the value of σ so achieved will be substantially higher than the empty section minimum. Of course the cavity itself, being only vapor, does not block the flow, but rather the strong jet of water which surrounds it can transmit only a limited quantity of fluid. As the angle of deflection or of attack of the model is increased, the attached cavity becomes larger and the tunnel area is reduced. This increase in the minimum possible σ with increasing angle of deflection or attack, is called tunnel blockage. It is the most obvious evidence of wall effects in closed jet cavity flow experiments. Similarly, the use of a larger model, i.e. a smaller H/ℓ, in a given tunnel, will result in a higher minimum cavitation number σ at each α. The minimum cavitation number, which occurs when the cavity has grown extremely long, is denoted σ_*, the blockage cavitation number.

At the σ_* condition the theoretical trailing cavity length is infinite by definition, and the flow is called "choked". In practice the cavity collapses in the diffuser, but no increase in flow speed is possible. Above σ_*, the cavity length is finite, and various potential flow models (see Wu, 1955) have been proposed to rejoin the separated free streamlines which surround the cavity. There are two groups of "wake models", open and closed. In the open wake model the streamlines never actually rejoin as the pressure recovers in the downstream wake. In a closed cavity wake model they may rejoin, or it may only be required that the wake flow is potential and continuous. All these models are artificial since the actual flow in the closure region is observed to be turbulent and

unsteady.

There is a marked similarity between closed-jet effects on cavity flows and the same flows in an infinite cascade of zero stagger. The latter may be solved theoretically by a simple singly periodic transformation. In fact, for the two-dimensional pure drag case the conditions are identical, by symmetry, since there is no flow turning. Blockage is also exhibited in the cascade flow, and σ_* depends on the solidity. The analogy for the propeller case is more difficult, since the primary flow restriction occurs as the fluid passes between the blades. Yet the individual blade cavities can join downstream to choke the tunnel (McDonald and Hecker, 1969).

So far the only theoretical results for tunnel wall effect apply to the two-dimensional flow case, where both linear and non-linear mathematical formulations are available. For the three-dimensional foil case, the unbounded flow model has been worked out, but the tunnel wall effects case has not. Systematic wall effects experiments on three-dimensional foils are only now being performed (Maixner, 1977). The propeller mathematical model without walls is currently under development with linearized and quasi-linear models. Tunnel wall effects may not be added for quite some time because of the mathematical difficulties. Experiments with geosym propellers in closed jet sections are well known, however (van de Voorde and Esveldt, 1962; Kruppa, 1963; McDonald and Hecker, 1969).

Though the main interest in wall effects experiments has been the measurement of force coefficients, this turns out to be not of primary importance. Often the wall effect on the force coefficients is small and of the order of the experimental inaccuracy itself, except in the case of bodies with inherently low force coefficients such as thin wedges or lifting flat plates at low angle of attack. Rather the large problems of wall effects are in two areas: first the value of σ_* in a tunnel may be larger than the free-stream value of σ being modeled; and second, the cavity length in a tunnel is dramatically larger than that in an unbounded stream for even large tunnel sizes, say $H/\ell = 5$. Meanwhile for hydrofoil operation at a fixed depth, the water surface above tends to suppress the cavity length at fixed σ (Dobay and Baker, 1974). Consequently a hydrofoil modeled in the tunnel and found to have a long full cavity might actually only be partially cavitating under operation at depth/chord ratio of one.

PURE DRAG CASE

Two-Dimensional Flow

The pure drag planar flow case was the earliest analytic example of wall effects to be attacked. The thesis of Valcovici (1913) followed by the textbook of Cisotti (1922) both carried the free streamline theory of Kirchoff into the case of the infinite cavity flat plate perpendicular to the flow, between parallel walls. In more recent times the work of Gurevich (1946,1953) extended this to the case of finite cavity by applying the previously developed re-entrant jet wake model, while Birkhoff, Plesset and Simmons (1950) did the more general case of solid body flows in channel, using the Riabouchinsky wake model. The first detailed mathematical treatment of the wedge in channel flow with closed cavity is that of Cohen and Gilbert (1957). They employed a singly periodic flow mapping (using the contangent function) to extend the classical linearized source-distribution representation of cavitating wedge flow to the infinite cascade case, which by symmetry is identical to the wall effects case. Their result clearly shows the blockage cavitation number σ_* increasing as the tunnel wall spacing H is decreased; and shows that the cavity length becomes infinite as $\sigma \to \sigma_*+$. In the channel flow case they showed that at $\sigma = \sigma_*$ the cavity width downstream approaches a definite maximum, while in the infinite stream case the downstream maximum cavity width at $\sigma = 0$ is unbounded. However, for some unknown reason their calculation of the choked case drag coefficient (their Figure 5) shows an increase with closer wall spacing, in glaring contradiction to the later more accurate computations of Wu et al (1969).

This discrepancy was apparently repeated in the earlier report of Oba (1962) but later corrected through the careful consideration of the wake momentum in the linearized theory, see Oba (1968). Oba's Figure 26, reproduced as our Figure 1, shows the proper behavior of C_D versus σ, including the decrease of C_D with increasing wall effect at constant σ, and the increase of σ_*. Oba's later wake model took account of the partially open wake which must remain behind the drag body to satisfy the conservation of momentum condition.

The report of Wu, Whitney and Lin (1969) is the first non-linear calculation of wall effects on planar, pure-drag flows. Numerical results are presented for the wedge flow case using the open wake parallel plate wake model and the closed wake Riabouchinsky wake model, as well as the background theory of those and the re-entrant jet flow model.

The non-linear mathematical formulation is elegant and simple in the two-dimensional pure drag case. The shape of the potential plane $f = \phi + i\Psi$ is

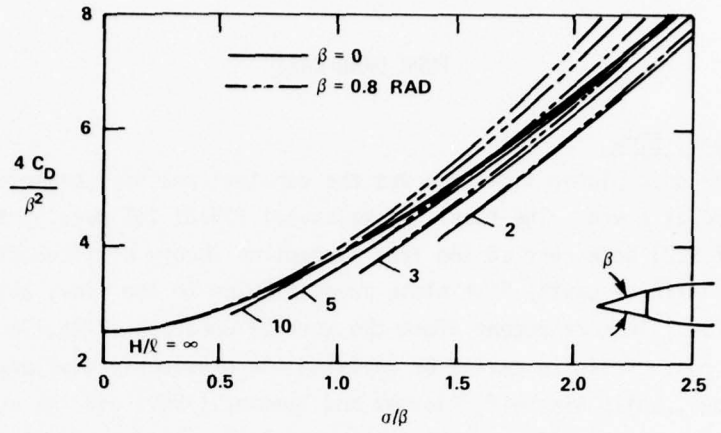

Figure 1 – Tunnel Wall Effect on the Drag Coefficient of a Symmetric Wedge, Opening Angle β, Chord L, Mounted in Mid-Channel

(From Oba, 1968)

either an open or closed straight-sided slit in the channel, but since only half the flow need be considered by symmetry, a condition of $\phi = 0$ may be applied on the center channel, so that the flow in either the upper or lower half plane is always simply connected. Therefore the Schwarz-Christoffel mapping theorem is sufficient to map the f-plane onto a common parameter upper-half plane, say $\Psi = \xi + i\eta$. The velocity problem is solved by considering not the complex velocity $w = u - iv$, but rather the logarithmic hodograph ω, where $w = u - iv = qe^{i\theta}$, $\omega = \log \frac{1}{w} = \tau + i\theta$, $\tau = \log \frac{1}{q}$, where q is the velocity magnitude and θ the velocity direction. Here ω is analytic and its map is also straight-sided since for the wedge flow, θ is constant and known on the wedge sides and on the tunnel walls, while q is constant on the free streamline by Bernoulli's theorem, and specified in terms of cavitation number σ. So ω can be easily mapped onto the Ψ plane also. The shape of the wedge and trailing cavity in the physical $z = x + iy$ plane is then recovered from the definition $w = \frac{df}{dz}$ or

$$Z(\Psi) = \int_a^{\Psi} \frac{1}{w} \frac{df}{d\Psi}\, d\Psi = \int_a^{\Psi} e^{w(\Psi)} \frac{df}{d\Psi}\, d\Psi$$

where a is the position of $z = 0$ in the common parameter plane, and the fluid flow boundaries correspond to the real axis, along which the integrations are taken. The drag force may be computed by integrating the pressure, obtained from Bernoulli's theorem and the known velocities $w(\Psi)$, acting along the pressure surface of the body, whose slope is given at each point from the known geometry. Thus for nonlinear wedge flows the flow quantities are usually expressed as

integrals of rational functions by the nature of the Schwarz-Christoffel Theorem.

Results from these non-linear calculations confirm that the wall effect (smaller H/ℓ)decreases the level of the C_D versus σ curves, and that the numerical amount of the decrease is quite insenitive to σ so long as $\sigma > \sigma_*$ for a given tunnel wall spacing. The surprising result is that the decrease as a fraction of C_D is largest (but not unlimited) as $\beta \to 0°$. Strikingly counter-intuitive, the implication is that tunnel wall effects should not be ignored even when making measurements on models which are quite small in relation to tunnel size.

At the choked condition the cavity length is infinite, there is no wake, and therefore no wake model is necessary. Discrepancies between the theoretical predictions of the various wake models become apparent at the larger cavitation numbers and shorter cavity lengths. The comparison of parallel plate versus Riabouchinsky wake model showed the parallel plate to predict a slightly higher C_D versus σ at the larger σ values, with identical tunnel wall spacing.

To resolve this discrepancy, experiments were conducted on supercavitating wedges by Whitney, Brennen and Wu (1970) in the C.I.T. water tunnel, using the narrow, rectangular working section. (Also reported in Wu et al 1971.) This report concludes that the Riabouchinsky wake model gives the more accurate comparison with drag measured by integrating the measured pressure distribution along the wedge. Unfortunately, corresponding theoretical data for the parallel plate wake model are not given for comparison. More importantly, the two wake models regarded as being the most representative in the unbounded flow case, namely the Wagner's re-entrant jet flow model and the Tulin single spiral vortex wake model, were not computed for the pure drag case with wall effect. The agreement between the Riabouchinsky theory and the experiment for the measured pressure distribution is excellent except near the leading and trailing edges where there are cancelling errors when the drag integral is computed. Agreement for the measured wall pressure distribution however is barely fair, and here the parallel plate wake model would have been superior, since the Riabouchinsky image shows a complete pressure recovery downstream, while the measurements clearly show a wake under pressure. Oba (1968) has shown this to be necessary in the finite cavity case due to the cavity drag. However Oba concludes theoretically that the parallel plate wake model would have over predicted the wake under pressure value.

Another difficulty of the Whitney experiments is the positioning of the static pressure tap only 1.16 chord-lengths ahead of the model. This was perhaps adequate for fully wetted flow, but near the choking condition, with its long trailing cavity, the flow sees a divided streamline many times that length. Indeed the measured data seems less accurate near the choking condition, as shown

by Whitney's Figure 5. One other point to be made is that the recorded drag from the force balance do not agree closely enough with the theoretical data to make any conclusions on wall effects or wake models. The direction is not consistent. The force balance data exceeds the integrated pressure coefficient drag for the 9° wedge opening but trails it for the 30° wedge opening, see Figure 2. Nevertheless this force balance measurement is the usual technique for determining model loads. The drag balance data were corrected for friction drag using the Falkner-Skan solution for laminar flow over a wedge. Rather high chord Reynolds numbers were involved, ranging from 1.15×10^6 to 2.3×10^6, corresponding to tunnel speed range of 25 feet/sec (7.62 m/s) to 50 feet/sec (15.2 m/s). It seems safe to conclude that the tunnel wall effects on force coefficients are generally smaller than the experimental accuracy in most pure-drag supercavitating flow experiments. The large tunnel wall effect is exerted on the cavity length.

In fact, as can be seen from the simple correction rules propounded in Whitney's report, the primary effect of tunnel walls appears as a reduction of the cavitation number (which enlarges the cavity); the reduction of drag coefficient at constant σ is of rather secondary importance numerically. A similar correction formula to σ has been proposed by Karlikov et al (1966), using a simpler procedure based on flow area.

A recent major addition to the literature in this area is the work of Popp (1975). He has re-derived the wedge flow in channel results using the parallel plate (also called Roshko) wake model, by a different mathematical method, which allows extension to the case of compressible fluid flows; though he reports that his solution series for that case may converge slowly. This work has applications for the design of flame tubes and stabilizers, using the well known analogy between cavity and separated wake flows.

Scale effect studies of cavitation behind circular cylinders in a closed-jet section have been reported by Shal'nev (1966) who investigated experimentally diameter/tunnel width ratios of 0.1-0.4. However his extrapolation of choking cavitation number to a positive value at infinite tunnel width (his Figure 8) is clearly incorrect - this value must be zero. But the dramatic increase in cavity length with increasing tunnel constriction, σ fixed, is very evident in his data.

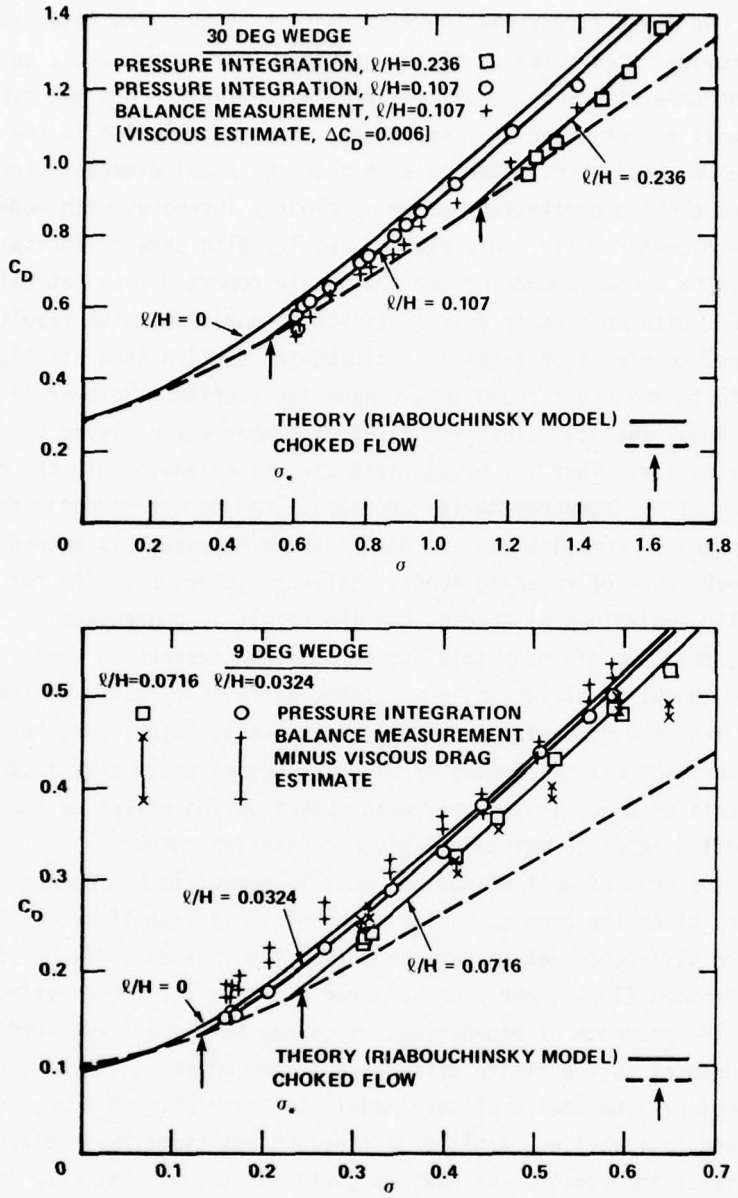

Figure 2 – Comparison of Prediction and Experimental Measurement for a Symmetric Wedge Mounted in Mid-Channel

(From Whitney, Brennen and Wu, 1970)

Axially Symmetric Case

Experimentally measured drag of axisymmetric discs was compared by Klose and Acosta (1964), who found no correlation with facility type. The later report of Dobay (1967) provides a good review of the previous literature, and a survey of the then current understanding of axisymmetric wall effects. His own experiments investigating wall effect, used very small drag discs in relation to the tunnel size (2 inch (5 cm) maximum diameter in a 36 inch (91.5 cm) diameter closed-jet). Yet the measured choking cavitation number σ_* clearly increases with model size-to-tunnel- diameter ratio. His plotted results also show an increase in the curves of C_D versus σ when comparing the previously reported open-jet data of Reichardt (1945), with open water data (infinite stream), and with results of increasing tunnel constriction cases in a closed-jet section (see his Figure 5). This is opposite to the usual trend in a closed-jet section. However in the experiments of Dobay the low value of cavitation number was achieved by ventilating the cavity. That is, pressurized air was released into the cavity to raise the values of P_c, measured cavity pressure, used in the computed definition of cavitation number. Correlations are not reported between this method and the usual tunnel techniques of reducing tunnel static pressure, P_∞. The two cases are theoretically equivalent of course, but the result is unexpected.

Similarly, the data of Dobay (his Figure 10) show decreasing cavity lengths with increasing tunnel constriction, σ constant, which is opposite to the expected trend from two-dimensional theory. Previously, Bate (1964) had reported the expected increased cavity lengths as the disc cavity moved away from a free surface. The data of Dobay is the only data extant on the effect of tunnel walls on required airflow rates to maintain a given cavitation number.

Theory in the area of wall effects on axially symmetric bodies has been in slow development since the complex variable technique is inapplicable. Results using the finite difference method have been reported independently by Jeppson (1969) and by Brennen (1969), who also compared his results with experimental measurements. The presence of boundaries, which may be either free surface or wall type, is natural to the finite difference scheme which must subdivide a finite fluid region. The choice of wake models is invariably an image of the upstream body and cavity; i.e., a plane of fore and aft symmetry is placed normal to the flow axis at the position of maximum cavity width, so that only the upstream flow need be subdivided into elements. The position of this symmetry plane is adjusted automatically with cavitation number and tunnel or jet boundary separation. This is the analog of the two-dimensional Riabouchinsky wake model.

The computed results from Brennen's paper for the drag of both the axisymmetric disc and the cavitating sphere in tunnel clearly show the trend of increased σ_* with increased tunnel constriction, and a reduction of the level of

the curves of C_D versus σ at constant σ as the wall effect is increased. As in the wedge flow case, the amount of reduction of C_D versus σ is quite insensitive to the actual value of σ, so long as $\sigma > \sigma_*$.

No three-dimensional non-axisymmetric wall effects cases are known. The unsteady two-dimensional (planar) case of a cavitating wedge moving fore and aft along its axis has been analysed by Song and Tsai (1962), using a linearised formulation and the parallel plate wake model. The case of a two-dimensional wedge impacting a constrained fluid has been analysed by Parkhomovski (1958), while the corresponding disc impact case with walls is the subject of an investigation by Borodachev et al (1967).

Observers of the natural wake oscillations behind supercavitating drag bodies have also been concerned about wall effects on the cavity vibrations, since the tunnel walls affect the cavity geometry so much more strongly than the force coefficients. As a speculation, it would seem that for cavities with $\sigma > \sigma_*$ any wake model is unstable (in time) in a sense analogous to the inviscid instability first studied by Lord Rayleigh. In practice two-dimensional wakes may be observed to oscillate in time even though the upstream conditions are steady. Some notes of the effect of walls on this oscillation may be found in the article of Shair et al (1963) for cylinder wakes. Young (1965) has made an investigation into the effects of cavitations on wakes and shedding frequencies. The mathemetical boundary conditions are similar for wakes and cavities; but the wall effect may not be the same due to different closure conditions and physics of the flow.

LIFTING FLOWS

Two-Dimensional Case

Lift, drag and moment coefficients are the usual measured quantities for experiments on supercavitating hydrofoil sections. The first theoretical paper to present numerical results for wall effects in the lifting case is that of Cohen, Sutherland, and Tu (1957). Their mathematical results apply to the linearized version of the parallel plate wake model, which in its non-linear form had been developed just previously by T.Y. Wu (1955). The simplest case of a flat plate at mid-channel (but also the off-center case) was analysed in detail. From their reported curves in this first report can be gleaned the three major conclusions which have stood for 20 years of subsequent development:

1. For a fixed foil geometry (i.e., given plate α) the choking cavitation number σ_* increases with increasing tunnel constriction (lower H/ℓ), and for fixed tunnel wall spacing H/ℓ, the choking cavitation number increases with

increasing angle of attack (their Figure 5).

2. The effect of tunnel walls is to reduce the level of the C_L versus σ curves from the infinite stream values; i.e., at fixed σ, C_L is reduced as the tunnel is constricted (their Figure 6, reproduced as Figure 3).

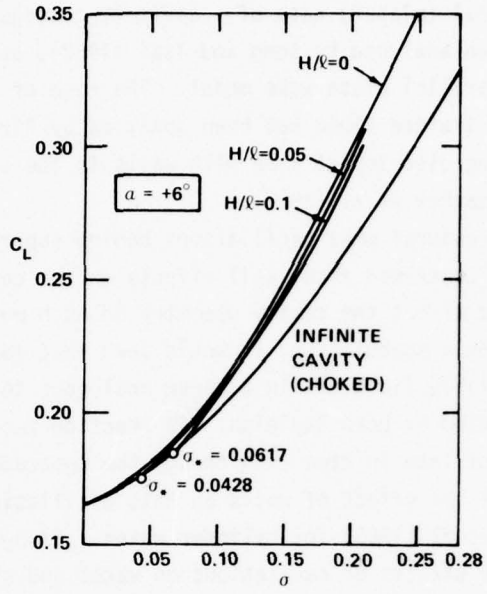

Figure 3 – Lift Coefficient versus Cavitation Number for a Lifting Flat Plate Hydrofoil Mounted in Mid-Channel

(From Cohen, Sutherland and Tu, 1957)

3. The numerical amount of the wall effect on the C_L versus σ curves is relatively insensitive to σ for each spacing H/ℓ, but the magnitude of the decrease as a fraction of C_L is larger at the smaller angles of attack, so that the relative wall effect is largest for precisely those thin foil cases where it would be expected to be the smallest (their Figure 10, reproduced as Figure 4).

With these results established at an early date, there remained only a need to improve the accuracy of the theoretical model and the calculation, and to improve the ease of application to the cambered foil case. The correct trends obtained with the parallel plate model for the lifting case tend to vindicate its previous use in the pure drag case, Cohen and Gilbert (1957), and point rather to a mathematical error in their incorrect report of the curves of C_D versus σ increasing with H/ℓ increase, rather than ascribing that fault to the linearization of the wall effect problem itself. This linearization has been discussed in detail by Parkin (1959). The early error was recognized by Whitney

(1970) in his experiments.

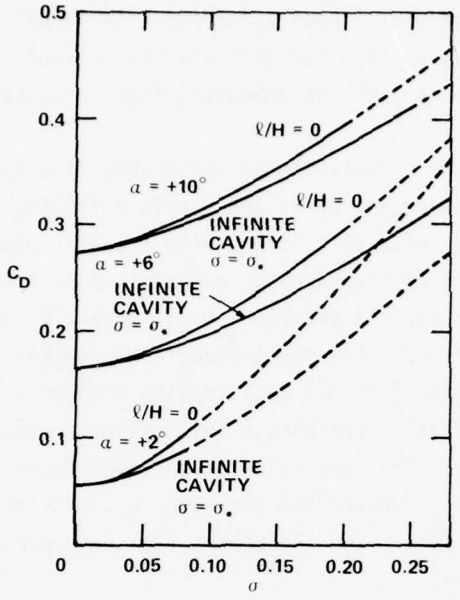

Figure 4 -- Force Reduction with Wall Effect on a Flat Plate Hydrofoil, Showing the Variation with Increasing Angle of Attack

(From Cohen, Sutherland and Tu, 1957)

Fabula (1964) derived linearized results for the case of a cambered foil in choked flow, i.e., infinite cavity length, for which no wake model is required. He allowed the added variable of an arbitrary free-streamline detachment point from the upper surface, at position e in percent of chord from the leading edge. The case e = 1 is fully wetted flow over the plate in tunnel, in which the wall effect increases the force coefficients over their unbounded values, as clearly shown by Fabula's Figure 3, wherein σ is actually σ_*, an implicit parameter in the non-fully wetted cases. His computed results are compared with the experimental measurements of Lang, Daybell et al (1959) on cambered ventilated hydrofoil sections in tunnel. By using forced ventilation, the cavity was so long that the flow could safely be concluded to be near choked. Lift prediction and experiment agree well for C_L versus α. Of course here σ is an output or dependent variable in the choked flow case. That is, σ_* is determined solely by the tunnel and model geometry.

The predicted and measured C_D versus α and σ_* versus α do not agree as well. Fabula blames this on the longitudinal pressure gradient effect of the growing tunnel wall boundary layers and on the location of the static pressure tap only 3 inches upstream of the 4 inch chord models, and he devised a numerical correction

which improved the agreement considerably. But the report of the data in his paper plotted versus α, with contours of the ventilation coefficient K_v (his Figure 7) show an odd pattern. Does C_D versus α in tunnel increase with increasing airflow rate, as if σ had increased by pressurizing the cavity? This would be quite at variance with the unbounded flow case measurements of Dobay and Ficken (1964).

The first non-linear calculation of the choked flow over an inclined flat plate in tunnel was carried out by Ai and Harrison (1965), using the conformal mapping technique. The infinitely long cavity actually simplifies the mapping process. The results of Ai and Harrison are similar in trend to those of Fabula. One curve in particular shows a striking result (their Figure 11, reproduced as Figure 5). The ratio of C_D - bounded choked flow case (in tunnel) to C_D - unbounded as plotted against tunnel wall spacing H shows a large increase for the lower plate angles of attack, reaching a wall effect reduction value of 80% for $\alpha = 5°$ and H = 3 chords. The same value is only 98% for $\alpha = 90°$, with the plate perpendicular to stream. However the parameter σ_*, choking cavitation number, does not appear here. This being the choked flow case means that its value changes along each curve.

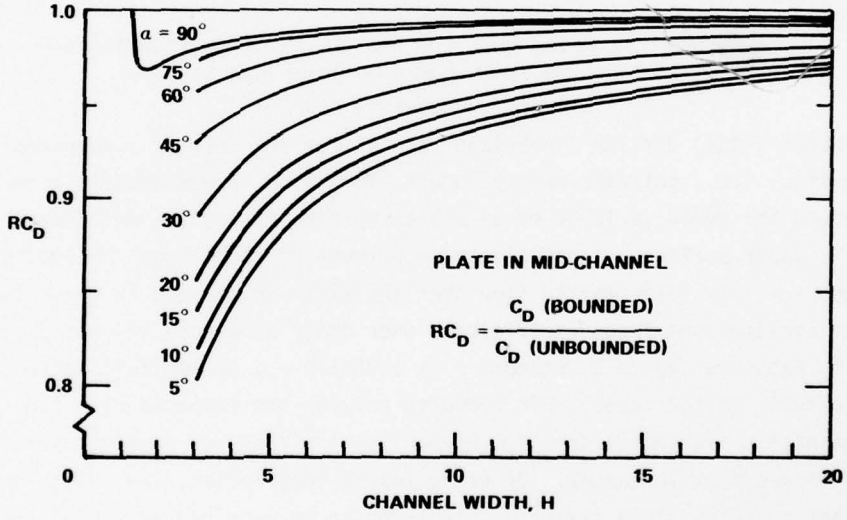

Figure 5 – The Ratio of C_D in Closed Jet Tunnel Section to C_D for Unbounded Flow, for a Lifting Flat Plate Hydrofoil Section in Mid-Channel in Fully Choked Flow (σ_* varies with H/L)

(From Ai and Harrison, 1965)

The case of off-center location in the tunnel was also investigated in this report. It was found that the force coefficients at choked condition decreased as the foil was brought near the upper tunnel wall, and increased near the lower

wall (wing in ground effect case). Similarly Ho (1963) had found an increase in lift coefficient as the foil nears the bottom of a channel, at a fixed submergence below the free surface. The opposite effect, i.e., foil approaching a free surface from below, in an infinitely deep stream, has also been analysed. There it was found (Ho, 1963; Dobay and Baker, 1974; Lazarev, 1970; and many others) that the opposite to the wall effect occurs in every regard. The force coefficients at constant α and σ are increased by the free surface proximity, and (contrary to intuition) the cavity length is reduced, though its vertical height above the foil section increases.

The report of Wu, Whitney, and Lin (1969) also contains a mathematical analysis of two lifting cases: choked flow past a cambered obstacle with fixed separation points and arbitrarily shaped tunnel walls, and finite cavity flow past a flat plate in tunnel, using the parallel plate wake model. For a comparison with the experiment of Parkin, see Figure 6. Mathematical results were reported for the latter, showing the expected trend of larger percentage wall effects on the plates at lower angles of attack. The growth of the tunnel wall boundary layers in the downstream direction means that most models are actually being tested in a convergent section outlined by the wall displacement thickness. Avoidance of the pressure gradient that this causes was the main reason for locating the static pressure tap near the model.

The report of Baker (1972) combined features of these two analyses to do the case of arbitrarily cambered foil sections in tunnel with a finite cavity, using the parallel plate wake model. As expected, the much higher lift coefficients of the cambered models meant that the relative wall effect on the force coefficients was much less than in the plate case, although the cavity length was much altered by the tunnel. Comparison of the computed results with previous tunnel experiments (Parkin, 1956) showed excellent agreement for the choked case, but spotty agreement for the trend of C_L versus σ. It was suspected that the wake model was the cause, since the results of all the wake models coalesce on the choked flow case. The infinite stream prediction of C_L versus σ for the flat plate case from the parallel plate wake model was compared to predictions for the closed-wake Tulin single-spiral vortex wake model and the Wu (1962) wake model. This was thought relevant to the tunnel wall effects case since the pure drag calculations of Wu, Whitney and Lin (1969) have shown the numerical amount of wall effect to be relatively insensitive to σ, at a constant angle of attack α, over the whole range of σ for which the termination model is needed. The two most highly favored wake models from that case in infinite stream, namely the Riabouchinsky and the Wagner's re-entrant jet, have not been applied to lifting foils however.

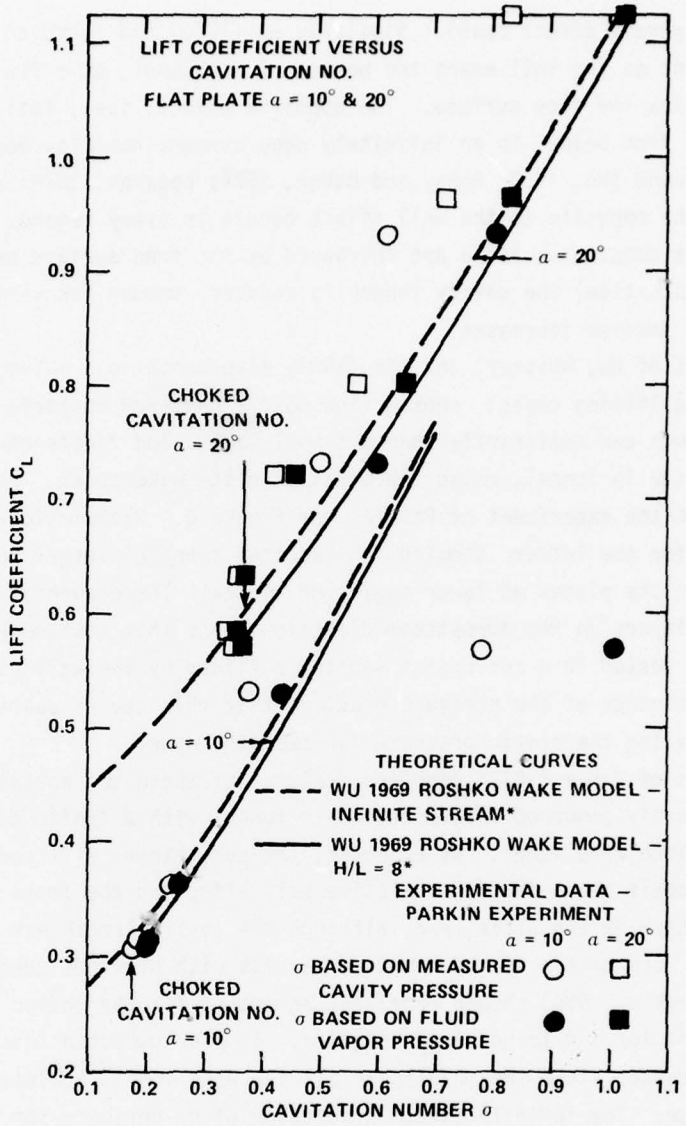

Figure 6 – Comparison of Predicted Data Using the Parallel Plate Wake Model, and Experimental Force Balance Measurements for a Flat Plate Hydrofoil Section in a Closed Jet Tunnel

(Theoretical Data from T. Y. Wu, Experiment of Parkin, 1956)

The agreement of the predicted C_L versus σ curves, for infinite stream flow, is excellent between the parallel plate wake model and the highly favored Tulin single spiral vortex wake model, and quite reasonable with the Wu (1962) wake model. Substantial differences in the predicted cavity location were noted, however. For the correct design of the section, the accuracy of this location is

very important. Sections with the same structural section modulus have a more favorable lift to drag ratio as the heavily loaded leading edge region becomes thinner, (Auslaender, 1962). But the limiting location of the material there is the free streamline location. In fact, one of the justifications for using the non-linear theory had been to gain accuracy in this region. The comparison between the wake models shows that the vertical height of the free streamline near the leading edge decreases with increasing σ for the parallel plate wake model, but increases for the other two models. Since the prime effect of the tunnel walls is to change the apparent cavitation number, as shown by the simple pure-drag correction rules, it may be that the tunnel walls change the shape of the cavity as well. The cavity location from the parallel plate wake model as affected by tunnel walls in the Baker(1972) report is probably not reliable enough to settle this point.

A major advance in applying these other more accurate wake models to the wall effect case was made by Schot (1971). He solved the closed-cavity asymmetrical (lifting) flow case in a tunnel by using a linearized formulation, and reported results for the flat plate case. Because the cavity length varies with σ to satisfy the closed cavity condition, the predicted C_L versus σ curve is not linear. The mathematical results for C_L versus σ closely resemble the linearized open wake results of Cohen et al (1957) except that the magnitude of the wall effect lift coefficient reduction seems to be slightly magnified near the choking condition $\sigma \to \sigma_*$, which is by definition an open wake condition.

Subsequent wall effects papers have also used the linearized formulation. Roman (1972) solved the design problem of the constant pressure camber distribution lifting foil shape in tunnel, showing that the thickness distribution can be decreased while maintaining the same cavity length. Yefremov (1972) has very clearly shown in his article how the source and vortex distributions can be used to represent the supercavitating lifting hydrofoil on the centerline of a straight tunnel by the method of images. The actual use of the words "source and vortex strength distribution" or "singularity strengths" to represent the flow disturbances due the supercavitating foil seems to have had its first major application in the report of Davies (1970), though of course most previous authors had recognized them in the jump conditions of the analytic complex velocity w on the flow boundary as used previously. Davies deduces an analytic result for the singularity strengths of a single foil in infinite stream. Meanwhile the use of cascade singularites, i.e., infinite rows of source or vortex elements to represent cascaded airfoils had been known for some time, and a similar method of imaged singularities has been used for fully wetted flow problems in tunnel. The numerical results presented clearly show the increase

of cavity length at a fixed σ due to the tunnel walls (a zero net source strength condition was used to close the cavity), but the effect of walls on C_L versus σ is so small as to be indistinguishable on the scale of the graphs used.

Many of the effects here described are summarized very succinctly in the recent paper of Ota (1974a). He used the open wake Tulin double-spiral vortex wake model to avoid the double-periodicity or infinite sum problem in his linearized mathemetical analysis of the lifting flat plate in bounded flow, and managed to present solutions for the force coefficients, as simple integrals of powers of rational functions, for four flow cases: a) infinite stream (unbounded fluid), b) solid wall tunnel, c) open- jet, d) open channel (foil below a free surface but above a wall). His paper presents the clearest and the most concise demonstration of all the conclusions that have been gained about boundary effects on lifting cavity flows:

a) The numerical amount of the wall effect is rather insensitive to σ (his Figure 6) as shown by Cohen, Sutherland and Tu, and by Wu, Whitney and Lin.

b) The tunnel wall effect dramatically lengthens the cavity at a fixed σ, while the open-jet effect shortens it (his Figure 9, reproduced as Figure 7), as shown by Lazarev (1970), Dobay and Baker (1974), and many others.

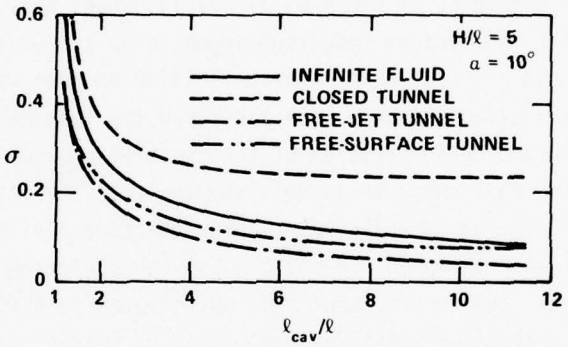

Figure 7 – Wall Effect on the Cavity Length of a Flat Plate Hydrofoil Section, Using the Double Spiral Vortex Wake Model

(From Ota, 1974)

c) Both the foil in an open-jet and the foil in a solid tunnel suffer a reduction in lift from the boundary effect (his Figure 11, reproduced as Figure 8). The open-jet effect may be inferred from the case of staggered cascade, where the foil riding above the cavity free surface from the foil beneath shows a very large loss of lift, more than enough to offset any gain from the free surface above in an open-jet.

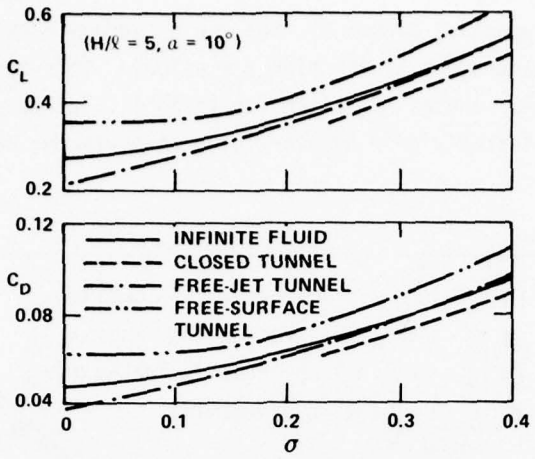

Figure 8 – Boundary Effect on the Force Coefficients of a Flat Plate Hydrofoil Section in Three Types of Facilities

(From Ota, 1974)

d) The foil in an open channel has its lift increased above the unbounded stream case. Here the mild increase in lift from the free surface above is augmented by lift due to the wall below, as shown by H.T. Ho (1963).

e) Only the solid wall tunnel can block the flow and exhibit choking. All the other cases can theoretically approach $\sigma = 0$.

The gathered data shown by Ota in his figures, taken from the C.I.T. closed-jet tunnel and the St. Anthony Falls Hydraulic Lab open-jet facility, clearly shows that the scatter in data measured by the force balance technique is often of the order of magnitude of the predicted boundary effect, so that it would be tempting to ignore the wall effect altogether. Yet for the suitable design of sections two questions remain unanswered: i) does the foil section achieve its design minimum angle of attack and hence lift-to-drag ratio in the tunnel? ii) is the free streamline in its predicted location above the foil material?

A recent report in preparation by Fisher and Baker (1977) is trying to answer the first of these questions for relatively high lift coefficient sections. The second question awaits the development of better experiment measurement techniques and perhaps more accurate wake model representations. In the report of Fisher and Baker, three cambered sections designed for open water performance at $C_L \simeq 0.30$ by either the Tulin single spiral vortex wake model or the parallel plate wake model are analysed for operation in a solid wall tunnel using the parallel plate wake model, and the results are compared with experiments. Due to the large lift coefficient there is very little numerical wall effect on the section performance. The agreement of lift and moment coefficients with the force balance measurements is quite good near the choking

condition (see for example, Figure 9), but the C_L versus σ curves sometimes diverge from the measurement at the higher σ values. This agreement does improve somewhat at the higher angles of attack (up to 15°). The comparison of the drag coefficient is consistently poor however, even when viscous corrections are considered.

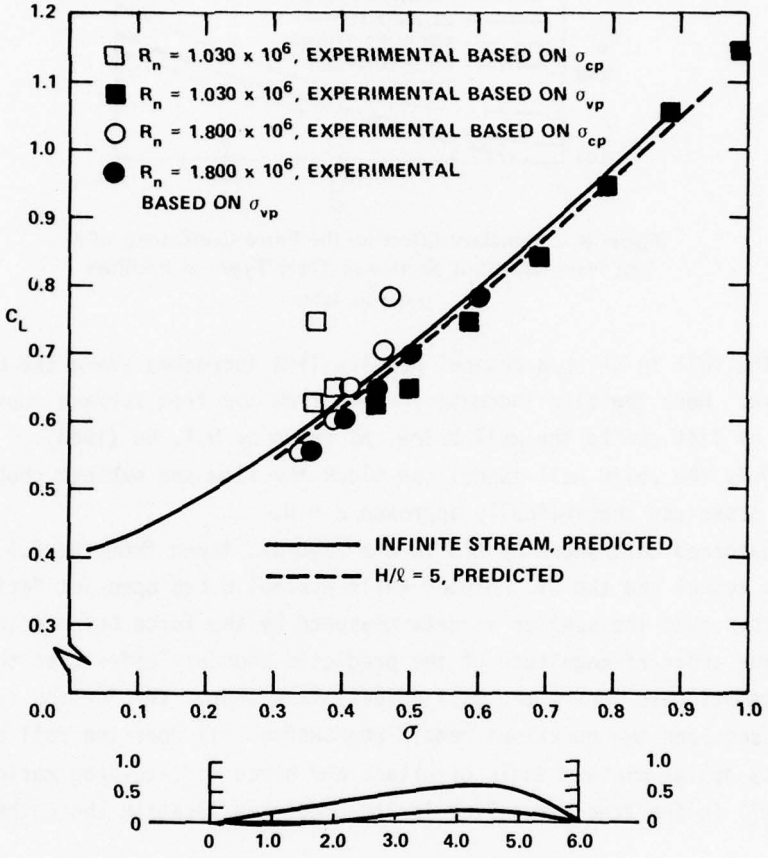

Figure 9 – Comparison of the Experimentally Measured Force Coefficient on a Highly Cambered Lifting Section with the Prediction Including Wall Effect, by Using the Parallel Plate Wake Model

(From Fisher and Baker, 1977)

THREE-DIMENSIONAL EFFECTS

No theoretical data exist here. One of the more important problems is the cavity closure condition. Current three-dimensional programs for supercavitating hydrofoils either leave the cavity length unchanged, in which case C_L versus σ is linear, or apply the two-dimensional closure condition to each section spanwise,

in which case the trailing cavity is approximately elliptical in planform (see Unruh and Bass, 1974; Tsen and Guilbaud, 1974; Acosta and Furuya, 1975). The effect of the flow boundaries distorts the cavity length versus cavitation number relation. This is shown, for example, in the data of Brennen (1969) for an axisymmetric, cavitating sphere, as reproduced in Figure 10. Therefore it is doubtful that the sectioning technique will be sufficiently accurate for the three-dimensional wall effect case. For instance, by using that method it would be easy to construct a case wherein the overall foil would operate at a cavitation number, below the choking value σ_* of the center hydrofoil section, which is obviously impossible.

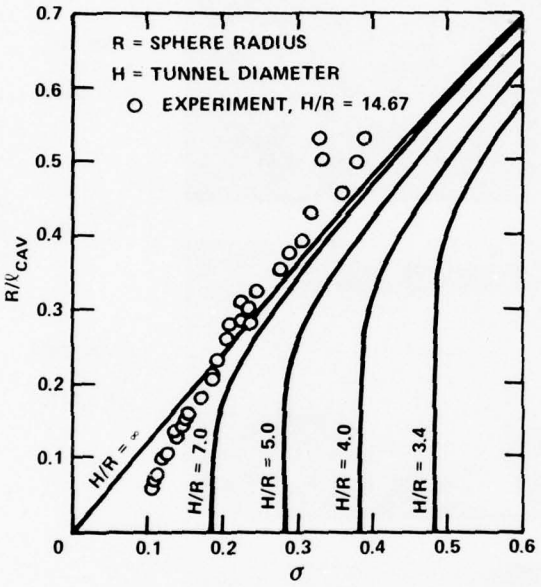

Figure 10 – Wall Effect on the Cavity Length of a Cavitating Sphere in Tunnel, versus the Cavitation Number σ
(From Brennen, 1969)

The experiments of Kermeen (1961) involved three-dimensional, rectangular planform wings of four different aspect ratios in a closed-jet rectangular tunnel. The largest two aspect ratios spanned the same percentage of the tunnel width, yet the C_L versus σ curve of the AR = 4 model was actually lower than that of the AR = 2 model. Though in the proper direction, these tests are not sufficient to conclude the intuitive notion that wall effects are more important on two-dimensional sections, i.e., AR $\rightarrow \infty$.

A series of experiments recently completed at the M.I.T. closed-jet section water tunnel (Maixner, 1977) compared steady forces and cavity planform outlines for three geosym elliptical planform hydrofoil models, of the same aspect ratio.

The largest spanned 75% of the test section (see Figure 11). Although the largest model should exhibit the most wall effect reduction of force coefficient, the proximity of the opposite tunnel wall may act as an end plate to increase its effective aspect ratio. In observing the experiments, it is noted that the natural oscillation of the short cavities, in the large σ case, is substantially more pronounced on the largest model.

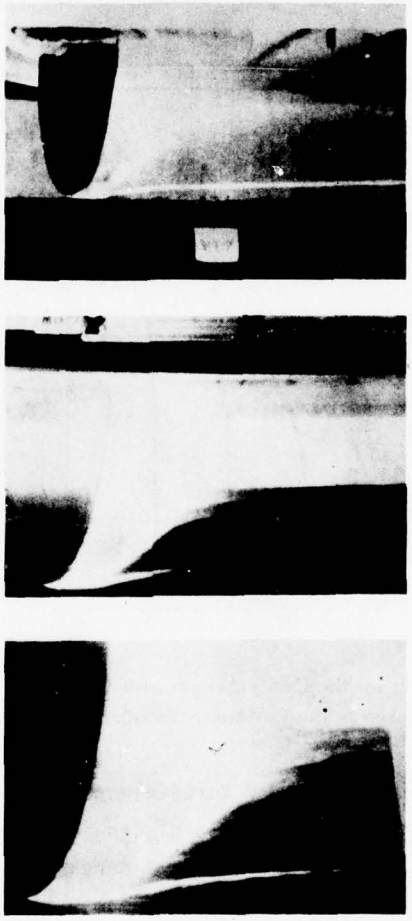

Figure 11 – Photographs Show the Cavity Outlines Behind Similar Elliptic Planform, Flat Faced Supercavitating Hydrofoils, Spanning Respectively 1/4, 1/2, and 3/4 of the 20″ × 20″ (51 cm × 51 cm) Water Tunnel

(From Maixner, 1977)

WALL EFFECT ON UNSTEADY FLOW

This is the subject of the recent paper of Kim (1972), who has analysed the two-dimensional choked flow case only, using the acceleration potential formulation. A flat-faced foil is considered to oscillate in heave, pitch or a combination of both. Of course the tunnel pressure or velocity must also oscillate to maintain the choked condition, so that σ_* is now a function of time. The mathematical flow model is a linearized time perturbation about the steady choked flow result.

The resulting curves show that the tunnel walls augment the unsteady loads, both in-phase and out of phase components (see Figure 12, reproduced from his report). This is opposite the steady flow case. Past attempts to run supercavitating flutter tests in water tunnels (Besch, 1969; Cieslowski and Pattison, 1965) have had difficulty in establishing flutter conditions in closed-jet water tunnels, while the same data is readily available from open-jet facilities, (Song, 1967, 1972).

WALL EFFECTS ON PROPELLERS

No theoretical results which consider the details of the blade section shape are available for wall effect on a propeller. The work of Tulin, using the momentum theory, (Tulin, 1962, 1965) has established that there are no wall effects at all on the propeller forces in a closed-jet tunnel, but his flow model may be an oversimplification. Nevertheless it is safe to conclude that the force coefficient change is indeed small. The lifting surface theory of the supercavitating propeller itself is only now under development, and it seems safe to conclude that it will be some time after its publication before a wall effect model is successfully devised and analysed. Here also, it is the problem of the spanwise cavity closure condition that is retarding development of the three-dimensional flow case. This is related to the problem of predicting possible flow choking between the blade rows.

Experimental results are, however, available for geosym propeller series in closed-jet tunnels. Early work at the David Taylor Model Basin with geosym propeller models 3767 (16 inch diameter (41 cm)) and 3768 (10 inch diameter (25 cm)), (Hecker and Peck, 1961), in a open-jet tunnel, established that the corrections to forces accounting for the boundary effects were very small. The so-called "thrust identity" procedure of testing does not eliminate the wall effect on the supercavitating models as the cavity geometry changes, but merely

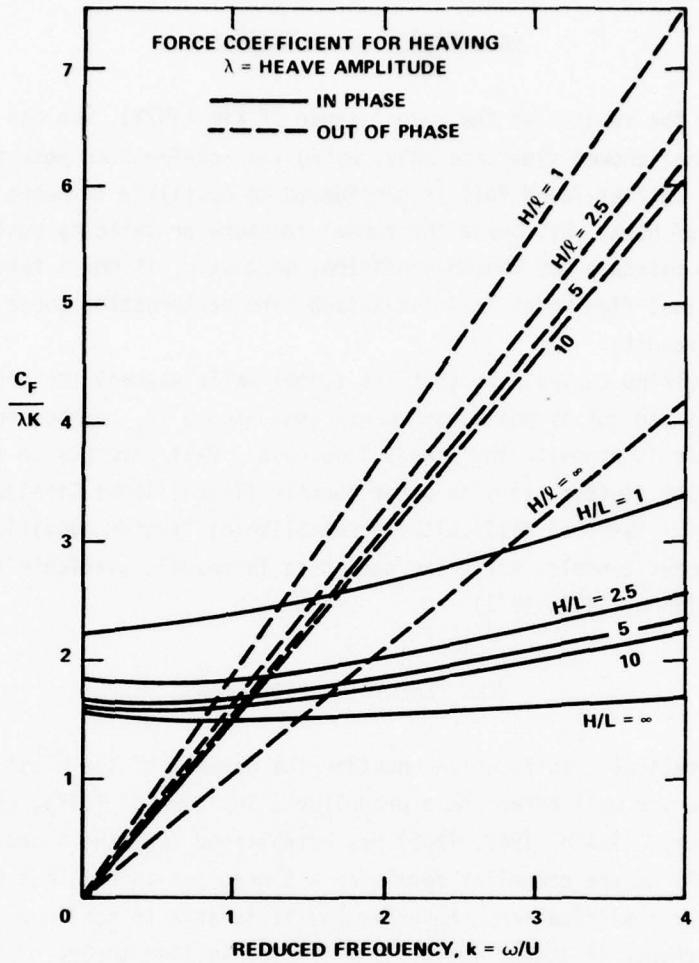

Figure 12 – Force Coefficient Normal to Heaving Flat Plate Hydrofoil Section in Closed Jet Water Tunnel, Fully Choked Condition (σ_* Varies with H/ℓ)
(From Kim, 1971)

accounts for the presence of the fully wetted model in the tunnel by changing the flow calibration curve of the upstream venturi. Careful comparison of the data for propellers 3767 and 3768 in the open-jet tunnel shows that the larger propeller has a slightly lower K_T, an effect that becomes less pronounced as J decreases into the fully cavitating range of fixed σ. The closed-jet data of (van de Voorde and Esvelt, 1962; see also Morgan, 1966; and Figure 13), show the slight trend of K_T to decrease with increasing geosym model size in a closed rectangular tunnel. There is a similar trend of K_Q; so that the wall effect trend on the efficiency can go in either direction. There was not sufficient experimental accuracy to determine which way, at least from this series of three

geometrically similar models. The data of Kruppa (1963) are more difficult to interpret. There are three different propeller sizes reported in the geosym series: 6 inch (15 cm), 8 inch (20 cm), and 10 inch (25 cm). In comparisons at the same J and σ, there appears to be a weak trend for K_T and K_Q to decrease very slightly with an increase in diameter from 6 inch to 8 inch as σ approaches low values of 0.25 (full cavitating). For the 10 inch model, the K_T and K_Q are consistently above the other results throughout the experimental range. This apparent discrepency may be resolved by noting that this experiment was carried out in a water channel (60 cm X 60 cm) with one free surface, and not in a closed tunnel. Further experiments have confirmed the trend toward larger K_T and K_Q versus J in this type of facility, on an 11.4 inch (29 cm) propeller.

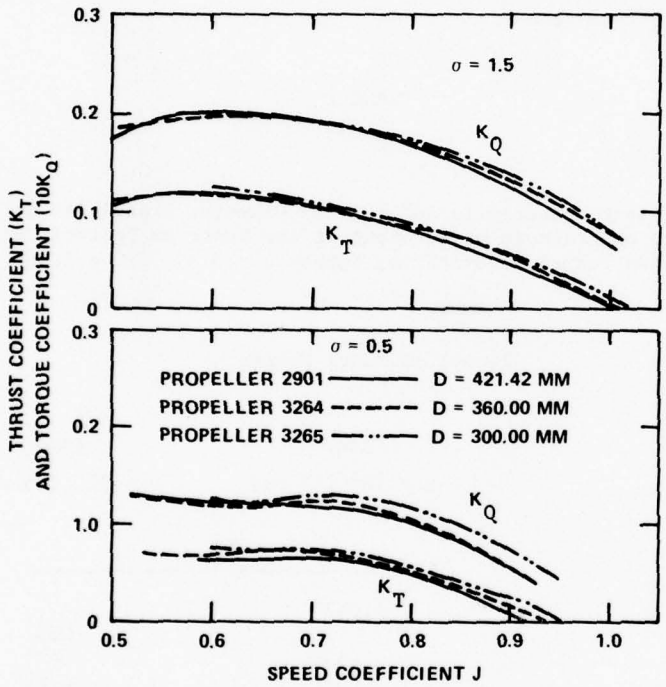

Figure 13 – Comparison of Test Results on Similar Propellers of Different Diameters in the NSMB 90 CM x 90 CM Tunnel
(From Morgan, 1966)

Later work at NSRDC resulted in the construction of a third geosym model of the propeller number 3767. This was denoted propeller number 4000, of 22 inch (56 cm) diameter (McDonald and Hecker, 1969). Compared with performance of propeller 3767 in the 36 inch (91 cm) water tunnel closed jet section, this larger model showed a further small decrease in K_T versus J, at constant σ, (see Table 1). There is a discussion by Morgan (1966) stating that the propeller 4000 may not have been a perfect geosym since the open water curves of it and model number

3767 (see McDonald and Hecker, 1969) differ slightly. The most likely manufacturing error would have been a pitch difference, which would not have affected the supercavitating result very much since such propellers are very insensitive to P/D (see Hecker, et al, 1967). Indeed the open water curves of models 3767 and 4000 at σ = 1.25 converge in the low J range where the flow was fully cavitating. Measurements indicate that the smaller propeller 3768 is a perfect geosym of propeller 3767 however. The comparison of propeller data for one model in open water and tunnel conditions shows a steady decrease from open water to open-jet tunnel to closed tunnel (see Figure 14), similar to the trend for two-dimensional hydrofoils found by Ota (1974). The wall effect on cavity size has not been systematically investigated for propellers, although the large model 4000 choked the closed-jet tunnel at a larger J = 0.8, at σ = 0.33, than the smaller model at the same σ.

TABLE 1

Thrust Coefficient Measured in 36" (91 cm) Diameter Closed Jet Section. Velocity Based on Pressure Measurement at the Upstream Venturi Calibrated for Unobstructed Tunnel. Cavitation Number σ = 0.33, P/D = 1.180

	Propeller Model Number	
	3767	4000
	D = 16" (41 cm)	D = 22" (56 cm)
J	K_T	
1.05	.013	
1.025		.026
1.00	.053	.047
.95	.081	.076
.9	.106	.101
.85	.117	.1165
.8	.128	.128
.75	.134	↓
.7	.149	choked

Unsteady wall effects on supercavitating propellers and blade edge flutter have not been investigated, nor has the presence of any natural cavity oscillations for this highly three-dimensional case.

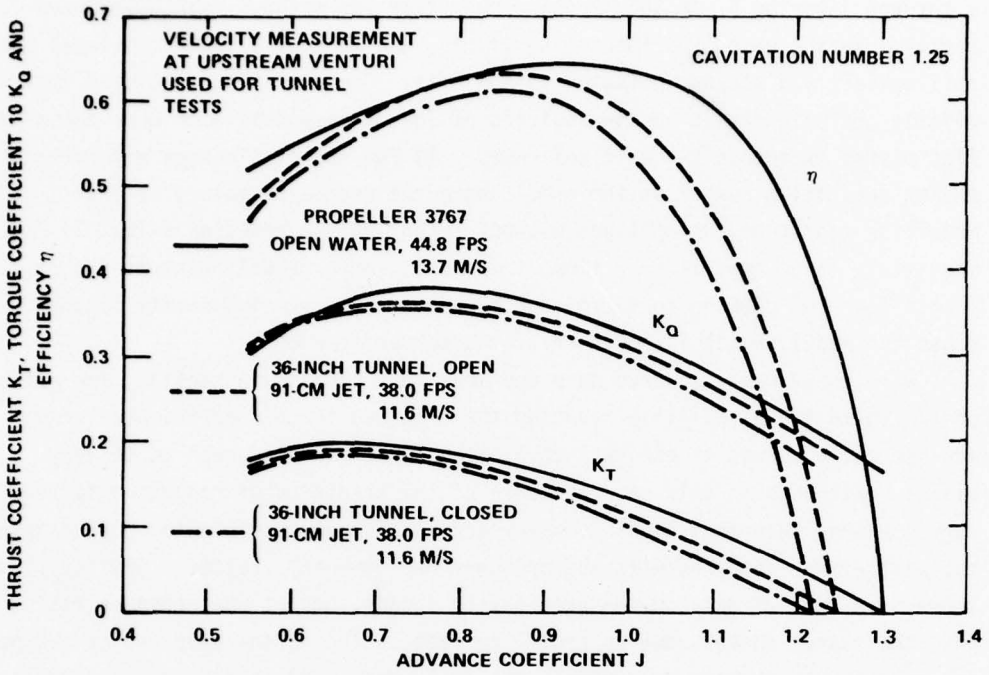

Figure 14 – Comparison of Open Water, Free-Jet Tunnel, and Closed Jet Tunnel Results for Propeller 3767
(From McDonald and Hecker, 1969)

CONCLUSIONS

Observers of tunnel experiments should beware of the effects of two other scaling parameters not mentioned here. These are the effect of a lowered Froude number, which seems to decrease C_L slightly at low σ and reduce the cavity size (Larock, et al 1966), and the effect of a lowered Weber number (surface tension parameter) which distorts the cavity shape (Oba and Matsudaira, 1974).

No disagreement has been found in this report with the original conclusions of Cohen and DiPrima (1958) and Morgan (1966) in previous surveys of fully cavitating tunnel wall effects. Namely, that the effect on force coefficients is a small decrease which may be comparable to the scatter in the force balance measurements; but the effect on the cavity length is a large increase near the choking condition which may confuse the model versus prototype correlation. This latter is very important in the design case, where accurate cavity location is crucial to obtaining high lift to drag ratios at low angles of attack.

The experiments using forced ventilation to simulate a low cavitation number (by raising P_c, the cavity pressure) in the tunnel show some unusual and

unexpected trends, sometimes contrary to the effects found by direct reduction of σ through lowering P_∞ in the tunnel. But these two methods have never been compared in the same experiment. Similarly, the lack of a two-dimensional geosym foil series is a strange omission in the data. Overall it is concluded that wall effects are unimportant in the analysis of forces on models with more camber than flat plates except in two critical cases: 1) The tunnel blockage may raise the choked cavitation number on the model above the prototype value, so that modelling cannot be accomplished without resort to a correction rule. 2) Even moderately large tunnels of 5 times the model length greatly distort the cavity length near the choking condition and may change the crucial cavity clearance above the model, which is necessary for good performance.

When experiments are run on propellers in a closed-jet section, the effect of the solid tunnel walls in reducing the measured force coefficients versus advance ratio curves at constant cavitation number is also seen to be very slight. Although in this case, because of the tradition of reporting faired curves rather than individual measurements, it is not possible to comment on how the wall effect compares with the ordinary experimental scatter. Similarly, there is a lack of data on measured cavity length, and at what advance ratio, if any, the tunnel chokes, during propeller tests. Though the open-jet tunnel has the tendency to shorten or suppress the fully developed cavity on two-dimensional models this is not thought to be the reason for the failure to achieve full cavitation of the originally developed supercavitating propeller series (Hecker, et al 1964).

SUMMARY

Theoretical methods for the steady, two-dimensional wall effect are now well known, yet in the pure-drag case accurate nonlinear numerical results have been calculated only for the parallel plate and Riabouchinsky wake models, which are not regarded as the most accurate. Since the doubly connected mapping technique has been developed, the way is open for further calculations which could better discriminate among the available wake models in the two-dimensional case.

Additionally, it is conceivable that the Froude number effect could be included also. This has already been computed for the infinite stream case with open wake models (Larock, 1966; Oba, 1972). This would be meaningful since the tunnel Froude number ordinarily differs considerably from that of the prototype. A difficult theoretical problem exists however for the choked flow case, commonly encountered in two-dimensional water tunnels. A wake model would still be required for finite Froude number to rejoin the separated streamlines, each now

at a different flow speed, to the downstream condition.

In contrast to the hydrofoil case, the development of a wall effect modelling program for propellers would be premature at this time. Here the prediction programs for the propeller in infinite stream are still under development. A particularly difficult problem here is how to apply the cavity closure condition in three-dimensions, which would be exacerbated in the tunnel case because of the distorted cavity length.

Experimentally, the most difficult data to interpret are those for which forced ventilation was used in the closed-jet tunnel section. Careful calibration experiments will be necessary before it can be safely concluded that cavitation number scaling alone, even using the measured cavity pressure, correctly models those experiments in the water tunnel in which forced ventilation is used. It may turn out that two independent parameters are required - both cavitation number σ and ventilation coefficient K_v. The scale size effect on ventilation air demand itself, without the presence of walls, is only partially understood.

The experimental results for the forces on hydrofoil models in the closed tunnel agree quite well with the theory when the cavity is long and the separation points are fixed. But the prediction of the minimum fully cavitating angle of attack, which determines the lift to drag ratio, is still spotty. In this regard, more emphasis is needed on measuring the length and position of the cavity. The unique feature of the tunnel wall effect is that the large changes occur not on the force coefficients but on the particle paths.

REFERENCES

1. Acosta, A.J. and O. Furuya, "A Note on Three-Dimensional Supercavitating Hydrofoils," Journal of Ship Research, Vol. 19, No. 3 (Sep 1975).

2. Ai, D.K. and Z.L. Harrison, "Wall Effects in Cavity Flow," California Institute of Technology Hydrodynamics Laboratory Report 111.3 (Apr 1965) ; see also Journal of Basic Engineering, Transactions American Society of Mechanical Engineers (ASME), Series D, Vol. 88, pp. 132-138 (Mar 1966).

3. Auslaender, J., "Low Drag Supercavitating Hydrofoil Sections," Hydronautics, Inc., Technical Report TR 001-7 (Apr 1962); see also TR 001-5.

4. Baker, E.S., "Analytical Prediction of Wall Effect on Fully Cavitating Lifting Foils, Using Nonlinear Theory," NSRDC Report 3688 (Nov 1972).

5. Bate, E.R., "A Preliminary Study of the Effect of the Free Surface on a Three-Dimensional Cavity Produced by a Circular Disk," California Institute of

Technology, Hydrodynamics Laboratory Report E-118.15 (Mar 1964).

6. Besch, P.K., "Flutter and Cavity-Induced Oscillation of a Two-Dimensional Cavitating Flow," NSRDC Report 3000, AD 690-096 (Apr 1969).

7. Birkhoff, G. et al, "Wall Effects in Cavity Flow, I and II," Quarterly Journal of Applied Mathematics, Part I: Vol. 8, No. 2, pp. 151-168 (1950), Part II: Vol. 9, No. 4, pp. 413-421 (1952).

8. Borodachev, N.M. and F.N. Borodacheva, "Ob Uchete Vliyaniya Stenok Pri Udare Kruglogo Diska o Zhid Kost", Inzheneryi Zhurnal, Mekhanika Tverdogo Tela, No. 1, pp. 177-82 (Jan, Feb 1967).

9. Brennen, C., "A Numerical Solution of Axisymmetric Cavity Flows, Parts 1 and 2," National Physical Lab, Teddington, Ship Division Report 114 (Jul 1968).

10. Brennen, C., "Numerical Solution of Axisymmetric Cavity Flows," Journal of Fluid Mechanics, Vol. 37, Part 4, pp. 67188 (Jul 1969).

11. Cieslowski, D.S., and J.H. Pattison, "Unsteady Hydrodynamic Loads and Flutter of Two-Dimensional Hydrofoils," Society of Naval Architects and Marine Engineers, Spring Meeting Hydrofoil Symposium, Paper 2-b (May 1965).

12. Cisotti, U., "Idromeccanica Piana," Libreria Editrice Politecnica, Milano, Vol. II, pp. 263-268, 298 (1922).

13. Cohen, H., and R.C. DiPrima, "Wall Effects in Cavitating Flows," Proceedings of the Second Office of Naval Research Symposium Naval Hydrodynamics, ACR-38, pp. 367-390 (Aug 1958).

14. Cohen H., and R. Gilbert, "Two-Dimensional Steady, Cavity Flow About Slender Bodies in Channels of Finite Breadth," Journal of Applied Mechanics, Vol. 24, No. 2, pp. 170-176 (Jun 1957).

15. Cohen, H., et al, "Wall Effects in Cavitating Hydrofoil Flow," Journal of Ship Research, Vol. 3, No. 3, pp. 31-40 (1957).

16. Davies, T.V., "Steady Two-Dimensional Cavity Flow Past an Aerofoil Using Linearized Theory," Quarterly Journal of Mechanics and Applied Mathematics, Vol. 23, Part 1 (Feb 1970).

17. Dobay, G.F. and N.L. Ficken, "Supercavitating and Ventilated Performance of Three Hydrofoil Sections," NSRDC Report 1828 (Jan 1964).

18. Dobay, G.F. and E.S. Baker, "Special Problems in the Design of Supercavitating Hydrofoils," AIAA/SNAME Second Advanced Marine Vehicles Conference, AIAA Paper 74-309 (Feb 1974).

19. Dobay, G.F., "Experimental Investigation of Wall Effect on Simple Cavity Flows," Proceedings, Symposium on Testing Techniques in Ship Cavitation Research, The Norwegian Ship Model Experiment Tank (Jun 1967).

20. Fabula, A.G., "Choked Flow About Vented or Cavitating Hydrofoils," Journal of Basic Engineering, Transactions American Society of Mechanical Engineers (ASME), Series D, Vol. 86, No. 3, pp. 561-568 (Sep 1964).

21. Fisher, B.F. and E.S. Baker, "Comparison of Experimental Data with Analytical Prediction (Including Wall Effect) for Three Supercavitating Hydrofoils," DTNSRDC, Ship Performance Departmental Report SPD-751-01 (Jul 1977).

22. Gurevich, M.I., "Symmetrical Cavitation Flow Around a Flat Plate Situated Between Parallel Walls," Bulletin of the Academy of Sciences, USSR (IZV Akad. Nauk. SSSR, Div. Technical Sciences) No. 4 (1946).

23. Hecker, R. and J.G. Peck, "Experimental Performance of TMB Supercavitating Propellers 3767, 3768, 3769, 3770, 3785, and 3820," DTNSRDC Hydromechanics Laboratory, Test Evaluation Report, No. 1553 (Aug 1961).

24. Hecker, R. et al, "Experimental Performance of TMB Supercavitating Propellers," NSRDC Report 1432 (Jan 1964).

25. Hecker, R. et al, "Experimental Performance of a Controllable-Pitch Supercavitating Propeller," NSRDC Report 1636 (Aug 1967).

26. Ho, H.T., "Linearized Theory for a Supercavitating Hydrofoil Operating in a Fluid of Finite Depth," Hydronautics, Inc., Report TR-119-7, AD 601-101 (Jun 1963).

27. Jeppson, R.W., "Finite Difference Solutions to Free Jet and Confined Cavity Flows Past Disks with Preliminary Analysis of the Results," Utah Water Research Laboratory, Utah State University, No. PRWG-76-1, AD 704-490 (Nov 1969).

28. Karlikov, V.P. and G.I. Sholomovich, "Metod Priblizhennogo Ucheta Vliyaniya Stenok Pri Kavitatsionnom Obtekanii Tel v Gidrodinamicheskikh Trubakh," Akademiya Nauk, Izvestiya, Mekhanika Zhidkosti i Gaxa, No. 4, pp. 89-93 (Jul-Aug 1966).

29. Kermeen, R. W., "Experimental Investigations of Three-Dimensional Effects on Cavitating Hydrofoils, " Journal of Ship Research, Vol. 5, No. 2, pp. 22-43 (Sep 1961); see also California Institute of Technology Report 47-14 (Sep 1960).

30. Kim, J.H., "Analysis of Unsteady Cavity in Internal Flows," ASME, 1972 Polyphase Flow Forum, Fluids Engineering Conference, San Francisco, California, pp. 25-26 (Mar 26-30, 1972).

31. Klose, G.J. and A.J. Acosta, "Some New Measurements on the Drag of Cavitating Disks," California Institute of Technology, Hydro. Lab. Report E-118.27 (Nov 1964).

32. Kruppa, C.F., "Axial Flow Cavitation Tests with Three Geosym High Speed Propellers," Tenth International Towing Tank Conference, London (1963).

33. Lang, T.G., D.A. Daybell and K.E. Smith, "Water-Tunnel Tests of Hydrofoils with Forced Ventilation," NAVORD Report 7005, NOTS TP 2363, ASTIA, AD 250-220 (Nov 1959); see also Journal of Ship Research, Vol. 5, pg. 1 (1961).

34. Larock, B.E. and R.L. Street, "A Nonlinear Theory for Fully Cavitating Flows Past an Inclined Flat Plate," Stanford Univ., Dept. of Civil Engineering, Technical Report No. 64 (Jun 1966).

35. Lazariv, V.A., "Cavitating Flow of Finite Width Jet Past a Flat Plate," IZV. AN SSSR Mekhanika Zhid Kosti i Gaza, Vol. 5, No. 1, pp. 127-133 (1970).

36. Maixner, M., Ocean Engineers Thesis, M.I.T., to be published 1977; see also presentation at ATTC (Aug 1977).

37. McDonald, N.A. and R. Hecker, "Water Tunnel Testing for Supercavitating Propellers - Measuring Velocity," NSRDC Report 3029, AD 700-692 (1969).

38. Morgan, W.B., "The Testing of Hydrofoils and Propellers for Fully Cavitating or Ventilated Operation," Proceedings of the 11th International Towing Tank Conference, Tokyo, Japan, pp. 202-216 (1966).

39. Oba, R., "A Study on Finite Cavity Supercavitating Blocked Flow," Institute of High Speed Mechanics, Tohoku Univ., Vol. 20, Report N . 208 (1968); in European language.

40. Oba, R. "Gravity Effects on Supercavitating Flow," Institute of High Speed Mechanics, Tohoku Univ., Vol. 25, Report No. 247 (1972).

41. Oba, R. and Y. Matsudaira, "Effects of Surface Tension on Supercavitating Foil Performance," Institute of High Speed Mechanics, Tohoku Univ., Vol. 29, Report No. 268 (1974).

42. Ota, T., "Comparison of Wall Effects on Cavitating Hydrofoils in Three Water Tunnels," Zeitschrift fuer Flugwissenschaften, Vol. 22, No. 6, pp. 201-206 (Jun 1974).

43. Ota, T., "A Separated and Reattached Flow on a Blunt Flat Plate in a Tunnel," Quarterly Journal of Mechanics, Applied Math., Vol. 27, No. 3, pp. 379-386 (Aug 1974).

44. Parkhomovski, S.I., "Impact of a Wedge in Bounded Flow with Symmetric Cavitation," Izv. Vyssh. Uchebn. Zavedenii, Mat., Vol. 6, pp. 215-225 (1958).

45. Parkin, B.R., "Experiments on Circular Arc and Flat Plat Hydrofoils in Noncavitating and Full Cavity Flows," Hydrodynamics Laboratory, C.I.T., Report HL 47-6 (1956); see also Journel of Ship Research, Vol. 1, No. 4 (1958).

46. Parkin, B.R., "Linearized Theory of Cavity Flow in Two Dimensions," Rand Corp., Physics Div., Report P-1745 (Jul 1959).

47. Popp, S., " Theoretical Investigations and Numerical Evaluations of Wall Effects in Cavity Flows," ASME Symposium on Cavity Flows, Minneapolis (May 5-7, 1975), ed. B. Parkin and W.B. Morgan.

48. Reichardt, H., "The Laws of Cavitation Bubbles at Axially Symmetrical Bodies in a Flow," Kaiser Wilhelm Institut fur Strommungsforschung, Gottingen (25 Oct 1945); (Reports and Translation No. 766, Ministry of Aircraft Production (15 Aug 1946), ONR No. MAP-UG69-T.

49. Roman, V.M., "Calculation of Supercavitated Flow Past Slender Profiles in a Finite Flow," Fluid Mechanics - Soviet Research, Vol. 1, No. 5, pp. 38-47 (Sep-Oct 1972).

50. Schot, S.H., "The Hydrofoil with Finite Cavity in a Solid Wall Channel," Journal of Ship Research, Vol. 15, No. 2 (Jun 1971).

51. Shair, F.H. et al, "The Effect of Confining Walls on the Stability of the Steady Wake Behind a Circular Cylinder," Journal of Fluid Mechanics, Vol. 17, pp. 546-550 (1963).

52. Shal'nev, K.K., "The Effect of Flow Boundaries Upon Cavity Flow Around a Cylinder, Zhurnal Prikladnoy Mekhaniki: Tekhnicheskoy Fiziki, No. 3, Foreign Technology Div., FTD-TT-65-1813, AD 626-973 (Jan 1966).

53. Song, C.S. and F.Y. Tsai, "Unsteady, Symmetrical, Supercavitating Flows Past a

Thin Wedge in a Solid Wall Channel," University of Minnesota, St. Anthony Falls Hydraulic Lab., Technical Paper No. 38, Series B, pp. 1-24 (1962).

54. Song, C.S. and J. Almo, "Experimental Study of Hydroelastic Instability of Supercavitating Hydrofoils," University of Minnesota, St. Anthony Falls Hydraulic Lab., Project Report No. 89 (Feb 1967).

55. Song, C.S., "Flutter of Supercavitating Hydrofoils - Comparison of Theory and Experiment," Journal of Ship Research, Vol. 16, No. 3 (Sep 1972).

56. Tsen, L.F. and Guilbaud, " A Theoretical and Experimental Study on the Planform of Superventilated Wings," Journal of Ship Research, Vol. 18, No. 3 (Sep 1974).

57. Tulin, M.P., "Supercavitating Propellers - History, Operating Characteristics, Mechanism of Operation," Fourth Office of Naval Research (ONR) Symposium on Naval Hydrodynamics, ACR-92, pg. 267 (Aug 1962).

58. Unruh, J.F. and R.L. Bass III, "Doublet Lattice-Source Method for Calculating Unsteady Loads on Cavitating Hydrofoils," Journal of Hydronautics, Vol. 8, No. 4 (Oct 1974).

59. Valcovici, V. "Uber discontinuierliche Flussigkeitsbewegungen mit zwei freien Strahlen, Thesis, Gottingen (1913).

60. van de Voorde, C.B. and J. Esveldt, "Tunnel Tests on Supercavitating Propellers," International Shipbuilding Progress, Vol. 9, No. 99, pp. 449-463 (Nov 1962); see also 4th ONR Symposium on Naval Hydrodynamics, pg. 312 (1962).

61. Whitney, A.K., "A Simple Correction Rule for Wall Effect in Two-Dimensional Cavity Flow," ASME, Cavitation State of Knowledge, New York (1969).

62. Whitney, A.K. et al, "Experimental Verification of Cavity-Flow Wall Effects and Correction Rules," C.I.T. Report E-97A-18, AD 717-393 (Nov 1970).

63. Wu, T.Y., " A Free Streamline Theory for Two-Dimensional Fully Cavitated Hydrofoils," C.I.T., Hydrodynamics Lab. Report HL 21-17 (Jul 1955).

64. Wu, T.Y., " A Wake Model for Free-Streamline Flow Theory. Part 1, Fully and Partially Developed Wake Flows and Cavity Flows Past an Oblique Flat Plate," Journal of Fluid Mechanics, Vol. 13, Part 2, pp. 161-218 (1962).

65. Wu, T.Y. et al, "Wall Effects in Cavity Flows," C.I.T. Report E-111A.5, AD 694-037 (Apr 1969).

66. Wu, T.Y. et al, "Wall Effects in Cavity Flows and Their Correction Rules," International Union Theoretical and Applied Mechanics Symposium on Non-Steady Flow of Water at High Speeds, Leningrad (Jun 1971).

67. Yefremov, I.E., "Effect of Water Tunnel Walls on Supercavitated Flow Past Profiles, Fluid Mechanics - Soviet Research, Vol. 1, No. 4 (Jul-Aug 1972).

68. Young, J.O., "Effects of Cavitation on Periodic Wakes Behind Symmetric Wedges," Ordinance Research Lab., Technical Memorandum TM 508.2451-02 (Feb 1965).

BIBLIOGRAPHY

1. Ai, D.K. et al, "Linearized Theory of a Two-Dimensional Planing Flat Plate in a Channel of Finite Depth - I," C.I.T., Hydro. Lab. Report E-110.2, AD 602-201 (Apr 1964).

2. Ai, D.K., "The Wall Effect in Cavity Flow," American Society of Mechanical Engineers, Fluids Eng. Conf., Paper No. 65-FE-13, Wash., DC. (Jun 1965); see also ASME J. of Basic Eng., Vol. 88, Series D, pg. 132-138.

3. Arakeri, V.H., "Water Tunnel Investigations of Scale Slender Bodies and Characteristics of Flow Past a Bi-Convex Hydrofoil," C.I.T., Div. of Eng. and Applied Science Report E-79A.12, AD 718-364 (Jan 1971).

4. Armstrong, A.H. and K.G. Tadman, "Wall Corrections to Cavities in Closed Jet and Open Jet Axially Symmetric Tunnels," Armament Research Establishment, Memo No. 3/52, presented at the Ninth Underwater Ballistic Conf., sponsored by ONR (9-11 Jul 1952).

5. Armstrong, A.H. and K.G. Tadman, "Wall Corrections to Axially Symmetric Cavities in Circular Tunnels and Jets," Armament Research Establishment Report No. 7/52 (Mar 1953).

6. Barr, R.A., "An Investigation of the Cavity Flow Behind Drag Discs and Supercavitating Propellers," M.S. Thesis, Univ. of Md. (1966).

7. Billet, M.L. et al, "Geometric Description of Developed Cavities on Zero and Quarter Caliber Ogive Bodies," Penn. State Univ., Applied Research Lab., Report TM-74-136 (May 1974).

8. Birkhoff, G. and E.H. Zarantonello, "Jets, Wakes, and Cavities," Academic Press, N.Y., pg. 39, pg. 116 (1957).

9. Birkhoff, G.B., "Hydrodynamics - A Study in Logic, Fact, and Similitude," Second Edition, Princeton Univ. Press, Princeton, N.J., Ch. III, Sec. 40, "Wall Corrections," pg.57 (1960).

10. Brennen, C., "Numerical Solution of Axisymmetric Cavity Flows," J. of Fluid Mechanics, Vol. 37, Part 4, pp. 671-88 (July 1969).

11. Cambell, I.J. and G.E. Thomas, "Water Tunnel Boundary Effects on Axially Symmetric Fully Developed Cavities," Admiralty Res. Lab., RI/G/HY/18/1 (1956).

12. Chandrasekhara, D.V. and B.C. Syamala Rao, "Effect of Pressure on the Length of Cavity and Cavitation Damage behind Circular Cylinders in a Venturi," Paper No. 27-WA/FE-6, J. of Fluids Eng., Trans ASME, Vol. 95, Series I, No. 2, pp. 197-206 (Jun 1973).

13. Chaplygin, Y.S., "Planing on a Fluid of Finite Depth," Prikl. Mat. Mekn., Vol. 5, No. 2 (1941).

14. Chen, C.F., "Feasibility Study of Supercavitating Propellers in Kort Nozzles, Phase I," Hydronautics, Inc., Technical Report TR 005-1 (Dec 1960).

15. Chen, C.F., "Final Report on the Feasibility Study of Supercavitating Propellers in Kort Nozzles," Hydronautics, Inc., Technical Report TR 005-5 (Sep 1961).

16. Chen, C.F., "Shrouded Supercavitating Propellers," Fourth Symposium on Naval Hydro. (ONR), Wash. D.C., ACR-92 (Aug 1962).

17. Cisotti, U., "Sul Moto di un Solido in un Canale," Rendiconti del Circolo Matematico di Palermo, Vol. 28, No. 9, pp. 307-352 (1909).

18. Cohen, H. and R.C. DiPrima, "Wall Effects in Cavitating Flows," ONR Second Symposium on Naval Hydro., ACR-38, pp. 367-390 (Aug 1958).

19. Cohen, H. and Y.O. Tu, "A Comparison of Wall Effects on Supercavitating Flows Past Symmetric Bodies in Solid Wall Channels and Jets," Proc. IX Int. Cong. of Applied Mech., Brussels, pp. 359-379 (1956).

20. Dinh, N.N., "Some Experiments on a Supercavitating Plane Hydrofoil with Jet-Flap," J. of Ship Research, Vol. 13, No. 3, pg. 207-219, AD 697-348 (Sep 1969).

21. Efremrv, I.I. and V.M. Roman, "Calculation of Supercavitational Flow Past Slender Profiles in Proximity to the Separation Boundary," J. of Appl. Mech. and Tech. Physics, Vol. 10, No. 3, pp. 390-5 (May-Jun 1969).

22. Eisenberg, P. and H.L. Pond, "Water Tunnel Investigations of Steady State Cavities," DTMB Report 668 (1948).

23. Epshtein, L.A., "About Minimum Number of Cavitations and Width of Cavern in a Flat and Axially Symmetric Channels," Foreign Tech. Div., Wright-Patterson AFB, Ohio, Report No. FTD-HT-23-748-67, translation from Akademiya Nauk SSSR. Izvestiya, Mekhankika Zhid Kosti i Gaza, No. 5, pp. 78-81, AD 676-176 (Sep-Oct 1966).

24. Epshtein L.A., "Approximate Calculation of the Effect of the Walls on a Model of a Cavity," J. of Fluid Dyn., Vol. 10, No. 6 (Dec 1976).

25. Ericson, D.M. Jr., "Observations and Analyses of Cavitating Flow in Venturi Systems," Ph.D. Thesis, Univ. of Mich., Dept. Mech. Eng. (Jul 1969).

26. Fage, A., " On the Two-Dimensional Flow Past a Body of Symmetrical Cross Section Mounted in a Channel of Finite Breadth," Report and Memoranda, No. 1223 (1929).

27. Furness, R.A. and S.P. Hutton, "Experimental and Theoretical Studies on Two-Dimensional Fixed-Type Cavities," ASME Symposium on Cavity Flows, Minneapolis (5-7 May 1975); ed. B.R. Parkin and W.B. Morgan.

28. Furness, R.A. and S.P. Hutton, "Experimental and Theoretical Studies of Two-Dimensional Fixed-Type Cavities," J. Fluids Eng., Trans ASME, Series I, Vol. 97, No. 4, pp. 515-522 (Dec 1975).

29. Furuya, O., "Nonlinear Calculation of Arbitrarily Shaped Supercavitating Hydrofoils Near a Free Surface," J. of Fluid Mech., Vol. 68, No. 1, pp. 21-40 (Mar 1975).

30. Furuya, O., "Three-Dimensional Theory on Supercavitating Hydrofoils Near a Free Surface," J. of Fluid Mech., Vol. 71, Part 2 (Sep 1975).

31. Gadd, G.E. and S. Grant, "Some Experiments on Cavities Behind Disks," J. of Fluid Mech., Vol. 23, Part 4, pp. 645-656 (1965).

32. Green, A.E., "The Gliding of a Plate on a Stream of Finite Depth,"

Proceedings Cambridge Philosophical Society, Part I, Vol. 31, No. 4, pp. 584-603 (1935); Part II, Vol. 32, pp. 67-85 (1936).

33. Guerst, H.A., "Linearized Theory of Two-Dimensional Cavity Flows," Doctoral Dissertation, Technical Univ. of Delft, The Netherlands (1961).

34. Gurevich, M.I., "Soprotivleniye Tsilindra i Klina Pri Malykh Chislakh Kavitatsii," Tr. Mosk. In-ta Rybn. Promyshl i Khoz, No. 5 (1953).

35. Gurevich, M.I., "Theory of Jets in Ideal Fluids," translated by R.L. Street and K. Zagwstin, Academic Press, N.Y., pg. 261ff, pg. 323 (1965).

36. Gurevich, M.I., Proceedings A.I. Mikoyan, Moscow Tech. Inst. of Fis., Ind. Econ.V (1953).

37. Hashimoto, H., "Progressive Waves on Swirling Cavity Flow in a Circular Pipe," Inst. of High Speed Mech., Tohoku Univ., Report No. 223, Vol. 22, pp. 137-159 (1970).

38. Hsu, Y.K., "A Brief Review of Supercavitating Hydrofoils," J. of Hydro., Vol. 2, No. 4 (Oct 1968).

39. Huse, E., "Cavitation Induced Hull Pressures, Some Recent Developments of Model Testing Techniques," Norwegian Maritime Research, Vol. 3, No. 2, pp. 24-40 (1975).

40. Jeppson, R.W., "Techniques for Solving Free-Streamline, Cavity, Jet, and Seepage Problems by Finite Differences," Stanford Univ., Dept. of Civil Eng., Tech. Report No. 68 (Sep 1966).

41. Kaplan, P. and A. Lehman, "An Experimental Study of Hydroelastic Instabilities of Finite Span Hydrofoils Under Cavitating Conditions," Joseph Nunn and Associates, Pasadena Calif., Report 6412, AD 603-265 (Feb 1964).

42. Khaskind, M.D., "The Plane Problem of Planing on the Surface of a Heavy Fluid of Finite Depth," Izv. Akad. Nauk. SSSR, Otd. Tekhn. Nauk, No. 1-2 (1943).

43. Kiceniuk, T. and A.J. Acosta, "Experiments on Gravity Effects in Supercavitating Flow," J. of Ship Research, Vol. 10, No. 2, pp. 119-21 (Jun 1966).

44. Kida, T. and Y. Miyai, "Wall Effect in Cavitating Flow Past a Thin Jet-Flapped Foil," Quarterly J. of Mech. and Applied Math., Vol. 25, Part I, pp. 83-104 (Feb 1972).

45. Kida, T. and Y. Miyai, "Lift Coefficients on a Supercavitating Jet-Flapped Foil Between Rigid Walls," Bulletin of the Japan Society Mech. Eng. , Vol 18, No. 116, pp. 151-158 (Feb 1975).

46. Kim, J.H., "The Wall Effect for Unsteady, Choked Supercavitating Flow," C.I.T., Div. of Eng. and Applied Science, Report E-79.A13, AD 718-816 (Jan 1971); see also J. of Ship Research, Vol. 16, No. 4 (Dec 1972).

47. Kim, J.H., "A Note on the Unsteady Cavity Flow in a Tunnel," J. of Fluids Eng., Trans. ASME (Mar 1974).

48. Kinoshita, M. and J. Shinoda, "Uber den Wandeinfluss auf das Flugel profil mit einer vollig ausgebildeter Kavitation, Der erste Bericht," Pub. Special

Paper Meeting of the Society of Naval Architects of Japan (Apr 1944).

49. Koiter, W.T., "Some General Theorems on Doubly-Periodic and Quasi-Periodic Functions," Proc. Kon. Nederi. Akad. Wetensch., Amsterdam, Vol. A62, No. 2, pp. 120-28 (1959).

50. Kruppa, C.F., "High Speed Propellers - Hydrodynamic and Design," Univ. of Mich., Dept. Nav. Arch. and Mar. Eng., Report 035 (Sep 1969).

51. Lammeren, W.P., "Testing Screw Propellers in a Cavitation Tunnel with Controllable Velocity Distribution Over the Screw Disc," International Shipbuilding Progress, Vol. 2, No. 16 (1955).

52. Landweber, L., "A Note on Blockage Effect," Van Lammeren Memorial Volume, pp. 49-51, Iowa Inst. Hydraulic Research Reprint 277, AD 727-415 (1970).

53. Lerbs, H., "Untersuchung der Kavitation an Schraubenpropellern," Hamburgische Schiffbau Versuchsanstalt, Report 131 (1936); DTMB Translation 46 (1937).

54. Meijer, M.C., "Some Experiments on Partly Cavitating Hydrofoils," International Shipbuilding Progress, Rotterdam, Vol. 6, No. 60, pp. 361-368 (1959).

55. Meijer, M.C., "Pressure Measurement on Flapped Hydrofoils in Cavity Flows and Wake Flows," C.I.T. Report E-133.2 (Oct 1965); see also J. of Ship Research, Vol. 11, No. 3, pp. 170-89 (Sep 1967).

56. Mendenhall, M.R. et al, "Theoretical Study of Ducted Propeller Blade Loading, Duct Stall, and Interference," Itek Corp., Palo Alto, Calif., Report Vidya-229, AD 646-022 (Sep 1966).

57. Michel, J.M. and A. Rowe, "The Influence of the Cavitation Number on the Behaviour of a Base-Vented Hydrofoil Beneath a Free Surface," Comptes Rendus Hebdom. des Seances de l'Acad. des Sciences, Series A, Sci. Math Vol. 280, No. 16 (Apr 1975).

58. Mogel, T.R. and R.L. Street, "A Numerical Method for Steady-State Cavity Flows," Stanford Univ. Dept. of Civil Eng., Report TR-155, AD 745-346 (Feb 1972).

59. Morgan, W.B., "The Testing of Hydrofoils and Propellers for Fully Cavitating or Ventilated Operation," Proceedings of 12th ITTC, Rome, Italy (1969).

60. Nelka, J.J., "Induced Field-Point Pressures of a Ducted Propeller System," NSRDC Report 4270 (Oct 1974).

61. Nishiyama T. and T. Ota, "Potential Flow Models of Cavity Termination for a Base-Vented Hydrofoil," Trans. Japan Society of Mech. Eng., Vol. 36, pp. 1851-1857 (1969).

62. Oba, R., "Theory of Wall Effects Upon Performance of Supercavitating Hydrofoil," Inst. of High-Speed Mech., Tohoku Univ., Vol 15, Report 145 (1962); see also proceedings of 1962 International Assoc. of Hydraulic Res., Sym. on Cavitation and Hydraulic Machinery, Sendai, Japan, pg. 167.

63. Oba, R., "Method to Remove Wall Effects on Supercavitating Flow - Slotted Wall Tunnel," Facilities and Techniques, pp. 95-100 (18-20 May 1964); see also Inst. of High-Speed Mech., Tohoku Univ., Vol. 16, No. 152 (1964).

64. Oba, R., "A Method to Remove the Wall Effects on Supercavitating Flow," (2nd report theoretical study on expanding wall tunnel), 41st National Meeting of the Japan Society of Mech. Eng. (Oct 8, 1963); see also Tohoku Univ. Inst. of High-Speed Mech., Report No. 162, Vol. 17, pp. 23-42 (1965, 1966).

65. Oba, R. and J. Higuchi, "Theory of Wall Effects Upon Performance of Supercavitating Hydrofoil," Inst. of High-Speed Mech.,Tohoku Univ., Vol. 22, No. 217 (1970).

66. Ota, T., "A Cavitating Hydrofoil in a Solid Wall Tunnel," Zeitschrift Fur Angewandte Mathematik Und Mechanik, Vol. 55, No. 5, pp. 227-233 (May 1975).

67. Parkin, B.R. and R.W. Kermeen, "Water Tunnel Techniques for Force Measurements on Cavitating Hydrofoils," J. of Ship Research, Vol. 1, No. 1 (Apr 1957).

68. Peck, J.G., "Tunnel Hull Cavitation and Propeller Induced Pressure Investigation," NSRDC, Ship Perf. Dept. Report SPD-597-01 (Nov 1974).

69. Pope, A., "Wind Tunnel Testing," Second Edition, John Wiley & Sons, N.Y. (1954).

70. Popp, S., "Roshko's Model in a Channel," Revue Roumaine de Mathématiques Pures et Appliquées, Vol. 14, No. 9, pp. 1340-1350 (1969).

71. Popp, S., "Corrections de Compressibilité dans le Problème de Cisotti-Villat," Comptes Rendus de L'Académie de Sciences de Paris, Vol. 270, pp. 1045-1047 (1970).

72. Popp, S., "Numerical Analysis in Problems of Flows with a Discontinuity Surface," Studii si Cercetari Matematice, Vol. 27, No. 3, pp. 345-357 (1975).

73. Reichardt, H. and W. Sattler, "Three-Component Measurements on Rectangular Wings with Cavitation," Max-Plank Institut fur Stromungsforschung, Gottingen (Mar 1967).

74. Rojdestvenskii, K., "High Aspect Ratio Surfaces Planing on the Free Boundary of a Finite Depth Fluid Domain," (in French), Journale de Mechanique, Vol. 14, No. 5, pp. 793-821 (1975).

75. Rowe, A. and J.M. Michel, "Two-Dimensional Base-Vented Hydrofoils Near a Free Surface: Influence of the Ventilation Numbers," J. of Fluids Eng., Trans. ASME, Series I, Vol. 97, No. 4, pp. 465-474 (Dec 1975); see also Comptes Rendus Hebdomedaires de Seances de l'Académie des Sciences, Series A, Sciences Mathématiques Vol. 280, No. 16 (Apr 1975).

76. Sedov, L.I., "Two-Dimensional Problems in Hydrodynamic and Aerodynamics," Trans. by C.K. Chu, H. Cohen and B. Seckler, Interscience Publishers, John Wiley & Sons, N.Y., pg. 212, pg. 275 (1965).

77. Shen, Y.T., "Wall Effects on Propeller Performance," NSRDC Ship Perf. Dept. Report SPD-666-01 (Mar 1976).

78. Silberman, E., "Experimental Studies of Supercavitating Flow about Simple Two-Dimensional Bodies in a Jet," J. of Fluid Mech., Vol. 5, pp. 337 (1959).

79. Simmons, N., "The Geometry of Liquid Cavities With Especial Reference to the Effects of Finite Extent of the Stream," Ministry of Supply, A.D.E., Report 17/48 (1948).

80. Song, C.S., "Measurements of the Unsteady Force on Cavitating Hydrofoils in a Free Jet," Univ. of Minn., St. Anthony Falls Hydraulic Lab., Tech. Paper No. 49, Series B (Jun 1964).

81. Stefan, H.G. and A.G. Anderson, "Cavity Formation and Associated Drag in Supercavitating Flow over Wedges in Boundary Layer," Minnesota Univ., St. Anthony Falls. Hydraulic Lab., Project Report 69 (Apr 1964).

82. Terentev, A.G., "Bounded Jet Flow Past a Thin Profile," Izv. Ak. Nauk. SSSR, Mekh. Zhid i Gaza, No. 2 (Mar-Apr 1972).

83. Troshin, V.I., Izvestija Akademii Nauk SSSR, O.T.N., Vol. 4, pp. 167-170 (1960).

84. Tsakonas, S. et al, "Propeller-Duct Interaction Due to Loading and Thickness Effects," Stevens Inst. of Tech., Davidson Lab., SIT-DL-75-1722 (Apr 1975).

85. Tulin, M.P., "Supercavitating Propellers - Momentum Theory," J. of Ship Research, Vol. 9, No. 3, pp. 153-169 (Dec 1965).

86. van de Voorde, C.B., "On Experiences with Strut Supporting System for Testing Two-Dimensional Fully Cavitating Hydrofoils in Cavitation Tunnel," ASME - Sym. on Cavitation Research Facilities and Techniques, pp. 88-94 (18-20 May 1964); see also International Shipbuilding Progress, Vol. 11, No. 118, pp. 269-75 (Jun 1964).

87. Villat, H., "Sur le Mouvement (à la Helmholtz) d'un Liquide Dans un Canal Symètrique," Bulletin de la Société Mathématique de France, Vol. 40, pp. 266-304 (1912).

88. Wade, R.B. and A.J. Acosta, "Experimental Observations on the Flow Past a Plano-Convex Hydrofoil," C.I.T. Hydro. Lab. Report E-79.8, AD 623-711 (Feb 1965); see also J. of Eng. for Power, pg. 1-10, pg.165.

89. Waid, R., "Water Tunnel Investigations of Two-Dimensional Cavities,"C.I.T. Hydro. Lab. Report E-73.6 (1957).

90. Wade, R., "Water Tunnel Observations on the Flow Past a Plane-Convex Hydrofoil," C.I.T. Report E-79.6, AD 436-087 (1964).

91. Weir, D.S., "Effect of Velocity, Temperature, and Blockage on the Cavitation Number for a Developed Cavity," Cavitation and Polyphase Flow Forum, Proceeding Joint Meeting of Fluids Eng. Div. and Lubr. Div. of ASME, Minneapolis, Minn., pp. 7-9 (5-7 May 1975).

92. Whittaker, E.T. and G.N. Watson, "A Course of Modern Analysis," 4th Edition, Cambridge Univ. Press, pg. 433 (1969).

93. Woods, L., "Compressible Subsonic Flow in Two-Dimensional Channels with Mixed Boundary Conditions," Quarterly J. of Math. Mech., Vol. 7, pp. 263-282 (1954).

94. Wu, T.Y., "Inviscid Cavity and Wake Flows," Section 1.10, "Wall Effect," article in "Basic Developments in Fluid Dynamics," ed. M. Holt, Vol. 2, Academic Press, N.Y., pg. 67 (1968).

95. Wu, T.Y., "Cavity Flow Analysis - A Review of the State of Knowledge," ASME Fluids Eng. and Applied Mech. Conf., Cavitation State of Knowledge Papers, pg. 130, ed. J.M. Robertson and G.F. Wislicenu, (1969).

96. Wu, T.Y., "Cavity and Wake Flows," article in "Annual Review of Fluid Mechanics," ed. M. Van Dyke and W.G. Vincenti, Vol. 4, Annual Reviews Inc., Palo Alto, Calif., Sec. 6: "Wall Effects in Cavity Flows: A Critical Examination of Flow Models," pg. 267, AD 747-860 (1972).

97. Wu, T.Y., et al, "Cavity Flow Wall Effects and Correction Rule," J. of Fluid Mech., Vol. 49, Part 2, pp. 223-256 (1971).

98. Wyler, J.S., "Probe Blockage Effects in Free Jets and Closed Tunnels," Am. Society Mech. Eng., Paper No. 74-WA/PTC-5 (Nov 1974).

99. Zwick, W., "Nichtlineare Methode zur Berechnung des Einflusses der Kavitation auf die Umstroemung eines Tragfluegels," Deutsche Akademie der Wissenschaften zu Berlin-Monatsberichte, Vol. 7, No. 2, pp. 77-83 (1965).

SCALE EFFECTS IN MODELS WITH FORCED OR NATURAL VENTILATION NEAR THE FREE WATER SURFACE

by

R. S. ROTHBLUM
David W. Taylor Naval Ship Research and Development Center

For hydrofoils and struts piercing or operating near the free water surface, there exists the possibility of venting of atmospheric air into the low pressure regions on the strut or foil, known as ventilation. Ventilation may or may not be accidental. It is often desired to deliberately introduce a measured amount of air into the flow field around a strut or foil to affect the hydrodynamic forces in a controlled manner. This is usually described as airbleed or superventilation. Whether or not air is being deliberately introduced, when a cavity connected to the atmosphere is formed, there is generally an abrupt change in the forces on the submerged body. According to Dobay[1], the greatest cause of inconsistency of measurements on a supercavitating hydrofoil tested in different facilities was due to the unpredictable variation in the onset and degree of ventilation to the atmosphere. The importance of ventilation inception on nominallly fully wetted surface piercing struts and foils is now well known, the subject of two review papers[2,3] in the towing tank community. Recently, ventilation has been shown to affect significantly the forces on a surface piercing strut with air bleed.[4]

As discussed by Shen[3], the phenomenon of ventilation is complicated, and depends upon so many different scaling parameters that no model test facility could possibly satisfy all of the required similarity constraints simultaneously. Therefore, a thorough understanding of the physical mechanism affecting the various aspects of ventilated flow and ventilation inception is necessary in order to conduct rational model tests.

For the case of surface piercing struts and foils, the elements of the flow important to ventilation inception have been established as[5-16]

> A region of flow of low momentum as measured by an observer stationary with respect to the strut or foil. This condition may be satisfied by separation, vapor cavitation, or possibly by thickening of the boundary layer.
>
> A pressure in the low momentum region of less

than atmospheric.

A high momentum layer of liquid which isolates the low pressure, low momentum region from the atmosphere, called the surface seal.

It is probable but by no means confirmed that these same elements are important in in ventilation of fully submerged hydrofoils operating near the free surface. In the case of surface piercing or fully submerged lifting surfaces, the critical mechanism to identify is that which causes the breakdown of the surface seal, allowing air to be introduced to the low pressure, low momentum region. One possibility is that the surface seal may become unstable because of the downward acceleration caused by the high atmospheric pressure above and the low pressure region below.[17,18] (Taylor instabilities). A second possibility which has been identified is broaching of the tip vortices. Encounter with a sufficiently large ambient disturbance is a third. There are others[5], but enough have been named to emphasize the importance of identifying the breakdown mechanism expected at full scale. To illustrate, if breakdown of the surface seal were most likely due to encounter with ambient disturbances, then a test in which the model is towed through undisturbed water might be completely misleading. The absence of disturbances would result in an undesirable scale effect. This particular example was alluded to by Eames in a discussion which took place during the Second Office of Naval Research Symposium on Naval Hydrodynamics, in 1958, when he made the following statement:

> ...Experience in the full-scale operation of hydrofoil craft suggests that significant retardation of ventilation by the influence of the constant-pressure water surface can only be obtained under laboratory conditions. In open water even the smallest ripples appear to be sufficient to initiate ventilation at the water surface. This of course is an advantage to full-scale operation since ventilation proceeds smoothly as speed is increased. The explosive type of phenomenon which results when large negative pressures are supported in calm water and subsequently tripped by a small disturbance could represent a very dangerous situation for a hydrofoil craft....
>
> ...In an "ad hoc" search for the smallest effective fence we have found that on a particular section designed for uniform pressure distribution it is only necessary to extend the fence over the leading 50 percent of the chord...I would have expected most of the low energy paths to exist behind this, and therefore the success of the half-fences surprises me....

Besides illustrating the fact that the consequences of ventilation are generally underestimated by designers of high speed craft, Eames implicitly raised three issues of the utmost importance to the analysis of scale effects for the correct interpretation of laboratory studies for application to full scale.

Identification of the differences which have been observed between full scale and laboratory instances of ventilation phenomena.

Identification of the characteristics of the open water and full scale conditions and environment which may affect ventilation.

Extrapolation of the effects of the prototype environment on the known elements of the mechanism of ventilation to predict and explain differences between model and full scale behavior.

The well documented[19] experience of the PCH-1 with its uncontrollable yaw rates in rough water, and the many other identifiable problems now associated with ventilation have disposed of the unjustified optimism which led to the belief that the dire consequences intimated by model tests would not be realized under full scale conditions.

DIFFERENCES BETWEEN MODEL AND PROTOTYPE BEHAVIOR

Smaller Attack Angles for Prototype. The most distinctive feature of prototype strut ventilation as observed on craft with fully submerged systems is that it probably occurs at sideslip (attack) angles much smaller than those observed on models in the laboratory. The qualification "probably" is required, because there is no satisfactory way to measure local sideslip as seen by a strut on a full scale vessel at sea. Discussions with designers familiar with the results of full scale tests, indicate that the sideslip angles expected are of the order of 2 or 3 degrees. This will vary depending on the conditions. In calm water, considering only fully coordinated turns, the sideslip angles are probably half or less than the amounts indicated. Even allowing for a generous margin of error in the estimation of full scale sideslip angles, (some people would concede up to 6 degrees of sideslip) the ventilation angles observed under laboratory conditions are largely outside the range of those apparently occurring naturally. Rothblum, et al.[12], observed ventilation at angles of about 6 degrees on surface piercing struts tested at full scale speeds of 55 knots in the David W. Taylor Model Basin in calm water. The only other data obtained which demonstrated angles this low were those of Wetzel[8], Kramer[20], and Rothblum et al[21]. These tests were made in rough water, in waves, and with a roughened model, respectively.

For foils, as opposed to struts, full scale data concerning inception of ventilation does not seem to be available at all. The fundamental difference between foils and struts, besides dihedral angle, is that foils are allowed to assume asymmetric shapes. The conclusions reached for struts may be extended, with caution, to foils which are surface-piercing or submerged close to the free surface. The angle of attack deviation from design condition is roughly comparable to sideslip angle.

Visual Appearance. To establish the flow anomalies observed on full scale craft as being the manifestation of ventilation on the struts is not trivial. The existence of a fully ventilated cavity on a surface piercing strut on a full scale boat has never been documented. The films of ventilation on a hydrofoil strut in open water available to

the author have shown partial cavities in a very unstable state, generally not as is observed under laboratory conditions. The laboratory test which reproduced visual behavior most similar to that reported in full scale tests was a model test at cavitating speed with roughness applied to a surface piercing strut in rather turbulent flow[21].

Cine films of ventilation taken on full scale craft must necessarily be shot through the water surface if the camera is carried aboard the craft. Even the calmest open water surface is less than ideal for looking through. Therefore details of underwater occurrences are difficult to observe. Ventilation is usually most easily identified under these circumstances by the characteristic change in the spray pattern. This has led to the identification of a phenomenon called waterline ventilation, in which the spray pattern at the water surface is observed to change to that associated with ventilation, and the typical behavior of the craft is observed simultaneously, but there is no evidence of an underwater cavity. The nearest analogy to this phenomenon observed in laboratory experiments was in work on fences[22] and on protuberances from the sides of surface piercing struts[23]. For fences, ventilation down to the barrier occurred at rather low angles, of about 4 degrees. The protuberances created shallow cavities and the surface seal was re-formed just below the protuberance. In either case, in spite of the fact that the cavities formed were extremely shallow, the spray pattern was still markedly different from ordinary fully wetted flow.

The existence on prototype surface piercing struts of waterline and partial ventilated cavities implies that the force changes due to natural ventilation inception are not so abrupt as smooth model tests would imply. Thus, Eames was not entirely wrong when he speculated that the large changes in forces, implied by the retarding effect of the surface seal on ventilation inception, would not be realized at full scale.

Different Effect of Fences. The anomalous effect noted by Eames was that leading edge fences on full scale surface piercing struts and foils were successful, despite the results of model studies which indicated that the low energy paths for air ingress to the low pressure separated regions were nearer the after part of the strut, if not in the wake. In fact, in model studies[22], the effect of nose fences was deleterious. On the other hand, in order to be effective, tail or whole body fences had to be extremely large, especially at the rearward part of the strut.

Summary of Differences. The differences between ventilation as it occurs on smooth models and as it seems to occur on prototypes can be summarized as follows:

PROTOTYPE	MODEL
inception at small attack angles	inception at large attack angles
partial and waterline cavities	full cavities follow inception

force changes may be small	force changes generally large
small nose fences effective	large tail fences effective, small nose fences harmful

DIFFERENCES IN AMBIENT CONDITIONS BETWEEN MODEL AND PROTOTYPE

Speed and Size. There are great differences in the ambient conditions influencing prototype and model. Most obviously, models are almost by definition smaller than full scale. Generally, they are necessarily tested at less than prototype speeds.

Waves and Turbulence. The character of the oncoming flow seen by a strut is probably the most important difference between conditions attainable in the laboratory and those existing in the ocean. The effect of waves and background turbulence is also the most difficult to assess on the basis of theoretical considerations without actual observations to provide a baseline. Full scale observations are difficult to make under the best of conditions. In bad weather it is nearly impossible to accurately correlate flow conditions with craft behavior. One thing certain is that rough water has an immensely adverse effect on the tendency of struts and foils to ventilate.

Surface Finish. Model construction methods and the highly polished finish of most models used in hydrodynamic testing bear little relationship to the final product of shipyards. Examples of the negative effects of weld beads, seams and cavities are abundant.

Wettability and Surface Tension. Wetzel[8] and Perry[24] found that suface tension and "wettability" had an effect on the ventilation inception boundaries of small, surface-piercing models -- 1/4 inch diameter (6 mm) rods and 2 inch chord (50 mm) struts. It is unlikely that surface tension and wettability will have any effect on full scale ventilation, but it is important to determine how it may affect model results.

Other Differences. Full scale observations are sparse, and because of this, it must be concluded that there are important differences in the ocean and laboratory environment affecting ventilation that have not yet been discovered. Wind driven surface currents can be as high as eight or nine knots, strongly varying with depth in the six or seven metres closest to the ocean surface. In bad weather, large amounts of air can be entrained in the the water near the surface. Besides air entrained in the gaseous state, the water near the ocean surface is supersaturated with dissolved air. Capillary waves as well as gravity waves may influence ventilation[25]. Since cavitation can supply the requisite low pressure separated region which is often the precursor of ventilation, anything which influences cavitation could be considered to have an effect on ventilation. These might include, besides many of the factors already mentioned, the tempera-

ture, solid nucleus population, atmospheric pressure, salinity and a host of other factors.

PROJECTED EFFECT OF PROTOTYPE ENVIRONMENT ON VENTILATION BEHAVIOR

Speed. Comparison of ventilation inception angles on geometrically similar surface piercing struts at different speeds did not show any significant effect of speed alone so long as the cavitation number and Froude number based on chord were invariant, and providing there were no surface disturbances or background turbulence[26]. For Reynolds number based on chord of less than about 10^6, a great deal of scatter in inception angle was found[27]. Tests in facilities where there was a great deal of background turbulence or surface disturbances, such that the nose mode of inception caused by encounter with a disturbance was possible, indicated that this mode of inception disappeared with increasing speed[5]. This was found to be the case for both towed, large models in regular waves, breaking waves and chop, and for smaller models in a rather turbulent free surface water channel. In the latter case, the mode of ventilation was observed to change with increasing speed from tail-type, initiated by Taylor instabilities, to a mixture of nose and tail types, then to a new mode which combined some features of both the nose and tail type. Finally, at the highest speed, the tail mode was the only one observed. However, the point of breakdown of the surface seal, though still tail mode, moved steadily forward and the actual inception point became more indistinct. The explanation for this was that, with increasing speed, the separated region, whether due to a vapor cavity or wetted separation, does not grow towards the surface in the vicinity of the nose. Therefore the thickness of the surface seal is relatively constant. But as speed increases, the momentum of the surface seal grows, resulting in greater strength and resistance to breakdown caused by disturbances. On the other hand, the increased downward pressure gradient and greater turbulence generated by higher speed enhances the growth of Taylor instabilities, encouraging tail ventilation farther and farther forward. It seems quite likely that this trend would apply to fully submerged as well as surface piercing foils.

Size. The effect of size on the inception of ventilation on surface piercing struts is discussed in Reference 5, based on calculations of boundary layer thickness and considerations of transition to turbulent flow, and the mechanism of growth of Taylor instabilities. The boundary layer is shown to be thicker on an absolute basis, but compared to the dimensions of the body, it is relatively smaller. However, it is likely to be the absolute size of the boundary layer which is the controlling factor in the ability of the surface seal to maintain its integrity.

The tendency to earlier transition on the larger sizes would promote greater mixing

of air and water in the surface seal, a phenomenon that can be observed along the side of ships. This greater mixing is thought to encourage earlier ventilation inception, although this is not clear.

Since the growth of Taylor instabilities is a non-linear function of time, the greater residence time of each instability in the accelerating region of the flow might hasten the breakdown of the surface seal, with the effect of moving the breakdown point forward, as well. The possible effect of longer residence times would also apply to fully submerged foils.

Waves and Turbulence. The available experimental evidence concerning waves is somewhat contradictory, in much the same way, perhaps, that the calm water experiments were apparently contradictory until the concepts of nose and tail ventilation were resolved. Work at the David W. Taylor Naval Ship R&D Center at high speeds showed that waves had little effect on ventilation inception boudaries of surface piercing struts. The investigation (unpublished) was conducted in head seas only, but included breaking waves as well as regular waves. Kramer[20], at Lockheed, who tested the same models at lower speeds in waves at reduced pressure, found vastly reduced sideslip angles compared to the calm water tests under similar conditions, and a tremendous amount of scatter in the boundary points. Kramer investigated both head and following seas, and suggested that ventilation was likely to occur in crests in head seas and in troughs in following seas. From this observation, he attempted to reduce the scatter of his data by correcting the cavitation number parameter for the orbital velocity of the waves. He was able to collapse his data somewhat, but the results were insignificant compared to the total scatter.

McGregor et al.[25], reported that inception took place predominately at wave crests in both head and following seas. By adding the effect of the acceleration of the water surface due to the waves to the acceleration obtained in calm water conditions he was able to obtain an empirical correlation between calm water and wave inception boundaries for limited circumstances. Swales et al.[15] were able to include some representative points of the McGregor et al. experiment in a different empirical correlation with considerable success.

The role of turbulence in the initiation of tail ventilation is explained by Swales et al[15]. The existence of background turbulence in a test facility, or the absence thereof, constitutes a genuine scale effect. Whether nose ventilation is an expected mode of inception on the prototype will determine whether the turbulence is desirable as a proper simulation of full scale. Any further role of turbulence has not been systematically investigated. At present, the effect of waves and turbulence cannot be explained or predicted, except in the most limited way.

Surface Finish (Roughness). The principal effect of roughness deliberately applied to model scale surface piercing struts is to drastically reduce the angle required for

ventilation inception.[5,8,9,24] A secondary effect is to introduce a dependence on speed, whereby at very low speeds, a lower asymptotic bound for inception angle is arrived at. The most remarkable aspect of the lower bound is that it is less than that angle at which separation or cavitation could be observed, or had been observed on the smooth models. With increasing speed, the behavior of the flow around the struts reported in Reference 5 became more like the behavior at full scale. The vented cavities often did not extend to the full depth of the struts, and were extremely unstable, forming and collapsing seemingly at random.

The observed behavior is compatible with the notion of a much-weakened surface seal and a decreased requirement for a separated region, which may have been replaced by a roughness-thickened boundary layer. The roughness undoubtedly stimulated turbulence in the surface seal, probably similarly to what happens at full scale with larger sizes, coarser surface finish and greater ambient flow disturbances.

Breslin[9] showed that the effect of a trip wire near the leading edge of a surface piercing strut has a similar effect to roughness. That the principal effect of the trip wire in encouraging ventilation is on the surface seal is corroborated by Isayev[28], who noted that when the trip wire was installed below the surface seal that premature ventilation did not occur, in spite of the fact that larger force coefficients were measured due to the elimination of a region of laminar separation by the trip wire.

Roughness is probably not important in creating differences between the ventilation behavior of ordinarily smooth models. In Reference 5 it was shown that for ordinary machined surfaces (about 0.006 mm peak-to-trough roughness height) additional polishing to a near-mirror finish (0.002 mm) did not make any difference. However, the introduction of controlled roughnesses created, besides the effects noted above, a critical speed effect which was a function of roughness size. For each size tested, at a particular speed, the ventilation angle would start to be affected, becoming smaller with increasing speed. Therefore, even though ordinary surface finish did not influence results at the sizes and speeds tested, it does not necessarily follow that this will be true at higher speeds. Attempts to explain this apparent transition phenomenon by correlating the critical speed with a roughness Reynolds number based on the roughness diameter and the velocity in the boundary layer at the roughness height did not yield anything meaningful. This was probably because of the uncertainty of the boundary layer calculation in the surface seal, the critical region.

It is interesting to note that nowhere was a "gradual" transition to the ventilated state observed even though the roughness "broke down" the surface seal. This also corresponds to the situation at full scale. It is likely that roughness would have a similar effect on fully submerged models, but the effect would be limited by the fact that the roughness could not act on the entire surface seal from the foil to the free water surface. Also, if a vapor or superventilated cavity was attached to the foil, the roughness would only be made manifest at the leading edge to the point of detachment of the cavity.

Wettability and Surface Tension. Besides the effects of surface tension mentioned previously, which applied only to very small models, it was observed[5] that wettability had a significant effect on the closure angle of ventilated cavities on a strut model of 125 mm chord, but no other effect was noted on inception angle or other observable behavior. This is another argument, if one is necessary, for not using the closure angle as a criterion for evaluating the ventilation resistance of struts or foils from model tests.

CONCLUSIONS

The major differences which have been observed between model and prototype ventilation behavior can be explained in terms of a weakened surface seal and a decreased requirement for a region of separation or cavitation prior to ventilation inception. Although most of the investigation of the phenomenon of ventilation has pertained to surface piercing struts not artificially ventilated, the basic principles can be applied to submerged or airbleed struts and foils.

The effectiveness of nose fences at full scale is seen as a consequence of the forward movement of the point of ventilation inception with increasing speed. The addition of controlled roughness may well simulate full scale conditions at model sizes. However, no quantitative criterion now exists for determining the proper roughness size to simulate given prototype conditions. The effects of surface tension or wettability do not seem to be important for model sizes and speeds which would satisfy the minimum Reynolds number criterion of 10^6. The effects of waves do not seem to be well understood. Turbulence at low speeds may lead to spurious nose ventilation.

Other unsteady aspects of the flow around ventilated or potentially ventilated hydrofoils have not been discussed, although the effects of acceleration, the possibility of flutter of ventilated surface piercing struts, and the time dependence of certain modes of ventilation inception are known.

Because of the lack of full scale data, there are certainly other scale effects to be discovered, and even the ones which are known cannot be properly quantified. More full scale observations are a necessity if progress is to be made in this area.

REFERENCES

1. Dobay, G.F., "Performance Characteristics of the BuShips Parent Hydrofoil," David Taylor Model Basin Report 2084, Aug 1965.

2. Morgan, W.B., "Surface-Piercing Struts (Strut Ventilation)," Proceedings of the 12th I.T.T.C., Rome, Italy, 1969.

3. Shen, Y.T., "General Scaling Problems on Fully Cavitating and Ventilated Flows," 17th ATTC, Jun 1974.

4. Rothblum, R.S., M.F. Jeffers, and R.P. Smith, "Methods for Controlling the Sideforce on Surface-Piercing Hydrofoil Struts," David W. Taylor Naval Ship R&D Center Report SPD-700-01, Jul 1976.

5. Rothblum, R.S., "Investigation of Methods of Delaying or Controlling Ventilation on Surface-Piercing Struts," Ph.D. Thesis, Department of Mechanical Engineering, The University of Leeds, Jan 1977.

6. Hoerner, S.F., "Some Characteristics of Spray and Ventilation," Gibbs and Cox Report 1351/S1/1,S1/10(1-1504), ONR Contract No. NONR-507(00), Sep 1953.

7. Wadlin, Kenneth L., "Mechanics of Ventilation Inception," Second Symposium on Naval Hydrodynamics, Office of Naval Research, 1958.

8. Wetzel, Joseph M., "Ventilation of Bodies Piercing a Free Surface," Second Symposium on Naval Hydrodynamics, Office of Naval Research, 1958.

9. Breslin, John P. and Richard Skalak, "Exploratory Study of Ventilated Flows about Yawed Surface-Piercing Struts," NASA MEMO 2-23-59W, Apr 1959.

10. Sottorf, "Experimental Investigation of Hydrofoils," Inst. Seeflugwesen, Hamburg, ZWB Document FB 1319, 1940. (Note: This reference is as it appeared in Reference 6.).

11. Kicenuik, Taras, "A Preliminary Experimental Study of Vertical Hydrofoils of Low Aspect Ratio Piercing a Water Surface," Cal. Inst. Tech. Report E55.2, 1955.

12. Rothblum, Richard S., Dennis A. Mayer, and Gene M. Wilburn, "Ventilation, Cavitation and Other Characteristics of High Speed Surface-Piercing Struts," Naval Ship R&D Center Report 3023, 1961.

13. Coffee, Claude W., and Robert E. McKann, "Hydrodynamic Drag of 12- and 21-Percent Thick Surface-Piercing Struts," NACA TN 3092, 1953.

14. Waid, Robert L., "Experimental Investigation of the Ventilation of Vertical Surface-Piercing Struts in the Presence of Cavitation," Lockheed Missiles and Space Company Report LMSC/DO19597, May 1968.

15. Swales, P.D., A.J. Wright, R.C. McGregor, and R.S. Rothblum, "The Mechanism of Ventilation Inception on Surface Piercing Foils," Jour. Mech. Eng. Sci., Vol. 16, No. 1, 1974.

16. Swales, P.D., A.J. Wright, R.C. McGregor, and B.N. Cole, "Separation and Ventilation Interaction Studies," Hovering Craft and Hydrofoil, Vol. 13, No. 3, pp. 8-12, 1973.

17. Taylor, G.I., "The Instability of Liquid Surfaces When Accelerated in a Director Perpendicular to Their Planes. I.," Proc. Roy. Soc., Vol. A201, pp. 192-6, 1950.

18. Emmons, H.W., Chang, C.T., and Watson, B.D., "Taylor Instability of Finite Surface Waves," Jour. Fluid Mech., Vol. 7, Part 2, Feb 1960.

19. Boeing Company Report, "Hydrofoil Patrol Craft High Point (PCH-1) Analysis of Strut Hydrodynamic Characteristics in Calm Water," HYSTU PLAN BE049APO44, Contract NOO 600-69-c-0618, 1968.

20. Kramer, Ray L., "An Experimental Study of the Effects of Waves on the Ventilation of Surface-Piercing Struts," Lockheed Missiles and Space Co. DO29678, Nov 1970.

21. Rothblum, R.S., R.C. McGregor, and P.D. Swales, "The Effect of Roughness, Wettability and Speed on the Ventilation Characteristics of Surface-Piercing Hydrofoil Struts," International Hovering Craft, Hydrofoil and Advanced Transit Systems Exhibition and Conference, London, May 1974.

22. Swales, P.D., R.C. McGregor, R.S. Rothblum, "The Influence of Fences on Strut and Foil Ventilation," 10th ONR Symposium, Boston, 1974.

23. Rothblum, R.S., N.L. Dailey, and J.H. Pattison, "Effect of a Protuberance and Aspect Ratio on the Inception of Ventilation on a Surface-Piercing Strut in Cavitating Flow," Naval Ship R&D Center Ship Performance Department Evaluation Report 479-H-02, Jun 1972.

24. Perry, Bryne, "Experiments on Struts Piercing the Water Surface," Cal. Inst. Tech. Report No. E-55.1, 1954.

25. McGregor, Robert C., A.J. Wright, and P.D. Swales, and G.D. Crapper, "An Examination of the Influence of Waves on the Ventilation of Surface-Piercing Struts," J. Fluid Mech., Vol. 61, Part 1, pp. 85-96, 1973.

26. Rothblum, R., "A Scaling Law for Ventilation Inception on Surface Piercing Struts," ASME Cavitation Forum, 1970.

27. Waid, R.L., "Experimental Study of Model Size Effects on Cavitation and Ventilation of Surface-Piercing Struts," LMSC/DO 26656, Nov 1970.

28. Isayev, I.I., "Scaling Effect on the Magnitude of the Lateral Force Acting on an Isolated Hydrofoil Strut," Sbornik Statey po Gidromekhanike i Dinamike Sudna, (Russian), pp. 158-162, 1967.

A REVIEW OF CAVITATION EROSION SCALING RESEARCH

by

Gurmukh D. Mehta and Andrew F. Conn
HYDRONAUTICS, Incorporated

ABSTRACT

Although many investigators have studied the phenomena of cavitation erosion over the past hundred years, systematic attempts to develop sound scaling laws started only a few years ago. The status of the subject was reviewed at the Seventeenth American Towing Tank Conference at CALTECH in June 1974. In this paper we have updated the previous review by presenting a brief discussion of the recent work on cavitation scaling by various researchers. Some of the important areas in which considerable research remains to be done are also outlined.

INTRODUCTION

Cavitation erosion is an important problem in many hydraulic and marine engineering components. In order to cope with the requirements of new, high performance systems, it is very desirable to develop appropriate scaling laws for cavitation erosion by which one can extrapolate laboratory experience to actual field systems. The status of cavitation erosion scaling laws was reviewed (1) at the last American Towing Tank Conference at CALTECH in June 1974. The purpose of this paper is to update the previous review by presenting a brief discussion of the recent work that has been done or is presently being done by various organizations. Some of the important areas, relevant to cavitation erosion scaling, in which considerable research remains to be done are also outlined in this paper.

The problem of cavitation erosion is an extremely complex one, requiring a sophisticated knowledge not only of the transient fluid mechanics and thermodynamics of two-phase flow, but also of material behavior and the interactions between the fluid and the solid. Using a simple heuristic approach, Thiruvengadam (2) developed scaling laws for flow

over foils. Recently, Kato (3) has presented an alternative approach to the development of cavitation erosion scaling laws by assuming an energy distribution of the cavitation bubbles. However, as will be discussed later in the present paper, Kato's theory cannot be used until several undetermined constants have been determined, a priori, by conducting controlled experiments in the laboratory.

In order to predict the erosion behavior and to choose suitable materials for use in cavitating environments, many investigators (4-8) have attempted to correlate the cavitation resistance of different materials and alloys with some bulk material property or combination of bulk properties. Although a wide range of properties have been tried, including strain energy, hardness, ultimate resilience, fatigue life, ultimate tensile strength and various combinations of properties, these attempts have met with very limited success. While for alloys of the same base metal a qualitative correlation may be obtained, for instance with hardness, only general trends with considerable scatter are found, as seen in Fig. 1 (8), if correlations of many alloys are attempted. The parameter, normalized erosion resistance, N_e , was suggested by Heymann (8) for relative comparisons of materials, and is based on hardness and rate of volume removal. For a reference material with a 170 DPH, N_e is given by:

$$N_e = \frac{\text{Volume loss rate of ref. material}}{\text{Volume loss rate of test material}} \quad .$$

Motivated by these failures to derive a general correlation between erosion rates and existing bulk material properties, Preece, et al. (9 and 10) decided to study the actual cavitation damage process at the microscale by optical metallography and x-ray diffraction. The results of their ongoing study are interesting and will be discussed in the next section.

RECENT STUDIES

In this section we will describe only that part of the recent work (since 1974) on cavitation erosion that has bearing on the scaling laws. Since the objective of this paper is to review those aspects which are relevant to scaling cavitation erosion, for more details the reader should refer to the particular references. In order to include all the work that is presently being done in this field, various teams working on cavitation erosion mechanisms, mainly in the United States, were contacted for their inputs. Although additional Russian studies may exist, these have not been included due to the usual difficulties of procuring references covering their current work.

It is fair to report that not much work has been done in this area since the last American Towing Tank Conference in 1974. For this reason, also included in this review is some new work which may be only of indirect importance to cavitation scaling laws. In the following paragraphs only brief descriptions of each study will be given, with any critical reviews being reserved for the Discussion section.

A Scaling Theory (Kato, Ref. 3)

As mentioned, Kato has attempted to provide new scaling laws to describe cavitation erosion. A number of assumptions underlie the results derived by Kato, including:

a. A particular form of the number density distribution for the cavitation bubbles (see Fig. 2), where n, the number of bubbles per unit time whose energy is between E and E + dE is given by:

$$n = AEe^{-BE}$$

where A and B are constants.

b. Material deformation is of two forms, either i) fatigue due to repeated collapse of many bubbles, or ii) due to a single blow from a highly energetic bubble (see Fig. 2). Furthermore, Kato assumes the deformation depends only on the density of bubble energy and hence does not include length or time scales in this part of his derivation.

c. The use of MDD (mean depth of deformation) as his basic measure of cavitation damage instead of one of the more familiar measures such as weight loss, erosion penetration, or numbers of pits (see Fig. 3).

d. A dependence only on hardness of the fraction of energy absorbed by the material from the total energy reaching the surface due to a cavitation bubble collapse.

From these basic assumptions, Kato derives, under a set of simplifying assumptions, the dependence of mean depth of deformation rate, MDDR, on flow velocity, v , characteristic length, L , hardness, H , and ultimate resilience, UR. For the examples chosen, MDDR was seen to vary as v^a, L^b, and $(H \cdot UR)^c$, with the exponents a, b, and c covering a very large range depending upon the material properties, velocity, and other operating conditions.

Cavitation Damage in the Incubation Zone (Stinebring, Ref. 12)

Most of the attention in cavitation erosion studies has focused on the later stages of the damage, either in the "maximum rate period", or

the "terminal rate (or steady state) period", where considerable damage has already occurred. From such studies, the so-called "sixth-power law" has evolved which says that the damage rate is proportional to the flow velocity raised to the sixth power. However, as discussed in the previous review (1), although many investigators using a variety of devices have reported this v^6 dependence, damage rates proportional to v^m, with m ranging from one to ten or more, have been cited. If one assumes the existence of a unique erosion property for materials such as the erosion strength, S_e, suggested by Thiruvengadam (2), and defines an intensity of cavitation damage, I (power absorbed per unit area), then $I \sim v^6$ is the resulting form for the "sixth power law".

Stinebring concentrated on the earliest part of the damage history, the "incubation zone". During this initial period the cavitation must overcome a material threshold of resistance to damage. Thus, if the intensity of cavitation is low relative to the material erosion resistance, a considerable time period can exist before measurable weight loss can be determined. During this incubation period, however, considerable damage in the form of isolated pits can be observed. As discussed below (19), removal of material occurs only after many, sufficiently energetic collapses have occurred near the same site.

Using 0.635-cm diameter zero-caliber ogives made of pure annealed aluminum in a flowing system with water, Stinebring observed damage in the form of small round depressions usually under 0.1 mm in diameter (with the majority of pits less than 0.025 mm) without any net material removal. The pitting rate per unit area (pits/cm^2-sec) was seen to vary as v^6, thus corroborating Knapp's (15) results. As shown in Fig. 4, it was found that for a flow velocity in the range from 14.9 to 59.3 m/sec, the average volume of each pit increases as about the fifth power of the flow velocity as previously reported by Sato, et al. (13). Since Knapp (15) has shown that individual bubbles produce individual pits in the incubation zone, Stinebring assumed that the pit volume is proportional to the energy absorbed and performed a dynamic hardness test to relate volume to the absorbed cavitation energy. Then, by combining the v^6 dependence of damage rate with the (approximate) v^5 dependence of pit volume, he deduced a v^{11} dependence for the total cavitation bubble collapse energy absorbed per unit area per second. Using the definition of intensity above, this implies: $I \sim v^{11}$. It should be emphasized that this result is for the initial or incubation stage of damage.

Stinebring also used the dynamic hardness test correlations of the energy required to form a given pit size to create density distributions

for the numbers of pits within each energy level. He reports that a large number of low energy bubbles are collapsing, causing relatively little damage, which tends to refute the distribution suggested by Kato (Fig. 2).

Stinebring also studied the effect of air content on the pitting rate. It was observed that for a range of air content from 7 ppm to 20 ppm the damage rate in the maximum damage zone changed approximately inversely with the air concent as shown in Fig. 5. It was also quantitatively noted that the pits at the lower air content appeared to be larger than their counterparts at higher air contents. The reason for this may be, as first suggested by Rayleigh (22), that if the gas inside the bubble undergoes adiabatic compression during the collapse, then as the air content decreases, the collapse pressure of a bubble increases resulting in a bigger pit. The experimental data of Stinebring (12) has conclusively demonstrated that minute differences in noncondensible dissolved gas can have a profound effect on the damage rates.

Some Correlations (Arndt, Refs. 17, 18)

Arndt (17) compared the experimental results of Stinebring (0.635-cm diameter zero-caliber ogives) (12) with the data of Knapp (15) (5.08-cm diameter hemispherical-nosed body); Sato, Kato and Tamiya (13) (1 cm hemispherical-nozed body); and Hackworth and Arndt (16) (0.635 cm step mismatch). He reduced the experimental data of these different investigators to one air-content, and the results are shown in Fig. 6. From this figure we see that despite wide variations in model sizes, geometry and different flow conditions, the same trend is observed, i.e., damage rate increases as the sixth-power of flow velocity. This correlation indicates that the variation of damage rate with velocity overrides the differences due to flow configurations and cavitation numbers.

Recently Arndt (18) has reanalyzed the previously published data for cavitation inception in the wake of sharp-edged disks. A simple, semiempirical analysis is presented which correctly predicts the correlation between the cavitation index and Reynolds number. According to this theory, for a laminar boundary layer at the face of the disk, the desinent cavitation number σ_d, increases as: $\sigma_d = C + FR_n^{\frac{1}{2}}$, where R_n is the Reynolds number and C and F are constants. As shown in Fig. 7, the correlation between the experiment and the analysis is good for the laminar boundary layer up to a Reynolds number of 2×10^5. However, for higher Reynolds numbers Arndt cites other experimental data which show a variation with Reynolds number raised to only the one-fifth power.

Arndt (17) has also briefly reviewed the current status of cavitation mechanisms including cavitation inception and the effects of turbulence and gas content on the cavitation erosion process. The cavitation number is the primary scaling parameter in turbulent flow fields; however, cavitation is dominated by both mean and the fluctuating pressure fields. Apart from that, many other hydrodynamic factors such as nuclei size distribution, viscosity, surface tension, temperature and corrosion also affect the cavitation process. For this reason, model tests often are not very reliable in predicting the cavitation erosion characteristics of the prototype because it is very difficult to model all these effects in the model tests.

Micromechanisms of Cavitation Damage (Preece and Vyas, et al., Refs. 9, 10 and 19)

Vyas and Preece (19) have investigated cavitation erosion mechanisms by measuring the stress pulse using quartz transducers. Their objective was to determine whether the damage in a vibratory cavitation erosion device was created by microjet impingement from individual bubbles near the surface, or by a shock-wave type of stress pulse created by the concerted collapse of a large aggregate of bubbles. From their experimental results, they concluded that the pressure changes in the vibratory device cause the shock-wave mechanism to be the dominant way for erosion to occur. As shown in Fig. 8, in each positive part of the cycle, a high amplitude spike, representing the pressure pulse due to concerted collapse of cavitation bubbles is observed. Also, the cavitation stress (the amplitude of shock-wave spike) is seen to increase with increasing amplitude of vibrations. The weight losses from aluminum samples exposed for the same time interval to cavitation are directly related to the magnitude of the shock wave emitted by the collapse of the bubble cloud as shown in Figs. 9 and 10.

Motivated by the failure to arrive at any correlation between erosion rates and bulk material properties, Preece, et al., (9 and 10) subjected several face centered cubic metals and alloys to vibratory cavitation in distilled water to study the mechanism of cavitation erosion at the microscale. The surface damage during the incubation zone was analyzed qualitatively by scanning electron micrographs and optical metallography and quantitatively by microhardness and x-ray diffraction. It is reported that the deformation of the surface is caused by a shock-like stress wave produced by the combined collapse of a large number of bubbles. These surface undulations are primarily responsible for erosion in that the undulations deepen to form craters as cavitation proceeds and material is

lost by ductile rupture from the lips of the craters.

CURRENT STUDIES

Apart from the recent work described above, a brief summary of the work relevant to cavitation erosion scaling, which is presently being conducted by various teams, is included in this section.

In an ongoing study, a team from Bell Aerospace* is investigating the effects of propeller design and simulated ship operating conditions on the collapse pressure of individual cavitation bubbles as determined from crater size and the rate of crater formation. Under this program full-scale propeller tests (to be done in conjunction with American Export Lines) will be correlated with model tests which are being conducted at the David Taylor Naval Ship Research and Development Center. The results of this study should be available by the end of this year. This study should provide more information on the important problems of length-scale effects on cavitation damage.

In another study*, of a more fundamental nature, the effects of wakes on cavitation bubble formation and damage rate are being examined in fresh water under conditions representative of actual operating conditions. The objective of this program is to reduce and possibly eliminate the erosion due to cavitation damage by proper modification of the propeller design.

It is reported that Preece, et al.** are presently studying the effect of corrosion on cavitation damage. Thiruvengadam† is continuing his studies of the effects of bubble-size distributions on cavitation erosion damage. This effort is an extension of his earlier efforts on the subject (2 and 20); however, no reports are as yet available on this new work.

DISCUSSION

The results of Preece, et al. are very interesting. It is clearly evident from their data that under vibratory cavitation the mechanism of material erosion is the concerted collapse of a group of bubbles rather than by a single bubble. However, as these researchers (19) indicate,

---

*Private communication with Dr. Vaughn Hackworth, Bell Aerospace Division of Textron, Buffalo, New Jersey, May 1977.
**Private communication with Dr. Carolyn M. Preece, Bell Laboratories, Murray Hill, New Jersey, March 1977.
†Private communication with Dr. A. Thiruvengadam, Daedalean Associates, Incorporated, Woodbine, Maryland, May 1977.

these results cannot be generalized to the cavitation erosion in flowing systems. Indeed, such nonlinear interactions depend on the localized size scaling and the severity of the turbulence which contributes to the bubble growth and collapse. Similar tests should be conducted on propeller blades, for instance, to examine the role of concerted bubble collapse in the erosion mechanisms of such a flowing system. Since the frequanty of bubble collapse is very large, the simultaneous collapse of many bubbles causing severe material failure is always a possibility. If concerted collapse is the principal mechanism, then the various theoretical analyses which model material failures by the simple superposition of the effects due to the collapse of individual bubbles (for example, Refs. 2 and 3) need to be reviewed in this light.

Over the air-content range of 7-20 ppm, the experimental results of Stinebring have clearly demonstrated that very small differences in noncondensible dissolved gas can have a profound effect on the damage rates. The data of Stinebring show that, over this range, erosion due to cavitation damage increases with decreasing air content. However, more work is desirable over a larger gas-content range. In particular, studies should be extended to below a certain minimum value of gas content whereby the number of available nuclei for cavitation bubbles, and therefore erosion, should decrease.

In Reference 12, the author has shown that in the incubation zone the rate of absorption of energy in creating pits at the surface of the material increases as the eleventh power of the flow velocity. These tests, however, were done on a ductile material (pure annealed aluminum) during the initial stage of damage such that no material loss was observed during these tests. It should be pointed out that these results cannot be compared with the well-known sixth-power law for weight loss in the maximum erosion zone because the mechanism of cavitation damage is significantly different in the two zones. In the incubation zone there is no material loss and damage is in the form of pits and surface undulations. In contrast, during the maximum damage zone the flow is significantly altered due to the presence of surface erosion and there is material failure due to fatigue as well as individual and concerted bubble collapse.

Kato (3) has derived scaling laws for cavitation damage which are based on a number of assumptions. He compares his own results with an alternate "empirical formula" that suggests much smaller effects from all relevant parameters, and says: "At the present stage, it is impossible to decide which one is better." We agree. Moreover, in light of the

recent work of Preece, et al. (9 and 10), Kato's assumption that the absorption ratio (energy absorbed by the material divided by total bubble collapse energy reaching the surface) is a function only of hardness is questionable. Also, the assumed form for the number density of cavitation bubbles (Fig. 2), which suggests few low energy bubbles, seems to be refuted by bubble distribution studies such as those of Stinebring (12). Thus, as suggested by Kato, experiments must be run which carefully control the key parameters under actual operating conditions in hydrodynamic equipment before we will begin to understand how to accomplish the modeling of cavitation erosion.

FUTURE RESEARCH AREAS

In this section we will outline some of the areas in which considerable research still remains to be done. These areas are important to develop suitable scaling laws for cavitation erosion. The first area that has not been explored is the effect of size-scaling on cavitation damage. Recently, the present authors completed a preliminary study (21) to evaluate estimated cumulative erosion depths in the 3K SES water jet propulsor. Due to lack of sufficient information on size-scaling, the propulsor manufacturer made preliminary analyses which assumed that the scaling factor between 1/6-scale model erosion and full-scale propulsor erosion is unity. However, from the limited data on the damage created by the collapse of a large cavity on 7.5-cm and 3.8-cm foils, generated at HYDRONAUTICS, Incorporated (2), it appears that the peak erosion intensity for the 7.5-cm foil is more than that for the 3.8-cm foil by a factor of about 2.5, as shown in Fig. 11. Indeed, the scaling laws developed by Thiruvengadam (2) predict that intensity of cavitation damage should increase linearly with the characteristic length of the foil. Hopefully, the current study of Bell Aerospace* will shed more light on this subject.

Another important area where considerable research is required is in the assessment of density and size distributions of nuclei in the ambient liquid. The authors are not aware of any model study in which the size and density of cavitation nuclei have been systematically scaled in the laboratory experiments. In general, model studies in which the cavitation number is kept equal to the field value, but which do not properly scale nuclei distribution, surface tension and viscosity, cannot be very reliable in predicting the cavitation characteristics of the prototype. Furthermore, in most of the laboratory testing devices the geometry and the

*Private communication with Dr. Vaughn Hackworth, Bell Aerospace Division of Textron, Buffalo, New Jersey, May 1977.

operating conditions are significantly different from those in the full-scale situation.

A third area which has received very little attention is cavitation under turbulent flow conditions. In turbulent flows, cavitation is influenced not only by the mean pressure field but also by the fluctuating pressure field. For further details, the reader should refer to the paper by Arndt (17) which reviews the work of different investigators on this subject.

CONCLUSIONS

In summary, although considerable progress has been made in understanding certain aspects of cavitation mechanisms, it is not yet possible to summarize the various effects in a few simple scaling laws because of the extremely large number of interrelated parameters. Systematic experimentation, which is presently lacking, is very desirable to make further progress in this important field. Some of the important areas, including the effects of size-scaling, nuclei distribution and turbulence on cavitation erosion need considerably more research.

On the basis of the available data, discussed in this paper, the following general conclusions can be drawn:

For flowing systems:

1. The average volume of the pits, and therefore the energy absorbed by the material during the incubation zone, increases as the fifth-power of the velocity.
2. The total collapse energy absorbed by the model per unit area per unit time in creating pits increases as v^{11} in the incubation zone, and
3. The damage rate in the maximum damage zone increases as the sixth-power of the flow velocity.

For vibratory cavitation systems:

4. Concerted bubble collapse is the principal mechanism for material failure, and
5. The surface undulations created during the incubation zone are primarily responsible for subsequent material loss which is caused by ductile rupture of the material from the lips of the craters.

ACKNOWLEDGMENTS

The authors wish to thank the investigators whose work is reviewed in this paper for their assistance in the compilation of these results. The suggestions and encouragement of Dr. T. R. Sundaram throughout the preparation is also gratefully acknowledged.

LIST OF SYMBOLS

A, B, C, F: constants
D: characteristic diameter
DPH: diamond pyramid hardness
E: energy
H: hardness
I: cavitation erosion intensity, power/unit area
L: characteristic length
MDD: mean depth of deformation, MDD = $\frac{1}{s}\int|\Delta|ds$
MDDR: mean depth of deformation rate (time derivative of MDD)
n: number of bubbles per unit time whose energy is between E and E + dE
N_e: normalized erosion resistance (see definition in text)
p_o: reference, or free stream pressure
p_v: vapor pressure of the liquid
R_n: Reynolds number
s: eroded area
S_e: erosion strength, force/unit area
UR: ultimate resilience, UR = (ultimate tensile strength)^2/ 2 (tensile modulus of elasticity)
v: flow velocity
Δ: deformed volume relative to the original surface
ρ: density of the liquid
σ: cavitation number, $\sigma = \frac{p_o - p_v}{\frac{1}{2}\rho v^2}$.

REFERENCES

1. Conn, A. F., "Cavitation Erosion Scaling," Proceedings of the Seventeenth American Towing Tank Conference, Caltech, September 1974.
2. Thiruvengadam, A., "Scaling Laws for Cavitation Erosion," HYDRONAUTICS, Incorporated Technical Report 233-15, December 1971 (also Proc., Sympos. on Nonsteady Flow of Water, IUTAM, Leningrad, June 1971).
3. Kato, H., "A Consideration on Scaling Laws of Cavitation Erosion," International Shipbuilding Progress, Vol. 22, pp. 305-327, Sept. 1975.
4. Garcia, R., and Hammitt, F. G., "Cavitation Damage and Correlations with Material and Fluid Properties," Trans. ASME, J. Basic Engineering, Vol. 89, No. 4, pp. 753-763, 1967.

5. Thiruvengadam, A., "High Frequency Fatigue of Metals and Their Cavitation Damage Resistance," HYDRONAUTICS, Incorporated Technical Report 233-6, December 1964 (also Trans. ASME, J. Engr. for Industry, Vol. 88, Ser. B., No. 3, pp. 332-340, 1966).

6. Lichtman, J. Z. and Kallas, D. H., Symp. on Cavitation Research Facilities and Tech., ASME, p. 185, 1964.

7. Eisenberg, P., Preiser, H. S., and Thiruvengadam, A., "On the Mechanisms of Cavitation Damage and Methods of Protection," Trans. SNAME, Vol. 73, pp. 241-286, 1965.

8. Heymann, F. J., "Toward Quantitative Prediction of Liquid Impact Erosion," Characterization and Determination of Erosion Resistance, ASTM STP 474, pp. 212-248, 1970 (also Westinghouse Engr. Report E-140, 1968).

9. Vyas, B. and Preece, C. M., "Cavitation Erosion of Face Centered Cubic Metals," Metallurgical Transactions (in press).

10. Preece, C. M., Dakshinamoorthy, S., Prasad, S., and Vyas, B., "The Influence of Microstructure on the Cavitation Erosion Resistance of FCC Metals and Alloys," Proceedings of the Fourth International Conference on the Strength of Metals and Alloys, Vol. III, p. 1397, France, 1976.

11. Hammitt, F. G., "Observation on Cavitation Damage in a Flowing System," J. Basic Eng., Trans. ASME, pp. 347-367, Sept. 1963.

12. Stinebring, D. R., "Scaling of Cavitation Damage," AIAA 13th Annual Meeting and Technical Display Incorporating the Forum on the Future of Air Transportation, Washington, D. C., Jan. 10-13, 1977 (also J. Hydronautics, Vol. 11, No. 3, pp. 67-73, July 1977).

13. Sato, R., Kato, H., and Tamiya, S., "Study on Cavitation Erosion," J. Soc. Naval Arch., (in Japanese), pp. 43-63, Japan, November 1973.

14. Thiruvengadam, A., "Cavitation Erosion," Applied Mechanics Reviews, pp. 245-253, March 1971.

15. Knapp, R. T., "Recent Investigations of Cavitation and Cavitation Damage," Trans. ASME, Vol. 77, pp. 1045-1054, 1955.

16. Hackworth, J. V., and Arndt, R. E. A., "Preliminary Investigations of the Scale Effects of Cavitation Erosion in a Flowing Media," Cavitation and Polyphase Flow Forum, ASME, 1974.

17. Arndt, R. E. A., "Cavitation and Erosion: An Overview," Corrosion/77, Annual Conference of the National Association of Corrosion Engineers (NACE), San Francisco, March, 1977.

18. Arndt, R. E. A., "Semiempirical Analysis of Cavitation in the Wake of a Sharp-Edged Disk," J. Fluid Engr., Trans. ASME, pp. 560-562, September 1976.

19. Vyas, B., and Preece, C. M., "Stress Produced in a Solid by Cavitation," J. Appl. Phys., Vol. 47, pp. 5133-5138, 1976.

20. Thiruvengadam, A., "Role of Physical Properties of Liquids in Cavitation Erosion," Proc. of the 19th Mechanical Failure Prevention Group, October 1973 (also Tung, S., Ph.D. Thesis, Catholic University, 1973).

21. Conn, A. F., and Mehta, G. D., "A Preliminary Evaluation of 3K SES Propulsor Erosion Damage Predictions," HYDRONAUTICS, Incorporated Technical Report 7750-1, March 1977.

22. Rayleigh, Lord, "On the Pressure Developed in a Liquid During the Collapse of a Spherical Cavity," Phil. Mag., Series 4, Vol. 34, pp. 94-98, 1917.

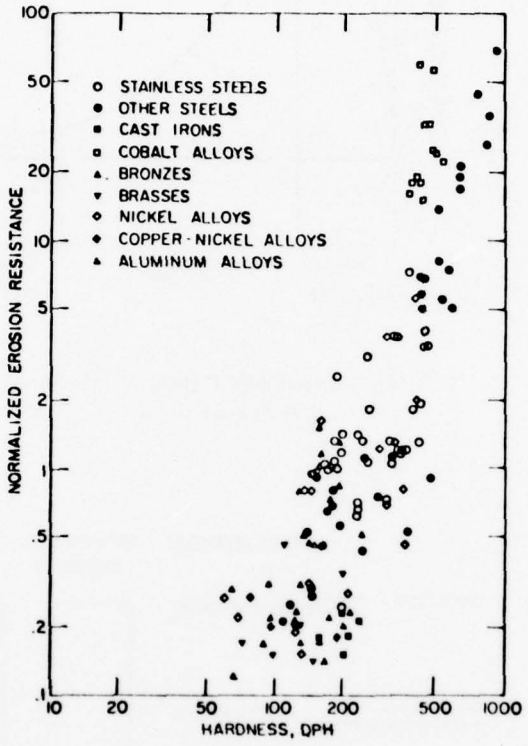

FIGURE 1 - VARIATION IN THE NORMALIZED EROSION RESISTANCE, N_e, OF VARIOUS ALLOYS AS A FUNCTION OF THE INITIAL DIAMOND PYRAMID HARDNESS, DPH. (Reference 8)

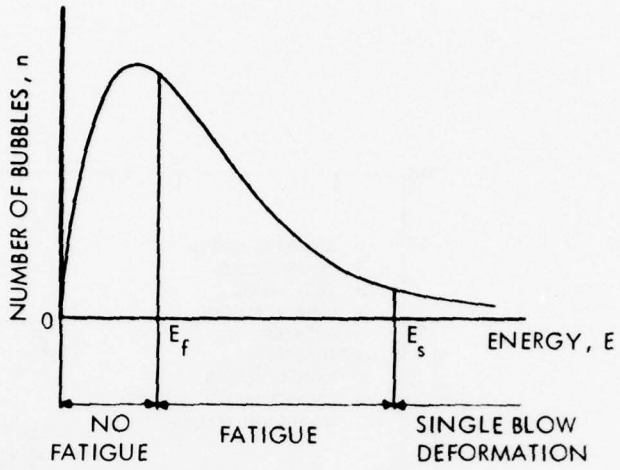

FIGURE 2 - NUMBER DENSITY OF CAVITATION BUBBLES
(Reference 3)

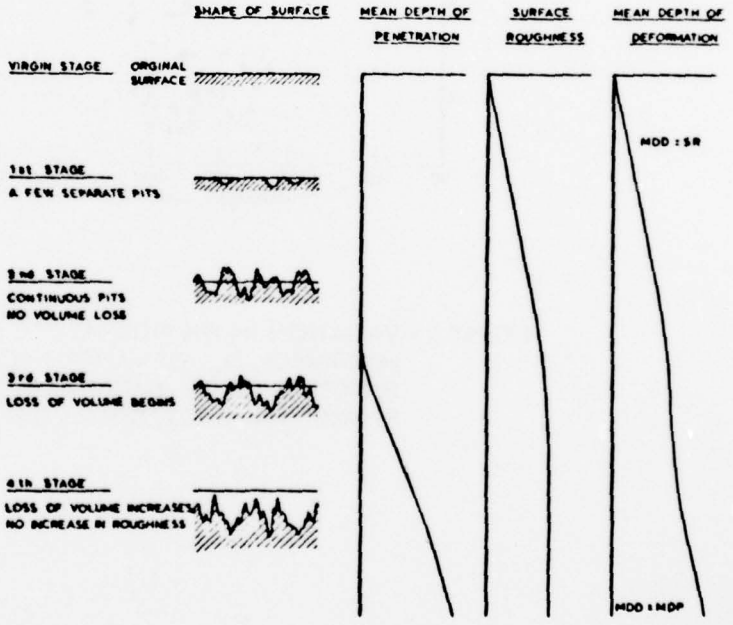

FIGURE 3 - DEFORMATION OF SURFACE BY CAVITATION ATTACK
(Reference 3)

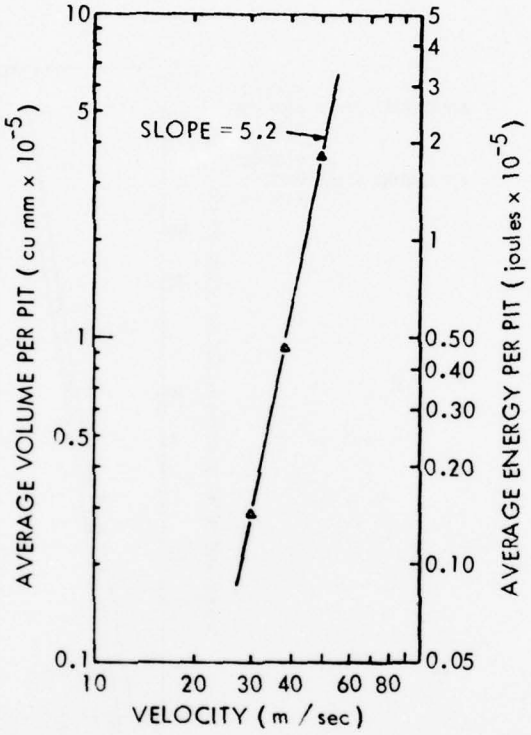

FIGURE 4 - AVERAGE PIT VOLUME (AVERAGE ENERGY PER PIT) VERSUS VELOCITY. For an aluminum, 0.635 - cm diameter, zero-caliber ogive with L / D = 3.0; air content: 10 ppm (Reference 12)

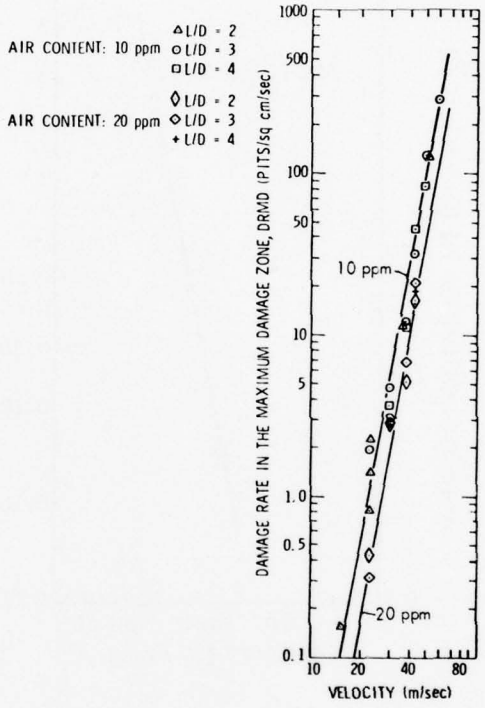

FIGURE 5 - EFFECT OF AIR CONTENT ON THE DAMAGE RATE IN THE MAXIMUM DAMAGE ZONE (Reference 12)

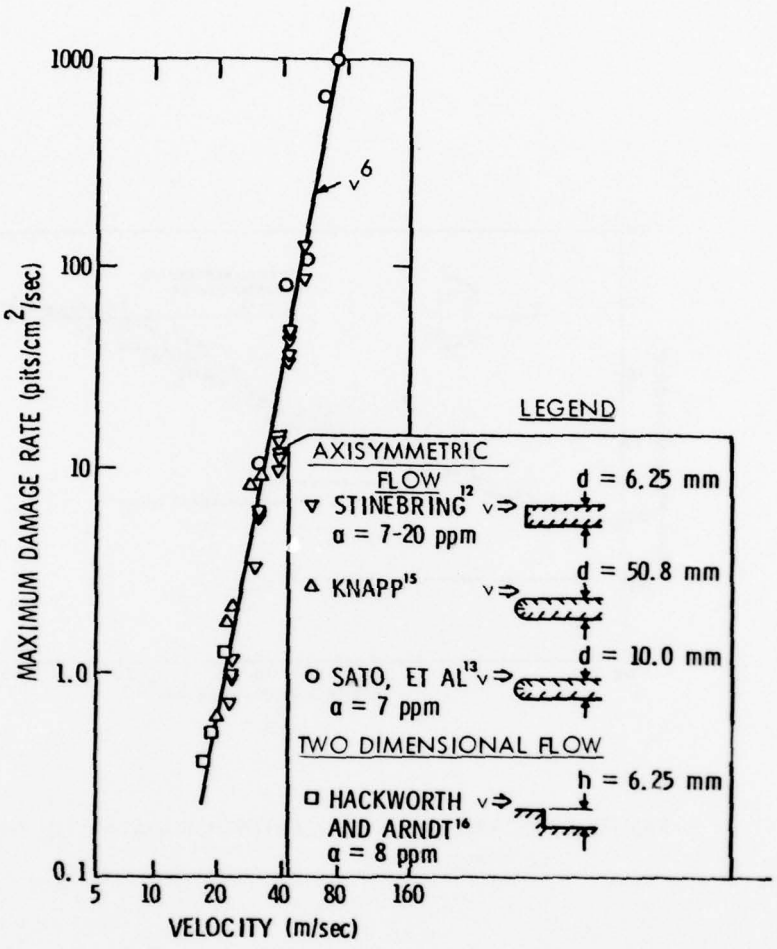

FIGURE 6 - DAMAGE RATE IN THE MAXIMUM DAMAGE ZONE VERSUS VELOCITY - CORRECTED FOR AIR CONTENT (Reference 17)

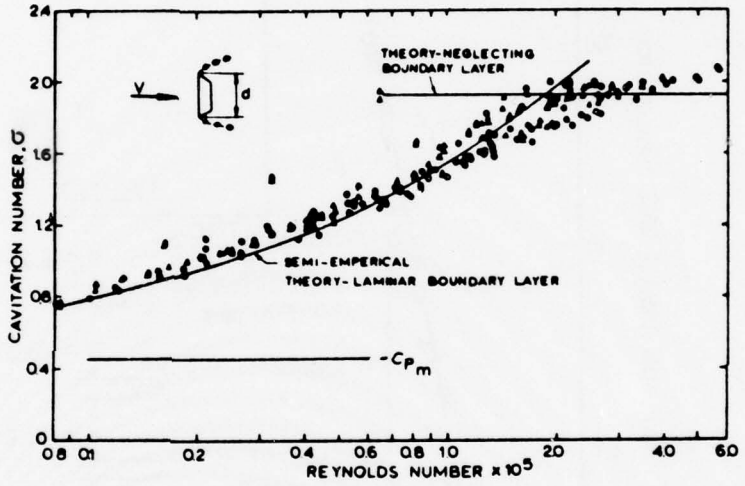

FIGURE 7 - CORRELATION OF CAVITATION DATA WITH THEORY
(Reference 18)

AD-A062 507 NAVAL ACADEMY ANNAPOLIS MD F/G 5/11
PROCEEDINGS OF THE GENERAL MEETING (18TH) OF THE AMERICAN TOWIN--ETC(U)
1977 B JOHNSON, B NEHRLING

UNCLASSIFIED NL

2 OF 3
AD A062507

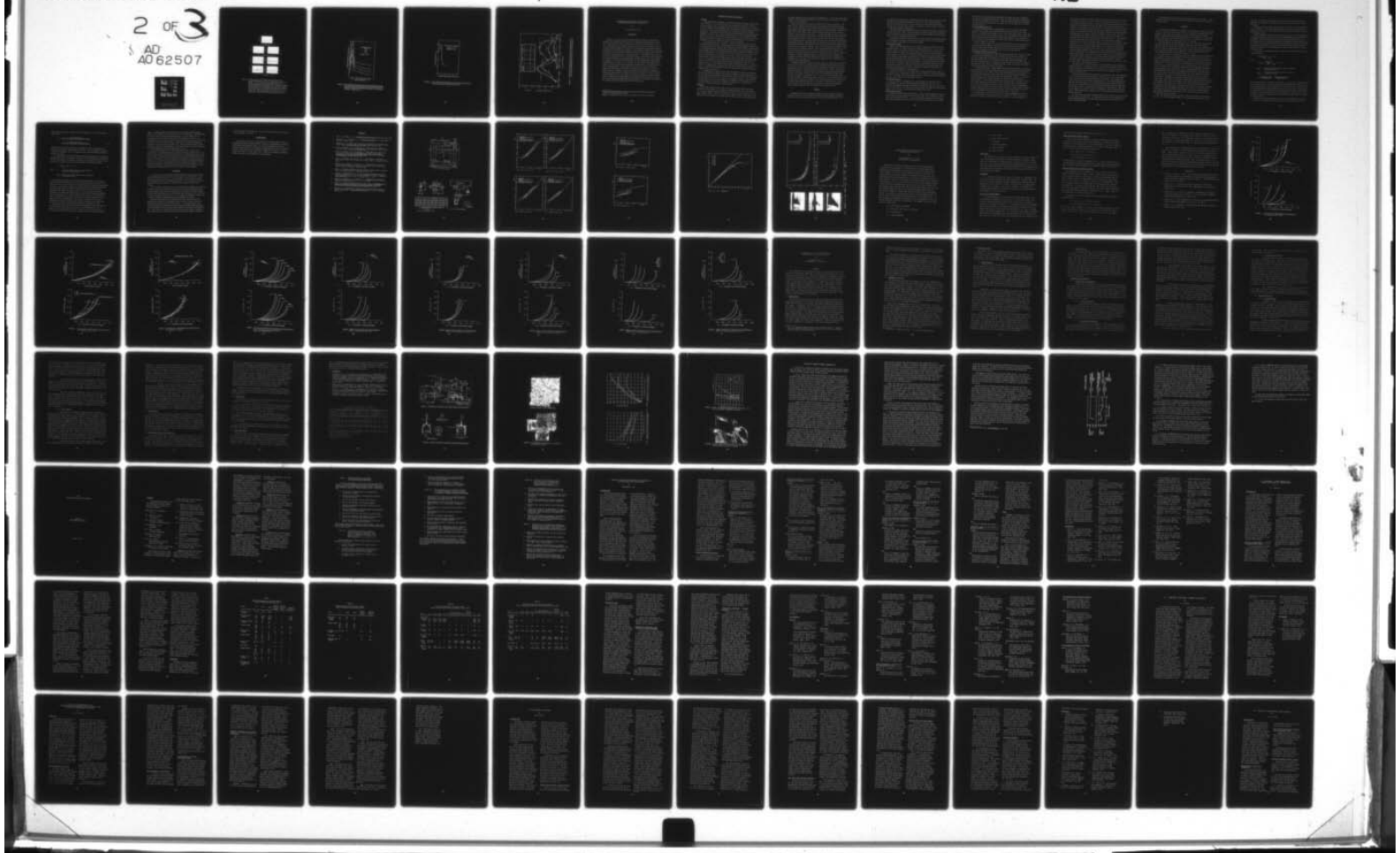

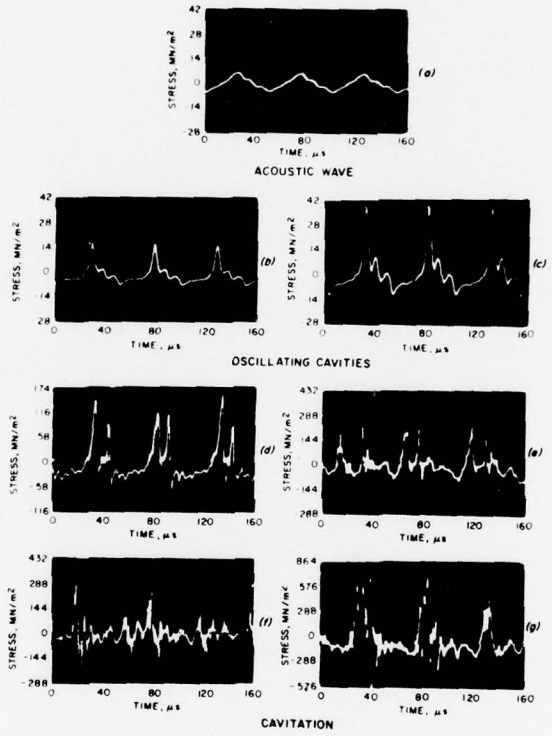

FIGURE 8 - OSCILLOGRAMS OF THE STRESS PULSE PRODUCED IN A QUARTZ TRANSDUCER BY 20- kHz VIBRATIONS IN DISTILLED WATER. (a) AT LOW VIBRATIONAL AMPLITUDES THE PRESSURE DIFFERENTIAL IS INSUFFICIENT TO NUCLEATE BUBBLES AND THE TRANSDUCER RESPONDS TO THE APPLIED ACOUSTIC WAVE; (b) AND (c) AT INTERMEDIATE AMPLITUDES, BUBBLES ARE NUCLEATED BUT COLLAPSE BY OSCILLATIONS; (d) - (g) CAVITATION, THE NUCLEATION AND VIOLENT COLLAPSE OF BUBBLES, OCCURS AT HIGHER AMPLITUDES (Reference 19)

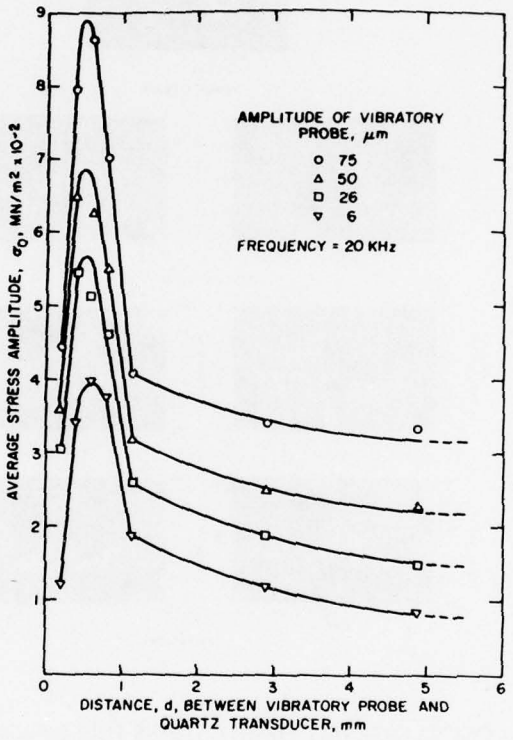

FIGURE 9 - THE VARIATION IN AVERAGE CAVITATION STRESS AMPLITUDE WITH DISTANCE BETWEEN THE QUARTZ TRANSDUCER AND THE VIBRATORY PROBE FOR DIFFERENT AMPLITUDES OF VIBRATION AT 20 kHz (Reference 19)

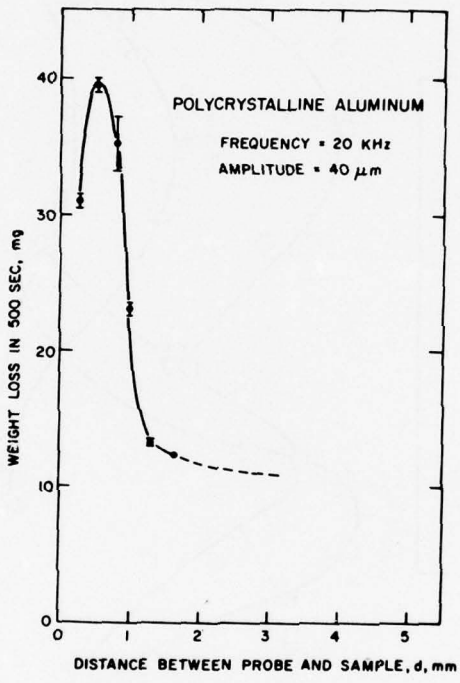

FIGURE 10 - THE VARIATION IN EROSION OF ALUMINUM WITH DISTANCE FROM THE VIBRATORY PROBE (Reference 19)

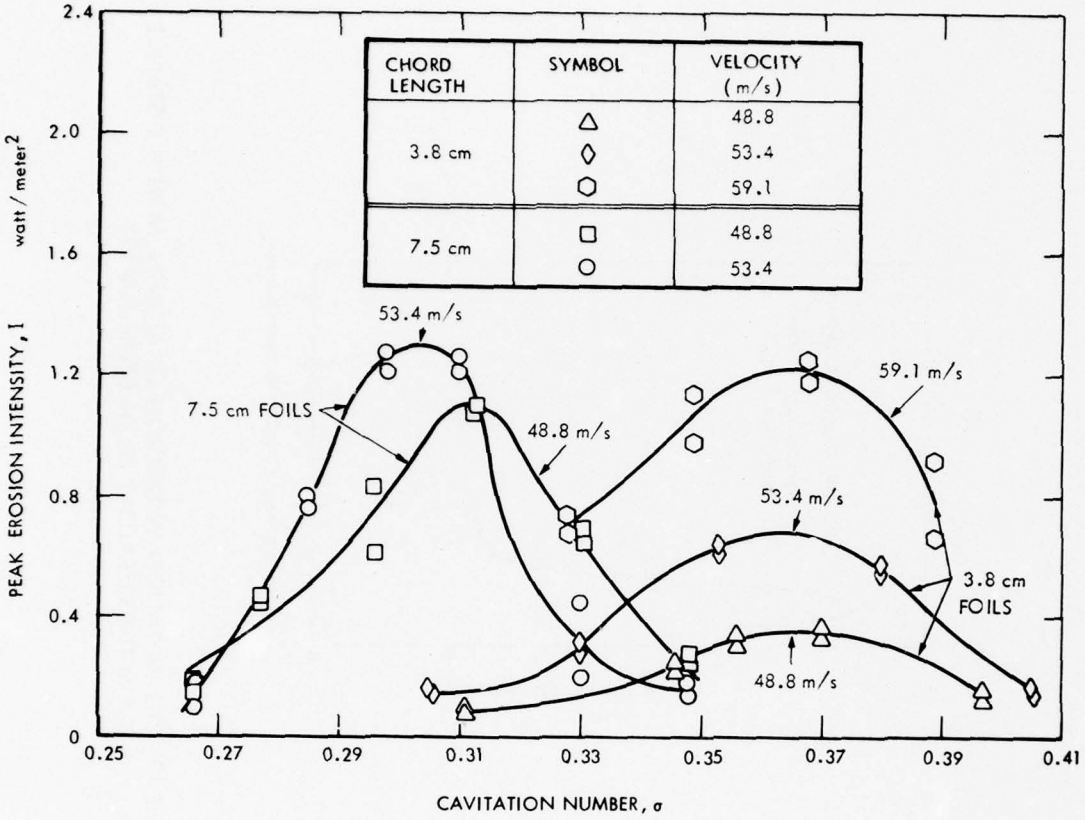

FIGURE 11 - RELATIONSHIP BETWEEN PEAK INTENSITY OF EROSION AND CAVITATION NUMBER FOR NACA-16-021 FOILS (Reference 2)

AN EXPERIMENTAL INVESTIGATION OF WALL EFFECTS ON SUPERCAVITATING HYDROFOILS OF FINITE SPAN

by

M. R. Maixner, LT, USN[1]

INTRODUCTION

Corrections for water tunnel wall effects during the testing of subcavitating hydrofoils are essentially the same corrections developed fifty years ago for use in wind tunnel testing of airfoils; references [1][2] and [2] are standard texts in this area. Only within the last twenty years have wall effects been considered in the case of supercavitating hydrofoils, with the majority of theoretical and experimental work concentrated on two-dimensional hydrofoils. The problem of blockage can be significant; the shape of the foil and cavity combination must be known in order to apply a blockage correction of the type utilized in subcavitating flow. Unfortunately, this proves to be an area of great difficulty in the various theories. Corrections to drag coefficient and cavitation number for the two-dimensional pure-drag case are given in references [3] through [7]; a nonlinear theoretical model of the two-dimensional lifting problem is formulated in reference [6]. In reference [8], Baker converts this model into a computer program which numerically calculates the wall effect on two-dimensional hydrofoils of arbitrary shape. It was hoped by Baker that these results would prove adequate for application to flows over high aspect ratio hydrofoils. Prior to the current research, a systematic series of experiments which exhibit wall effects on a geometrically similar family of hydrofoils had not been carried out in either the two- or three-dimensional case. The purpose of the present research is to make available data on a geometrically similar family of three supercavitating hydrofoils of finite span, and to apply existing two-dimensional corrections in an attempt to bring the data into agreement with three-dimensional, unbounded flow theory.

---

[1]Graduate student, Department of Ocean Engineering, Massachusetts Institute of Technology, Cambridge, Massachusetts.

[2]Numbers in brackets refer to the list of references at the end of the paper.

EXPERIMENTAL APPARATUS AND PROCEDURE

Apparatus

The experiments were conducted in the MIT recirculating, variable pressure water tunnel (Figure 1). Test section velocity was variable between 0 and 9.1 m/sec; a velocity manometer read the difference in pressure across a contraction in the tunnel one meter upstream of the dynamometer axis. The assumption was made that the blockage caused by the foil and cavity combination did not affect the velocity manometer appreciably. Test section static pressure was variable between 90 mm Hg absolute and atmospheric pressure; static pressure readings were taken using a mercury manometer connected to either or both of two taps on the centerline of a side wall of the test section. These taps were located 62 cm upstream and downstream of the hydrofoil dynamometer, which was located at the center of the test section.

Foil dimensions are given in Figure 2. The three semi-span, aspect ratio five foils had sharp leading edges. Geometrically similar elliptic planforms were chosen even though foils of this type were more difficult to fabricate than, for example, foils of rectangular planform; elliptic planform foils exhibit less tip loading effect than do rectangular planform foils, thereby rendering them more amenable to analysis. Each foil was drilled with a hole terminating in a pressure tap on the cavity side of the foil. The medium foil was the aspect ratio five foil utilized by Leehey and Stellinger [9], except that the cavity pressure tap was relocated to a position nearer the tip. The composition of the medium foil was of type 304 stainless steel, while that of the small and large foils was of type 614 aluminum bronze. Each foil was welded to its own 10.16 cm diameter mounting plate; the mounting plates, in turn, were bolted to the dynamometer so that the small, medium, and large foils protruded one-quarter, one-half, and three-quarters of the way, respectively, downward from the top window into the test section.

The dynamometer was capable of measuring three moment and three force components, but only the moment about midchord and the forces tangential to and perpendicular to the span and chord were measured. Zero geometrical angle of attack was set by aligning the flat (wetted) side of each foil with the test section side wall. Upon alignment, a sighting telescope, which was attached to the dynamometer, was aligned with a scale on the laboratory wall; this scale, graduated in increments of 0.05 degree, was utilized in varying the geometrical angle of attack.

Procedure

Before test runs were begun on any one day, the tunnel was operated at medium velocity for twenty minutes at a pressure of 300 mm Hg absolute; this removed almost all of the air trapped in remote locations of the tunnel. Prior to each test run, the bubble chamber shown in Figure 3 was utilized to collect and draw off any gases or air which may have been trapped in the static pressure sensing line; once cleared of gases,

the bubble chamber was merely a reservoir of common pressure. On the other hand, small amounts of air were bled intermittently into the cavity pressure sensing line in order to keep it free of moisture.

Each foil was tested at a variety of attack angles from 8 to 21 degrees. The lower limit of 8 degrees was chosen so that the cavities would not terminate on the foil. For all test runs, the test section velocity was set at 8.5 m/sec, whereupon static pressure was reduced until a cavity covered the entire planform. Readings were taken of lift, drag, moment, static pressure (with pressure taps U and D open; see Figure 3), cavity pressure, and velocity. A Polaroid photograph was taken of the foil and cavity from the wetted side of the foil, utilizing an exposure time of 1/40 second with bottom flood lighting. Pressure tap D was then closed, and the same reading taken; reopening pressure tap D and closing pressure tap U, the same series of readings was repeated once more. (Photographs were not taken for these last two pressure tap combinations since hardly any variation in cavity shape was noted when compared to the situation where both pressure taps were open.) This completed the measurement of three data points at one controller setting. Both pressure taps were then opened, and the static pressure was reduced by 20 to 30 mm Hg, whereupon the above procedure was repeated. The static pressure was reduced in this fashion until an excessive number of recirculated cavitation bubbles resulted in either extremely poor conditions for photography or rapidly fluctuating instrument readings. Prior to and immediately following a run of this type, the room and water temperatures were recorded, as were the tares on the instrumentation.

A computer program was utilized in the data reduction. Wetted surface frictional drag (for each foil and its mounting plate) and dynamometer shaft twist were taken into account, and test section static pressure readings were modified for static head difference to give the static pressure at the foil centroid. (Gravity effects were otherwise neglected.) Cavitation number was computed using measured cavity pressure, and also by using vapor pressure at the ambient water temperature (computed using equation (2) on page 151 of reference [10]). Lift, drag, and moment coefficients were also calculated. Standard wind tunnel corrections [1,2] were applied to the data to account for the effect of the images of the trailing vortices; this resulted in an increase in drag coefficient and also in an increase in effective angle of attack (α_T is the "true" angle of attack in a free stream). Utilizing the photographs, cavity lengths were measured from the midchord at the centroid position.

RESULTS

Experimental results were compared with predictions calculated from Leehey's linearized theory [11], which utilizes the method of matched asymptotic expansions; the theory is valid to first order in angle of attack, and to second order in the

reciprocal of the aspect ratio. Comparisons were also made with a more detailed linear lifting surface calculation developed by Jiang at MIT. This numerical theory is expected to be more accurate at the lower values of σ/α, where the cavity length is the same size as the foil span or longer; it should also be more accurate, in general, for prediction of moment coefficients.

The wall boundary layer momentum thickness, as measured by Stellinger under similar conditions [9], was 1.91 mm. Since this resulted in almost no reduction in effective foil wetted surface area, the upper wall boundary layer was assumed to have negligible effect on the force and moment coefficients.

It should be noted that the only correction for wall effect which has been applied to the data shown in Figures 4 through 10 and in Figures 12 and 13 is the correction for the effects of the images of the trailing vortices.

Lift (Figures 4 and 5)

There is very good agreement, overall, between theoretical predictions and the experimental data. For small values of the similarity parameter σ/α (i.e., for long cavities), there is much better agreement with the numerical theory; the foil and cavity combination no longer has a large aspect ratio, so that a better theoretical prediction might, in fact, be obtained from slender body theory. For the higher values of σ/α, Leehey's theory appears to underpredict, the effect becoming especially pronounced at attack angles of 16 degrees and higher. This is in apparent contradiction with Figure 4 of reference [9]; it should, however, be noted that the data of reference [9] was based on cavitation numbers calculated with vapor pressure rather than with measured cavity pressure. It can be seen from Figure 10 of the present paper that, when based on measured cavity pressure, the cavitation number will be smaller, so that the above contradiction is only apparent.

Of particular interest is the strange "hook" in the data trend which occurs at high values of σ/α at high angles of attack (18 and 21 degrees). The small and medium foil data plot almost on top of one another, whereas, for the most part, the large foil data plot lower than the small and medium foil data.

Drag (Figures 6 and 7)

When the effects of streamwise foil or flow curvature are negligible, linear theory predicts $C_D = \alpha_T C_L$, so that the drag data are plotted as C_D/α_T^2 vs. σ_c/α_T. C_D/α_T^2 plotted somewhat higher than the theoretical predictions except for very long or for very short cavities. As with the lift data, the small and medium foil data plotted together, with the large foil data plotting somewhat below these.

Moment (Figures 8 and 9)

As pointed out by Leehey and Stellinger [9], Leehey's matched asymptotic expansion theory neglected lifting surface corrections (third order in the reciprocal of aspect ratio) for the moment coefficient. It is not surprising, therefore, that the current experimental data agrees best with the more detailed lifting surface theory of Jiang.

The load cell utilized for moment measurements on the small foil was of inadequate sensitivity, and consequently, much of the small foil data may be less accurate than the data for the medium and large foils. Comparisons must therefore be made between the large and the medium foil data; once again, the large foil data plot below that of the medium foil.

Cavitation Number (Figure 10)

Below a cavitation number of approximately 0.4, there is almost no difference between cavitation number calculated with measured cavity pressure or with vapor pressure. It should be noted, however, that in this region there exists a large variation in cavity length from very short to very long. This indicates that for even short cavities, where ram jet effects have heretofore been thought to have a pronounced effect on measured cavity pressure, the actual cavity pressure is approximately equal to the vapor pressure of the water.

Above a cavitation number of 0.4, the disparity between σ_v and σ_c increases with increasing cavitation number; the data in this region is for only large angles of attack and small cavity lengths, indicating that there may indeed be some effect caused by the impinging of the reentrant jet on the cavity pressure tap.

Cavity Length (Figures 11, 12, and 13)

Representative photographs of the large, medium, and small foils at the same angle of attack and at approximately the same cavitation number are shown in Figure 11. The cavity shapes shown are averaged over the exposure time of 1/40 second; visual observations showed that the instantaneous cavity shape was highly unsteady. For the small and medium foils, the general outline of the cavity is elliptic, as predicted by theory; the cavity length is undoubtedly reduced toward the tip due to the hydrostatic pressure gradient existing in the tunnel.

As mentioned previously, cavity lengths were measured from midchord at the centroid position rather than from the leading edge, since this convention was utilized by both Jiang and Leehey. Cavity length (L) was nondimensionalized on the foil mean chord (c). The cavity length data for the small and medium foils plotted on top of one another (consequently, of these two, only the plot for the small foil is shown); in both cases, the cavity lengths were slightly less than those predicted by either Leehey's or Jiang's theory, but the overall agreement with theory was good. In contrast, there was a marked deviation in the large foil cavity length and shape, especially at the root, where local blockage was the worst. The tip vortices seen in the photographs had no evident effect upon the force or moment coefficients. Neither Leehey's matched asymptotic expansion theory nor Jiang's numerical lifting surface theory accounts for the roll-up effects which these trailing vortices produce in the wake.

As stated earlier, readings were taken for the various combinations of the two static pressure taps; this was done in order to determine the effect of blockage on pressure and velocity at the two different tap positions. It was anticipated that

this variation in static pressure tap combination would have no effect on the forces and moments experienced by the foil. Due to the location within the system of the static pressure controller (Figure 3) (which was inadvertently overlooked), the forces and moments varied significantly when the combination of static pressure taps was changed. The explanation for this is as follows. Before data were taken, both static pressure taps were opened and the controller setting reduced to $\tilde{p}$; the actual static pressure in the tunnel was decreased by the control system until the combined signal from both taps was $\tilde{p}$. When the instrument readings settled out, data were taken. The downstream static pressure tap was then closed, so that the only signal to the controller was p_U, which was greater than the controller setting, $\tilde{p}$. The controller therefore lowered the actual static pressure in the tunnel until p_U equaled $\tilde{p}$. Consequently, the effective cavitation number (as seen by the foil) decreased, causing the cavity to grow. This reduced the effective camber of the foil and cavity combination; this loss of effective camber resulted in a reduction of the force and moment coefficients from their previous values. On the other hand, the measured cavitation number increased slightly due to a small decrease in measured cavity pressure; the presence of the controller prevented the measured static pressure from changing significantly. The opposite effect was observed with the upstream tap open and the downstream tap closed (i.e., an increase in force and moment coefficients, an increase in effective cavitation number, and a slight decrease in measured cavitation number when compared to the case when both pressure taps were open); there were only a few of these data points taken.

The general trend of the data agrees with the experimental results obtained by Kermeen (see page 37 of reference [12]); he observed that the longer the cavity in supercavitating flow, the smaller the force coefficients. The same conclusion follows from the theoretical results of Leehey, as may be seen from equation (35) and Figure 4 of reference [9].

Although the desired pressure readings were not obtained in the current experiment (i.e., the actual tunnel static pressure was different for each of the tap combinations), the results do show the significance of the blockage. When comparing the results obtained with the different tap combinations for the small and medium foils, there was very little change in the plotted data points; the increased blockage in the case of the large foil resulted in significantly different force and moment data. For the sake of clarity, the data for the different tap combinations are shown only for the large foil at an angle of attack of 14 degrees. Unless otherwise specified, further remarks concerning foil data will be for the data obtained with both static pressure taps open.

At a later time, the system indicated by dashed lines in Figure 3 will be utilized to obtain data on the large foil. It should be noticed that this configuration will allow pressure measurements to be made without affecting the input signal to the static pressure controller.

Only enough data plots to show the data trends are given in this paper. A more detailed and complete listing of all the data and plots for all angles of attack will be reported later.

DISCUSSION

For the small and medium foils, it appears to be necessary to correct only for the effects of the images of the trailing vortices in accordance with standard wind tunnel procedure. These corrections to drag coefficient and effective angle of attack brought the data into good agreement with theory; the lift, moment, and cavity length data also agreed well with theoretical predictions. For the most part, the plots for the small and medium foils were extremely close to each other.

Upon application of the same corrections to the large foil data, good agreement with theory was seen for the force and moment coefficients; they were, however, generally lower than the data for the smaller foils. The plot of cavity length for the large foil, however, showed substantially longer cavities than predicted by either of the two theoretical models used for comparison. The most pronounced deviations in cavity length occurred for the long cavity (lower σ/α) data.

When compared with the data obtained from the two smaller foils, the general trend of the large foil data is in agreement with Baker's predictions for wall effects on two-dimensional supercavitating hydrofoils [8]. Baker makes the point that the wall effect is negligible for tunnel height-to-foil chord ratios (H/c) greater than 10 for cambered foils. Although he makes no such generalizations concerning supercavitating flat plates, (i.e., the case applicable to the current research), it is seen from Figures 4 through 9 that the effect of blockage on the force and moment coefficients is not exceedingly large. The following line of reasoning explains why the force and moment data for the large foil are somewhat lower than for the two smaller foils. For the three foils at the same cavitation number and at the same angle of attack, the magnitude of the velocity on the cavity wall of all three foils is $\sigma/2$ (from linear theory); consequently, all three foils have identical pressure coefficients on the cavity. The largest foil experiences significantly more blockage than do either of the smaller foils, so that the velocity on the wetted surface of the large foil is much higher than for either of the smaller foils; the pressure coefficient on the wetted surface of the largest foil is therefore the least of all three foils, resulting in smaller lift, drag, and moment coefficients than for either of the smaller foils. It is interesting to note that this overall effect is contrary to blockage effects experienced in subcavitating water tunnel or wind tunnel testing, where force and moment coefficients are increased.

Baker also questioned the sharp increase in wall effect predicted by Wu, Whitney, and Lin [6] for thin symmetric wedges or for small attack angles in the lifting

flow case. The results of the present work do not show a marked increase in wall effect on force and moment coefficients at the lower angles of attack, in agreement with Baker.

Conversely, Baker's results indicate that the wall effect on the cavity plus wake can be tremendous. In the current research, this is, in fact, the most significant departure of the large foil data from the theoretical predictions and from the data of the two smaller foils.

Several attempts were made to bring the large foil data into closer agreement with the small and medium foil data by using existing two-dimensional blockage corrections. Wu, Whitney, and Brennen [4] give wall effect correction procedures for the two-dimensional pure-drag (wedge) case, employing the open-wake and Riabouchinsky models. Wu, Whitney, and Lin [6] consider wall effects in two-dimensional lifting cavity flows, a situation more applicable to the current research; Baker [8] utilized a computer program to translate this into information which could be readily applied to correct experimental data.

The pure-drag, open-wake model employs corrections to both drag coefficient and cavitation number:

$$C_D = \left(\frac{1+\sigma'}{1+\sigma_{meas}} \right) C_{D_{meas}} + O(\lambda^2) \tag{1}$$

where

$$\sigma' = \sigma_{meas} - \left(\frac{1+\sigma_{meas}}{\sigma_{meas}} \right) C_{D_{meas}} \lambda + O(\lambda^2) \tag{2}$$

σ_{meas} = measured cavitation number, based on conditions at upstream infinity

$C_{D_{meas}}$ = measured drag coefficient, based on velocity at upstream infinity

$$\lambda = \frac{\text{foil frontal width}}{\text{tunnel width}} \simeq \frac{\text{(mean chord) x sin}(\alpha)}{\text{tunnel width}} \tag{3}$$

For the large foil with λ defined in this fashion, $\lambda = 0.3015 \sin(\alpha)$. Application of the above corrections to the large foil data shifted the data points down and to the left on the plot of C_D/α_T^2 vs. σ_c/α_T (Figures 6 and 7), but did not bring the data into any closer agreement with the small and medium foil data. When the cavity length data for the large foil were replotted using the corrected cavitation numbers, the data points in Figure 13 were moved downward; this downward movement was not sufficient, however, to bring the large foil cavity lengths into agreement with either theory or the small and medium foil data.

Actually, the straightforward application of such a two-dimensional correction to the case of a finite-span wing should over-correct for blockage, making λ much

larger than it should be. Perhaps a better representation of λ for the finite-span case would be

$$\lambda_{3D} = \frac{\text{foil frontal area}}{\text{tunnel cross-sectional area (without foil)}}$$

$$= \frac{\text{(foil area) x sin}(\alpha)}{\text{tunnel cross-sectional area (without foil)}} \qquad (4)$$

Recalculating the corrections using λ_{3D} in equations (1) and (2) would make the corrections even smaller than previously calculated. Since the previous corrections proved to be inadequate, there is no reason to believe that the modified corrections should be any better.

To correct measured cavitation number and measured drag coefficient utilizing the Riabouchinsky model, it is necessary to obtain p_m, the minimum pressure reading along the wall in the region of the cavity. Equation (1) is again used to correct the drag coefficient, but now the corrected cavitation number is calculated as follows:

$$\sigma' = \frac{2}{3}\sigma_{meas} + \frac{1}{3}\sigma'' + O(\lambda^2) \qquad (5)$$

where σ'' = cavitation number based on minimum pressure, p_m, and on maximum velocity.

σ_{meas} = measured cavitation number, based on conditions at upstream infinity.

It had originally been hoped that a reasonably close measurement of this minimum pressure could be obtained by using only the downstream tap (tap D in Figure 3); as was shown earlier, the interaction of the controller precluded making this measurement accurately. In an attempt to apply the correction based on the Riabouchinsky model, the gross assumption was made that the maximum frontal area of the cavity was approximately the same as the frontal area of the foil; utilizing a continuity argument and the steady-flow Bernoulli equation, the pressure minimum was estimated, thus allowing application of the wall effect correction based on the Riabouchinsky model. Unfortunately, this procedure gave results which were comparable to those obtained using the open-wake model. The failure of both models in the current application should not be surprising since they were designed for two-dimensional, pure-drag cavity flows, and not for three-dimensional, lifting cavity flows.

Whereas the pure-drag wall effect corrections changed both drag coefficient and cavitation number, Baker presents the results of his computerization of the Wu lifting case wall effect model in terms of a change to the force coefficients (i.e., drag and lift coefficients in this case), referenced to the uncorrected cavitation

number. Accordingly, Baker's corrections to the lift and drag coefficients are expressed as a percentage difference from the free stream condition. He presents data for only one ratio of tunnel height-to-arclength (i.e., chord length), H/c = 4. Calculating this ratio using the mean chord of the large foil gives H/c = 3.32; recalculating H/c as the ratio of tunnel cross-sectional area to foil area, H/c = 4.48 is obtained. It was concluded, therefore, that the H/c = 4 corrections should be suitable for correction of the large foil data. Upon application of these additive corrections to both lift and drag data, it was found to bring the large foil data into very close agreement with the small and medium foil data.

Because he is dealing with an infinite wake model, Baker's results give no correction for the extremely large cavity lengths recorded for the large foil. His results do show, however, that as blockage increases, the nondimensional cavity thickness increases. This was borne out nicely when the cavitation characteristics of the three foils utilized in the current research were compared at an angle of attack of 8 degrees. On the small foil, which produced the least blockage, supercavitation was never totally achieved, no matter how low the static pressure was brought. For the medium and large foils, which produced more blockage than did the small foil, cavity termination was achieved behind the foil over a range of static pressures.

CONCLUSIONS

As a general rule, the agreement of the experimental data with theory was good for the small and medium foils, whose ratios of semi-span to tunnel width were one-quarter and one-half, respectively. It appeared that in order to bring the small foil and medium foil data into agreement with theory, it was necessary to apply only standard wind tunnel procedures in correcting for the images of the trailing vortices.

For the largest of the three foils, which protruded three-quarters of the way into the tunnel, the force and moment data was close to the small and medium foil data, although slightly lower; the cavity length data for the large foil differed greatly from the small and medium foil data, showing much longer cavities for the same ratio of cavitation number to angle of attack. It is evident that blockage corrections are required in addition to the standard wind tunnel downwash corrections.

Application and modification of blockage corrections based on various two-dimensional pure-drag cavity flow models failed to bring the large foil data into agreement with the data for the two smaller foils. It was found, however, that corrections based on a two-dimensional lifting cavity flow model brought the large foil force coefficient data into much closer agreement with the small and medium foil data. While these force coefficient corrections were found to give an "engineering order of accuracy," no corrections have been found which give adequate corrections

to the large foil cavity length data; it is clearly evident that further analytical work is necessary in this area.

ACKNOWLEDGMENTS

This research was carried out under the Naval Sea Systems Command, General Hydromechanics Research Program, Subproject SR 009 01 01, administered by the Naval Ship Research and Development Center. The author is exceedingly grateful to Professor Patrick Leehey of the Department of Ocean Engineering at the Massachusetts Institute of Technology for his inspiration, suggestions, and guidance. Special thanks are also due to S. Dean Lewis and C. W. Jiang, also from MIT, who rendered valuable assistance in the performance of the experiments.

REFERENCES

1. Pope, A., and Harper, J. J., Low Speed Wind Tunnel Testing, Wiley, New York, 1969.

2. Pankhurst, R. C., and Holder, D. W., Wind-Tunnel Technique, Sir Isaac Pitman & Sons, LTD., London, 1965.

3. Whitney, A. K., "A Simple Correction Rule for Wall Effect on Two Dimensional Cavity Flows," Cavitation State of Knowledge, ASME, New York, 1969.

4. Wu, T. Y., Whitney, A. K., and Brennen, C., "Cavity-Flow Wall Effects and Correction Rules," Journal of Fluid Mechanics, Vol. 49, Part 2, 1971, p. 223.

5. Wu, T. Y., Whitney, A. K., and Brennen, C., "Wall Effects in Cavity Flows and Their Correction Rules," Non-Steady Flow of Water at High Speed, Proceedings of the IUTAM Symposium in Leningrad, June 22-26, 1971, Nauka Publishing House, Moscow, 1973, p. 461.

6. Wu, T. Y., Whitney, A. K., and Lin, J. D., "Final Report: Wall Effects in Cavity Flow," Calif. Inst. of Tech. Div. of Eng. & App. Sci. Report No. 111A.5, 1969.

7. Whitney, A. K., Brennen, C., and Wu, T. Y., "Experimental Verification of Cavity-Flow Wall Effects and Correction Rules," Calif. Inst. of Tech. Div. of Eng. & App. Sci. Report No. E-97A-18, 1970.

8. Baker, E., "Analytical Prediction of Wall Effect on Fully-Cavitating Lifting Foils Using Nonlinear Theory," NSRDC Report 3688, 1972.

9. Leehey, P. and Stellinger, T. S., "Force and Moment Measurements of Super-cavitating Hydrofoils of Finite Span with Comparison to Theory," Journal of Fluids Engineering, Vol. 97, No. 4, December 1975, p. 453.

10. Smith, L. B., Keays, F. G., and Gerry, H. T., Proceedings of the American Academy of Arts and Sciences, Vol. 69, No. 137, 1934.

11. Leehey, P., "Supercavitating Hydrofoils of Finite Span," Non-Steady Flow of Water at High Speed, Proceedings of the IUTAM Symposium in Leningrad, June 22-26, 1971, Nauka Publishing House, Moscow, 1973, p. 277.

12. Kermeen, R. W., "Experimental Investigation of Three-Dimensional Effects on Cavitating Hydrofoils," Journal of Ship Research, Vol. 5, No. 2, September 1961, p. 22.

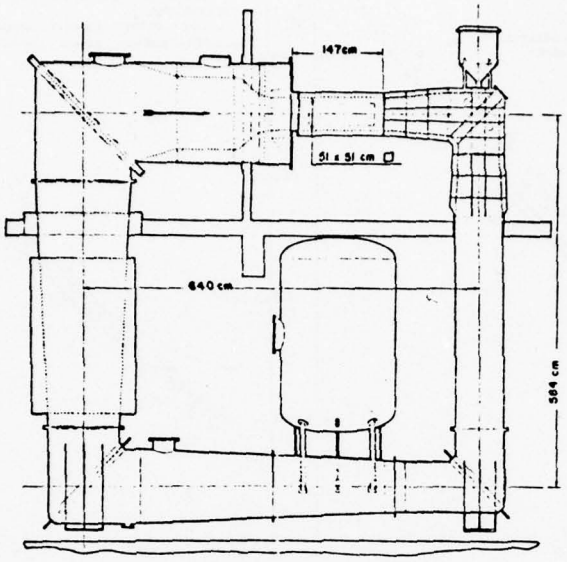

FIG. 1 : M.I.T. TEST FACILITY

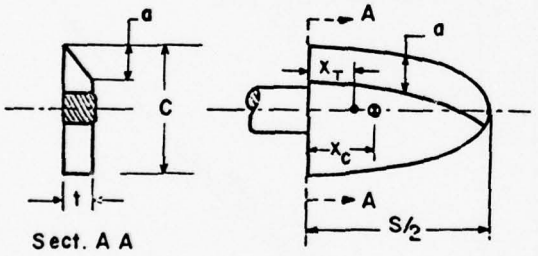

FOIL	C	S/2	α	AREA	X_C	X_T	t
LARGE	19.50	38.10	7.65	580.6	16.17	12.55	1.60
MEDIUM	13.00	25.40	5.10	258.1	10.78	8.18	1.20
SMALL	6.50	12.70	2.55	64.5	5.39	4.67	.65

X_T = distance of cavity pressure tap from foil baseplate

FIG. 2: FOIL DIMENSIONS (cm)

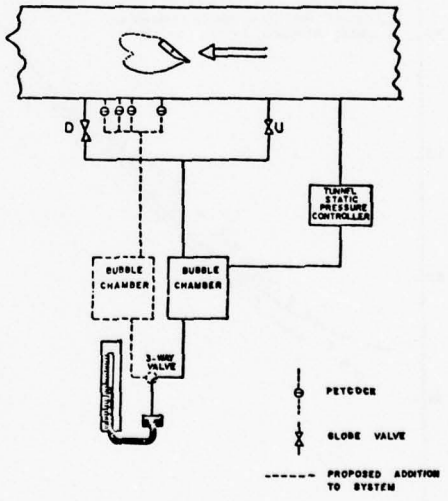

FIG. 3 : STATIC PRESSURE MEASUREMENT

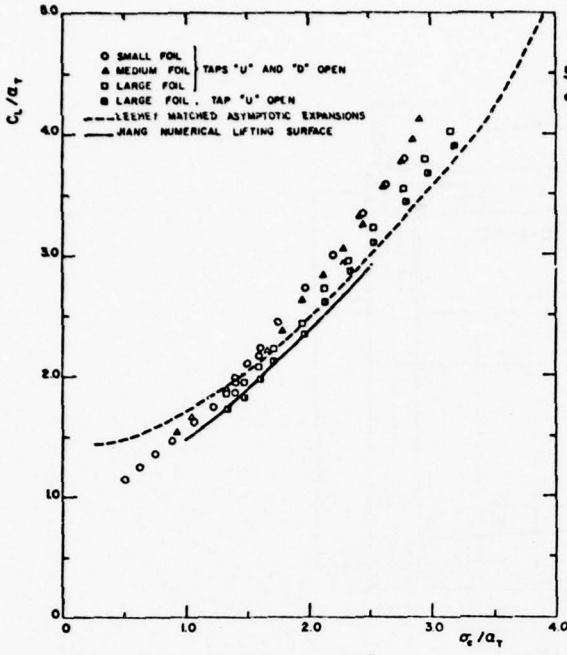

FIG. 4: C_L/a_T vs σ_c/a_T, $\alpha = 14.0°$

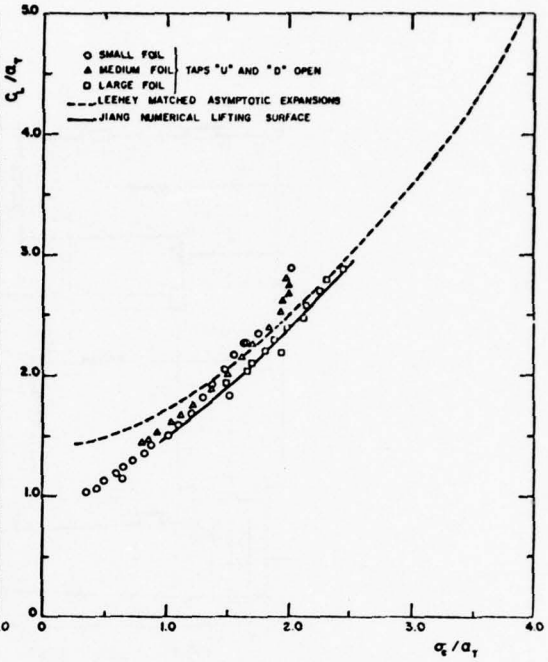

FIG. 5: C_L/a_T vs σ_c/a_T, $\alpha = 21.0°$

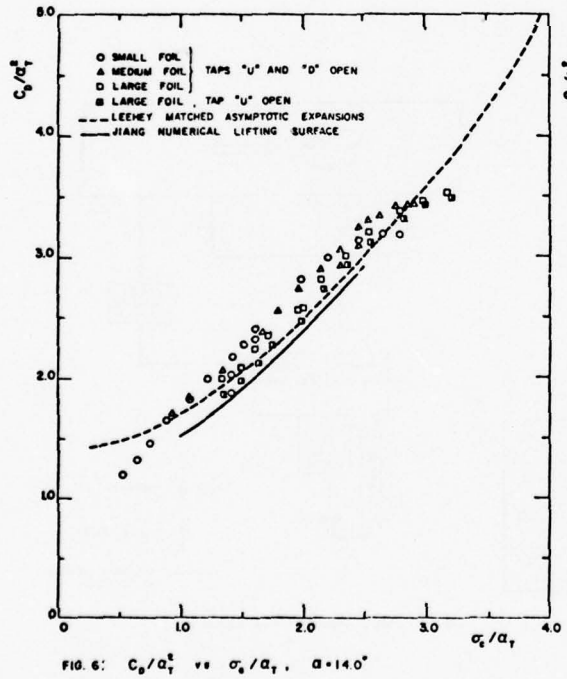

FIG. 6: C_D/a_T^2 vs σ_c/a_T, $\alpha = 14.0°$

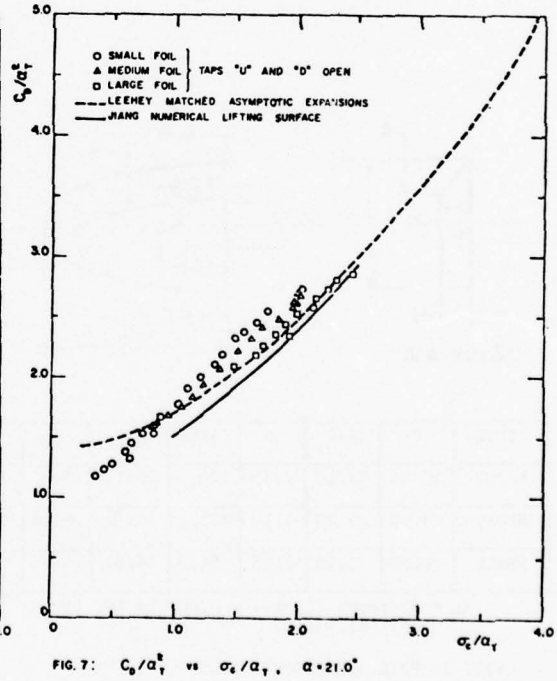

FIG. 7: C_D/a_T^2 vs σ_c/a_T, $\alpha = 21.0°$

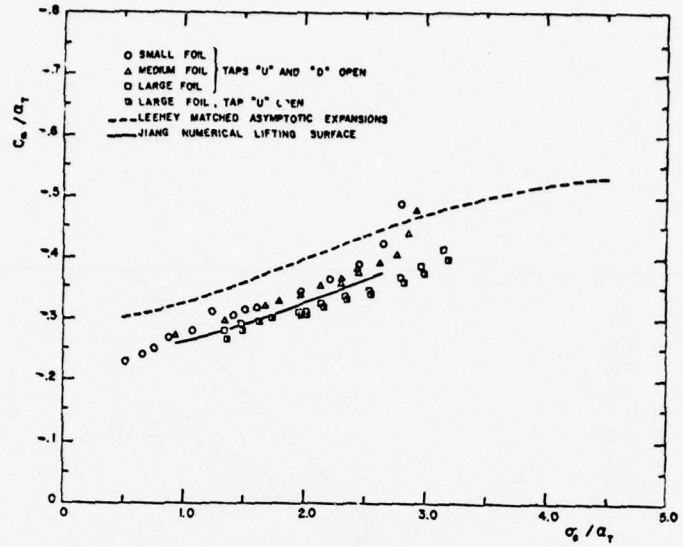

FIG. 8: C_m / α_T vs σ_s / α_T, $\alpha = 14.0°$

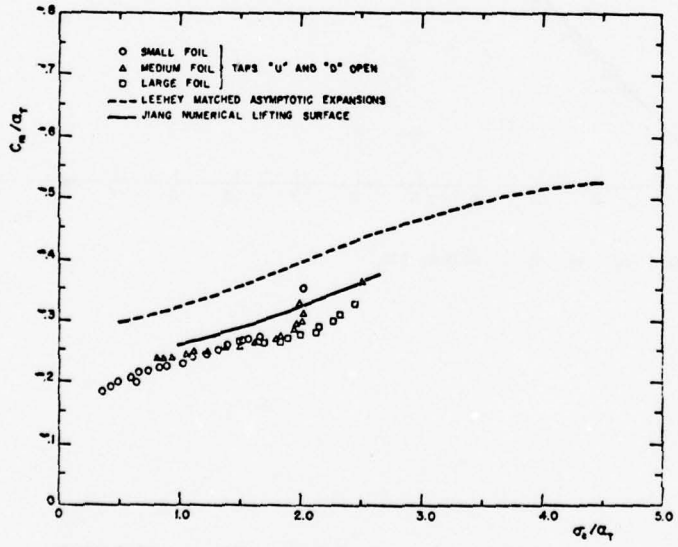

FIG. 9: C_m / α_T vs σ_s / α_T, $\alpha = 21.0°$

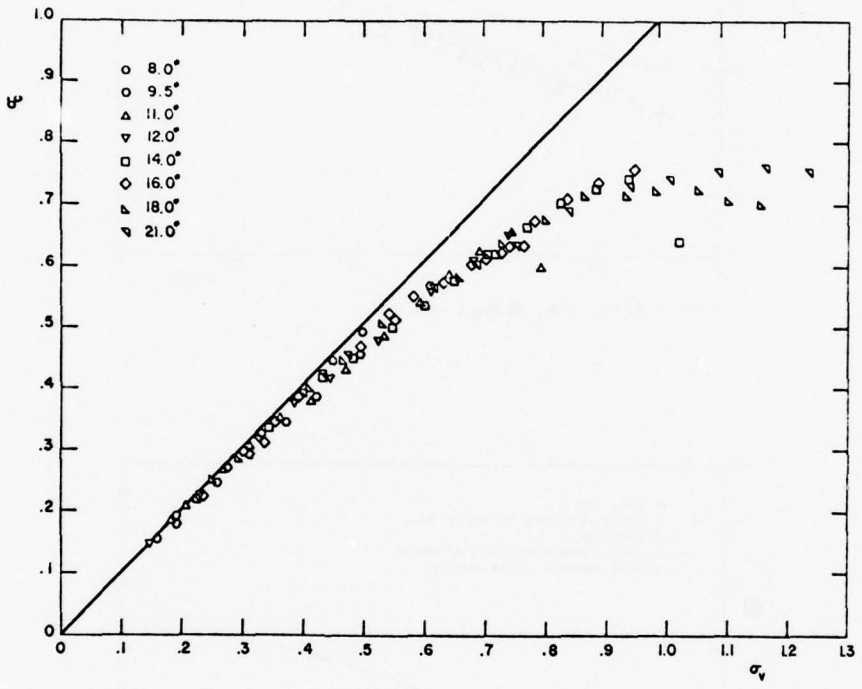

FIG. 10: σ_c vs σ_v, MEDIUM FOIL

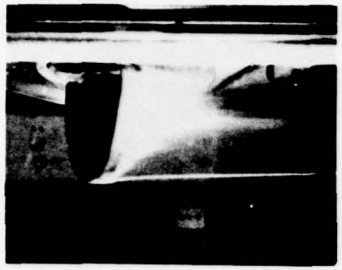

(a) SMALL FOIL: $\alpha = 12^\circ$, $\sigma_c = .3545$, $L/c = 1.3$

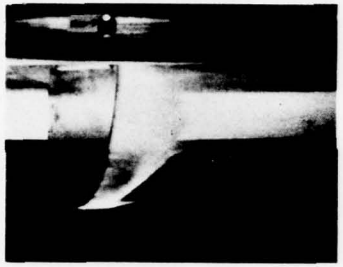

(b) MEDIUM FOIL: $\alpha = 12^\circ$, $\sigma_c = .3473$, $L/c = 1.55$

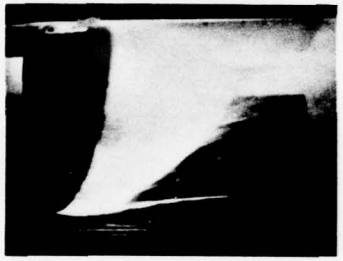

(c) LARGE FOIL: $\alpha = 12^\circ$, $\sigma_c = .3265$, $L/c = 2.1$

FIG. 11: COMPARISON OF CAVITY LENGTHS

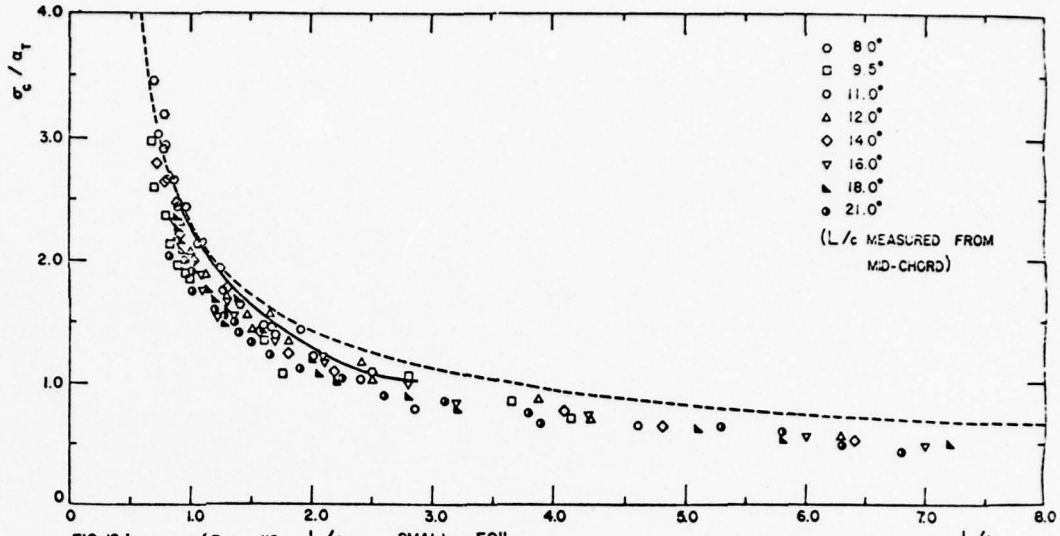

FIG. 12: σ_c / α_T vs L/c, SMALL FOIL

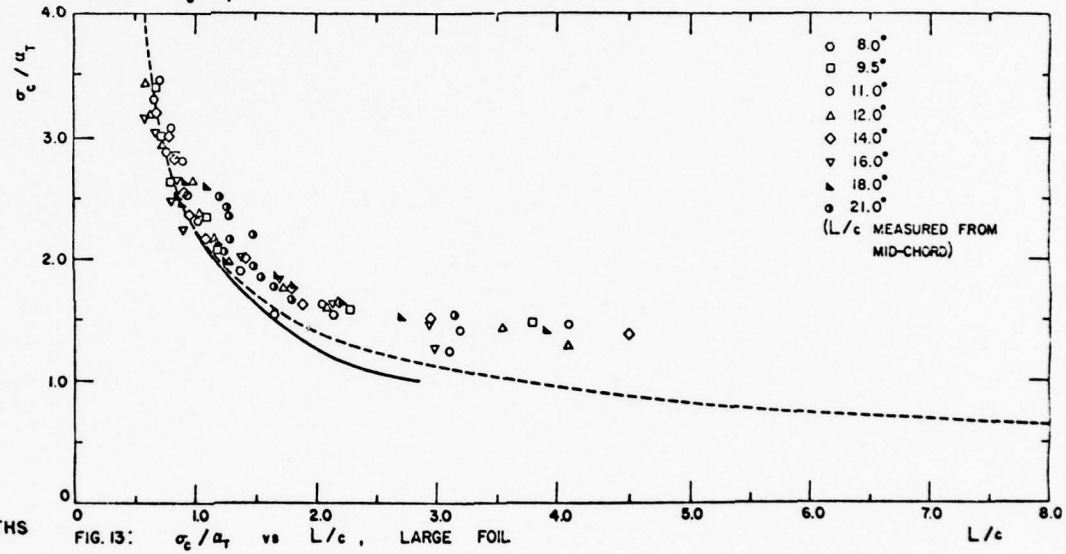

FIG. 13: σ_c / α_T vs L/c, LARGE FOIL

LEADING EDGE CAVITATION ON LIFTING SURFACES WITH THICKNESS

by

M. P. TULIN and C. C. HSU
HYDRONAUTICS, Incorporated

The extent and volume of partial cavities on lifting hydrofoil sections are very important in determining the unsteady pressures generated by their growth and collapse. In turn, the cavity volume itself depends on the foil shape and particularly on flow near the leading edge and the foil thickness distribution near the nose. The determination of time-varying partial cavities on a propeller blade is made extremely difficult on account of both finite span effects and flow unsteadiness. As a step in the direction toward a more complete theory, a new treatment of leading edge cavitation in steady flow around lifting surfaces with thickness have been developed by Tulin and Hsu in [1]. The theory assumes that the flow around the lifting surface without cavitation is known in advance and then perturbed by the leading edge cavity. The cavity is assumed to be short in extent compared with its span so that the perturbed flow may be treated as two-dimensional. In the following, some numerical results, based on the approach of [1], for various hydrofoil sections are presented. The symbols used in the figures are listed below:

L_o = lift without cavitation

L_1 = additional lift due to cavitation

V_c = cavity volume

k = camber parameter

ℓ = foil chord

r_n = nose radius of foil

α = incidence

σ = cavitation number

τ = foil thickness

AR = aspect ratio

Flat Plate

The results for flat plate of zero thickness are shown in Figure 1. It is interesting to note that the cavity length calculations agree with the conventional linearized results of Acosta, [2], in the limit of small α, but diverge significantly for angles beyond 5° or so; however, the non-linear effects on cavity length are in good agreement with the non-linear calculations of Kutznetzov and Terentev, [3], based on the re-entrant jet model.

Bi-Convex

Calculations have also been made in the case of a symmetric foil with circular-arc thickness and sharp leading and trailing edges. The results are shown in Figure 2 where a comparison is made with the experimental data of Meijer, [4], for a bi-convex foil of four percent thickness and for angles of 2, 3, and 4 degrees. The agreement is generally good; there is a tendency for the measured cavity length to be somewhat less than predicted.

Flat Plate with Thickness

The profound effect of the fully wetted flow immediately at the leading edge is demonstrated in the case of a flat plate with small constant thickness which is rounded off at the nose to a radius r_n. The results are shown in Figure 3. The calculations show that leading edge radius ameliorates the effect of incidence; a radius of only 0.5 percent reduces the cavity volume by something like an order of magnitude. This effect demonstrates: (i) the central importance of leading edge radius in determining short cavity effect; (ii) the advantage of the approach of [1], which does deal adequately with the rounded leading

edge, while conventional linearized does not at all.

High Speed Foil, NACA 16 Series

These foil involve camber and thickness distributions providing good cavitation characteristics when operated at or near their design incidence (on the bottom of the cavitation bucket). We have carried out calculations for two-dimensional (AR = ∞) 16 series (modified camber line 0.8) with the following characteristics:

$\tau/\ell = 6\%$; k = 0; $\alpha = 2,3,4,6^{\circ}$

$\tau/\ell = 6\%$; k = 0, 0.1, 0.2; $\alpha = 4^{\circ}$

$\tau/\ell = 0,6,9,12\%$; k = 0; $\alpha = 4^{\circ}$

and the results are shown as Figures 4-6. It is to be noted that increasing design camber increased cavity volume, while increasing thickness decreases volume especially for thickness beyond nine percent.

Elliptic Wings with 16 Series Sections

The approach of [1], assuming as it does the fully wetted flow, would seem applicable to wings of finite aspect ratio, at least in the limit of short cavities. The idea is to treat the perturbed flow at a given spanwise section as two-dimensional in view of the high aspect ratio of the cavity. In doing so, of course, it is essential to take into account the effect of finite span on the fully wetted velocity distribution. It is only in this way that the effect of finite span enter this approximate strip-like theory. We treat elliptic wings here, using the appropriate but simple corrections of R. T. Jones, [5], for the estimation of the fully wetted flows.

Calculations have been carried out for wings with the following characteristics:

$\tau/\ell = 6\%$; k = 0; $\alpha = 4^{\circ}$; AR = $2,4,8,\infty$

$\tau/\ell = 0,6,9,12\%$; k = 0.1; $\alpha = 6^{\circ}$; AR = 2

The cavity volumes, Figure 7, are seen to be markedly affected by aspect ratio, especially for smaller values, which are of a magnitude appropriate to propellers. This result, approximate as it is, does suggest

that two-dimensional estimates of short cavities, whether based on theory or experiment, are likely significantly to overpredict both the occurrence and severity of leading edge cavitation. The importance of foil thickness (leading edge radius) in the case of finite span wings is shown by the calculations, Figure 8, especially for large values of α/σ.

The importance of leading edge radius in controlling the properties of partial cavitation is clearly demonstrated from the above calculations. These results suggest that foils selected for minimization of short cavity volume should have larger values of leading edge radius than are normally associated with foils designed to optimize inception characteristics at design incidence (i.e., shock-free entry). The result for wing also shows the marked effect of aspect ratio, revealing the importance of considering the finite span effect in both design and estimation and in the interpretation of test results.

REFERENCES

1. Tulin, M. P. and C. C. Hsu, "The Theory of Leading Edge Cavitation on Lifting Surfaces with Thickness," Symposium on Hydrodynamics of Ship and Offshore Propulsion Systems (Sponsor: DET NORSKE VERITAS), March 1977, Oslo, Norway.

2. Acosta, A. J., "A Note on Partial Cavitation of Flat Plate Hydrofoils," California Inst. Tech. Hydrodynamic Lab. Report No. E19.9, 1955.

3. Kutznetzov, A. V. and A. C. Terentev, "On Analysis of Partially Cavitating Flow Around Flat Plate," Izvestia Vysshikh Uchebnykh Zavedenii Mathematika No. 6 (97), 1970.

4. Meijer, M. C., "Some Experiments on Partially Cavitating Hydrofoils," Inter. Shipbuilding Progress, Vol. 6, No. 60, 1959.

5. Jones, R. T., "Correction of Lifting Line Theory for the Effect of Chord," NACA TN 817, 1941.

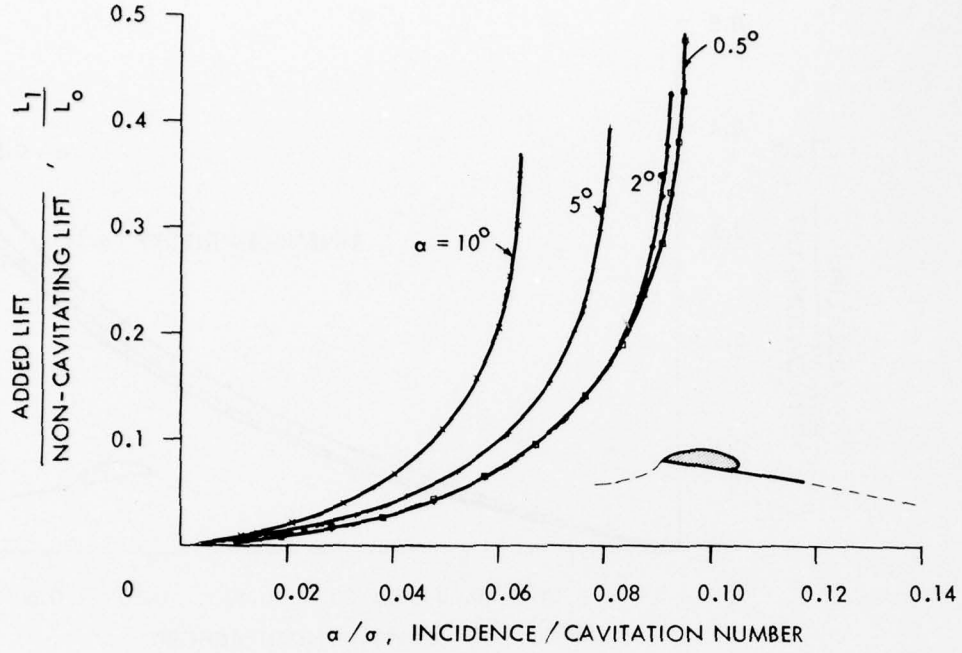

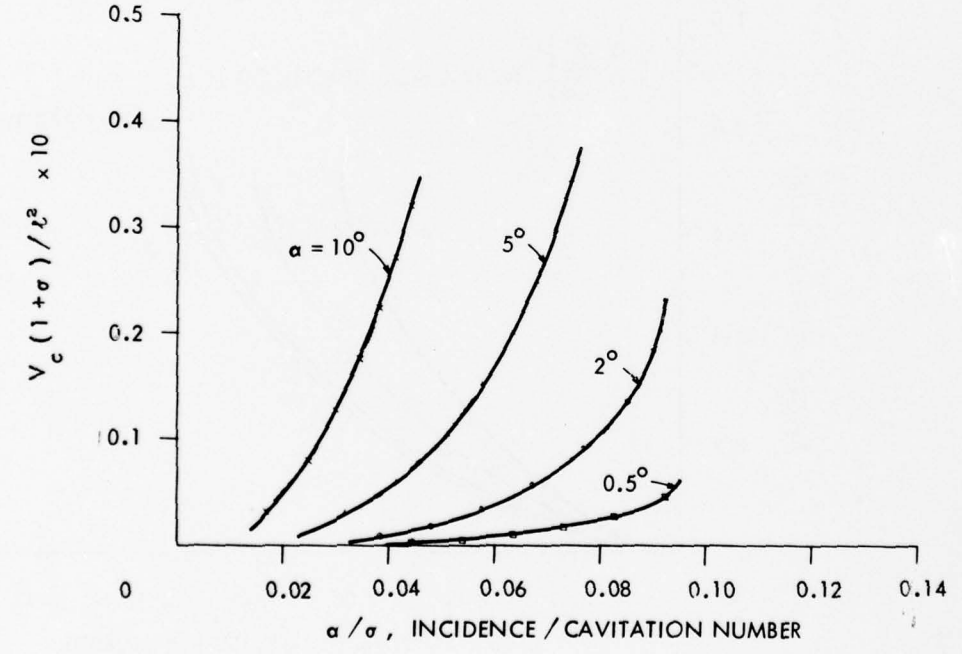

FIGURE 1a - FLAT PLATE FOIL CHARACTERISTICS WITH SHORT CAVITY
$\tau / \ell = 0$; AR = ∞; α = 0.5 - 10.0°

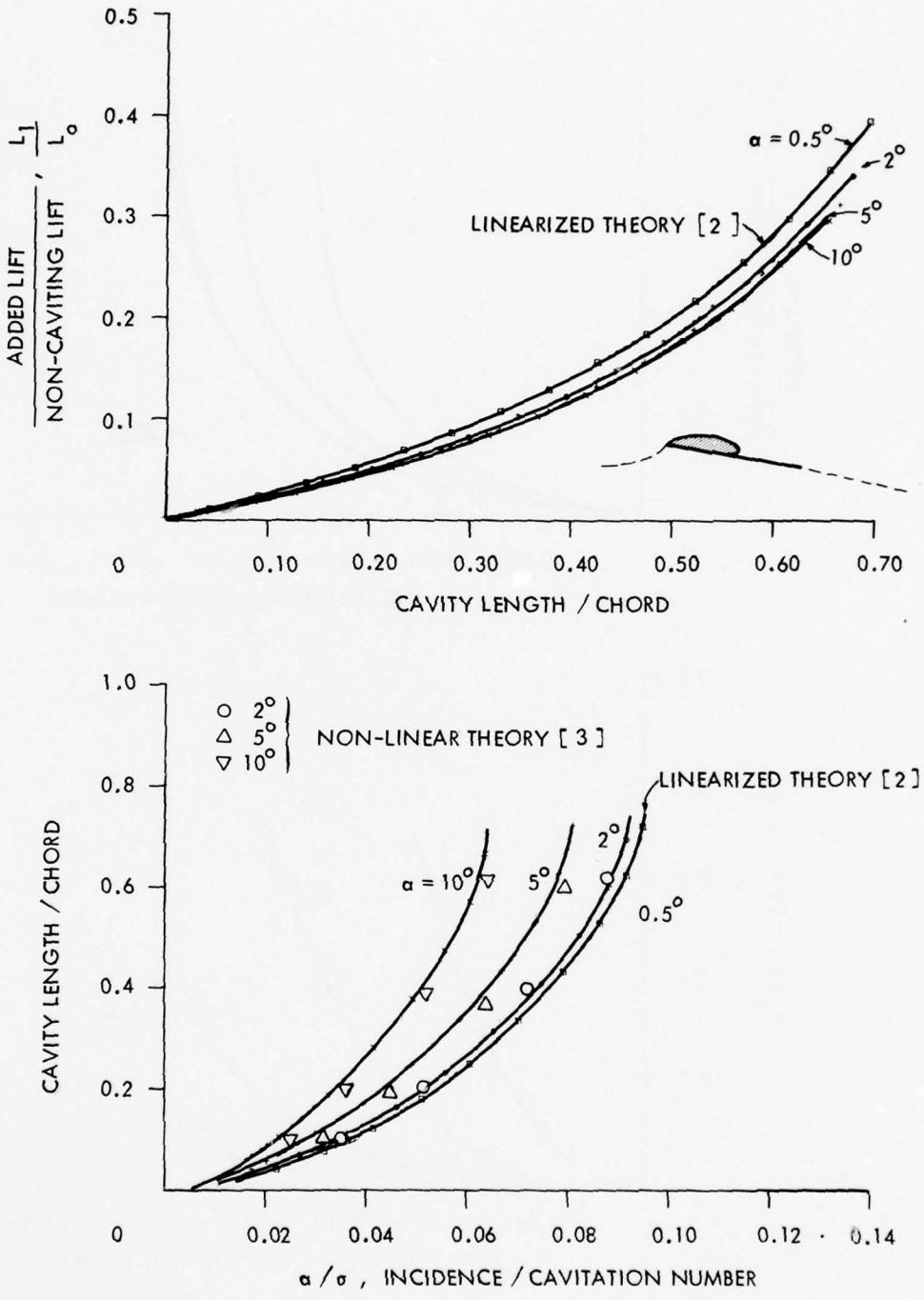

FIGURE 1b - FLAT PLATE FOIL CHARACTERISTICS WITH SHORT CAVITY
$\tau / \ell = 0$; AR = ∞; α = 0.5 - 10.0°

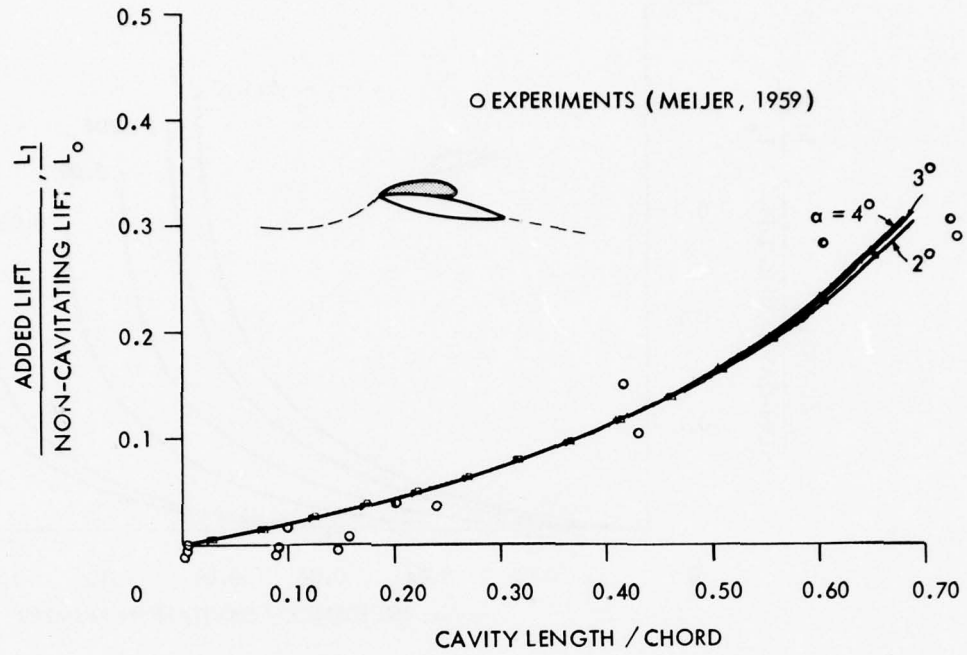

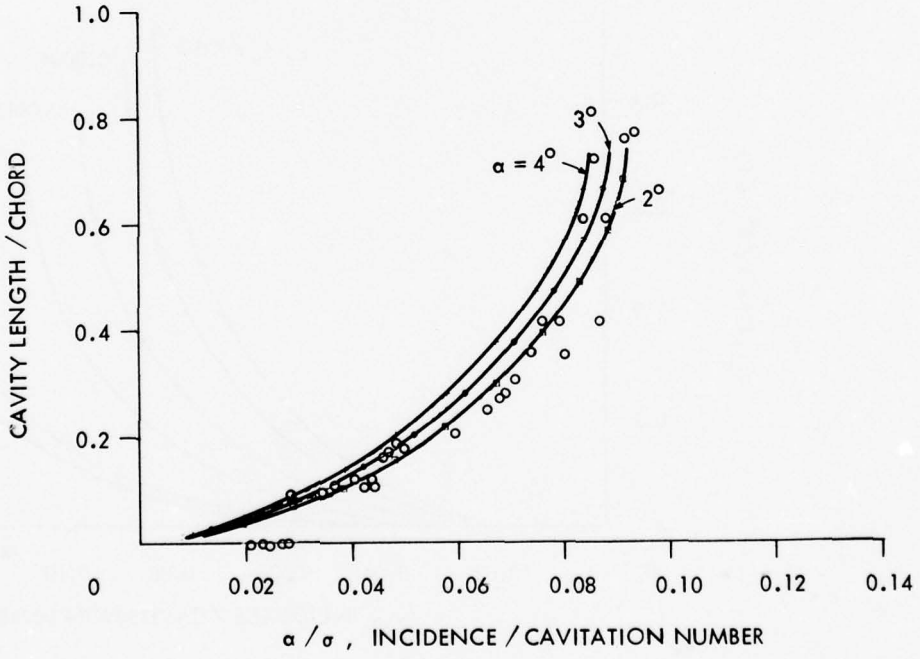

FIGURE 2 - BI-CONVEX FOIL, CHARACTERISTICS WITH SHORT CAVITY
$\tau / \ell = 4\%$; AR = ∞; α = 2,3,4°

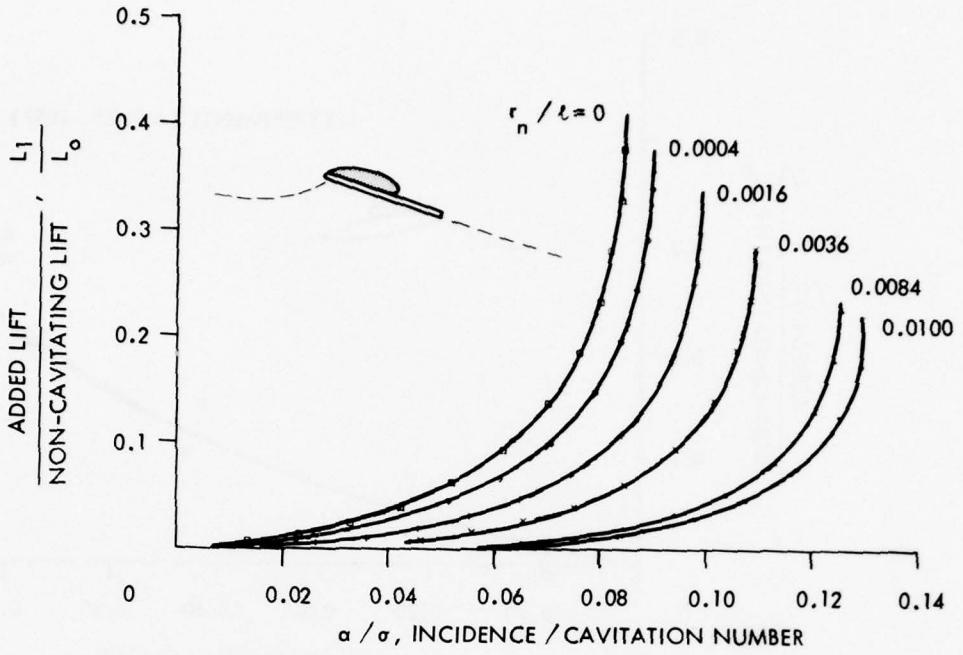

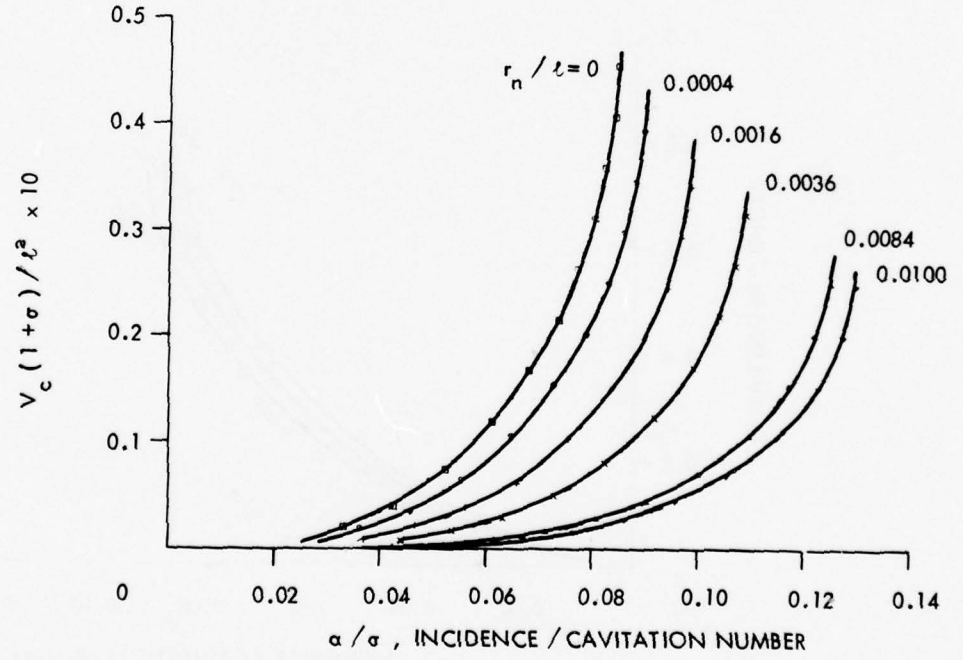

FIGURE 3 - FLAT PLATE WITH CONSTANT THICKNESS AND ROUNDED LEADING EDGE, CHARACTERISTICS WITH SHORT CAVITY
AR = ∞; r_n/ℓ = 0-1%; α = 4°

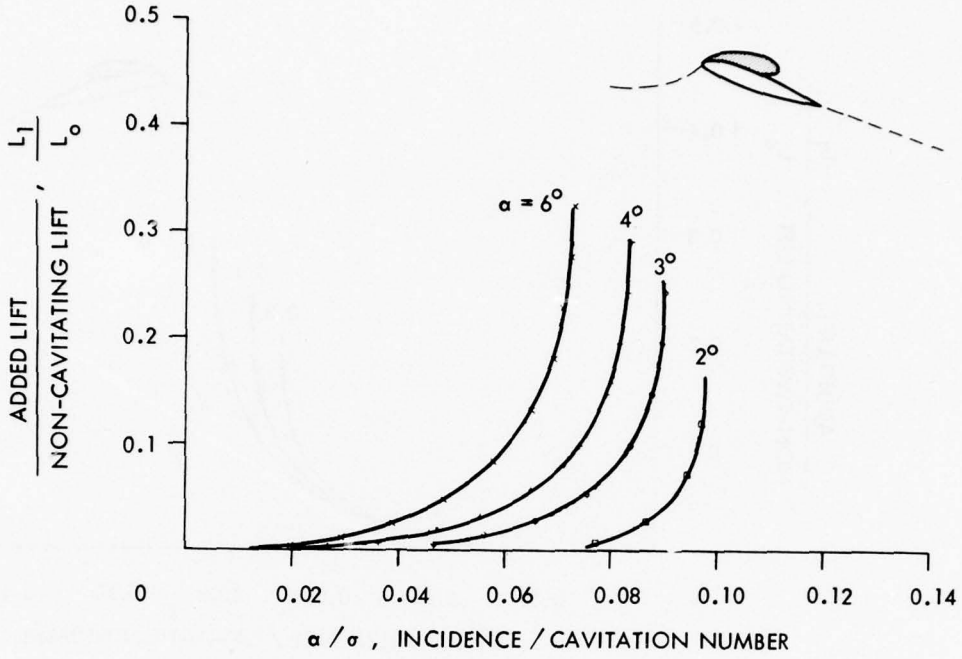

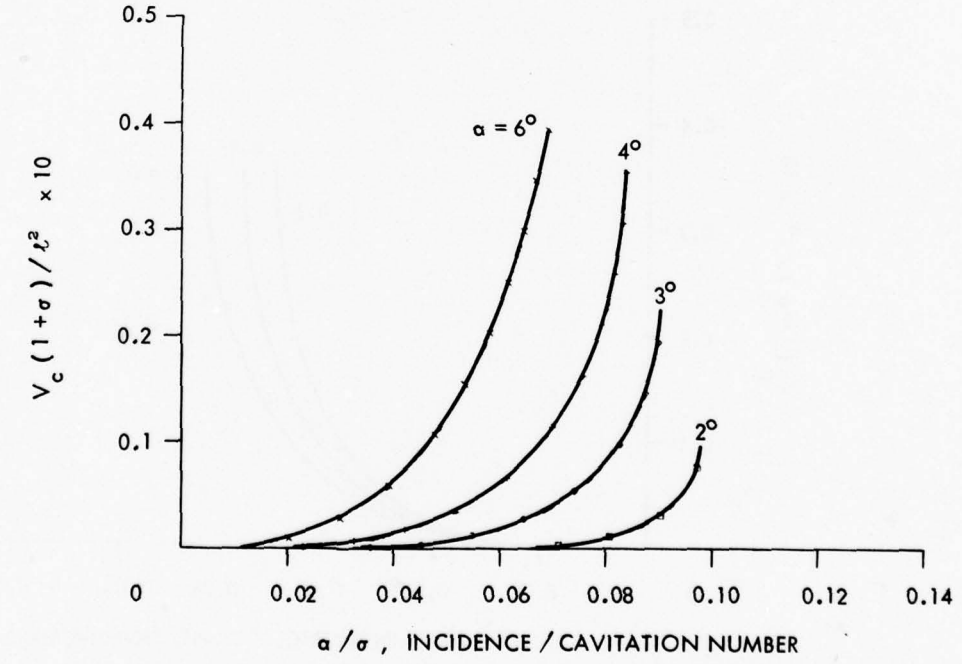

FIGURE 4 - SERIES 16 FOILS, SHORT CAVITY CHARACTERISTICS
AR = ∞; τ/ℓ = 6%; α = 2 - 6°; k = 0

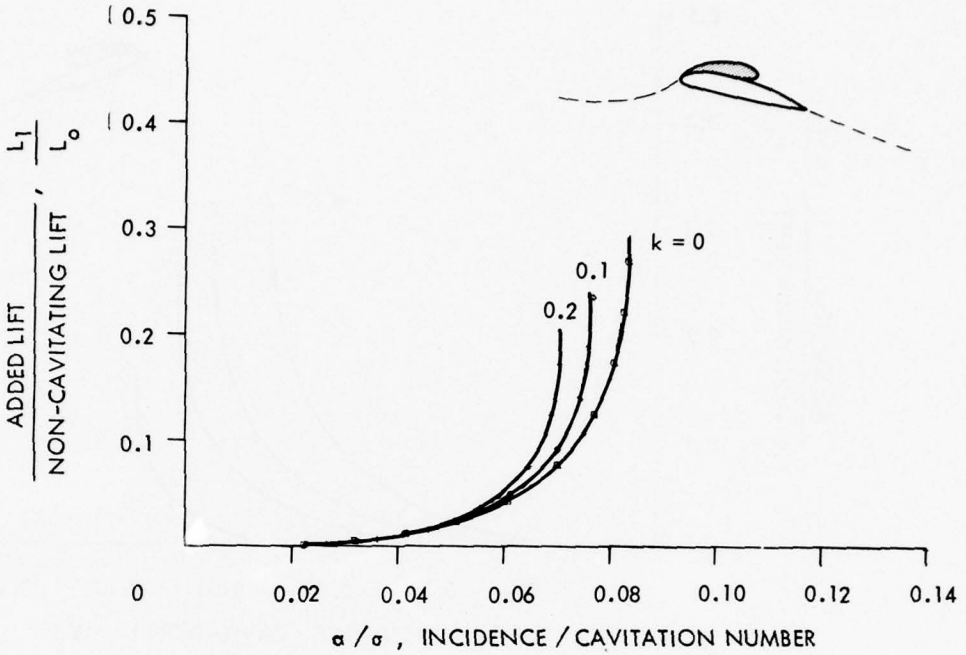

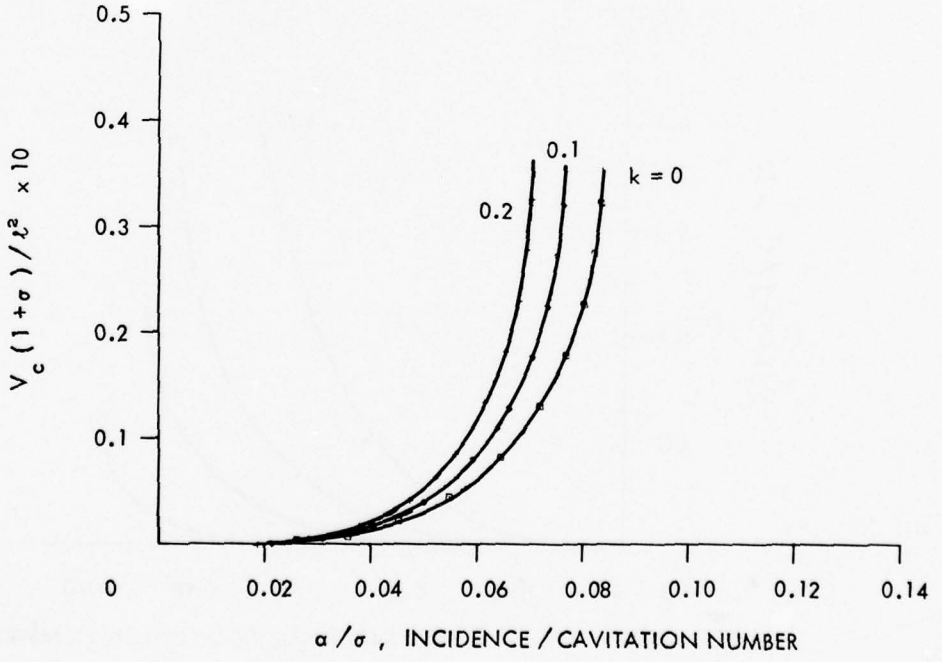

FIGURE 5 - SERIES 16 FOILS, SHORT CAVITY CHARACTERISTICS
AR = ∞; τ/ℓ = 6%; α = 4°; k = 0, 0.1, 0.2

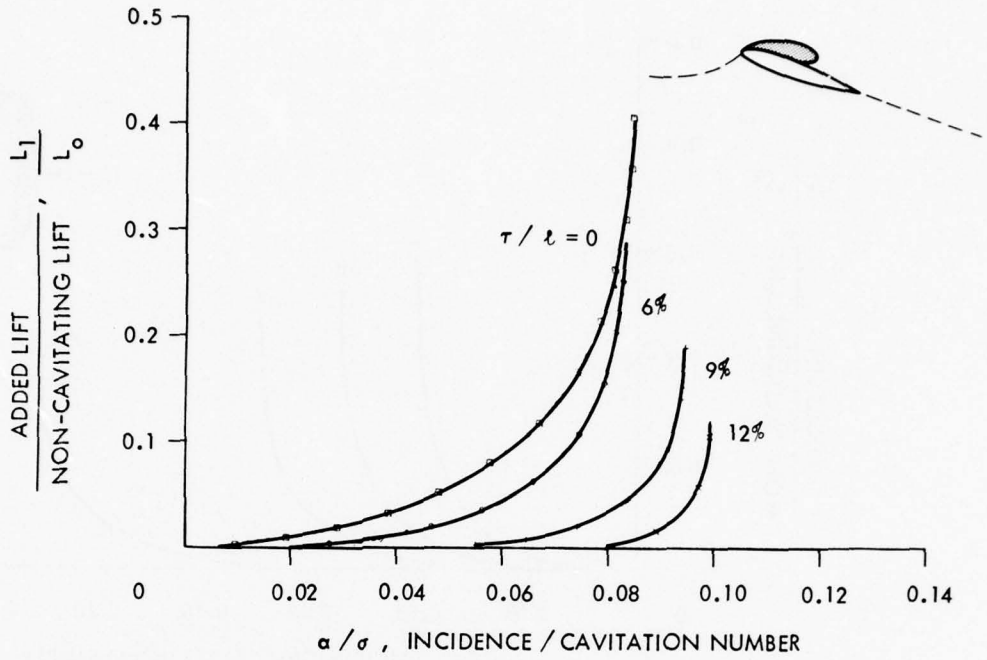

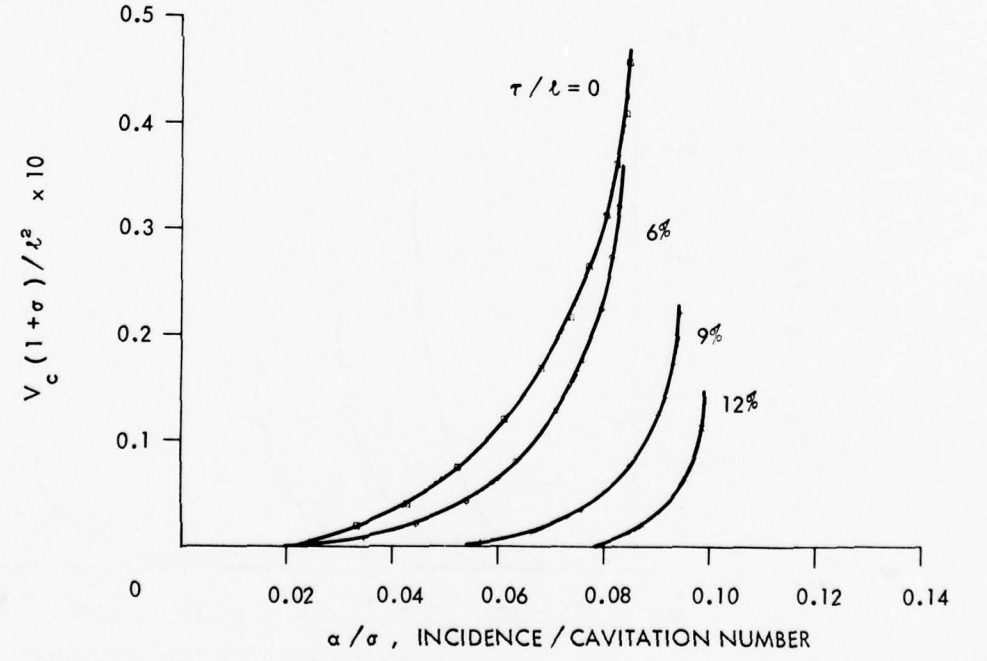

FIGURE 6 - SERIES 16 FOILS, SHORT CAVITY CHARACTERISTICS
AR = ∞; τ / ℓ = 0, 6, 9, 12%; α = 4°; k = 0

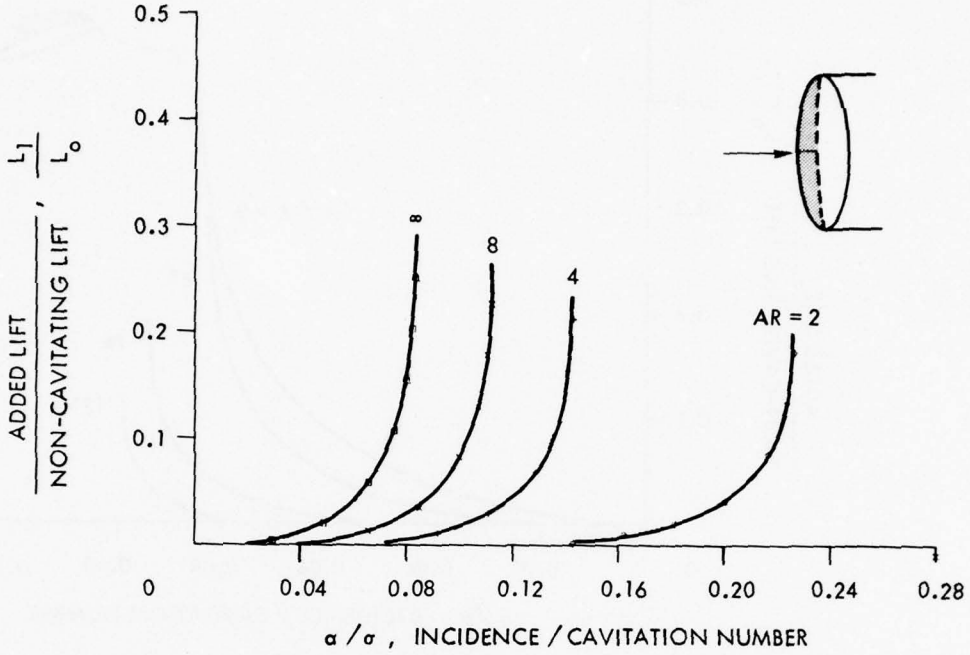

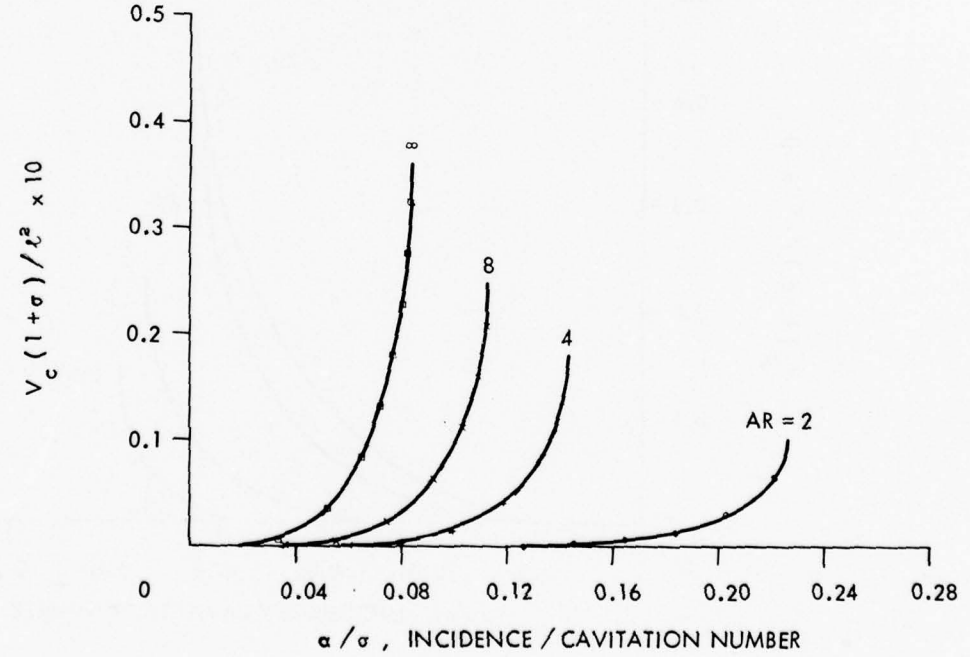

FIGURE 7 - SERIES 16 ELLIPTIC WING, SHORT CAVITY CHARACTERISTICS
AR = 2, 4, 8, ∞; $\tau/\ell = 6\%$; $\alpha = 4^\circ$; k = 0

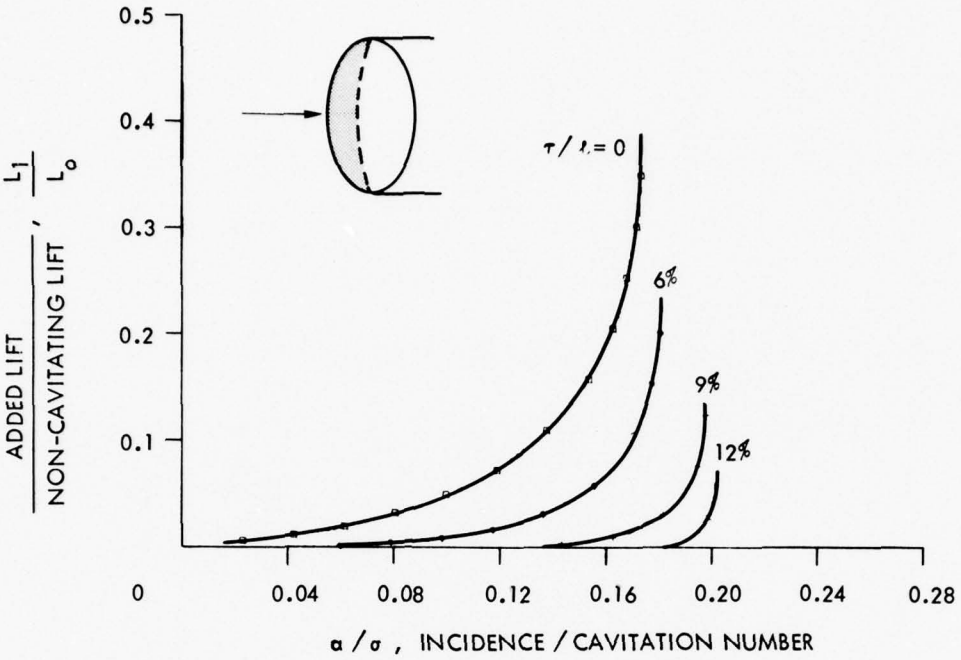

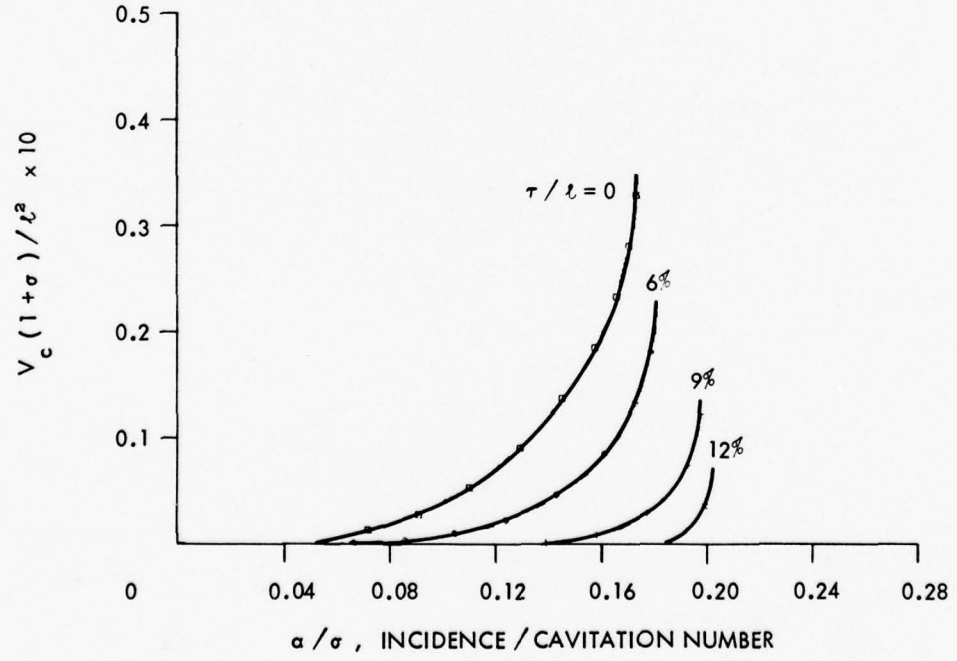

FIGURE 8 - SERIES 16 ELLIPTIC WING, SHORT CAVITY CHARACTERISTICS
AR = 2; τ / ℓ = 0, 6, 9, 12%; $\alpha = 6^{\circ}$; k = 0.1

APPLICATION OF A CAVIJET™ SYSTEM FOR REMOVING MARINE FOULING AND RUST

by

Andrew F. Conn
HYDRONAUTICS, Incorporated

SUMMARY

The CAVIJET™ is a turbulent water jet in which vapor and gas cavities are deliberately stimulated to enhance the destructive power of a relatively low velocity jet. This paper describes a systematic, ongoing study of the parameters required for new commercial CAVIJET™ equipment to remove marine fouling and rust from ship hulls and other surfaces, either in drydock or while submerged. In laboratory trials, fouling from submerged panels was removed at 100 m^2/hr (1030 ft^2/hr) using two 3.2-mm (⅛-in.) diameter CAVIJET nozzles at 13.8 MPa (2000 psi) at a power cost of only 1.5¢/m^2 ($1.50 per 1000 ft^2). For severely rusted steel panels, cleaning rates better than conventional techniques are possible by using a twin CAVIJET system at 41.4 MPa (6000 psi). Field trials of this system are now underway.

1. INTRODUCTION

The air and water pollution and cleanup problems associated with surface preparation by sand or grit blasting has made this process very undesirable and there is a growing trend toward banning this process in many areas. In addition, such sand and grit blasting techniques cannot be performed on submerged areas. For these reasons considerable attention has been focused on the use of high pressure, steady jets of water for cleaning purposes. The CAVIJET cavitating water jet delivers a much higher cleaning rate for the same jet velocity, and it is therefore a safer and more economical device than a high pressure steady jet. Steel test panels, either covered with fouling, or severely rusted and pitted, were used to make this study in the laboratory. Details may be found in the report (Reference 1) presented to the sponsoring agency* which

---

* The U. S. Maritime Administration under Purchase Order No. RT-3700 with Todd Research and Technical Division for the National Maritime Research Center, Galveston, Texas.

describes the first phase of this program. Under Phase II, now underway**, a CAVIJET fouling removal system is now being evaluated on ship hulls.

The cavitating water jet represents one of the few successful attemps to harness the destructive power of cavitation which for decades has plagued the designers of hydrodynamic equipment. In its most basic conceptualization, the CAVIJET technology involves the growth of vapor filled cavities within a relatively low velocity jet, which later collapse in the high pressure stagnation region where the jet impacts the material. Since the collapse energy is concentrated over many very small areas of collapse, extremely high localized stresses are produced. This local pressure amplification provides the cavitating water jet with a great advantage over steady noncavitating jets operating at equivalent pump pressures and flow rates.

2. LABORATORY FACILITY

An experimental facility was designed and built at HYDRONAUTICS, Incorporated for studying and developing practical devices which utilize the cavitating water jet principle. The primary components of the facility, shown schematically in Figure 1, include a pump, reservoirs to recover and store the water, suitable filters, controls, pressure and temperature gages, flow measuring devices for precisely measuring all system parameters, and a large test chamber which contains an hydraulic cylinder for translation of the CAVIJET nozzle relative to test specimens at precisely controlled rates of motion and at any desired angle of attack. Within this new test chamber, tests may be conducted on specimens either in air or in a submerged configuration.

Three nozzle configurations were used in these tests. The first was the center body configuration (see Figure 2) while the second was the turning vane configuration, also shown in Figure 2. The third configuration, to be referred to as the "plain" nozzle, was the basic CAVIJET nozzle housing without the use of either the center body or the vanes. It was found that essentially the same results were obtained with either the vanes or the plain nozzle. The center body configuration tended to give a more complete cleaning over a narrower path relative to the results with the plain nozzle. However, as the cavitation pattern from the plain nozzle tended to give a wider cleared path for any given test condition, it was decided early in the program to concentrate on the use of the plain CAVIJET nozzle for most of these tests.

** Contract No. 7-38001 from the U. S. Maritime Administration.

3. MATERIALS TESTED

The fouled panels were provided by Miami Marine Research, Incorporated (MMRI), located in South Miami Beach, Florida. This company specializes in the exposure and testing of various types of anti-fouling systems and concepts. The rusted panels were provided by the Todd Research and Technical Division in Galveston, Texas.

3.1 Fouled Panels

The majority of the panels used for fouling exposures were cut from 12 gauge steel plate into 0.3 x 0.3 m (12 inch by 12 inch) squares. The panels were sandblasted prior to spray painting. The coating applied to the panels is a commercial epoxy-phenolic primer, known as "Rust Ban", manufactured by EXXON, and is designated EP6841. The color designation is Oxide Red. After the paint had dried, it was scrubbed by hand with soap and water to remove any residual oils which might tend to delay the on-set of fouling. In this manner the fouling process was accelerated as much as possible. This process has resulted in the majority of the panels received from MMRI being uniformly encrusted with the number and size of barnacles required to acquire reproducible and meaningful test results.

Barnacles, plus Encrusting Bryozoan, and Tube Worms, comprise the primary types of encrusting marine organisms found on our test panels; that is, the organisms which are the most difficult to remove, and hence of main interest in these fouling removal tests with the CAVIJET. Air shipment of the panels, in wet wrappings, from Biscayne Bay to the specimen holding tank in the laboratories of HYDRONAUTICS, Incorporated was used so as to minimize the time the organisms were out of the water and thereby keep as many alive as possible. It should be emphasized that, dead or alive, the barnacles and other encrusting organisms are equally difficult to remove. However, from the point of view of odors and handling, it was extremely desirable to keep the fouling alive.

Also, we have observed that the difficulty of barnacle removal seems to be quite independent of the size; that is, barnacles larger than 10 mm in diameter are no more difficult to remove than those which are only about 2 or 3 mm in diameter. Thus, if sufficient encrustation on these panels of reasonably sized barnacles (larger than about 2 or 3 mm in diameter) is available, so that a clear contrast can be made between a cleared path and the uncleared panel areas, then valid test results were achieved. Depending on the time of year, the desired barnacle conditions required immersion times which varied from 10 to over 30 weeks.

3.2 Rusted Panels

The rusted panels, which were from large steel plates 3.2 to 6.4 mm ($\frac{1}{8}$" to $\frac{1}{4}$") thick, were cut into twenty-four 0.3 x 0.3 m (12 in. by 12 in.) squares and left near the shore in order to be exposed to salt spray. The total exposure time of these panels is not known as the prior experience of the large plates was not recorded. However, once cut into panels they were exposed for about six months. As desired, considerable variation in the nature of the rust on these panels was available, which provided a broad spectrum of test results with the CAVIJET. Although all the panels were received with a heavy reddish oxide coating, this loose scaly material came off quite easily under exposure to the CAVIJET. Once this outer scale was removed, the various degrees of locked-on rust were exposed and all test results are reported relative to the removal of the hard rust underneath.

4. LABORATORY TEST RESULTS

4.1 Description of Parameters

During this investigation the following parameters were varied: translation rate, nozzle pressure, stand-off distance, flow rate, impingement angle, nozzle size and configuration, and operating mode. From these parameters and the measured width of cleared path, other variables such as delivered hydraulic power, cleaning rate, input power, system size and weight, power and cleaning costs per square foot can be derived. In this section we will describe the effects of some of these parameters on rates of fouling and rust removal.

4.1.1 System Parameters

The three system parameters which are the essential variables in these tests are the nozzle size and configuration, the nozzle pressure, and the flow rate. From the values of pressure and flow rate the delivered hydraulic power can be calculated. Two CAVIJET nozzle sizes were used in the fouling removal and rust removal tests, a nozzle with a 3.2 mm ($\frac{1}{8}$-in.) orifice diameter and one with a 6.4 mm ($\frac{1}{4}$-in.) orifice diameter. For convenience these will usually be referred to merely as the $\frac{1}{8}$-in. and the $\frac{1}{4}$-in. nozzles from now on in this paper.

4.1.2 Operational Parameters

The parameters which might be varied during the operation of the CAVIJET for fouling and rust removal include the translation velocity, the stand-off distance, the impingement angle, the operating mode, and various other operational factors such as the use of multiple nozzles,

rotation of one or more nozzles, and the use of drag reducing polymers in the jet flow. The translation velocity, V, in cm/min (ipm: inch per minute) was measured during each test using a stop watch to determine the travel time over a premeasured distance. The translation was made with the test panel in a predetermined position and the nozzle moving in a straight line above the surface of the panel. The stand-off distance was pre-set before each test and was measured as the distance between the face of the nozzle and the surface of the steel panel.

The impingement angle refers to the angle between a normal vector to the surface and the jet direction vector. This angle may have two different orientations. In the "in-plane angle" case, the flow of the jet across the panel is ahead; i.e., in the same direction as the translation velocity, and hence washes across areas which will subsequently be directly impinged by the primary cavitation action. However, in the "out-of-plane" case, the washing of the flow across the panel after impingement is in a direction which is perpendicular to the translation of the jet.

Tests were run with both in-plane angles of impingement as well as out-of-plane angles. Although some slight improvement was seen with the out-of-plane configuration, the results were not substantially different than those with the jet perpendicular to the panel surface. Thus for hand-held operation of a CAVIJET hull cleaning lance, it will not be necessary for the operator to always keep the jet directed perpendicularly to the surface. Indeed, if he sweeps left-to-right, using the out-of-plane orientation, some improvement in cleaning rate will be made.

Three operating modes were used in these tests: in air, submerged, and artificially submerged operations. The submerged tests were performed with the test panels submerged at a depth of about 0.3 m (12 inches), Several methods were used to provide artificial submergence of the jet flow; that is, with the test panel in air but with a means provided to surround the high velocity jet with relatively slow or stagnant water. Two different types of methods were used to provide this artificial submergence: (a) "mechanical sheathing", where a container surrounding the nozzle reaching to, or near to, the surface to be cleaned, traps a volume of the water from the CAVIJET; and (b) "dynamic sheathing", using low pressure, low velocity water from a secondary pump, which flows around the high velocity CAVIJET water.

A few tests were run with a long-chain polymer introduced into

the jet flow. With up to 1000 ppm of this polymer, no changes in the cleaning rates were detected.

4.1.3 Performance Parameters

The parameter which was used to evaluate performance is the width of the cleared path. The typical cleared pattern (see Figure 5) consists of a central region which is totally cleared of all protruding marine growth except for some remaining traces of the barnacle "feet" (adhesive) on the panel. As these "feet" are less than 0.18 mm (0.007 inches) thick, and usually only about 0.08 to 0.12 mm (0.003 to 0.005 inches), these may be painted over in service. This fits standard sand-sweeping practices. Thus, the "cleared path width", w, was defined as that width where only some barnacle adhesive pads remained, but no barnacle shells or any other crustaceans. On either side of this totally cleared path is a region wherein approximately 80 percent of the barnacles are moved. This partially cleared part of the path is often twice as wide as the totally cleared path. However, in all of the path widths reported, we refer only to the cleared path width, w.

The cleaning rate, A, in m^2/hr (ft^2/hr) was calculated as the product of the path width, w, and the translation velocity V. An "area effectiveness", e_A, which indicates the area rate of clearing per unit of power, was derived by dividing A by the hydraulic power in kw (hp).

4.2 Some Test Results

4.2.1 Fouling Removal

A summary of some of the results from fouling removal tests are shown in Figure 5. Here, we compare the submerged operating mode for the $\frac{1}{8}$-in. and $\frac{1}{4}$-in. CAVIJETS. These curves are the averaged results from curves which were faired through the arithmetic averages of individual data points. At least three, and usually more, measurements were made at each translation velocity. For the velocities of interest (namely above 12.7 m/min (500 ipm)) and discarding an occasional very high or low width measurement, the faired curves for submerged testing fell within a scatter band of about $\pm$15 to $\pm$20 percent.

Similar comparisons were made for in-air operation, and the highlights of these are seen in Table 1. In Figure 6, the cleaning rates derived from the widths in Figure 5 are plotted. It is seen that rates for the $\frac{1}{4}$-in. jet are about twice those achieved for the $\frac{1}{8}$-in. jet for the present values of operating conditions. However, since the power requirements at corresponding pressures are four times greater for the $\frac{1}{4}$-in.

CAVIJET, the most economical operation favors the use of two $\frac{1}{8}$-in. nozzles. Moreover, in laboratory testing, the use of two side-by-side $\frac{1}{8}$-in. CAVIJETS achieved cleaning rates greater than the single $\frac{1}{4}$-in. nozzle. With a spacing of 3.8 cm (1.5 in.) between the two submerged $\frac{1}{8}$-in. nozzles, at 22.9 m/min (900 ipm), cleaning rates of about 100 m^2/hr (1030 ft^2/hr) were achieved. The corresponding area effectiveness was 4.33 m^2/kw-hr (34.8 ft^2/hp-hr), almost three times that for the single $\frac{1}{4}$-in. CAVIJET.

A comparison of the three operating modes is given in Figure 7, for the $\frac{1}{4}$-in. nozzle operated at 13.8 MPa (2000 psi). As seen in Table 1, the cleaning rate for the dynamically sheathed $\frac{1}{4}$-in. CAVIJET is 69% greater than the in-air operation. This is 78% of the potential gain that is represented by the actual submerged operation relative to in-air cleaning rates.

The other operating parameters, namely, standoff distance and impingement angle, were found to have some influence on the test results. However, if kept within 3.2 to 6.4 cm ($1\frac{1}{4}$ to $2\frac{1}{2}$ in.) for $\frac{1}{8}$-in. jet and between 8.9 to 11.4 cm ($3\frac{1}{2}$ to $4\frac{1}{2}$ in.) for the $\frac{1}{4}$-in. jet, the results were within the general data scatter. The variations of impingement angle showed that slightly better results could be achieved with out-of-plane angles of 30 to 40 degrees between the normal to the plate and the jet direction.

4.2.2 Rust Removal

Preliminary rust removal testing with the CAVIJET had shown that although tests up to 13.8 MPa (2000 psi) are capable of providing the type of "white metal" finish required on steel surfaces prior to repainting, this process was extremely slow at these pressures. As the in-house facility at HYDRONAUTICS was capable of providing pressures only up to about 13.8 MPa (2000 psi) it was necessary to lease higher pressure equipment for this phase of the study. Two "Liqua-Blaster" units, manufactured by the PARTEK® Corporation, Houston, Texas, were rented for this purpose. The outputs from these two units were run in parallel into the test chamber in order to provide sufficient flow for the desired pressure range up to 41.4 MPa (6000 psi). Each of these units was rated for 0.63 liter/sec. (10 gpm) flow at 61.4 MPa (6000 psi). Thus, we were able to utilize an $\frac{1}{8}$-in. CAVIJET up to 41.4 MPa (6000 psi), as about 1.26 liters/sec. (20 gpm) is required for this nozzle at that pressure.

Tests were conducted with rusted panels, using both in-air and submerged modes, at pressures of 27.6 MPa (4000 psi) and 41.4 MPa

(6000 psi). At translation velocities less than 6.4 m/min (250 ipm) the results for submerged and in-air panels are the same at 27.6 MPa (4000 psi), namely, a fully cleared path width ("white metal") of about 6.4-mm ($\frac{1}{4}$-in.). However, at higher translation velocities, although the tests on the submerged panels continued to provide this same 6.4-mm ($\frac{1}{4}$-in.) width of cleared white metal, up to translation velocities of about 12.7 m/min (500 ipm), the fully cleared path for the in-air tests fell to a level only about half as wide. These differences between the in-air and the submerged CAVIJET are as usually encountered in drilling applications.

However, at a nozzle pressure of 41.4 MPa (6000 psi), the results for the submerged and in-air testing are essentially the same. Observation of the test panels suggest one may consider these data to actually represent a mean cleared white metal path of about 7.1 mm $\pm$0.8 mm (0.28 inches $\pm$0.3 inches) over the entire range tested up to about 12.7 m/min (500 ipm) at 41.4 MPa (6000 psi). This corresponds to a cleaning rate for a single $\frac{1}{8}$-in. nozzle of 5.6 m^2/hr (60 square feet per hour). From the work with twin $\frac{1}{8}$-inch nozzles, one might expect that for rusted panels two $\frac{1}{8}$-inch CAVIJETS would provide the cleaning rate of 11.1 m^2/hr (120 ft^2/hr), and perhaps higher due to jet interactions. If twin $\frac{1}{8}$-in. nozzles can indeed achieve 11 m^2/hr, this would exceed the rates of conventional dry sandblasting, which is generally below 9.3 m^2/hr (100 ft^2/hr), and would be comparable to wet sandblasting methods (Reference 4).

5. FIELD TRIALS

Under the second phase of this program, a system has been developed which is suitable for controlled testing of the CAVIJET method on actual ship hulls. This system, shown in Figure 8 being operated on a hull in drydock, has also been designed for underwater cleaning. A cleaning head, consisting of an array of six CAVIJET nozzles, each with an orifice diameter of 3-mm (0.120-in.) can be moved by hydraulic drives at translation velocities of over 0.9 m/s (3 ft/sec). Thus, potential cleaning rates of over 464 m^2/hr (5000 ft^2/hr) are indicated by some of the preliminary results from these field trials.

6. COMPARISONS WITH OTHER TECHNIQUES

A calculation was made to estimate the CAVIJET power costs per 1000 square feet of cleaned area. These calculations were based on a cost of five cents per kilowatt hour and a system efficiency of 80 percent was assumed. The laboratory results for submerged cleaning provide estimates of about $1.50 per 1000 square feet cleared using two $\frac{1}{8}$-inch CAVIJETS and about $3.50 per 1000 square feet for a single $\frac{1}{4}$-inch CAVIJET hull cleaning

device. At comparative rates of sandsweeping, the costs, obtained during discussions with shipyard and Navy personnel experienced in such cleaning operations, are $28/1000 ft^2, merely for the "grit". It should be noted that the operating cost quoted for the sandsweeping method does not include power costs. Also, none of the operating costs include the labor which, during dry dock hull cleaning, would be the same for comparable rates of cleaning. However, considerable additional set-up and clean-up costs should be added to the sandsweeping method due to the requirements for screening other portions of the ship during these procedures. In addition, periodic dredging in the vicinity of the dry dock may be required if buildups of the sand or slag material become severe. Also, sandsweeping methods cannot be used on submerged surfaces.

The hand-held wire brush method can be operated by a diver under water. However, rates of only about 37 m^2/hr (400 ft^2/hr) are achieved, which are about half the rates obtained with the CAVIJET method during the present tests.

7. CONCLUSIONS

From the results obtained during the laboratory phase of this investigation, the following conclusions are drawn:

(a) In laboratory testing with various CAVIJET nozzles, using water at 13.8 MPa (2000 psi) or less, with no additives or abrasives, fouling removal rates have been achieved which are comparable to the hand-held sandsweeping methods now used for dry dock cleaning.

(b) A CAVIJET system, using two submerged $\frac{1}{8}$-inch nozzles at 13.8 MPa (2000 psi), can provide fouling removal rates of about 100 m^2/hr (1030 ft^2/hr), at power costs of about $1.50 per 100 m^2 (1000 ft^2). This should be compared with the grit cost of about $28 per 100 m^2 (1000-ft^2) for sandsweeping.

(c) A single $\frac{1}{8}$-inch CAVIJET system, at 41.4 MPa (6000 psi), has achieved white metal finishes on severely rusted steel panels at rates of 5.6 m^2/hr (60 ft^2/hr).

8. ACKNOWLEDGEMENTS

The authors wish to express appreciation for the support and suggestions from Mr. Lloyd Fink at MARAD; and Mr. Michael T. Gracey and Mr. E. Ervin Linnstaedter at Todd Research and Technical Division, Galveston. We gratefully acknowledge the testing and data analysis by Stephen J. Harrison, Robert L. Leavel, Paul R. Hartmen, Robert A. Munson, Philip M. LeBlanc, David J. Ayres, Stephen C. Howard and Gary S. Frederick. We also

want to acknowledge the assistance and support of Mr. Carlos Perez, Miami Marine Research, Incorporated, and Mr. Richard Seitz and Mr. Michael Manning of the Maryland Shipbuilding and Drydock Company. This study was supported by the U. S. Maritime Administration.

9. REFERENCES

1. Johnson, V. E., Jr., Kohl, R. E. and Conn, A. F., "Tunneling, Fracturing, Drilling, and Mining with High Speed Water Jets Utilizing Cavitation Damage," First Int'l Sympos. on Jet Cutting Technology, Coventry, England, Paper A3, 1972; Conn, A. F., "Recent Developments of the Cavitating Water Jet (CAVIJET) Method," First Int'l Sympos. on Jet Cutting Technology, Coventry, England, Suppl. to Paper A3, (April 1972).

2. Conn, A. F. and Johnson, V. E., Jr., "Further Applications of the CAVIJET™ (Cavitating Water Jet) Method," Second Int'l Sympos. on Jet Cutting Technology, Cambridge, England, Paper D2, (April 1974).

3. Conn, A. F. and Rudy, S. L., "Parameters for a Ship Hull Cleaning System Using the CAVIJET™ Cavitating Water Jet Method," HYDRONAUTICS, Incorporated Technical Report No. 7510-1, (July 1975).

4. PARTEK® Corporation of Houston Catalog, "Abras-I-Jector® High Pressure Water/Abrasive Blasting System," (1975).

Table 1. Comparison of Operating Modes: Fouling Removal from Epoxy Coated Panels; Pump Pressure: 13.8 MPa (2000 psi)

CAVIJET™ Nozzles	Cleared Path Width[1], w. cms (inches)			Cleaning Rate[4], $\dot{A}$ m^2/hr (ft^2/hr)			Area Effectiveness, e_A $m^2/kw\text{-}hr$ ($ft^2/hp\text{-}hr$)		
mm (inch)	Air	Dynamic Sheathing	Submerged	Air	Dynamic Sheathing	Submerged	Air	Dynamic Sheathing	Submerged
One - 6.4 dia. ($\frac{1}{4}$)	4.0 (1.6)	6.8[2] (2.7)	7.5 (3.0)	44.5 (480)	75.2 (810)	83.6 (900)	0.90 (7.2)	1.51 (12.1)	1.68 (13.5)
One - 3.2 dia. ($\frac{1}{8}$)	1.5 (0.6)	2.5[3] (1.0)	3.8 (1.5)	16.7 (180)	27.9 (300)	41.8[5] (450)	1.52 (12.2)	2.54 (20.3)	3.80 (30.4)
Six - 3.0 dia (0.120)	-	15.2[3] (6.0)	-	-	167 (1800)	-	-	2.73 (22.0)	-

[1] Averaged for 600-800 ipm translation velocity testing
[2] With 20 to 40 gpm sheathing flow
[3] With 15 gpm sheathing flow per nozzle
[4] Using 720 ipm translation velocity
[5] At 600 ipm

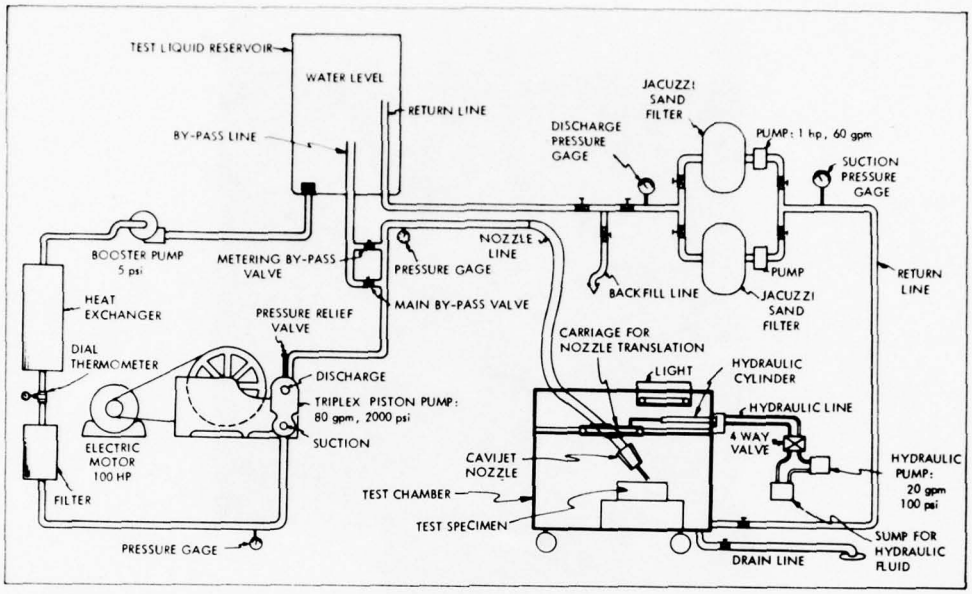

FIGURE 1 - SCHEMATIC OF CAVIJET™ CAVITATING WATER JET TEST FACILITY

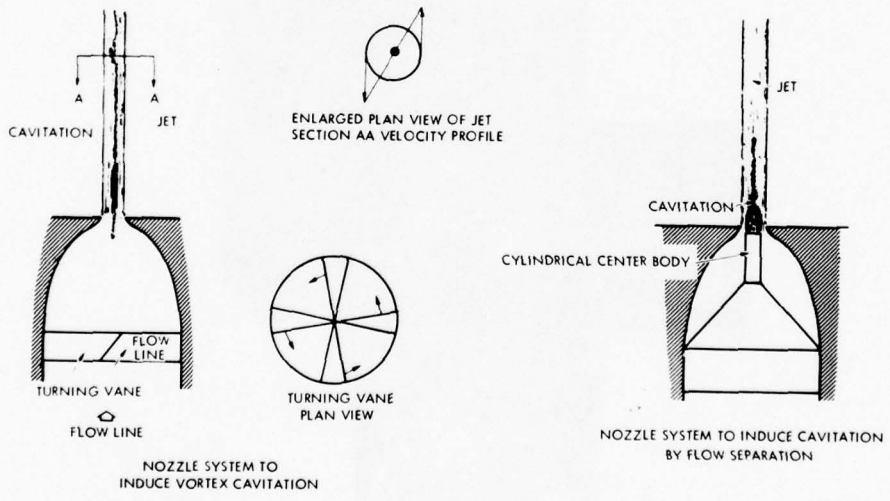

FIGURE 2 - TYPICAL CAVITATING WATER JET NOZZLE CONFIGURATIONS

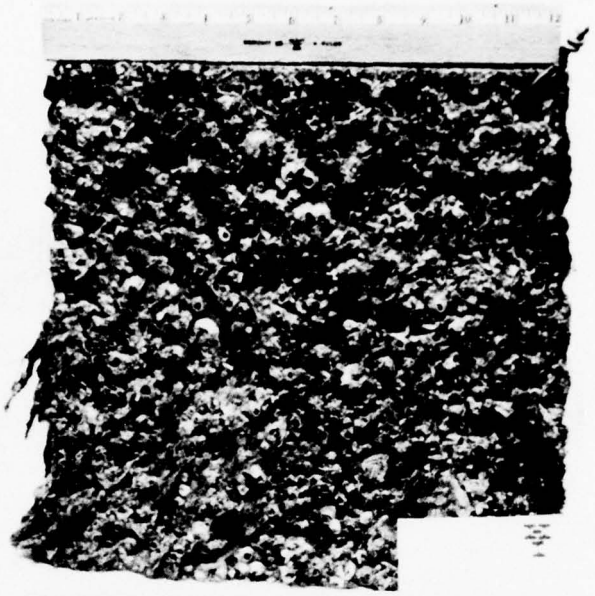

FIGURE 3 - PLATE 1, SIDE A BEFORE TEST

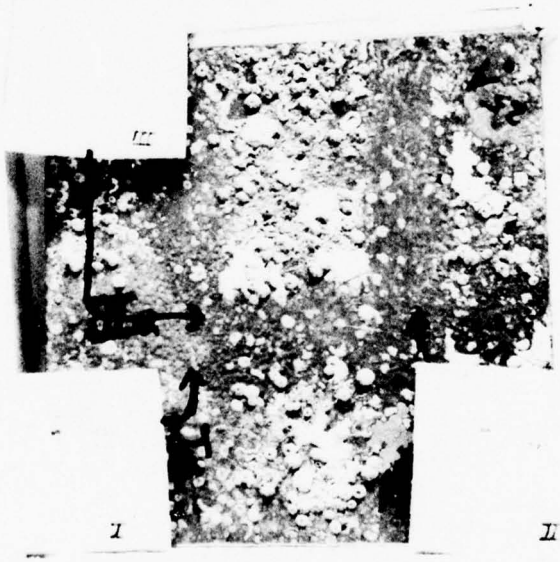

FIGURE 4 - FOULED PANEL TESTED WITH 1/4-in. CAVIJET™ AT 1500 PSI (10.3 MPa)

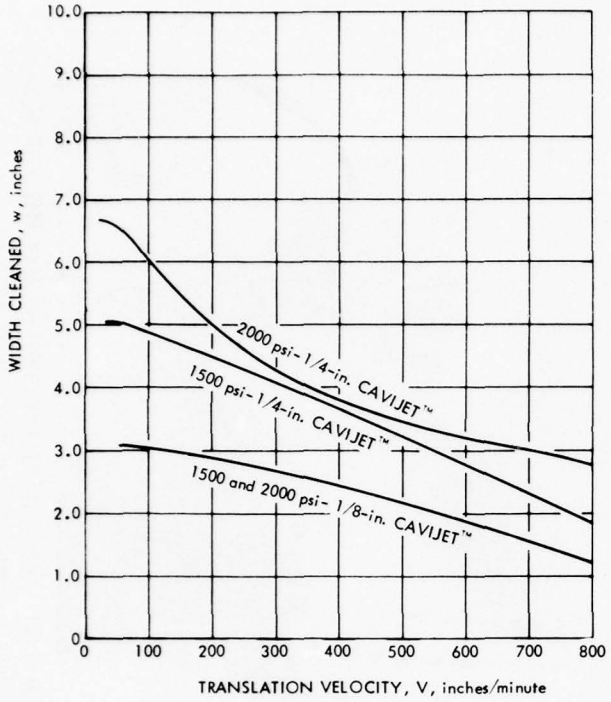

FIGURE 5 - COMPARING AVERAGE FOULING REMOVAL PATH WIDTHS OF 1/8-IN. (3.2 mm) AND 1/4 - IN. (6.4 mm) CAVIJET™ SUBMERGED

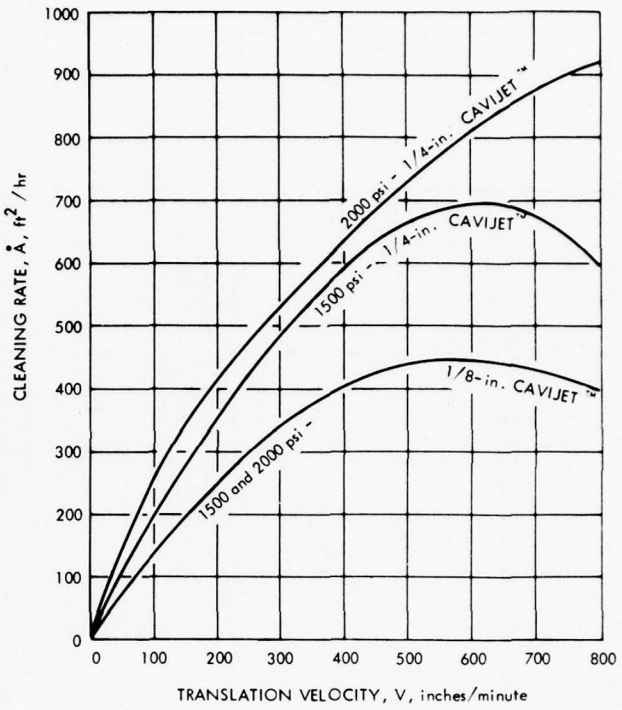

FIGURE 6 - COMPARING AVERAGE FOULING CLEANING RATES OF 1/8-IN. (3.2 mm) AND 1/4 - IN. (6.4 mm) CAVIJET™ SUBMERGED

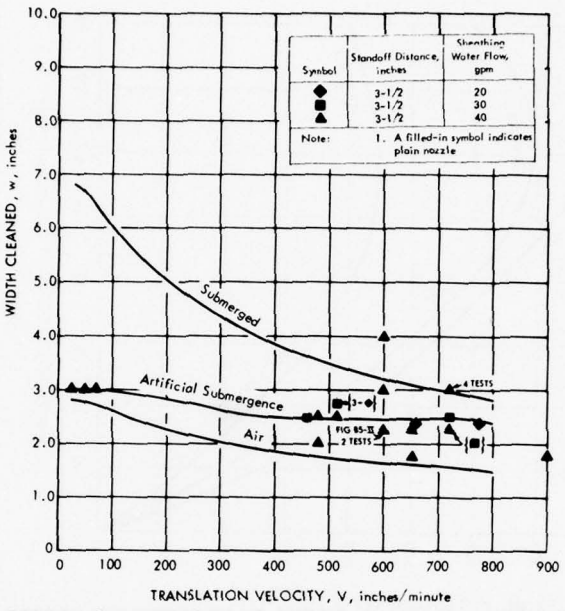

FIGURE 7 - EFFECT OF OPERATING MODE ON PATH WIDTH FOR 1/4 IN. (6.4 mm) CAVIJET™ AT 2000 PSI (13.8 MPa)

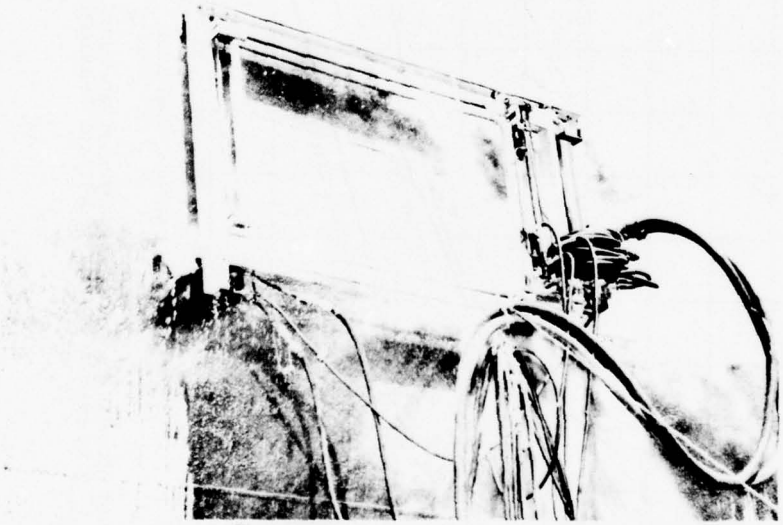

FIGURE 8 - CAVIJET™ HULL CLEANING SYSTEM FOR FIELD TRIALS: shown in operation on a ship hull in drydock

DISCUSSION OF COMMITTEE REPORT & CONTRIBUTIONS

Dr. Arndt (of St. Anthony Falls Hydraulic Laboratory) made the following comments about the summary, the review of cavitation inception by Morgan and Peterson, and the review of cavitation erosion research by Mehta and Conn.

1. First, I would like to take strong exception to the suggestion on page 2 of the summary that polymer additives be used to eliminate scale effects due to viscous effects. This would only add further complication to the overall scale effect problem and can only lead to further disparity between model and prototype. It should also be pointed out that trip wires are not a panacea for scale effects. As is well known, cavitation scale effects are related in a very complex way to both bubble dynamics and viscous effects. The trip wire is only effective for certain problems that are dominated by the presence of a laminar separation bubble. In addition, it is very difficult to design a trip wire which is large enough to properly induce turbulent flow while being small enough to avoid being a source of cavitation itself. This problem and other experiences with using trip wires on model propellers was first discussed by me in 1974 at the Wageningen conference on high powered ship propulsion. A written version of this discussion is contained in the proceedings of the 1976 ASME Polyphase Flow Forum.

2. I would like to congratulate the authors of the review paper on cavitation. It might be appropriate to point out to the audience the significance of cavitation research and its relationship to practical marine engineering problems. One of the most pressing problems existing today is the noise and vibration resulting from the periodic growth and collapse of sheet cavitation as each blade of a ships propeller passes through the wake. The magnitude of the pressure pulses suffered at the stern of a ship is sufficiently high enough for significant damage to the stern plating to occur. The intensity of these pressure fluctuations is directly related to the time rate of change of volume of the cavitation sheet. It is not difficult to envision a significant scaling effect on this phenomenon if cavitation inception is delayed by a few degrees of travel as the model propeller blade enters the wake peak. Recent work of Keller and Weitendorf at the Hamburg tank show that a dearth of cavitation nuclei can have a significant effect on the amplitude of pressure pulses sensed at the stern of a model.

Continuing along this vein, it is important to note that most of the work reviewed in the paper deals with viscous effects on cavitation inception. Again it must be said that various details of the flow and also various features of the bubble dynamics are uniquely interrelated. For example, consider flow over a body of revolution at sufficiently low Reynolds for a laminar separation bubble to exist. In laboratory experiments cavitation is observed at the point of reattachment, the value of the cavitation number at inception being a function of both the mean static pressure and the intensity of pressure fluctuations at the point of reattachment. It is well known that the length of a laminar separation bubble scales with the square root of the Reynolds number and

hence both the cavitation index and the location of the inception point will be Reynolds number dependent. However, it should not be overlooked that there is a negative pressure or tension at the minimum pressure point. The degree of tension that can be sustained with a given size distribution of nuclei in the free stream is a function of exposure time which is proportional to the quotient of body diameter and speed, d/U, with more tension being sustained with lower values of d/U. Thus one could hold Reynolds number constant by increasing the scale and decreasing the speed to the point where significantly different cavitation phenomena would be observed. The current concern with viscous phenomena to the exclusion of concern with other effects is a myopic way to look at the whole problem.

Another minor point concerns the discussion on the influence of polymer additives. Work to date shows that there is a significant difference in the way cavitation is attenuated in the free shear flow experiments of Hoyt and Baker et al and the way cavitation is attenuated on a head form. This is discussed in detail by Arndt et al (1976) and by Baker et al (1976). It is important to make this distinction. It is also gratifying to see the hypothesis for the attenuation mechanism, first proposed in the papers of Holl et al (1974) and Arndt et al, so quickly verified by the beautiful experimental work of van der Meulen and Gates working independently in different parts of the world.

Finally, the current review underscores the need for some careful attempts at correlating laboratory experiments with full scale observations. This is no small task, but it has become evident in several situations that data of this type are necessary to bolster our confidence in the ability of model studies to predict full scale phenomena.

3. The review of cavitation erosion by Mehta and Conn is most welcome at this time. It should be emphasized that research along these lines has traditionally fallen into three categories. The first deals with the mechanism of damage and focuses on the complex interaction between the pressures due to bubble collapse and the response of the material to the pressures generated. Research work in this area has tended to be very elegant, both theoretically and experimentally. The second area has focused more on the needs of the practicing engineer and has been concerned with methods for predicting erosion rates and with the classification of materials in terms of erosion resistance. Many different test devices have been developed which can create significant amounts of erosion in sufficiently short periods of time. These techniques make possible the study of a vast number of different materials. Finally, some study is now being made of the relative erosive potential of various types of flow fields, cavitation patterns etc. Under normal flowing conditions the rate of erosion is too slow for study by normal methods. Thus, this area of research generally relies on the ductile probe technique whereby a soft material is placed in areas where erosion is possible and erosive potential is determined by the rate of formation of microscopic pits on the surface of this ductile proble. There is no measurable weight loss and the erosion mechanicsm is

in many ways quite different from the erosion mechanism that occurs after measurable weight loss is observed. The authors have done a fine job of describing the differences between the various types of research and also the interrelationship between the various facets of the problem.

Some expansion of certain points in the paper should be made. First, the V^6 law in the incubation period has been determined by studies under steady flow conditions. This law may not be applicable to nonsteady cavitation phenomena such as the repetitive formation and collapse of sheet cavitation on propellers operating in a ships wake. Some soon to be published work by Hackworth and his colleagues will address itself to this problem.

Secondly, the work of Stinebring and Stinebring et al* indicating the strong influence of dissolved gas as shown in Figure 5 should be underscored since it has not been common practice to measure this quantity in erosion studies. The theory of how this factor enters into the erosion problem is discussed in Reference 17. It should be added that the ductile probe technique, pioneered by Knapp and utilized by Stinebring and others has not been utilized to its full potential. This technique would be very useful for the determination of the erosive potential of various different types of flows. Information of this type would be very useful to the designer.

Finally, the dearth of information on cavitation erosion in pumps is unfortunate. As shown schematically in the accompanying figure (reproduced from Reference 17), the critical cavitation number is normally defined by performance breakdown. Maximum noise and, presumably erosion, occurs at higher cavitation numbers. High performance water-jet propulsion systems often contain pump units which have evolved from the rocket industry where there was little concern for long-term operation. These pumps are usually installed in a system with excess inlet head available to prevent performance breakdown. However, in some cases this excess inlet head may force the pump to operate under exactly the conditions necessary for maximum erosion rate. Obviously, appropriate acceptance tests should be devised to allow for proper selection and installation of a pump to avoid this possibility.

---

*Stinebring, Arndt, Holl, Jour. Hydronautics, July 1977.

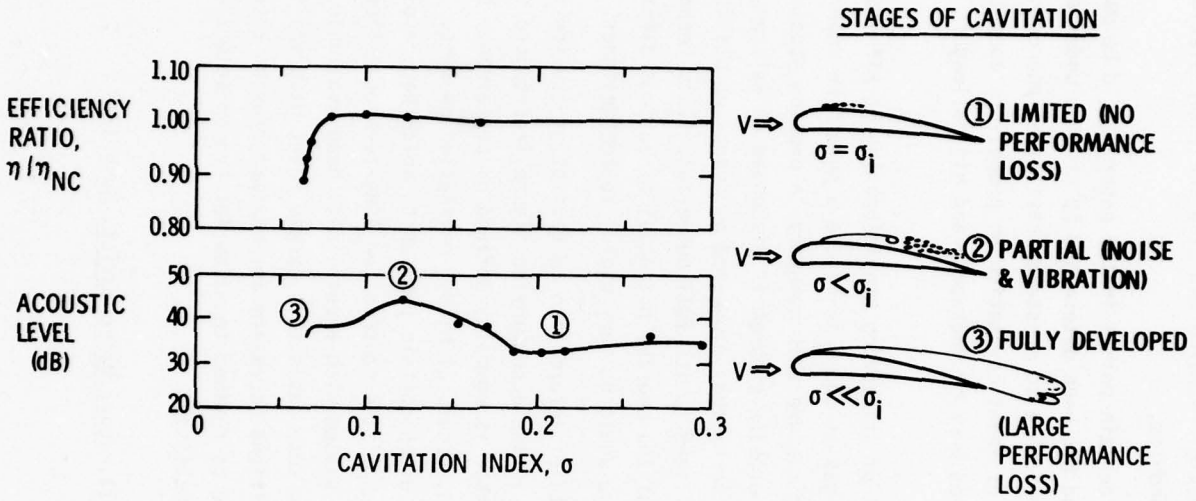
STAGES OF CAVITATION
EFFICIENCY RATIO, η/η_{NC}
1.10
1.00
0.90
0.80
ACOUSTIC LEVEL (dB)
50
40
30
20
0
0.1
0.2
0.3
CAVITATION INDEX, σ
V⇒
σ = σi
① LIMITED (NO PERFORMANCE LOSS)
V⇒
σ < σi
② PARTIAL (NOISE & VIBRATION)
V⇒
σ ≪ σi
③ FULLY DEVELOPED (LARGE PERFORMANCE LOSS)

4. Mr. Dobay (co-author of Cavitation Committee Report) replied to Dr. Arndt's comments. It is rather difficult to provide a brief summary on such a diverse subject as cavitation inception. The design of laboratory experiments and how they may apply to a given full scale situation are not free of controversy. The significant point in the summary, which should not escape the careful reader, was that the simulation of the open-sea environment is important for a meaningful model experiment. Although quantitative measures for the "correct" simulation are not known, it was suggested that the experimental facility should have a relatively high level of free-stream turbulence and, either the model should be large enough so that it possess a fully turbulent boundary layer or, the turbulent boundary layer should be induced by artificial devices. Mentioned in parenthesis, only as some possible examples were trip wire and polymer solution. Perhaps erroneously, the writer assumed that workers in this field, (especially the attendees of this conference), are familiar with at least some of the shortcomings of these and other devices used to stimulate a turbulent boundary layer. A considerable amount of literature is available on just this subject. The writer is grateful, however, that Dr. Arndt has dwelt on some of these shortcomings in his discussion.

This writer stated in the Summary that carefully controlled full-scale experiments should be promoted so that a quantitative assessment of model full-scale correlation in cavitation-inception may be made. I am grateful that Dr. Arndt shares the same view.

5. Dr. Morgan (co-author of Cavitation Inception - A Review - Progress Since 17th ATTC)also replied to Dr. Arndt's comments. The author agrees that the intensity of pressure fluctuations is related to the time-rate of change of volume of the cavitation sheet. The time-scale would be different between model and full scale.

The dificulties involved in the use of trip-wires in simulating a turbulent boundary layer are well known, and are reported in the state-of-the-art review.

6. Dr. Morgan (of DWTNSRDC) made the following comment about the contribution entitled "Scale Effects in Models with Forced or Natural Ventilation Near the Free Water Surface." The phenomena of cavitation inception and ventilation inception are different. Mr. Dobay however, has drawn a significant conclusion in the Summary Report that is important to note: The reasons for scale effects in both phenomena are very similar.

7. Dr. Peterson (of DWTNSRDC) made the following comment about the paper entitled "A Review of Cavitation Erosion Scaling Research." When one considers cavitation-erosion, it is important to note the difference between the "Real World" and the Laboratory. In the real world there are no steady cavities; the gross cavity collapses Judging from Full Scale observations, if no cloud-cavitation is present, no material erosion takes place.

8. Mr. Dobay (of DWTNSRDC) submitted the following discussion on leading edge cavitation by Tulin and Hsu. Mr. Baker's review of wall effects on fully developed cavity flows indicates that there is a large effect on the length of the cavity in confined flows. LT Maixner in his contributed paper ("An Experimental Investigation of Wall Effects on Supercavitating Hydrofoils of Finite Span") also shows significant differences in cavity length dependent on model size (tunnel wall effect). With the above in mind, I find the excellent agreement between theory and experiment in Figure 2 of the paper very surprising. The experimental data shown in this figure were obtained by Mr. Meijer (reference 4 of the paper) in the California Institute of Technology Water Tunnel. One would think that the experimental data would show longer cavities than predicted by the theory. As stated in the paper, "there is a tendency for the measured cavity-length to be somewhat less than predicted." How do the authors interpret the relatively excellent agreement between theory and experiment in light of the above?

It appears that the experimentally observed cavity length in confined flows should be longer than those predicted for infinite fluid.

9. Mr. Tulin (of Hydronautics) replied that he did not know the answer to Mr. Dobay's question.

18th

AMERICAN TOWING TANK CONFERENCE

REPORT OF SEAKEEPING COMMITTEE

August 1977

FOREWORD

The Seakeeping Committee for the Eighteenth American Towing Tank Conference includes the following members:

- Professor M. A. Abkowitz
  M. I. T.
- Dr. Roderick A. Barr
  Hydronautics
- Mr. Francis N. Biewer
  Offshore Technology Corp.
- Mr. Geoffrey G. Cox
  DWTNSRDC
- Mr. John F. Dalzell
  Davidson Laboratory
- Professor Dan Hoffman
  Webb Institute
- Mr. D. C. Murdey
  Marine Dynamics and Ship Laboratory, Ottawa
- Professor J. R. Paulling (chairman)
  University of California

This state-of-the-art report consists of seven chapters, each prepared by an individual member of the committee and the chapter titles are listed below:

I. Review of status for prediction of unstabilized and stabilized ship motions (Cox)

II. Experiment-theory correlation: linear ship motion and loading theory (Dalzell)

III. Performance prediction - slamming and wetness (Murdey)

IV. Facilities for seakeeping tests, including means of generating waves, currents, winds and other environmental conditions (Abkowitz)

V. Environmental conditions (Hoffman)

VI. Testing of unconventional ocean platforms (Biewer)

VII. Model testing for safety, including capsizing of ships and platforms (Barr)

Chapter I outlines the current status of the prediction of roll motion and the performance of stabilizing systems. In the past,

the problem of accurately predicting roll damping has hampered the development of a completely theoretical procedure for predicting roll motion and this situation persists. A summary is given of the methods used in different organizations for basic studies on the theoretical prediction problem as well as the development of semi-empirical methods for application to practical problems of ship performance prediction.

Chapter II contains a summary of the current status of the linear prediction of motions and loads of conventional displacement ships. An extensive reference list is included.

Chapter III deals with two very practical and often limiting aspects of ship seakeeping performance, wetness and slamming. Attention is directed to the correlation of theory and experience and it is noted that the latter topic was covered extensively at the 1976 ISSC.

Chapter IV reviews recent developments in hardware and methodology of reproducing various environmental conditions in the laboratory. Towing tanks are being called upon with increasing frequency to create heretofore unusual conditions including wind, currents and complex wave spectra in the testing of unusual or complex ocean systems and these needs have resulted in new hardware and testing techniques.

Chapter V discusses the present status of our ability to describe the wave environment and outlines some of the applications, needs, and shortcomings of existing formulations and data compilations.

Chapter VI outlines some of the unusual floating or ocean systems which have formed the subject of model testing in recent years. Some of the unusual problems of instrumentation and environmental conditions are described.

Chapter VII is addressed to the problem of the dynamic stability of ships and boats which, in recent years, has received significant attention. This has encompassed the gamut of vessel types from small pleasure boats to ocean-going ships, and has been motivated primarily by a desire to understand and to help prevent losses due to capsizing or swamping.

In preparation for this report, the committee circulated a questionnaire to about twenty member and nonmember organizations. Approximately ten replies were received and these replies are incorporated in the various chapters of our report. The questions asked are listed below.

Topic I Experiment-Theory Correlation for Roll Motion Predictions

If your organization is actively concerned with this topic, it would be appreciated if you could provide a brief description of your current practices and R&D. Answers to the following questions, where possible, will be very helpful.

a. Do you use a single degree-of-freedom roll equation of motion?

b. Do you use the coupled roll/yaw/sway equations of lateral motion?

c. How do you estimate natural roll period?

d. How do you estimate roll damping moment?

e. How do you recognize nonlinear aspects of roll damping moment?

f. How do you estimate the hydrodynamic coefficients and wave excitation terms?

g. How do you allow for the effect of bilge keels?

h. How do you allow for the presence of active anti-roll fins, including nonlinear effects?

i. How do you allow for the presence of anti-roll tanks, including nonlinear effects?

Please quote published references where possible. Any available comparison material showing predicted and measured data will be most useful.

Topic II Performance Prediction Including the Correlation of Experiment and Theory. Especially Attention to be given to Problems of Slamming, and Water on Deck

Please answer the following with reference to both slamming and wetness:

a. Do you make predictions from model tests or theory or both?

b. If model tests, specify wave conditions used, measurements made and method of analysis. Note any special problems encountered.

c. If theory, give reference or outline briefly the method used.

d. Can you give examples of correlation between model and theory or between predictions and full scale measurements?

e. Are you presently engaged in a program to improve prediction techniques in these areas? If so, outline its aims and line of approach.

Topic III Unconventional Ocean Platform Problems, e.g., OTEC Platforms, Jacket Launching or Upending, Offshore Terminals and Berths

a. Indicate which of the above you have tested in model form. For those you have tested indicate approximately how many of each.

b. What was/were the specific objective(s) of the model testing, i.e., structural, seakeeping, etc.?

c. What materials of construction were used in the models?

d. What approximate range of model scales was employed?

e. How were the models instrumented?

f. Was it necessary to model flooding rates for ballast tanks and flooded members?

g. What new and innovative techniques were employed in the tests?

h. What environmental conditions were you required to reproduce, i.e., wind waves, swell, combinations of these, seismic waves, current, wind?

i. When required, what techniques were used to model shallow water?

j. Did any of the work require hydraulic modeling?

Any further comments which would contribute to a report on the state of the art would be appreciated. If you have 35 mm slides which illustrate any techniques, models, etc. the use of these for the presentation would also be appreciated.

Topic IV Facilities for Seakeeping Tests Including Means of Generating Waves, Currents, Wind and Other Environmental Conditions

a. Does your establishment have the capability of conducting model tests in waves? If yes, proceed to the other questions.

b. What are the principal dimensions of the tank(s) or basin(s) in which the seakeeping tests are performed?

c. Describe the technique and type of apparatus used in generating regular and/or irregular waves.

d. Describe the type of beach or wave dissipator used.

e. If your facility has the capability of generating wind, currents, and/or other environmental conditions, please describe the methods and equipment used.

f. Describe the methods, techniques, and apparati used to record and reduce measured data -- for example, how is a motion response measured and reduced to spectrum form?

Topic V Description of Environmental Conditions Including Wind, Waves, Ice and Experience Feedback with Respect to the Use of Standard Spectra such as that of the ITTC

a. Type of wave maker and size of tank in which it operates.

b. Method of generation of regular and irregular waves.

c. Data base for the wave formulation and its format, i.e. ISSC, ITTC, measured data.

d. Exposure to special conditions such as shallow water, breaking waves, wave group experiments, etc.

e. What is the standard way of generating a transfer function (regular or irregular waves, number of frequencies, wave heights, etc.)?

f. How do you extrapolate from the short term statistical data to long term predictions, and what is the standard format of presentation of such data?

I. REVIEW OF STATUS FOR PREDICTION OF UNSTABILIZED AND STABILIZED SHIP ROLL MOTION

by

Geoffrey G. Cox

INTRODUCTION

This overview deals mainly with conventional surface ships but draws attantion to unconventional ship information where possible. It also covers the topic of roll stabilization since one of the major purposes in generating roll motion characteristics is to determine the need for, and effect of, roll reduction devices such as bilge keels, tanks and fins.

When unstabilized and stabilized ship roll motion characteristics are required for the design or performance evaluation of roll stabilizers, the concern is mostly with behavior in short crested seas. This implies reliance on computer predictions and/or simulation procedures for this information. Conventional seakeeping and other facilities tend to find their main use in determining input data or performance of specialized experiments in calm water, regular and long crested irregular waves to improve and upgrade the accuracy of computer/simulation techniques.

It is commonly agreed that completely theoretical procedures for the prediction of roll motion are unsatisfactory. Japanese investigators such as Tasai (1), Fujii and Takahashi (2) and the comprehensive efforts reported under the auspices of the Ship Research Project No. 161, strongly emphasize the need to cope adequately with the nonlinear character of the roll damping moment coefficient by the use of empirically derived, or experimentally measured, data in conjunction with correctly specified quasi-linear approaches. It is interesting to note that Fujii and Takahashi found that the other hydrodynamic coefficients of the lateral equations are quite reasonably predicted by strip theory.

There have been considerable efforts to understand and develop hydrodynamic knowledge and prediction techniques for bilge keels, antiroll fins and tanks since the 1960's, and reference 3 provides a recent state-of-the art report. Due to U.S. Navy interest in antiroll tanks, DTNSRDC has developed its Antiroll Tank Facility using a large model tank to represent tank dynamics in combination with a time

domain simulation of ship and wave excitation dynamics. Baitis (4), provided a description of this approach to the 17th ATTC. Hydronautics (5,6) have also reported considerable effort in this area using Webster's (7) time and frequency domain lateral equations of motion. Most of the development work necessary to understand and specify the hydrodynamic action of antiroll fins has been carried out by the British Royal Navy using experiments on models and full-scale ships to develop prediction tools (8,9). At present many state-of-the-art procedures use Kato (10) to allow for bilge keel effects but attention is drawn to the methodical series data reported by Bolton (11) and to the oscillating flat plate data obtained by Martin (12) and Ridjanovic (13).

Basic investigations by Dalzell (14,15) used the functional series method for nonlinear roll using a one-degree-of-freedom roll problem previously specified in the time domain. He replaced quadratic damping by a cubic damping model to obtain an analytic expression at zero roll velocity. He showed that this is an acceptable approximation in a separate study (16).

CURRENT PRACTICES AND PLANS

A questionnaire was circulated and literature surveyed in an attempt to determine current practice and proposed plans for the prediction of unstabilized and stabilized ship roll motion characteristics. In addition to the information summarized below

i) The Offshore Technology Corporation stated that they have only been concerned with the experimental measurement of roll motions.

ii) Information on the current practices at Hydronautics can be obtained from references 6 and 7.

Do you use a single-degree-of-freedom roll equation?

DTNSRDC

Yes, use the Conolly roll equation (8) in conjunction with an iterative procedure to recognize dependence of roll decay coefficient on roll angle. It is used for early ship design studies due to simple input based on certain overall ship particulars. It is also used for bilge keel and fin sizing in addition to which it can also be considered for tank sizing using time history simulation.

MIT, NRC

No.

Boeing Marine Systems

Yes, method combines model tests with nonlinear roll time simulation for a hydrofoil ship as described in the Boeing document entitled "Intact Lateral Stability of a Hydrofoil Ship."

Do you use coupled roll/sway/yaw equations of motion?

DTNSRDC

Yes, as part of the six-degree-of-freedom NSRDC Ship Motion and Sea Loads theory and program (17,18). It is also used for antiroll tank sizing and performance assessment using time history simulation. Lee and McCreight (19,20) have developed and programmed a six-degree-of-freedom theory for small waterplane catamarans, and which is also applicable to conventional catamarans and monohulls. The coupled lateral equations of motion are included as a part of this theory.

MIT

Yes, as part of MIT five-degree-of-freedom computer program (20).

NRC

Yes, as part of modified version of DTNSRDC six-degree-of-freedom program (17).

Boeing Marine Systems

Yes, use MIT computer program for conventional ships. Have developed coupled six-degree-of freedom, nonlinear time history simulation for analyzing hydrofoil ship motions, primarily in foilborne operation.

How do you estimate natural roll period?

DTNSRDC (1 DOF)

By standard formula when not available from model test or ship trial data.

DTNSRDC (6 DOF), MIT, NRC

Not directly required, but obtained from calculated or empirically estimated roll radius of gyration, calculated metacentric height and computer predicted added mass moment of inertia in roll.

Note: NRC estimates radius of gyration by $0.52(KG^2 + 0.25\,B^2)^{\frac{1}{2}}$ when calculated value not available.

How do you estimate roll damping moment and recognize its nonlinear character?

DTNSRDC (1 DOF)

Preferably from calm water roll decrement tests or scaled from comparable hull data. Nonlinear effects of bilge keels are estimated from empirical data based on the material of reference 13 if necessary. An outer loop iterative procedure is used to ensure choice of appropriate roll decay coefficient for finally predicted rms roll angle in the sea state of interest.

DTNSRDC (6 DOF)

The nonviscous speed independent wave generation part of the roll damping coefficient is computed and the nonlinear viscous part, based on equivalent linearization with the work of Tanaka (23) and Kato (24), is computed for a given wave slope and initial assumed peak roll angle.

An iterative procedure is used to compute the final roll transfer function. See reference 18 for small waterplane catamaran case.

MIT

Similar to DTNSRDC (6 DOF) but computation of nonlinear viscous part for constant wave amplitude rather than wave slope.

NRC

Similar to DTNSRDC (6 DOF) but includes allowances for drag of skegs, rudders, shaft brackets, etc. Rudders are treated as hydrofoils and damping due to lift is calculated.

How do you estimate the hydrodynamic coefficients and wave excitation terms?

DTNSRDC (1 DOF)

See Appendix 1 of reference 8.

DTNSRDC (6 DOF)

By means of slender body strip theory using Frank close-fit technique (25) for two-dimensional potential added mass and damping terms. For small waterplane catamarans as above but including additional contributions due to (a) twin hull interactions, (b) viscous effects, (c) stabilizing fins.

MIT

Similar to DTNSRDC (6 DOF) but using Lewis transformations for normal ship sections and MIT Bulb transformation for bulb-like sections when computing two-dimensional added mass and damping terms.

NRC

Similar to DTNSRDC (6 DOF) but including allowances for drag of skegs, rudders, shaft brackets, etc. Rudders are treated as hydrofoils and lift damping included.

How do you allow for the effect of bilge keels?

DTNSRDC (1 DOF)

As a speed independent nonlinear increment to roll decay coefficient determined by empirical relationships based on the data of reference 13.

DTNSRDC (6 DOF)

As an addition to roll damping coefficient according to nonlinear viscous contribution described previously.

MIT

According to empirical formulations by Japanese authors.

NRC

Kato's method (10).

How do you allow for the effect of antiroll fins?

DTNSRDC (1 DOF)

By techniques and methods extending and modifying the approach of Appendix 2 of reference 8. These incorporate findings/theory/data obtained by the British Royal Navy. Formulas and empirical expressions are used to predict

fin lift degradation due to (a) hull boundary layer, (b) fin/bilge keel and fin/fin interference, (c) fin induced sway and yaw motions, see reference 9.

DTNSRDC (6 DOF)

Does not include this feature.

MIT

Program the linearized effects, the control coefficients being estimated from hydrofoil theory and for any specified fin rate and time lag. Do not correct for "nonlinear effects" since roll response considered sufficiently within linear range to provide acceptable engineering accuracy.

NRC

Does not include this feature.

How do you allow for the effect of antiroll tanks?

DTNSRDC

The presence and performance of antiroll tanks is always predicted by a simulation technique which uses a large model of the tank in the loop. This is fully described in reference 4, and involves either a one or three-degree-of-freedom representation of the ship dynamics depending on the circumstances.

MIT

The presence of antiroll tanks is handled by treating the roll equation as a one-degree system which then becomes a two-degree system when the freedom of tank fluid is included. These coupled linear equations are then solved for the roll and slope angles. The nonlinear effects (U tube equivalent) are handled through equivalent linearization of the damping coefficients. By keeping track of the slope angle, in the linear solution, we can determine the limits of validity of the linear solution due to tank saturation.

PLANS

DTNSRDC is presently involved in a major effort to upgrade its Ship Motion and Sea Loads Program, particularly the lateral equations of motion and treatment of nonlinear roll damping moment effects. Theory has also been developed for a set of simplified lateral equations of motion suitable for early design purposes and roll stabilization investigations.

Boeing Marine Systems are studying the possible applicability of the MIT program to planing hulls.

The U.S. Naval Academy consider that initial studies probably will begin with very basic correlation studies. Coupled roll/yaw/sway equations of motion at zero forward speed probably will be used for the basic hull (without appendages). Lewis-form characteristics will be adopted to estimate hydrodynamic coefficients, probably

by applying a twenty-station strip-theory integration. The solution would be linear in form, and could be modified by inclusion of piece-wise-linear terms representing bilge keels, antiroll fins, or antiroll tanks. All available data suggest that the derivatives associated with such devices cannot be scaled adequately, and the use of separate test programs (such as antiroll tank "bench" tests) to obtain such derivatives will be pursued. Thus final predictions would be based on unappended model response measurements, corrected by the ratios of predicted responses for the model with and without various antiroll devices. Such programs probably will not be implemented within the next year.

REFERENCES

1. Tasai, F., "The State-of-the-Art of Calculations for Lateral Motions," Appendix 6 of the Seakeeping Report to the 13th ITTC, 1972.
2. Fujii, H. and Takahashi, T., "Measurement of the Derivatives of Sway, Yaw and Roll Motions by Forced Oscillation Tech niques," Journal of the Society of Naval Architects of Japan, Vol. 130, 1971.
3. Cox, G. G. and Lofft, R. F., "State-of-the-Art of Roll Stabilizers," Appendix 5 of the Seakeeping Report to the 14th ITTC, 1975.
4. Baitis, A. E. and Meyers, W. G., "Progress Report on the NSRDC Antiroll Tank Facility," 17th ATTC, 1974.
5. Barr, R. A. and Ankudinov, V. K., "Development of Technical Practices for Roll Stabilization Tanks during Later Ship Design Stages," NAVSEC Report 6136-75-12 (and Hydronautics Report 7401.26-1), Apr 1975.
6. Barr, R. A. and Ankudinov, V. K., "Ship Rolling, Its Prediction and Reduction Using Roll Stabilization," Marine Technology, Jan 1977.
7. Webster, W. C., "Analysis of the Control of Activated Antiroll Tanks," Trans. SNAME, Vol. 75, 1967.
8. Conolly, J. E., "Rolling and Its Stabilization by Active Fins," Trans. RINA, Vol. 111, 1969.
9. Lloyd, A.R.J.M., "Roll Stabilizer Fins - A Design Method," Trans. RINA, Vol. 117, 1975.
10. Kato, H., "Effect of Bilge Keels on the Rolling of Ships," Memoirs of the Defense Academy of Japan, Vol. 4, No. 8, 1966.
11. Bolton, W. E., "The Effect of Bilge Keel Size on Roll Reduction," AEW Report 19/72, Mar 1972.
12. Martin, M., "Roll Damping Due

to Bilge Keels," Report prepared by Iowa Institute of Hydraulic Research, Nov 1958.

13. Ridjanovic, M., "Drag Coefficients of Flat Plates Oscillating Normally to Their Planes," Schiffstechnik Bd. 9, Helf 45, 1962.

14. Dalzell, J. F., "Estimation of the Spectrum of Nonlinear Ship Rolling: The Functional Series Approach," SIT Report SIT-DL-76-1894, May 1976.

15. Dalzell, J. F., "A Note on the Distribution of Maxima of Ship Rolling," Journal of Ship Research, Vol. 17, No. 4, Dec 1973.

16. Dalzell, J. F., "A Note on the Form of Ship Roll Damping," SIT Report SIT-DL-1887, May 1976.

17. Salvesen, N. et al., "Ship Motions and Sea Loads," Trans. SNAME, Vol. 78, 1970.

18. Meyers, W. G. et al., "Manual: NSRDC Ship Motion and Sea Load Computer Program," NSRDC Report 3376, Feb 1975.

19. Lee, C. M., "Theoretical Prediction of Motion of Small-Waterplane-Area-Twin-Hull (SWATH) Ship in Waves," DTNSRDC Report 76-046, Dec 1976.

20. McCreight, K. K. and Lee, C. M., "Manual for Mono-Hull or Twin-Hull Ship Motion Prediction Computer Program," DTNSRDC Report SPD-686-02, June 1976.

21. Steen, Atle, "5-D Seakeeping Program User's Manual," Dept. of Ocean Engineering, MIT, Cambridge, Mass. (unpublished).

22. Webster, W. C., "Analysis of the Control of Activated Anti-roll Tanks," Trans. SNAME, Vol. 75, 1967.

23. Tanaka, N., "A Study of Bilge Keels, Part 4, on the Eddy Making Resistance to the Rolling of a Ship Hull," JSNA, Vol. 109, 1960.

24. Kato, H., "On the Frictional Resistance to the Roll of Ships," JZK, Vol. 102, 1958.

25. Frank, W., "Oscillation of Cylinders In or Below the Free Surface of Deep Fluids," NSRDC Report 2357, 1967.

II. EXPERIMENT - THEORY CORRELATION: LINEAR SHIP MOTION AND LOADING THEORY

by

J. F. Dalzell

INTRODUCTION

In the present review the concern is only with conventional displacement ships -- and specifically only with those aspects of experiment and theory which have to do with motions and wave induced loads in moderate (or linearizable) regular wave conditions. In this, there is an overlap with two other sections of the present report. Thus in the process of surveying the literature appearing since the last conference, the present reviewer has largely ignored work which appeared to be specialized to the subjects of ship rolling, stabilization, slamming, and deck wetness. With these exclusions, those relatively new references which have bearing upon the present topic are noted in the attached Bibliography.

THEORY AND EXPERIMENT -- MOTIONS and QUASI-STATIC LOADS

In the programming of most versions of theory it is now common to include as many structural load related responses as possible. In addition to the basic rigid body motions, the most elaborate programs now appear to incorporate vertical, lateral and longitudinal accelerations as functions of position within the ship, wave induced moments in the form of vertical, lateral, and torsional moments as a function of longitudinal position, wave induced shear forces (vertical and lateral) also as a function of longitudinal position, and dynamic pressures on the hull.

One basic problem faced in a general review is that there are numerous versions of "theory", and that the various published comparisons do not ordinarily involve the same ship. As most if not all members of ATTC are aware, a comparative computation exercise addressing part of this problem is now underway under the auspices of ITTC. The "bench mark" ship in this exercise is a relatively fine containership at moderate speed. Results are not expected until 1978.

A second, equally important, problem in a general review is that of quantifying the discrepancies between experiment and theory, as well as the probable precision of the experiments. There seems no agreed upon way of doing either.

The probable precision of experiment is not always stated -- perhaps because experiment time is ordinarily not available for a thorough assessment of reproducibility. It may be merely a defective memory on the part of the present reviewer, but it appears that ship motion experimentalists never plot response amplitudes on a logarithmic scale. This suggests that in nearly all cases the experimenter's confidence in his own results is related to an absolute rather than a percentage tolerance. In those cases where multiple data points are available, the scatter for small and large responses is often very little different.

The problem in quantifying experimental/theoretical discrepancies is apparent in this context. There have been many comparisons made in the last two decades in which the agreement was considered very good while at the same time the difference between theory and experiment was several hundred percent in the wave length range where response was relatively small. It is clearly unfair to expect theory to correctly reflect experimental results of low significance.

While it cannot be advanced as any kind of standard, it is the present reviewer's observation that when both theoretician and experimentalist are content with the results of a comparison of amplitude response, the maximum deviation between theory and experiment is usually not more than 10% of the largest response magnitude observed in the experiments as a function of wave length or frequency. When the corresponding number is 30% or more agreement is almost universally not considered good.

For the present review of relatively new correlation studies, the above was used as a numerical index of correlation in hopes of avoiding the use of words with many shades of meaning. In all cases to be noted the data is presented as a function of wave length. The largest experimental response amplitude as well as the largest deviation between theory and experiment can be estimated and the index is just the approximate ratio of the two in percent. In application, this index is quite sensitive to discrepancies in trends or the location of peaks.

The correlations shown in the recent references indicated in the Bibliography (as well as one or two previous ones) were examined in this light and the results are given in Tables 1 through IV. The tables cover head, following, bow and quartering seas. In each case a number of the more important motion or load responses are singled out. There are at least a half-dozen analytical methods

represented in the tables and altogether a dozen ships. There are three pairs of sources involving the same experimental data (Salvesen (1970) and Wahab (1975); Flokstra (1974) and Wahab (1975); and Kaplan (1974) and Kim (1975). Correlation indices of 5 and 10 involve situations where the correlation is amongst the best yet seen. Indices of 20 are primarily marginal cases. An index of 30 and above usually indicates an obvious problem.

Table 1 for head seas suggests that the major correlation problem with pitch and heave involves Froude numbers above 0.3. An indication of an isolated problem with vertical bending moment is indicated in the table. This particular correlation is known to be under review and entry should be considered tentative. Midship vertical shear has always been a problem of sorts -- probably due to the great difficulty in measuring it.

The following sea situation, Table II is not materially different than the head sea case and the same comments apply.

In bow and quartering seas, Table III and IV, there are indicated a great many relatively large correlation problems -- deviations between theory and experiment about equal to the magnitude of peak response. Rolling appears to be the basic offender. Both lateral and torsional moments are quite sensitive to rolling. There appears no way that improvement in prediction of loads can be expected in oblique seas until the roll prediction problem is rationalized. Pitch and heave correlations appear less good in bow seas than any other heading. In the context of the oblique sea roll correlation problem, note should be made that a great deal of serious work in this area is apparently being done in Japan (Takagi (1974), Fujii (1975)).

A few general observations can be advanced about the results in Tables I through IV. Though the data is sparse, it appears that correlation problems with lateral motions and loads start to be serious at a lower ship speed than seems to be the case for pitch and heave in head seas. (The results shown for Fn of 0.15, taken as a group, probably cannot be taken to be particularly disturbing.) It is not clear from the tables that any combination of theory and experiment has the correlation market cornered.

CROSS-SEAS

Kitagawa (1976) has presented one of the first studies involving model tests in experimentally produced cross seas. Some potentially important conclusions are made. Essentially he was unable to confirm

TABLE I

Approximate Measures of Correlation Between
Theory and Experiment for Head Seas

Source	Fn	Pitch	Heave	Midship Vertical Moment	Midship Vertical Shear	Relative Bow Motion
Baitis, et al (1974)	.13 → .2	5-10	10-20	-	-	-
Cox and Gerzina (1975)	.22	5-10	5-15	-	-	5-10
	.30	10-15	5-15	-	-	5-30
	.37	20	10-30	-	-	5-30
Baitis and Wermter (1972)	.15	10	10	-	-	-
	.46	40	20	-	-	-
Flokstra (1974	.22	-	10	-	-	-
	.245	10	10	10	20	10-15
	.27	-	10	-	-	-
Wahab and Vink (1975)	.15	5	-	10	15	15
	.245	15	25	15	20	25
Journee (1976)	.15	10	20	-	-	-
	.20	10	25	-	-	-
	.25	10	25	-	-	-
	.30	10	20	-	-	-
Kaplan, et al (1974)	.25-.30	10-15	-	30	20	-
Kim (1975)	.25	-	-	10	30	-
Loukakis (1975)	.15	10	10	-	-	-
	.20	15	10	-	-	-
	.25	15	10	-	-	-
	.30	15	10	-	-	-
	.09-.14	-	-	10	-	-
Salvesen, et al (1970)	.2	5	5	-	-	-
	.45	20	10	-	-	-
	.15	-	-	10	10	-
Oosterveld and van Oossanen (1975)	.3 → .4	-	-	-	-	10

TABLE II

Approximate Measures of Correlation Between
Theory and Experiment for Following Seas

Source	Fn	Pitch	Heave	Midship Vertical Moment	Midship Vertical Shear
Baitis and Wermter (1972)	.15	10	15	-	-
	.46	150	80	-	-
Journee (1976)	.15	10	5	-	-
	.20	20	10	-	-
	.25	15	10	-	-
	.30	15	15	-	-
Kaplan, et al (1974)	.25→.30	15	-	60	80
Kim (1975)	.25	-	-	25	15
Wahab and Vink (1975)	.15	5	-	25	100

TABLE III

Approximate Measures of Correlation Between
Theory and Experiment for Bow Seas (Headings 120 to 150°)

Source	Fn	Pitch	Heave	Roll	← Midship Moments → Vertical	Lateral	Torsional	Midship Vertical Shear	C_B	GM/B
Baitis and Wermter (1972)	.15	10-15	5-10	10-50	-	-	-	-	.486	12%
	.46	30-60	10-20	25-60	-	-	-	-	.486	12%
	.15	10	10	50	-	-	-	-	.486	6%
Salvesen, et al	.15	10	-	-	15	15	20	15	.80	5
Flokstra (1974)	.245	20	30	15	15	25	40	30	.598	3.6
Fujii and Ikegami (1975)	.195	15	25	-	20	30-50	30-50	-	.6994	4.1
Kaplan, et al (1974	.25 → .30	-	-	-	40	20-40	20-90	40-90	.56	2.5
	.25 - .30	-	-	-	40	20-40	20-90	40-90	.56	5.0
Wahab and Vink (1975)	.15	10	-	-	25	20	30	30	.80	5.0
	.245	10-30	20-30	20	30-50	25	20	50-100	.598	3.6

TABLE IV

Approximate Measures of Correlation Between
Theory and Experiment for Quartering Seas (Headings 30 to 60°)

Source	Fn	Pitch	Heave	Roll	Midship Moments — Vertical	Midship Moments — Lateral	Midship Moments — Torsional	Midship Vertical Shear	C_B	GM/B
Baitis and Wermter (1972)	.15	10	10	10	-	-	-	-	.486	12%
Salvesen, et al (1970)	.15	10	-	-	15	20	20	-	.80	5
Flokstra (1974)	.245	15	15	90	10	25	-	30	.598	3.6
Fujii and Ikegami (1975)	.195	15-20	15-20	20-35	20-25	20-80	30-40	-	.6994	4.1
Kaplan et al (1974)	.25 →.30	-	-	90	50	30-100	10-50	60-80	.56	2.5
	.25 →.30	-	-	30	50	20-70	40-90	60-80	.56	5.0
Kim (1974)	.25	-	-	50-100	20-40	30-40	30-90	40-100	.56	2.5
Wahab and Vink (1975)	.15	10	-	-	20	50	30	100	.80	5.0
	.245	10-15	-	30-40	20-40	30-50	50-60	50-100	.598	3.6

linear superposition for rolling in quartering/following seas to an acceptable degree of (engineering) accuracy.

ANALYTICAL WORK

Since last conference several sets of results have appeared from relatively basic investigations. Faltinsen (1974) has evaluated pitch and heave added mass, damping and cross coupling coefficients according to the Ogilvie-Tuck formulation and found equal or better agreement between these results and experiment than between experiment and the results of the Salvesen, Tuck and Faltinsen formulation. Ursell (1974), with a linear mathematical, model has provided a fundamental analysis of the nature of the observed variation of wave elevation near the hull not predicted in ordinary strip theory. In a related endeavor, Mauro (1975) has made a three-dimensional analysis of the pressures on a slender ship in head waves, thereby demonstrating improved agreement with experiment relative to results from strip theory. Troesch (1976) has approached the problem of short waves approaching from an oblique heading with a strip method and obtains good agreement for dynamic pressures near midship. Sayer and Ursell (1976) give results for virtual mass of a heaving circular cylinder in water of finite depth for the limiting, long-wave, case. Newman (1976) collects and extends the reciprocity relations which have had significant influence upon contemporary ship motion theory. Wang (1976) finds some new terms in equations of motion appropriate to the "strip" method, in a derivation involving the application of classical dynamic theory.

Since last conference the documentation of one existing ship motions program has appeared (Meyers, et al (1975)).

THEORY AND EXPERIMENT, SOME SPECIALIZED MOTION PROBLEMS

With respect to ship motions in restricted water (depth between 2 and 4 times draft), Hooft (1974) has developed analytical methods for reducing the motions from the motions in deep water. Some comparisons between this method and other earlier theories are indicated in the review by van Sluijs and Gie (1975). There appears to be much more theory than experiment available on this problem. Given the paucity of data, its possible scatter, and the moderate magnitude of change in motions induced by the restricted depth, it is difficult to assess what the situation really is.

Restricting attention to zero speed and shallow water (water depth less than twice draft), van Oortmerssen (1975) has presented a

new "three-dimensional source" computation technique, as well as supporting model test data for a range of headings. Wave excitation as well as forced oscillation experiments were carried out. Theory and experiment for wave excitation look to be with ±10% except in the case of rolling in bow seas, and in the case of surge, pitch and yaw in beam seas. The correlation of theory and experiment for added mass, damping and coupling coefficients was mixed. Quite wide discrepancies were noted for the generally small coupling coefficients, the added mass inertia in pitch and roll, and the roll damping. Motion response was also determined, and wide deviations between experiment and theory were noted for rolling, while discrepancies in the other five modes were in the 10 to perhaps 20% class.

Ohkusu (1976) considered the motions of a ship moored to a much larger floating structure. Correlations with experiment were presented for heave and sway in beam waves. Discrepancies in heave were of 10% magnitude, those for sway up to 30%.

Kaplan, et al, (1975) reduced a three-dimensional correction to be applied to strip theory in the case of a moored barge of very low length/beam ratio, obtaining heave and pitch correlations with experiment to 20% or better.

Schmitke (1976) shows 10% or better correlation between low speed head sea experiments and a special theory for one hullborne hydrofoil boat and between 10 and 30% deviations for another.

THEORY AND EXPERIMENT -- DYNAMIC RESPONSE

Within the confines of the present review "dynamic response" should be taken to mean springing. The subject is one of the concerns of Committee No. 1.2 of ISSC. The incidence of the problem and its place in the overall structural design problem may be found in the reviews of Lewis and Stiansen. Since last conference two reviews of the hydrodynamic aspects of subject have also appeared (Tasai (1975) and Kumai (1974)). The paper by Hoffman and van Hooff (1976), which involves experiments described at last conference, demonstrates reasonable correlation between a modified linear theory and experiments with jointed models. Wereldsma and Moeyes (1976) describe wave excitation force experiments with a highly segmented model. Excitation forces were measured for very short waves as well as those of more ordinary proportions. Agreement of observation with strip theory was not considered good -- the implication being that a new theoretical model is needed for short wave exciting forces.

To the non-specialist, a

comparison of the various reviews of this problem indicate that the specialists are by no means unanimous in their views of how to finally achieve and validate prediction methods for springing. Committee 1.2 of ISSC continues to place many aspects of springing in the "Unresolved Problem" category.

BIBLIOGRAPHY

Reviews

5th International Ship Structures Congress Report of Committee 2, Wave Loads, Hydrodynamics, Hamburg, 1973.

6th International Ship Structures Congress Report of Committee 1.2, Loads Induced by Wind, Waves and Motions, Boston, Mass., 1976.

Lewis, E. V. and Zubaly, R. B.
Dynamic Loadings due to Waves and Ship Motions, Ship Structure Symposium '75, Washington, D.C., (SNAME) 1976.

van Sluijs, M. F. and Gie, T. S.
The Effect of Water Depth on Ship Motions, Appendix 7 to Seakeeping Report, 14th International Towing Tank Conference, Ottawa, 1975.

Stiansen, S. G.
Structural Response and Computer Aided Design Procedure, Ship Structure Symposium '75, Washington, DC, (SNAME) 1975.

Takagi, M.
An Examination of the Ship Motion Theory as Compared with Experiments, Symposium on the Dynamics of Marine Vehicles and Structures in Waves, London, 1974.

Tasai, F.
Distribution of Forces Around the Hull in Waves, Including Whipping and Springing, Appendix 4 to Seakeeping Report, 14th International Towing Tank Conference, Ottawa, 1975.

Analytical

Faltinsen, O. M.
A Numerical Investigation of the Ogilvie-Tuck Formulas for Added Mass and Damping Coefficients, JSR, Vol. 18, No. 12, 1974.

Maruo, H.
On the Wave Pressure Acting on the Surface of a Slender Ship, Volume 4, 14th International Towing Tank Conference, Ottawa, 1975.

Meyers, W. G.; Sheridan, D. J. and Salvesen, N.
Manual - NSRDC Ship-Motion and Sea Load Computer Program, Report 3376, Naval Ship Research and Development Center, February 1975.

Newman, J. N.
The Interaction of Stationary

Vessels with Regular Waves, Eleventh Symposium on Naval Hydrodynamics, London, 1976.

Sayer, P. and Ursell, F.
On the Virtual Mass, at Long Wave Lengths, of a Half Immersed Circular Cylinder Heaving on Water of Finite Depth, Eleventh Symposium on Naval Hydrodynamics, London, 1976.

Troesch, A. W.
The Diffraction Potential for a Slender Ship Moving through Oblique Waves, Report 176, Department of Naval Architecture and Marine Engineering, University of Michigan, February 1976.

Ursell, F.
Note on the Refraction of Head Seas by Long Ships, Tenth Symposium on Naval Hydrodynamics, Cambridge, Mass., 1974.

Wang, S.
Dynamical Theory of Potential Flows with a Free Surface: A Classical Approach to Strip Theory of Ship Motions, JSR, Vol. 20, No. 3, Sept. 1976.

Theory/Experiment: Motions and and Quasi-static Loads

Baitis, A. L.; Bales, S. L. and Meyers, W. G.
Design Acceleration and Ship Motions for LNG Cargo Tanks, Tenth Symposium on Naval Hydrodynamics, Cambridge, Mass., 1974.

Cox, G. G. and Gerzina, D. M.
A Comparison of Predicted and Experimental Seakeeping Characteristics for Ships with and Without Large Bow Bulks, Appendix 2 to the Seakeeping Report, 14th International Towing Tank Conference, Ottawa, 1975.

Flokstra, C.
Comparison of Ship Motion Theories with Experiments for a Containership, ISP, Vol. 21, No. 238, June 1974.

Fujii, H. and Takahashi, T.
Experimental Study on Lateral Motions of a Ship in Waves, International Conference on Stability of Ships and Ocean Vehicles, University of Strathclyde, Glasgow, March 1975.

Fujii, H. and Ikegami, K.
Measurement of Torsional and Bending Moments Acting on a Ship Hull in Regular Oblique Waves, Volume 4, 14th International Towing Tank Conference, Ottawa, 1975.

Hooft, J. P.
The Behavior of a Ship in Head Waves at Restricted Water Depths, ISP, Vol. 21, No. 244, December 1974.

Journee, J. M. J.
Motions, Resistance and Propulsion of a Ship in Longitudinal Regular Waves, Report 428, Ship Hydrodynamics Laboratory, Delft University of Technology, May 1976.

Journee, J. M. J.
Motions and Resistance of a Ship in Regular Following Waves, Report 440, Ship Hydromechanics Laboratory, Delft University of Technology, September 1976.

Kaplan, P.; Sargent, T. P. and Cilmi, J.
Theoretical Estimates of Wave Loads on the SL-7 Containership in Regular and Irregular Seas, SSC-246 (SL-7-4) Ship Structure Committee, 1974.

Kaplan, P. and Sargent, T. P.
The Application and Extension of Ship Motion Theory to Prediction of Motions and Loads of Various Types of Offshore Platforms, Offshore Technology Conference, OTC 2284, 1975.

Kim, C. H.
Theoretical and Experimental Correlation of Wave Loads for the SL-7 Containership, SIT-DL-75-1829, Davidson Laboratory, Stevens Institute of Technology, June 1975.

Kitagawa, H.
Some Aspects of Ship Motions and Impulsive Wave Loads on an Ore Carrier Model in Two Directional Cross Waves, Eleventh Symposium on Naval Hydrodynamics, London, 1976.

Loukakis, T.A. and Chryssostomidis,C.
Seakeeping Standard Series for Cruiser Stern Ships, Trans. SNAME Vol. 83, 1975.

Ohkusu, M.
Ship Motions in Vicinity of a Structure, BOSS '76, Behavior of Offshore Structures, Trondheim, 1976.

van Oortmerssen, G.
The Motions of a Moored Ship in Waves, Publication No. 510, NSMB, Wageningen, The Netherlands, 1976.

Oosterveld, M.W.C. and van Oossanen, P.
Ship Research Activities in the Netherlands, Report No. M315933/259839, Royal Netherlands Navy, Publication 481 of NSMB, March 1975.

Schmitke, R. T.
Prediction of Wave-Induced Motions for Hullborne Hydrofoils, Paper 76-852, AIAA/SNAME, Advanced Marine Vehicles Conference, Arlington, VA, 1976.

Wahab, R. and Vink, J. H.
Wave Induced Motions and Loads on Ships in Oblique Waves, ISP, Vol. 22, No. 249, May 1975.

Theory/Experiment: Dynamic Response

Hoffman, D. and van Hooff, R. W.
Experimental and Theoretical Evaluation of Springing on a Great Lakes Bulk Carrier, ISP Vol. 23, No. 262, June 1976.

Kumai, T.
On the Exciting Force and Response of Springing of Ships, Symposium on Dynamics of Marine Vehicles and Structures in Waves, London, 1974.

Stiansen, S. G. AND Mansour, A. E.
Ship Primary Strength Based on Statistical Data Analysis, Trans. SNAME, Vol. 83, 1975.

Wereldsma, R. and Moeyes, G.
Wave and Structural Load Experiments for Elastic Ships, Eleventh Symposium on Naval Hydrodynamics, London, 1976.

Older References Cited in the Text

Baitis, A. E. and Wermter, R.
A Summary of Oblique Sea Experiments Conducted at the Naval Ship Research and Development Center, Appendix VIII to the Seakeeping Report, 13th International Towing Tank Conference, Hamburg, 1972.

Salvesen, N.; Tuck, E. O. and Faltinsen, O.
Ship Motions and Sea Loads, Trans. SNAME, Vol. 78, 1970.

III. PERFORMANCE PREDICTIONS (SLAMMING AND WETNESS)

by

D. C. Murdey

For the past decade much effort has been directed at the prediction of ship slamming and the associated ship stresses. This work has been the concern not only of experiment tanks but also research organizations whose primary interest is in ship structures and the report of the International Ship Structures Congress Committee 11-3 (Slamming and Impact) published in 1976 (Ref. 1) presents a detailed survey of the state of the art. It is concluded that, although several areas remain to be studied, sufficient progress has been made during the last three years to enable results of research now available to contribute significantly to the rational solution of practical design problems. A survey of members of the A.T.T.C. confirms the optimistic conclusion. No current programs for improvement of prediction techniques were reported. However, several areas still require further study. In particular, ship model correlation investigations are required if progress is to be made in improving currently available techniques and comprehensive seakeeping model experiments are needed to clarify the physical properties of bow flare impact phenomena. More work is required if prediction techniques are to be extended to the realm of high performance marine vehicles.

The subject of deck wetness is not as advanced as slamming. It is well known that predictions based on geometric freeboard and relative motion calculated from pitch and heave amplitudes and phases are generally in poor agreement with the results of direct measurements made during model tests. Because of difficulties in the analytical approach, predictions of wetness are often made directly by testing a model in irregular waves and observing the shipping of water on a video tape record, or using catch tanks to establish the weight of water shipped per unit time. Alternatively, tests are carried out in regular waves and relative motion response measured either with a probe or visually from a video record. Predictions of wetness then follow using standard statistical techniques.

Whilst such approaches yield practical results in the short term, they are unlikely to lead to a greater understanding of the problems of wetness, freeboard

selection or design of above water hull form.

At the present time, analytical methods need to be supplemented by empirical data. Relative motions calculated from pitch and heave amplitudes and phases (either from theory or model tests) are corrected for dynamic effects due to the distortion of the incident wave by the presence of the hull and the dynamic swell-up as the hull moves down into the waves. The freeboard used in wetness calculations is corrected for sinkage and trim, and the height of the wave profile. These corrections are currently obtained from model experiments or by empirical methods based on model tests.

Recent work (Ref. 2) has shown that neglect of these corrections may not always lead to a conservative estimate and suggests that the effects of the dynamic swell-up and incident wave distortion on relative motion may be different in head seas from those in following seas.

Many questions remain unanswered. The effects of changing relative wave direction and of motions other than pitch and heave, (particularly roll), need to be studied. The empirical corrections to relative motion and freeboard need to be related to hull form (above and below water) and the assumption that the calm water wave profile may be used in calculating the freeboard in waves requires further justification.

The empirical parts of the calculations should be replaced by theory. However, the extreme non-linear nature of the problem makes this a major challenge.

REFERENCES

1. Report of Committee 11-3, Slamming and Impact, International Ship Structures Congress, Boston, 1976.

2. Bales, N. K. and Watkins, R. M. Validity of Analytical Predictions of Deck Wetness for an Offshore Supply Vessel in Following Waves, DTNSRDC Report SPD-726-01, 1976.

IV. FACILITIES FOR SEAKEEPING TESTS, INCLUDING MEANS OF GENERATING WAVES, CURRENTS, WIND AND OTHER ENVIRONMENTAL CONDITIONS

by

M. A. Abkowitz

TANK SIZE

Nine member institutions reported facilities capable of performing model seakeeping tests. These are Boeing Marine Systems (BMS, no tank - use lake and sound); David Taylor Naval Ship Research and Development Center (DTNSRDC, 360' x 240' x 20' deep); Davidson Laboratory (DL, 313' x 12' x 5.5' d; 75' x 75' x 4.5' d); Lockheed Ocean Laboratory (LOL, 320' x 12' x 6' d); Massachusetts Institute of Technology (MIT, 100' x 8.5' x 4.5' d); National Research Council, Canada (NRC, 450' x 25' x 10' d; 400' x 200' x 10' d - outdoors); Offshore Technology Corporation (OTC, 295' x 48' x 15' d); St. Anthony Falls Hydraulic Laboratory (SAF, 220' x 9' x 6' d; 80' x 28' x 2' d); and the U.S. Naval Academy (NA, 380' x 26' x 16' d; 120' x 8' x 5' d; 54' x 40' x 2' d).

WAVE GENERATING FACILITIES

The three general types of tank wave generators, namely movable paddle (flap), plunger, and pneumatic, plus Mother Nature are used at one or more of the above institutions. BMS uses natural waves in the Lake Washington and Puget Sound, plungers (usually wedged shaped) are used at the DL, LOL, and in the wide tank at SAF, and pneumatic generators are used at DTNSRDC and NRC. All the remaining tanks (MIT, OTC, SAF large tank, and NA) use some sort of paddle type generator, mostly single paddle hinged at the floor, except for the NA, where dual (lower and upper) individually positioned flaps are used. The towing tanks at DTNSRDC, DL (75' x 75' x 4.5'), NRC, and SAF (80' x 28' x 2') have the capability of generating waves in a direction(s) other than along the longitudinal tank axis or have the ability to tow models in directions not aligned with the wave propagation. All the remaining tanks can only tow in head or following seas.

The facilities at NRC and SAF are presently limited to the generation of regular waves, the remaining tanks being capable of generating irregular seas. Of these, only DTNSRDC is able to generate short crested irregular seas. (BMS must accept whatever seaways nature presents.)

All tanks resort to some form of regular frequency generator to

generate their regular waves, the frequency usually being controlled by an electronic signal generator and the height usually being controlled by the signal amplitude of the generator, except in the case of those tanks which use pneumatic generators. In these cases, amplitude is basically controlled by the air pressure, along with other adjustments to the system. For the generation of irregular seas, DTNSRDC uses a pre-recorded magnetic tape for frequency adjustment, DL uses a pre-programmed sequence of plunger frequencies at fixed stroke, LOL and MIT use pre-programmed tape which controls a hydraulic servo valve, the tape having been prepared by white noise generators and elctronic filters; OTC uses a magnetic tape control, the tape having been prepared by a program which sums the output of 256 sine waves; and NA uses computer controlled dual flaps, programmed so as to correct the spectrum being generated in the tank (measured and analyzed on line in real time) to the desired spectrum, with rapid convergence.

WAVE ABSORBERS - DISSIPATORS

A variety of wave dissipators are used among the various tanks - sloping beaches, slatted beaches, matts, meshs - all located on the tank side or sides opposite to the side where the wave generators are located.

DTNSRDC and LOL use slatted beaches with one or more layers of slats, NA (380' x 26' x 16'; 120' x 8' x 5') and SAF (220' x 9' x 6') use matts made up of one or several layers of square bars or tubing (wood or metal), MIT and OTC use substantial meshs of stainless steel turnings (machinings), SAF (80' x 28' x 2') uses wire mesh or a pebble beach, DL (313' x 12' x 5.5') and NA (40' x 54' x 2') use plane surface sloping beaches, and DL (75' x 75' x 4.5') and NRC (both tanks) use a sloping beach with circular hole perforations of special design. In addition, in order to dampen model generated waves between test runs, LOL has installed slatted side beaches and DL (313' x 12' x 5.5') tows a transverse plank in each direction after a run.

ENVIRONMENTAL CONDITIONS OTHER THAN WAVES

Only two member tanks reported a capability of generating environmental conditions other than waves. OTC employs several large blowers whose volume can be controlled to produce the desired wind velocity and current is produced by inducing a circulation in the tank by means of large pumps. SAF (220' x 9' x 6') simulated wind over the waves by means of a variable speed blower within a temporily constructed duct (for a special test on spray over

breakwaters) and current can be generated by means of a gravity water supply flowing underneath a raised wave generator. SAF (80' x 28' x 2') can establish currents which pass under the plunger, by flow through perforated manifold pipes located behind the plunger wavemaker. Of course, BMS is subject to the wind, currents, and waves existing on the lake or sound at the time of testing.

METHODS, TECHNIQUES, AND INSTRUMENTATION FOR DATA RECORDING AND REDUCTION

BMS: Accelerations at several ship locations are measured using Systron/Donner Model 4310 servo accelerometers. Roll and pitch angles are measured by a Lear Siegler Model 9000-C vertical gyro. Roll and pitch are also measured together with ship heading by a LITEF PL-41E Stabilized Gyro Platform. Instantaneous wave height measurements are made using a Boeing-built wave height sensor which employs an acoustic height sensor together with a stabilized gyro platform. Data are generally recorded on 14-track magnetic tape and are time division multiplexed and pulse code modulated (PCM) at 100 Hz. Statistical analyses including spectrum computations are performed using standard digital programming on an IBM 360/65 computer.

DTNSRDC: Gyroscopes are used to measure angular displacements, and ultrasonic probes are used to measure linear displacements. Strain type pressure gages and force balancing accelerometers are also routinely employed. Time histories are recorded on strip charts and on analog and digital magnetic tapes. The digital magnetic tape is input to an on-carriage computer which uses FFT software to reduce steady state time history data. Data on transient phenomena are reduced manually.

DL: Motion or force sensors produce output voltages which pass through signal conditioners. DC output of conditioners, in analog form, is (1) displayed on UV chart recorder, (2) recorded on magnetic tape, and (3) digitized by PDP-8e digital computer. Digital time history of response to irregular waves reduced to (1) statistical averages of peaks and troughs by PDP-8e, or (2) to spectra on central digital computer, PDP-10. Regular wave responses may be reduced by peak-trough statistical averages or by harmonic analysis, both using PDP-8e.

LOL: Motion responses, accelerations, and pressures are measured by high frequency response sensors. Wave contours are measured by an ultrasonic wave sensor. These sensor signals are recorded simultaneously on analog magnetic tape and then sampled and digitized at a rate of approximately 250

samples/sec. These data are reduced to engineering units and statistical and/or spectral (power density and/or one-third octave) analyses performed by a PDP-8e digital computer. Resulting analyses are presented as hard copy tabulations. Results may also be plotted and recorded on digital magnetic tape.

MIT: All motion transducers are of the variable reluctance type (linear transformer). Also, accelerometers, sonic devices, and resistance wire wave probes are used. Measurement signals come in analog form and are simultaneously recorded on multi-channel graphical recorder and magnetic tape. Irregular motion data is then digitized and spectrally analyzed on a digital computer giving the wave and motion response spectra and the associated statistics such as significant response and average of 1/10th and 1/100th highest responses.

NRC: Gyro-stabilized platform used to measure roll, pitch, yaw angles and surge, sway, heave accelerations. Ultrasonic wave probes are used to measure incident waves. All data are recorded on digital magnetic tape at 25 samples/second on each channel. Although tests are done in regular waves, all data are analyzed using spectral methods to eliminate harmonic distortion. Amplitudes and phases of all transfer functions are calculated by averaging the cross spectrum of each response with the encountered wave over a narrow frequency band containing the main peak of the encountered wave spectrum. For tests of smaller models in head seas, unstabilized accelerometers are used to measure heave, pitch, and surge with software corrections for earth-field components. A sonic probe is used to measure the mean surge position of the model relative to the carriage-mounted wave probe so that phases can be related to the incident waves at the model LCB.

OTC: Data are obtained from a variety of transducers: anemometers, wave gages, rotary and linear motion transducers, potentiometers, accelerometers, pressure transducers, strain gages, etc. These signals are conditioned, multiplexed, converted to digital, and then fed to a computer for analysis and readout. The computer performs a statistical analysis on the data and provides such items as maximum, minimum, average, standard deviation, etc. as well as a spectral analysis of desired channels. Typically, the computer performs a spectral analysis of the wave which is then put on an X-Y plotter. A heave RAO is produced by dividing the heave spectrum by the wave spectrum.

SAF: Wave heights are measured using either resistive or capacitive type wave probes, or with an

ultrasonic wave transducer. The sonic transducer has been used to detect heave and pitch motions of ship models moored to a pier subjected to regular wave action. The sonic beam ranged off targets attached to the bow and stern of the model. Data were recorded on strip chart recorders which were adequate for the accuracy required in this application.

NA: Anticipated heavy use of sonic transducers to monitor motions. Currently use RVDT's. Data acquired by direct computer access links. Software includes complete statistical package capable of identifying means, peaks, determining spectra, etc.

V. ENVIRONMENTAL CONDITIONS

by

Dan Hoffman

INTRODUCTION

The need to simulate realistic environmental conditions in the tank, in order to observe and evaluate the performance of a model or extend analytically measured data to extrapolate beyond the short-term predictions to which tank results are generally limited, requires a careful and accurate specification of the environment.

Recent extension of tank work to offshore applications has led to more stringent requirements with regard to wave data, such as specific locations and/or seasons of the year, as well as promoted the need to consider combined effects of wave, wind and current. Since the tank test provides a qualitative as well as quantitative measure of the performance of the model under the selected test conditions, the combination of all or several environmental effects can be ideally simulated experimentally. The parameters defining wind and current are fairly simple, i.e. the wind is applied as a steady state force classified by its speed and direction. The current is defined in terms of its mean velocity and often a profile is applied as a function of depth, and the direction of application relative to the model is also specified. Though the definition of wind and current is far from satisfactory, the means of simulating more sophisticated conditions in the tank are rather limited, and very few tanks are capable even of providing wind and current effects in the simplistic form described above. Waves by contrast can be reproduced by most tanks. The problem, however, is defining the specific wave spectrum representing the desired conditions.

Description of the available facilities and apparatus used in generating waves, currents and wind and other environmental conditions was given in the previous section of this report. The purpose of this section is to review the current state of the art of wave data availability and representation for direct simulation in the towing tank as well as for purposes of extending tank test results to long-term predictions, operability criteria, etc.

TOWING TANK SPECTRAL REPRESENTATIONS

Practically all towing tanks offer the two-parameter Bretschneider

spectrum, also referred to as the modified Pierson-Moskowitz, ITTC or the ISSC spectrum, as standard wave data unless other requirements are specified by the client in terms of other theoretical formulations or specifically a representative measured spectrum for the location or route. Generally, most formulations require as input the desired wave height and some characteristic period. Some of the more recent spectral formulations require some additional parameters. A measured spectrum is usually defined in terms of its ordinates and can be reproduced in the tank by trial and error.

The major drawback of the ITTC/ISSC spectrum formulation is its inability to reproduce a wide variety of conditions such as cross seas, as can be represented by increase in energy in the high frequency range of the spectrum, multi-directional seas consisting of sea and swell or two swell systems. In reality the multiple spectral shapes which can occur are by far in excess of the single distribution which results when the ITTC/ISSC spectra are plotted non-dimensionally. These deficiencies could lead to erroneous results, particularly when systems sensitive to low threshold of wave height are being tested.

In order to generate the formulated or measured spectrum two basic sources of data are required: the height and period correlation for the mathematical spectra and the spectral ordinates for the measured spectra. The major source of height and period wave data is based on voluntary observation from passing ships. These data have been compiled by the U.S. Naval Weather Service Command to cover the U.S. continental shelf (1)* (ten volumes) and the rest of the world (2) (seven volumes). Other sources covering world-wide locations include (3) and North Atlantic data only based on weather ship data (4). Though these summaries are extremely useful in the absence of any other data, the reliability of the data should be carefully considered with respect to the nature of the problem which it is being used for. An alternate source of data for observed wave characteristics which offers wider flexibility is the actual magnetic tapes which are used to store this information, which in some cases extend over 100 years of observations. These tapes, which are available for each Marsden square, or even just portions of it, can be used to characterize a grid point or a route, providing wave height and period data, directional distribution, wind statistics, etc. for which wave exceedance tables can be formulated yielding data to compute the long-term responses or

*Numbers in parentheses refer to references listed at the end of this section.

the long-term wave statistics such as the 100 year wave, etc. Furthermore, the format of the wave data as stored on the magnetic tape facilitates the determination of wave persistence, since the chronological occurrence of the wave height is available; thus the probability of a specific wave height persisting for 8, 24 or 48 hours can be determined.

As previously indicated, some more recent spectral mathematical formulations require the input of additional parameters over and above the wave height and period. In the JONSWOP formulation (5) an assumption must be made of the shape parameter γ (for $\gamma = 1$ the JONSWOP is identical to the Bretschneider spectrum). Other shape parameters are defined as constants, due to lack of more extensive information. The six parameter spectrum (6) requires separate height and period values for sea and swell, (or primary and secondary directions) as well as shape parameters. It is apparent therefore, that these formulations are not practical as yet for tank simulation use, since if the actual spectra are available from which the parameters can be defined, the spectral ordinates can be used for the tank simulation rather than the mathematical formulation.

The simulation of actual spectra in the tank is possible if a sample is available for the case to be reproduced. Since spectral shapes can vary significantly, a specific spectrum representing a limited short-term period should only be used when that specific condition is to be simulated. Generally, average conditions representing spectral characteristics at the location or along the route are more meaningful and can be simulated by averaging a sample of several spectra all representing the same average conditions. This mean spectrum does not necessarily represent an actual 20-30-minute record but provides a good coverage of the frequency range and the corresponding spectral ordinates. It is also desirable to generate the lines corresponding to mean $\pm$ standard deviation of spectral ordinates so as to provide reasonable limits within which the simulated tank spectrum should fall.

The actual source of data for such mean spectral families can be measurements in the actual location, close by or in a location having similar characteristics (7) (8). Since for many locations no measured wave data are available, particularly in spectral form and in adequate quantity to allow for sampling, an alternative source of data currently being evaluated is based on the hindcasting of directional spectra using the U.S. Navy SOWM model at Monterey, Calif. Recent analysis

of spectral data at two locations, for which extensive measurements have previously been made, indicates that the mean spectral characteristics within the wave height group selected, obtained for hindcasting, give a fair representation of the corresponding data based on measurements. Though further verifications are necessary it is apparent already that the hindcast wave data should become a major source for design wave data in the near future and simple application to tank wave simulation should be feasible.

Since tank tests are limited to short-term responses and long-crested waves, the extrapolation into long-term and generalization into more realistic environmental conditions, such as short-crested seas or multi-directional wave systems, must be done analytically. The definition of the wave data required for these calculations is just as important as the simulation of waves in the tank, since in most cases tank tests cannot cover all operational conditions and supplementary analytical work must therefore be done.

WAVE DATA FOR POST-TEST ANALYSIS

Though the sources of data for the post-test analysis are essentially the same as those used for simulation of irregular seas in the tank, the format of the wave data is not necessarily the same. The analytical application of wave spectra using the principle of linear superposition allows for the use of many spectra, not necessarily a single spectrum or a mean curve representing a family of spectra. Each group of spectra can be represented by the total number of spectra composing it, hence resulting in a mean response spectrum and information on the scatter about it. Spectral families based on measurements for the North Atlantic and Pacific oceans are available from measurements as well as from hindcasts. Each family includes a large enough variety of spectra to account for the several different conditions under which the range of wave height is expected to occur at the specific locations.

The effect of the spectral shape on the resulting responses was discussed at length in several references (9) (10) illustrating the limitations of the mathematical formulations. A slightly different approach was recently used in (11), illustrating the type of bounds which must be applied to various spectral formulations in order to overcome the limitations of the single line mathematical spectrum.

The expansion of model test data from regular or irregular waves to yield long-term predictions such as the highest expected value to be exceeded once in a 30-hour storm, a year or a lifetime is possible

if wave exceedance data are available. The probabilities of occurrence of each wave height can be used as weighting factors and hence the extreme values can be determined by using some statistical distributions which are naturally beyond the scope of the more simple Rayleigh distribution or its various modifications. Wave exceedances can be compiled for observed wave heights as reported by passing ships, and experience has shown that, apart from the fact that ships generally try to avoid the worst storms, and hence may lack the high wave height groups, the reliability of the observed wave height data for the purpose of obtaining exceedance tables is more than satisfactory.

For operability critieria, such as expected downtime or the ability of the vessel to complete a mission at a certain location during a specific time of the year, wave persistence data must be applied. As previously indicated, one source for such data, and a fairly reliable one, is the observed wave height data files from passing ships discussed above. Alternatively, as the hindcasting of directional spectra currently underway at FNWC is expanded over longer periods of time and eventually to 20 years of data, it would no doubt provide an excellent alternative source for creating wave persistence data. Measured wave data do not usually cover long enough uninterrupted periods of time for a meaningful analysis.

SPECIAL WAVE DATA REQUIREMENT

The need to simulate experimentally or theoretically special wave conditions in the tank -- such as shallow water, breaking waves in deep or coastal environment, and more recently realistic wave group conditions (in order to study problems such as ship-single point mooring behavior , capsizing or other specific operational scenarios)-- cannot be overlooked. Yet most tanks are currently not capable of offering such services in spite of the growing demands.

The problem in shallow water is twofold: it requires the definition of a realistic wave spectrum to be generated as well as the simulation of physical conditions (shallow water) in the tank to allow for the correct modelling of the model behavior. Shallow water wave data are practically non-existent in meaningful quantities. Some general guidance was given in (12) specifically for tank test modelling. The future, however, does hold a possible solution by use of hindcasting models such as those that are currently being developed for the Great Lakes (13). Furthermore, a NOAA program to install waverider

buoys along the entire coast of the U.S. at 200 -mile intervals should shed some additional light on the problem in the near future.

Breaking waves are usually defined by the observance of the physical phenomena rather than by a more exact mathematical definition. The ability to control the location in the tank at which the break occurs has been demonstrated in (14). However, the mechanism of transfer of energy for the breaking wave to the model is not an easy phenomenon to describe theoretically. High-speed photography seems to be of value in such experiments because of the lack of any other instrumentation.

The understanding of the wave group phenomenon and hence the ability to simulate such conditions experimentally or theoretically should be given some serious consideration. One example relating to capsizing in waves was shown in (15). It is apparent that in this case the knowledge of the highest expected wave is not enough. It is necessary also to know the second, third, fourth, etc., highest waves and their sequence and duration in order to assess the effect of the wave train on the model. Similar knowledge is required in calculating the maximum expected tension in a bow hawser connecting a tanker to a single-point mooring. From the operational point of view, there may be a need to predict a "lull" in the ship motion, in order to perform a critical operation such as a heavy lift or transfer at sea, which requires only a very short duration. This lull must be defined in terms of those wave parameters used by the industry to define the wave contours.

Though some work is being carried out on the above special wave conditions, the state of the art is as yet far from satisfactory.

CONCLUDING REMARKS

In the preceding state-of-the-art review emphasis was given primarily to developments since the last ATTC. During the past three years updating reviews became available i.e., the 14th ITTC seakeeping report (16) and much more extensively the 6th ISSC committee I.1 report (5). Since the question of environmental conditions has been of prime interest, the present state of the art reflects continuous development over the past three years in the area. In this note we have attempted to emphasize the most recent ideas and sources of data available to date, thus underplaying those developments that have been extensively covered in (5) (16) (17).

This short note should serve as a reminder to those concerned with the behavior of models in waves that much work must still be in order to facilitate a realistic

simulation of the sea environment.

REFERENCES

1. "Summary of Synoptic Meteorological Observations", (North American Coastal Marine Areas), U.S. Naval Weather Services, Asheville, N.C.
2. "Summary of Synoptic Meteorological Observations", U.S. Naval Weather Services, Asheville, N.C.
3. N. Hogben and F. E. Lumb, "Ocean Wave Statics", HMS Stationery Office, London, 1967.
4. H. Walden, "Die Eigenschaften der Meereswellen im Nordatlantischen Ozean", Deutscher Wetterdienst Einzelveroffentlichungen, No. 41, 1964.
5. "Environmental Conditions", Report of Committee I.1, 6th ISSC, Boston,1976.
6. M. K. Ochi and E. N. Hubble, "On Six-Parameter Wave Spectra", Fifth Conference on Coastal Engineering, Hawaii, July 1976.
7. D. Hoffman and M. Miles, "Analysis of Stratified Sample of Ocean Wave Records at Station 'India'", SNAME T & R Bulletin 1-35, May 1976.
8. D. Hoffman, "Analysis of Wave Spectra at Station 'Papa'", NMRC-KP-173, Maritime Administration, October 1977.
9. D. Hoffman, "Wave Data Application to Ship Response Predictions", Webb Institute Report to DTNSRDC under GHR program, 1975.
10. D. Hoffman and T. Zielinski, "The Effect of Spectral Shape on Predicted Wave Bending Moment Trends", Webb Institute Report No. 10-31 to ABS, September 1975.
11. M. Ochi and S. L. Bales, "Effect of Various Spectral Formulations in Predicting Responses of Marine Vehicles and Ocean Structures", OTC 2743 Houston, 1977.
12. J. R. Scott, "A Coastal Spectrum for Model Tests", Vickers Ed., St. Albans, 1966.
13. D. T. Resio and C. L. Vincent, "Design Wave Information for the Great Lakes", Report No. 3, Lake Michigan, U.S. Army Engineer Division, North Central Chicago, Ill. 60605, November 1976.
14. G. L. Petrie and D. Hoffman, "Validation of a Time Domain Simulation of Buoy Motion in Breaking Waves", HMC Report 7753, May 1977.
15. S. J. Chou et al, "Ship Motions and Capsizing in Astern Seas", Report CG-D-103-75, USCG, December 1974.

16. Seakeeping Committee Report, 14th ITTC, NRC, Canada, 1975.

17. Seakeeping Committee Report to 17th ATTC, Environmental Condition Representation, Pasadena, California, June 1974.

VI. TESTING OF UNCONVENTIONAL OCEAN PLATFORMS

by

F. N. Biewer

INTRODUCTION

Since the last conference there has been an increasing emphasis on unconventional ocean platforms. This seems to be a reasonable progression as greater demands are placed on the ocean for energy resources whether these resources are in the form of thermal energy or fuel with the ultimate conversion ashore into energy. Although no reports were received on ocean platforms in support of aqua-culture, there is activity in this area indicating that when funding becomes available there will be projects aimed at exploiting more fully the food products of the sea - mammal, fish, and vegetable. These and OTEC plants hold great promise for future developments.

MASSACHUSETTS INSTITUTE OF TECHNOLOGY

MIT reported tests for the purpose of obtaining predictions of relative motion between ships in order to design a control system for the transfer of cargo in a seaway. A unique acoustical system was used to obtain relative distance by measuring the time for sound to transit from the transmitter to a receiver. The 1:96 scale models were constructed of fiberglass and tested in both wind waves and swells.

DAVID TAYLOR NAVAL SHIP RESEARCH AND DEVELOPMENT CENTER

DTNSRDC reported testing a semi-submersible pipe laying barge and a triangular platform drilling vessel. The models were instrumented to obtain motions, acceleration, pressures, and forces.

Wind waves and swell were represented separately and in combination. Wind and current loading were simulated by the use of constant loading devices.

NATIONAL RESEARCH COUNCIL, CANADA

NRC has tested a variety of ocean platforms: a moveable gravity structure, a ring assembly of 8 caissons, a drill ship, and another drill ship for use in shorefast ice.

The gravity structure involved a 1:60 scale plexiglass model and the model tests included towing resistance, motions, set down and lift off flodding sequences.

A 1:40 scale wood model of an eight caisson ring assembly was tested for resistance and behavior on tow. Cable tension was measured

AD-A062 507 NAVAL ACADEMY ANNAPOLIS MD F/G 5/11
PROCEEDINGS OF THE GENERAL MEETING (18TH) OF THE AMERICAN TOWIN--ETC(U)
1977 B JOHNSON, B NEHRLING

UNCLASSIFIED NL

3 OF 3
AD
AD62507

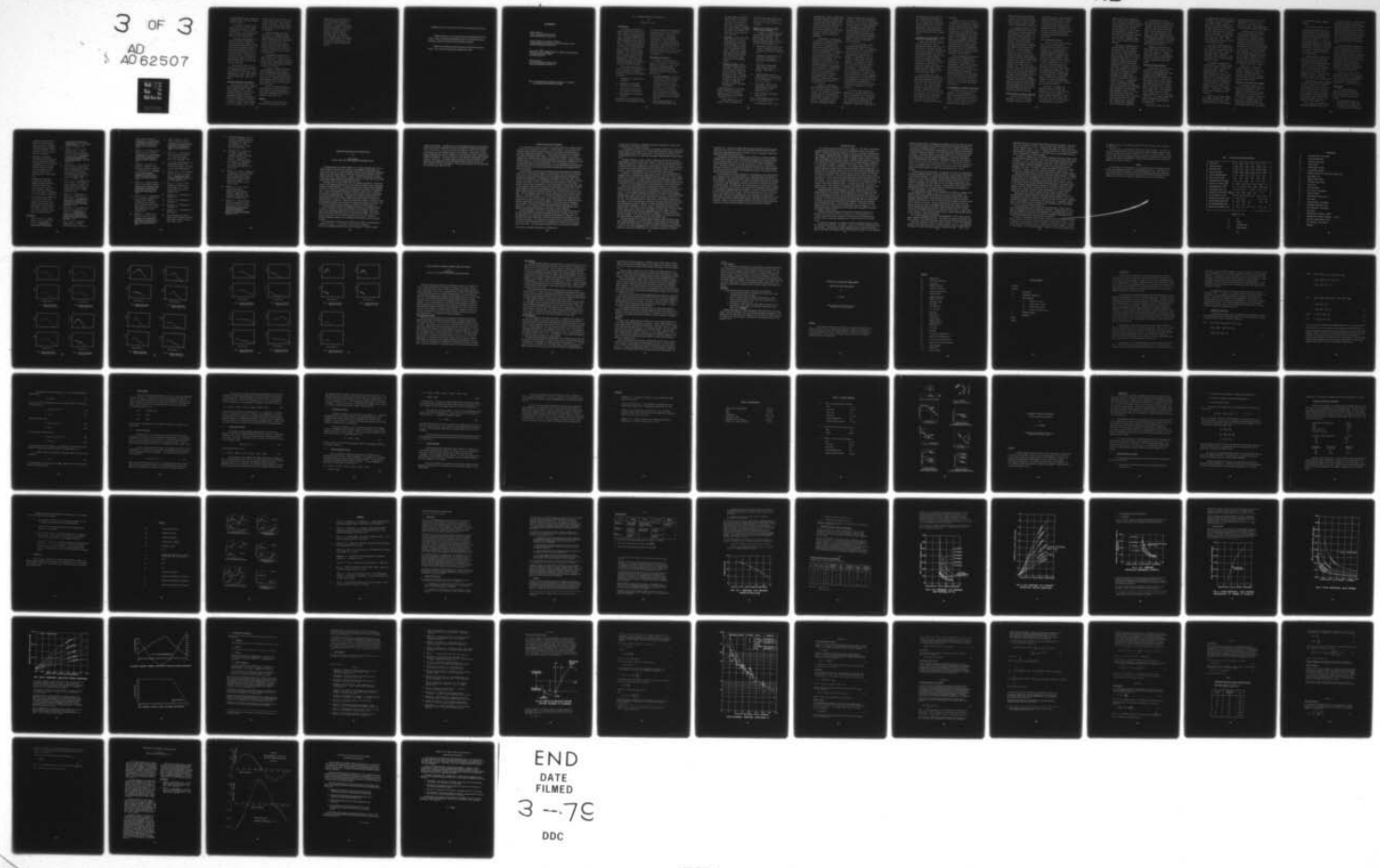

END
DATE FILMED
3-79
DDC

in pre-tensioned cable joining the caissons as was the joint deflections in waves.

The test of the drill ship in ice utilized a partial model constructed of wood to a model scale of 1:12. In this test, the use of engine cooling water to keep ice at bay was studied.

Although instrumentation in these tests was conventional, several innovative testing techniques were employed such as, the use of spring mounted winches to simulate the combined effect of crane lift and sinkage and trim of crane barges. A moveable ice deflection collar on the gravity structure was used to assist in the set down and lift off of the gravity structure.

When shallow water was required, the tests were performed in a separate shallow tank. For current tests, a tank with current simulation was used. Wave testing involved both wind, waves, and swell.

OFFSHORE TECHNOLOGY CORPORATION

OTC has model tested a number of the offshore production platforms used worldwide. These programs generally involve tests of stability during upending, seakeeping enroute to the area, and the development of techniques to cope with inadvertent flooding of buoyant members. Model scales are in the range of 1:40 to 1:60 with preference being given to the largest model that can be accomodated in the tank. When shallow water is required the water depth is adjusted to provide the proper scaled depth.

Because weights, mass distribution, and floodable volumes are important in jacket upending tests, these models are constructed of thin walled aluminum. The models are fitted with remotely operated flood and vent controls so that operators can be trained to upend the jacket using an operational console.

Environmental conditions imposed include: wind waves, swell, wind, and current. Wind and current effects may be simulated by imposing a load or by actual scaled wind and currents in the basin.

In testing offshore terminals, the requirement for very shallow water necessitates pumping the tank down to a few feet. For situations such as this, separate shallow water wave generators are installed along with required wind and current generation devices.

A test of an OTEC platform was also reported in which the objectives were to obtain seakeeping and structural characteristics of the model and cold water pipe.

GENERAL

Although it is believed that additional unconventional ocean

platforms have been tested, the above represents the material furnished to the committee in response to a questionnaire sent to all participants. A specific question regarding hydraulic modeling produced negative responses from all respondus. It would appear that this is an area in which basins will become involved as offshore ports, LNG terminals and the like become a reality.

Addendum to Topic III, received from the Lockheed Ocean Laboratory in San Diego

Although Lockheed did not report any unconventional ocean platform work, they conduct a number of programs having seakeeping, stability, and structural objectives. Materials of construction include wood, metal, fiberglas, and plastic.

Shallow water conditions are achieved by the use of false bottoms on sloping beaches. They did not report any hydraulic modeling in their work.

BIBLIOGRAPHY

Sheets, Herman E.
OTEC - A Survey of the State of the Art
Second STAR Symposium, SNAME 1977

Praught, Michael W., and Metcalf, Michael F.
Evaluating Stability Characteristics of Self-Floating Offshore Towers
Second STAR Symposium, SNAME 1977

_____, and _____
Verification of a Man - Computer System for Offshore Platform Upending Simulation by Scale Model Testing
OTC Paper 2163, 1975

Wilcox, Howard A.
The Ocean Food and Energy Farm Project
Second STAR Symposium, SNAME 1977

Note: To accompany *Report of Seakeeping Committee*; "VI Testing of Unconventional Ocean Platforms", by Biewer.

VII. DYNAMIC STABILITY AND CAPSIZING

by

Roderick A. Barr

INTRODUCTION

The dynamic stability of marine vessels has received, in recent years, significant attention. This has encompassed the gamut of vessel types and sizes from recreational boats under 20 feet in length to large containerships. The primary motivation is the desire to understand and thus to prevent losses due to capsizing and, for small boats, swamping. The scope of recent work on dynamic stability and capsizing is reflected in the proceedings of the 1975 International Conference on Stability of Ships and Ocean Vehicles.

This review discusses the state-of-the-art for understanding of and prediction of dynamic stability, capsizing and swamping, including:

1. Mechanisms of capsizing and swamping.
2. Methods for evaluating stability and capsizing.
3. Correlation of stability and capsizing predictions.
4. Establishment of stability criteria.

In addition, three extensive experimental and theoretical studies of dynamic stability and capsizing supported by the U.S. Coast Guard are highlighted. These three studies are felt to encompass collectively, state-of-the-art techniques for evaluating dynamic stability. No attempt is made to review the history of work in this area before 1974, but this is hardly necessary since a good review of earlier work is given by Bird and Odabasi (1).

MECHANISMS OF CAPSIZING

A number of mechanisms can result in capsizing. In some cases, capsizing will result from a combination of these mechanisms. Important mechanisms which are related to waves and wave induced motions are:

1. Low Cycle Resonance - Operation in a group of large following waves can result in a rapid increase in rolling motion and capsizing in a few cycles of motion. This unstable rolling occurs at one half the wave encounter frequency and is similar to the unstable motion described by the Mathieu equation.
2. Pure Loss of Stability - In large following waves, when

the ship speed is approximately equal to wave group velocity (one half phase velocity), wave length is one to two times ship length and a wave crest is amidships, the vessel can suddenly capsize due to total loss of roll stability.

3. Broaching - A group of large waves can force a vessel progressively farther off desired heading or course until the vessel broaches or turns broadside to the waves. These large waves, particularly when combined with strong gusting winds from the beam can cause capsizing of the broached vessel.

4. Shipping of Water - With low vessel freeboard and/or open deck, large relative motions between vessel and wave surface can result in shipping of water, followed by swamping due to loss of buoyancy or capsizing due to loss of stability. Swamping is often followed by capsizing.

A good description of the first three mechanisms is given by Oakley, et al (2) while the fourth mechanism is discussed by Sargent, et al (3).

Other mechanisms of capsizing, such as tripping of towing vessels, described by Amy, et al (4), are not related to operation in or ship motions due to waves.

METHODS FOR EVALUATING DYNAMIC STABILITY AND CAPSIZING

A number of methods have been used to study or predict dynamic stability and capsizing. The basic methods, and some of the recently reported studies in which they have been employed, are:

1. Theoretical predictions using linear, frequency domain predictions of motions, References 2, 3.

2. Theoretical predictions using nonlinear, time-domain simulations, References 2, 3, 4, 5, 6.

3. Theoretical predictions using various stability methods, References 6, 7, 8, 9, 10.

4. Laboratory model tests in unidirectional (long-crested) waves, References 4, 5, 9, 10, 11, 12, 13 and 14.

5. Field model tests in unidirectional or directional (short-crested) waves, References 2, 12.

6. Tests of small prototypes, Reference 15.

All of these methods have limitations, as described below.

In References 2 and 3 it is

concluded that linear, mathematical seakeeping methods are useful only for indicating the ranges of ship characteristics and operating conditions (ship speed, sea state or wave height and wave heading) which may be dangerous, and cannot be used to predict capsizing or swamping, which are nonlinear phenomena.

In Reference 2 the solution of coupled, six degree-of-freedom equations of ship motions for operations in irregular waves with no wind and resulting prediction of several modes of capsizing are discussed. In Reference 5 the solution of coupled roll, sway and heave equations for beam waves only is discussed. In Reference 4 the solution of an uncoupled equation of roll for irregular beam waves and gusting wind is discussed. In Reference 3 the solution of coupled roll, sway and yaw equations for irregular waves is discussed. The capabilities of these methods for predicting capsizing and swamping are discussed in a later section.

A number of investigators have considered direct solutions of a nonlinear equation of roll motion. The variety of approaches to solutions are illustrated by References 6-10 and by an earlier survey paper by Haddara, Reference 16. Approaches include various perturbation methods which are widely used in stability analysis. Casting of the equation of motions in the form of the Mathieu equation has been widely considered. The end products of such analyses are boundaries between stable and unstable operating regimes. As noted by Haddara, such solutions are useful for defining dangerous operating conditions but generally cannot be used for predicting actual capsizing.

All of the laboratory model tests have been carried out in unidirectional waves. In References 11 and 14 tests in regular waves and irregular waves modeling a prescribed wave spectrum are reported. In References 4 and 12, tests in regular waves only are reported. In Reference 5 tests only in irregular waves, which do not model a real wave spectrum, are reported. In References 10 and 13 tests in regular waves and wind are repeated. A gusting wind and waves whose height was modulated by the addition of a second regular low frequency wave were used in the tests reported in Reference 13. Correlation of model and full scale results are discussed in a later section.

The field tests reported in Reference 2, and described in more detail in Reference 17, were carried out in directional waves, although the directional distribution was more narrow banded than might be expected in open ocean environments.

The directionality of waves is not discussed in Reference 12. The directionality of waves in the full scale tests of pleasure boats, Reference 15, was not determined. The winds acting during testing were apparently not recorded during any of these tests.

CORRELATION OF PREDICTIONS, MODEL TESTS AND PROTOTYPE DATA

There have been few correlations of model test data or mathematical predictions with full scale data for extreme rolling motions and capsizing. Correlations for capsizing appear to be primarily qualitative, with only the occurence of capsizing under similar conditions correlated. Correlation of swamping for small recreational boats has been carried out where model tests and predictions were made for conditions closely matching those in the full scale tests.

Kure and Bang (13) have demonstrated good correlation of model test conditions and actual ship conditions for capsizing of a 60 meter long tanker in light condition. The model capsized with GM's between 100 and 115 percent of the estimated ship GM at capsizing. Amy, et al (4) provide model data for capsizings, with plausible operating GM's, for vessel types for which a number of actual capsizings have occurred.

Kaplan, et al (11) found no correlation of model test results and full scale results for swamping of small recreational boats, while Sargent, et al (3) found poor correlation of time domain mathematical simulations and full scale results for swamping of the same boats. It is somewhat surprising that the mathematical simulation duplicated three of 12 full scale swampings while the model tests duplicated none of the swampings. This may be due to the fairly poor correlation of the model and full scale wave energy spectra.

Good or acceptable correlation of model test and mathematical simulation of capsizing has been demonstrated by a number of investigators. Morall (5) has shown good quantitative correlation, while Oakley, et al (2) have shown some qualitative correlation. Boroday and Nikolaev (9) have shown good correlation of the statistics of rolling motions up to about 40 degrees. In all cases the correlation is for non-linear time domain simulations.

ESTABLISHMENT OF STABILITY CRITIERIA

The ultimate goal of stability studies is the establishment of rational stability criteria to be used in the design and operation of vessels. There appears, at present, to be some controversy on how to assess existing criteria or to

develop new rational stability criteria, which account for dynamic as well as static considerations, using results of model tests or mathematical simulations.

A primary problem in establishing stability criteria is the sensitivity of dynamic behavior, and capsizing in particular, to details of vessel geometry. For some types of vessels such as fishing, towing and supply vessels, the problem is acute. For ocean going ships the effect of geometry may be more easily defined. A recent attempt by Amy, et al (4) to establish stability criteria for fishing, towing and supply vessels based on model test data and operational experience met with a rather mixed response (see discussions of Nickum (18), Gilbert (19), and Townsend (20). The whole question of the rational basis for stability criteria and the relationship between static and dynamic stability has been raised by Odabasi (21). Despite such questions, however, it seems clear that well designed model tests and non-linear mathematical simulations can be useful for establishing new criteria and are particularly valuable for evaluating existing criteria.

THREE STUDIES OF DYNAMIC STABILITY

The U.S. Coast Guard has supported, since 1970, studies of dynamic stability of small recreational boats, towing, offshore supply and fishing boats, and fast container and cargo ships. These studies have been selected for a more detailed review because they represent the most significant U.S. activity in dynamic stability during the past five years and because they illustrate state-of-the-art technology.

Small Recreational Boats

Under U.S. Coast Guard sponsorship, a multi-phase study of recreational boat safety has been carried out. Various types of accidents were considered, with greatest emphasis on swamping and capsizing due to inadequate freeboard or initial stability, waves or wakes of passing boats or shift in load. References 3, 11, 14, 15 and 22 and 24 describe typical studies of actual accidents data, full scale boat tests, model tests and theoretical predictions. The studies by Oceanics, Incorporated of the feasibility of using model tests or theory for predicting swamping or capsizing, References 3 and 11, are of particular interest, and are described below.

Reference 11 compares the motions, shipping of water and swamping of a 12 foot long jon boat and a 15 foot long runaboat at various loading conditions as determined from full scale trials and from tank tests of 0.4 scale models. A comparison of full scale and

model motions and accelerations for a range of boat loading conditions and wave headings indicates that agreement with the Jon Boat is only fair, while agreement for the runaboat is fair to good. The agreement for swamping is very poor, the model test indicatting no cases of swamping and only one case of shipping water for 7 cases in which full scale swamped.

Reference 3 compares wave induced motions and freeboards for the jon boat and runabout from linear, frequency domain and nonlinear, time domain mathematical simulations and from full scale and model tests. In this reference, average differences between predicted motions and measured full scale motions are presented. Agreement is generally poor, particularly for pitch in beam seas and runabout lateral acceleration in beam seas. Agreement is somewhat better with the time domain simulation, except for roll. A comparison of rms freeboards predicted using the time domain simulations and from the model tests indicates poor agreement, with agreement being somewhat better for following seas than for beam seas. Time domain simulations for twelve cases in which the full scale boat shipped water, predicted only three cases of shipping water, rather poor agreement.

In References 3 and 11, a number of reasons are advanced for the generally poor correlation of results. The primary reason advanced is the lack of full scale data on wave directionality and wind. The significance of wave generation due to vessel motions, as described by Dudziak (12), could be a significant factor in the poor agreement of calculated and full scale shipping of water.

Swamping and capsizing of small recreational boats, such as jon boats, result in the loss of many lives each year. Adequate stability criteria and economical means for evaluating the safety of such recreational boats are needed.

Towing and Fishing Vessels

An extensive set of tests of four models of representative towing and fishing boats have been carried out by HYDRONAUTICS, Incorporated and are described in References 4 and 25. The vessel types tested were selected because they appeared to be likely candidates for capsizing due to high power, small size or low stability in following seas. Both tripping tests (tests in which a towing vessel capsizes due to its motions or those of the towed vessel) and tests in waves were conducted. Only the tests in waves will be discussed here.

Tests were carried out only

in regular head, beam and following waves. No tests were conducted in irregular waves. Tests in head and following seas were conducted over a range of speeds up to speed length ratios of 1.0 while tests in beam seas were conducted only at zero speed. In the head sea tests, both straight and zig zag courses were used. Tests were conducted for ranges of wave length and wave height.

One model, representing an 87 foot long Pacific Coast harbor tug, capsized in head waves. This model did not capsize in beam or following waves. Capsizing followed a rapid buildup of water on the deck and a resulting rapid increase in heel.

This model, representing a towing vessel, an offshore supply boat and a crabber, capsized in following waves. Capsizing always occurred in one of two modes described previously, low cycle resonance or pure loss of stability. No capsizings due to broaching occurred, perhaps due to the limitation on broaching imposed by the tank walls. No capsings occurred at low vessel speeds. The presence of water on deck was a prerequisite for capsizing.

Models of the towing vessel and crabber capsized, for limited wave conditions, in beam seas. Capsizing was due to slow heeling into the waves over 8 to 12 wave encounters, with little or no rolling, as a result of water pile-up on deck. Capsizing generally occurred in short, steep waves.

Capsizing was also studied using a time domain solution of an uncoupled, nonlinear roll equation motion assuming random beam waves and gusting beam wind. Capsizes could be simulated for realistic wave and wind conditions, and appeared to be a random function of roll angle, wave elevation and wind velocity. It was concluded that capsizing would occur if the rms roll angle exceeded one-quarter of the range of stability to leeward, a result that was used, together with the model test data, to formulate stability criteria.

Capsizing of towing and fishing vessels is a serious problem, resulting in large loss of life. Adequate stability criteria and means for evaluating the stability of given vessel designs are badly needed.

Capsizing of Ships at High Speeds

An extensive study of capsizing of container and break bulk cargo ships operating at high speeds in following seas has been carried out at the University of California at Berkeley. References 2, 17 and 26 describe this work. This work is presently being extended with laboratory model tests and documentation of the six-degree-

of-freedom time-domain computer program.

The primary efforts of this study were extensive tests of self-propelled, radio-controlled models of the SL-7 containership and American Challenger (C4-557a) class cargo ships in irregular, directional waves in San Francisco Bay and development of a nonlinear, time-domain, six-degree-of-freedom mathematical simulation. The use of a linear, seakeeping program for predicting ship motions was also investigated.

Numerous model capsizes were achieved in following and stern quartering seas, and resulted from one of three modes described earlier; low-cycle resonance, pure loss of stability or broaching. In all cases the initial stability was low (GM's of 2.3 percent or less of beam and 1.95 percent or less of beam for light and heavy load, respectively).

Capsizing was usually observed to occur when the model encountered a group of large waves. Other investigators, such as Ewing (27), have also pointed out the importance of wave groups in capsizing. The presence of large wave groups in the ocean, particularly with directional waves, has been confirmed by oceanographic data.

Wave spectra for these field tests were measured by an array of four wave probes. Sophisticated numerical methods were developed for obtaining good directional wave spectra (see Oakley (26)). The spectra deduced from the wave probe data were relatively narrow, particularly for the higher sea states, but are certainly more representative of ocean waves than are the unidirectional waves in laboratory tests.

The time domain mathematical simulation was used to study capsizing in modulated regular waves which are generated by a pair of regular waves of different frequency. These modulated waves have many of the characteristics of a wave group. Capsizing of the cargo ship in following quartering seas were simulated, capsizing occurring in both the low cycle resonance and pure loss of stability modes.

Capsizing of large, ocean-going ships operating with reasonable GM's is rare. All capsizings in this study occurred with GM's which are lower than would be permitted in actual operation.

CONCLUSIONS

This review suggests a number of general conclusions about current state-of-the-art for dynamic stability and capsizing.

1. Laboratory model tests may not adequately predict capsizing due to the absence of a realistic test environment

incorporating directional waves and gusting winds. Model tests in a carefully selected field environment can be more useful, but are much more difficult and expensive to conduct.

2. Nonlinear, time domain mathematical simulations are able to predict the general conditions for the occurrence of capsizing, but are, at present, primarily useful as a qualitative or comparative rather than a quantitative or predictional tool.

3. Mathematical stability anlayses can accurately predict unstable operating conditions where large rolling motions occur but cannot predict capsizing for a wide range of operating and environmental conditions.

4. It is difficult to generalize full scale or model test results into rational stability criteria which are applicable to whole classes of vessels, although such data are valuable for evaluating existing criteria.

REFERENCES

1. Bird, H. and A. Y. Odabasi, "State of Art: Present and Future," Proceedings of International Conferences on Stability of Ships and Ocean Vehicles, C. Kuo, Editor, Glasgow, Scotland, 1975.

2. Oakley, O. H., Jr., J. R. Paulling and P. D. Wood, "Ship Motions and Capsizing in Astern Seas," Proceedings of the Tenth Symposium on Naval Hydrodynamics, ACR-204, June 1974.

3. Sargent, T. P., M. N. Silbert and P. Kaplan, "Feasibility Study of Mathematical Simulation of Loading Related Recreational Boat Accidents," U.S. Coast Guard Report CG-D-44-77, December 1975.

4. Amy, J. R., R. E. Johnson and E. R. Miller, "Development of Intact Stability Criteria for Towing and Fishing Vessels," Transactions of the SNAME, Volume 84, 1976.

5. Morral, A., "Simulation of Capsizing in Beam Seas of a Side Trawler," Proceedings of International Conference on Stability of Ships and Ocean Vehicles, 1975.

6. Wellicome, J., "An Analytical Study of the Mechanisms of Capsizing," Proceedings of International Conference on Stability of Ships and Ocean Vehicles, 1975.

7. Kuo, C. and A. Y. Obahasi, "Application of Dynamic Systems Approach to Ship and

Ocean Vehicle Stability," Proceedings of International Conference on Stability of Ships and Ocean Vehicles, 1975.

8. Abicht, W., "On Capsizing of Ships in Irregular Waves," Proceedings of International Conference on Stability of Ships and Ocean Vehicles, 1975.

9. Boroday, I. K. and E. P. Nikolaev, "Methods for Estimating the Ship's Stability in Irregular Seas," Proceedings of International Conference on Stability of Ships and Ocean Vehicles, 1975.

10. Tamiya, S., "Capsize Experiments of Box Shaped Vessels," Proceedings of International Conference on Stability of Ships and Ocean Vehicles, 1975.

11. Kaplan, P., T. P. Sargent and M. N. Silbert, "Feasibility Study of Tank Modeling Environmentally Affected Loading Related Recreational Boat Accidents," U.S. Coast Guard Report CG-D-52-76, December 1975.

12. Dudziak, J., "Safety of a Vessel in Beam Sea," Proceedings of International Conference on Stablility of Ships and Ocean Vehicles, 1975.

13. Kure, K. and C. J. Bang, "The Ultimate Half Roll," Proceedings of International Symposium on Stability of Ships and Ocean Vehicles, 1975.

14. Hires, R. I., "Recreational Craft Performance Study," U.S. Coast Guard Report CG-D-7-76, September 1975.

15. U.S. Coast Guard Research and Development Center, New London, Connecticut, Log Books of Full Scale Experiments.

16. Haddara, M. R., "On Nonlinear Rolling of Ships in Random Seas," International Shipbuilding Progress, Volume 20, No. 230, October 1973.

17. Chou, S. J., et al, "Ship Motions and Capsizing in Astern Seas," U.S. Coast Guard Report CG-D-103-75, December 1974.

18. Nickum, G. C., Discussion of Reference 4.

19. Gilbert, J.W., Discussion of Reference 4.

20. Townsend, C., Discussion of Reference 4.

21. Odabasi, A. Y., Discussion of Reference 4.

22. Wyle Laboratories, "Safe Loading Test Procedure Development Report," Report 58201-2 (DR), April 1972.

23. Operations Research, Incorporated, "Guidelines for the Investigation of Capsizing and Swamping of Small Recreational Boats," AD/A-007 076, March 1974.

24. Sautkulis, C. M. Knack and J. Borman, "Capsizing/ Swamping Accident Investigations for 1974 Season, Volume I - Research Report and Volume II - Appendices," U.S. Coast Guard Reports CG-D-139-75 and CG-D-140-75, April 1975.

25. Miller, E. R. and V. Ankudinov, "Evaluation of Current Towing Vessel Stability Criterion and Proposed Fishing Vessel Stability Criteria," U.S. Coast Guard Report No. CG-D-4-76, 1976.

26. Oakley, O. H., Jr.,"Directional Wave Spectra Measurement and Analysis Systems," SNAME Panel H-7 Seakeeping Symposium, Webb Institute, October 1973.

27. Ewing, J. A., "Environmental Conditions Relevant to the Stability of Ships In Waves," "Proceedings of the International Symposium on Stability of Ships and Ocean Vehicles, 1975.

SEAKEEPING DESIGN BASE FOR AIR CUSHION VEHICLES

by

David D. Moran
David W. Taylor Naval Ship Research and Development Center

The understanding of the dynamic behavior of air-cushion-supported ships is in its infancy relative to the history of research on the seakeeping of displacement ships. The air cushion vehicle is a relatively modern concept and the international hydrodynamic community has only recently begun to examine the unique problems associated with the dynamic performance of these vehicles. Further, a complete understanding is hampered by the paucity (again compared with displacement ships) of full scale vehicles to clarify problem areas through full scale observations and trials.

The design of air cushion vehicles (ACV) for acceptable habitability and the evaluation of the seakeeping characteristics of ACVs during the design process have remained technically unsolved problems. The seakeeping design tools consist of three techniques. The first is the testing of geometrically and dynamically scaled models in a seakeeping basin. Model scale seakeeping experiments are presently limited in their reliability for design by an uncertainty over the special scaling procedures which are appropriate to air-cushion-supported vehicles. Experiments also require the construction of an expensive model of a specific design, thereby often making parametric evaluation for design difficult or impractical. Model scale testing does, however, allow the full range of experimental techniques such as regular and irregular wave testing, oscillation, wave excitation and transient waves techniques to be applied to a design evaluation.

The second method of analysis is mathematical simulation of the dynamic response of the ACV. The major difficulty with this method is that presently available air cushion vehicle seakeeping simulations have not been fully validated. Many investigators have published mathematical models of varying utility; however, none of these models has been proved to be a general engineering and design tool. Completely validated mathematical models will allow parametric design analysis when they become available.

The third method of design analysis outlined in this review is the development of a seakeeping data base. In the absence of other methods of seakeeping analysis this seakeeping data base would serve the designer as a guide to expected

response of the vehicle. The application of the data therefore requires a classification guide which describes as completely as possible the geometric and operational characteristics of the vehicle. The designer may then match expected or design craft characteristics against the system response contained in the data base. Alternatively, the seakeeping information may be used to optimize an air cushion vehicle design to meet special seakeeping requirements. The major limitation of this approach is the expected occurrence of gaps in the data set. The designer would be required to interpolate between known quantities while recognizing that the information obtained should be used only as a guide to design under these circumstances. The continued accumulation of data should make this limitation less severe with time.

SEAKEEPING CLASSIFICATION PARAMETERS

Air-cushion-supported vehicles may only be described completely by a seemingly endless catalog of design and operational properties. Each ACV design is unique, and new craft incorporate design features untested in previous ships in addition to modifications of previously implemented characteristics. Strictly, therefore, each ACV can be classified only through an exhaustive design summary. Certain general properties of air-cushion-supported craft do demand greater attention and appear to be critical in any ACV design or evaluation exercise. In this review ten nondimensional characteristic parameters are chosen to quantitatively classify an ACV configuration. It is also necessary to specify six qualitative descriptors of the ACV design which aid in the understanding and interpretation of the design but are not required for quantitative comparison of the seakeeping performance of the vehicle.

These descriptors include the type of cushion seal provided around the circumference of the craft. Surface piercing sidewalls of surface effect ships (SES) provide the best cushion seal and also furnish a portion of the lift through hydrostatic displacement at low speed and a combination of displacement and hydrodynamic lift at high speed. Alternatively, the flexible side seals of amphibious air cushion vehicles provide less efficient sealing and practically no lift. Bow and stern seals are available in a wide range of designs. Bag and finger or peripheral cell seals are designed to allow movement over water or solid material in more than one direction, and planing seals of either rigid or flexible design optimize cushion sealing and hydrodynamic drag. Quantitatively the lift of the cushion sealing system may be assessed through the ratio of cushion support force to craft mass. This lift parameter ($p_c A/m$)* has near unity magnitude for fully skirted air cushion vehicles. Excess pressure ($p_c A/m > 1$) is required to overcome the loss of energy attributed to the loss of air under the skirts. An air cushion vehicle just touching the free surface with no cushion air losses would display a lift parameter with a magnitude of unity. Vehicles incorporating surface piercing sidewalls in their design show lift parameters less than unity. The exact value depends upon the magnitude of hydrostatic and hydrodynamic lift. For all conditions the lift parameter is normally speed dependent and is therefore most appropriately presented at zero speed for design comparison.

The overall geometry of the vehicle is characterized by the length-to-beam ratio and the cushion planform block coefficient designated as (A/B_e^2) and ($A/B_e L_c$) in the table. The length-beam ratio is based upon an effective cushion length ($L_e = A/B_e$) which is defined by the cushion planform area A divided by the effective cushion beam B_e as shown in the definition table. The definition of an effective length is motivated by the fact that most air-cushion-supported vehicles are longitudinally prismatic but may have curved bow and stern seals. The cushion beam and planform areas are usually easily obtainable.

*All variables and symbols are defined in the Nomenclature.

A cushion block coefficient is a necessary classification parameter for vehicles with curved nonlinear or nonprismatic bow seals.

A third geometric factor of importance in ACV dynamics classification is the ratio of cushion length to cushion depth (L_e/d). Cushion depth influences but does not define the limiting operational sea state for the vehicle. The pitch and roll stability of air-cushion-supported vehicles is significantly affected by length-to-depth and beam-to-depth ratios.

The dynamic response of an ACV is greatly influenced by the existence of cushion compartmentation and active cushion pressure control. These two items are required qualitative descriptors of air cushion craft. Active cushion control may take the form of a pressure relief valve as implemented on an existing SES as a heave alleviation system or as an active flow valve directing cushion fluid to individual regions of the cushion as required. Cushion compartmentation is usually interpreted as passive control.

In addition to active cushion control, some air cushion craft are appropriate for hydrodynamically or aerodynamically induced motion control. Foils may be fitted to the sidewalls of SES and vertical plane aerodynamic forces and moments may be easily produced for air powered vehicles. The effect of these devices upon the dynamic response of air-cushion-supported craft can be established only qualitatively in a design comparison without recourse to the exact geometry and lift-drag characteristics of the control device.

The two major cushion characteristics which must be identified in any dynamics comparison are the cushion density given in nondimensional form as $p_c/\rho g L_e$ and the ratio of the seal, bag or loop pressure to the cushion pressure or the over-pressure ratio (p_s/p_c). The cushion density determines the payload of the vehicle and the wavemaking resistance and is a major factor in the structural design of an ACV. Recent design trends have been toward higher cushion densities particularly in the design practice of the U.S. Navy. The over-pressure ratio is a major factor in the stiffness and stability of seal systems. In this area the modern trend seems to be toward lower over-pressure ratios than those employed in early ACV designs. The seal over-pressure may not be constant around the seal circumference. The seal pressure is determined by the nature of flow through the seal to the cushion and by the existence of internal seals in the seal system. The major opportunity for seal pressure nonuniformity occurs in sidewall sealed air cushion ships where the seals may have completely separate lift system air supply and distribution designs. For vehicles falling in this category it is necessary to classify the design according to separate bow and stern over-pressure ratios.

The rigid body motion of air-cushion-supported vehicles hinges upon the mass and overall damping properties of the entire system. The specification of inertial properties requires the identification of one additional quantity proportional to the moment of inertia of the vehicle and presented here as the radius of gyration normalized by the effective cushion length ($\sqrt{I/mL_e^4}$) where I is the moment of inertia for a specified

rotational axis. Ideally the designer wishes to know this quantity for all three rotational axes of the craft but in reality the pitch moment of inertia often must be estimated from a known yaw moment and the roll moment of inertia is frequently missing from published ACV performance characteristics.

Two additional classification parameters which describe the stiffness and damping characteristics of the overall ACV lift system may be computed from the cushion pressure and lift system discharge. The entire lift system performance may be represented as a pressure/discharge relationship in a manner very similar to a normal fan performance curve. The slope of the curve at the craft operating point (p_c, Q) is a measure of the stiffness of the entire lift system and determines the vertical plane frequency response. This quantity should be specified as the nondimensional derivative $(Q/p_c)(dp_c/dQ)$ evaluated at the craft operating point.

The craft damping is inversely proportional to the magnitude of the system discharge and is related to other lift system properties in a complicated fashion not examined in this presentation. The system discharge Q should be specified whenever possible for each ACV classified in a design data base. The significant parameter associated with discharge is the cushion volume replenishment time which is the ratio of the cushion volume to the lift system discharge. Correspondingly, the system damping may be classified by a characteristic decay period which is equal to the reciprocal of the exponential decay coefficient β. The appropriate nondimensional design parameter is the ratio of those characteristic periods in the following form, $Q/B_eL_e d\beta$. The decay coefficient used in this ratio should refer to heave damping, but the availability of such information may dictate another response mode. The system discharge determines the flying height of the ACV which in turn has a significant effect on overland dynamic response, resistance and obstacle crossing capability. Further, the system discharge affects the craft overwater drag and hence has an effect on both the required system power and on the resistance of the vehicle.

SEAKEEPING DATA BASE

An air cushion vehicle description must be reduced to a small number of quantitative and qualitative descriptions to be of value to the designer as noted in the previous section. Similarly the seakeeping response of an ACV may be specified in complete detail only through an indeterminate number of graphical representations showing the effects of speed, heading, craft trim, sea state, degrees of freedom of motion, propulsive characteristics and immediately previous motion history. Meaningful design application of the data base requires that the most significant aspects of the seakeeping behavior be summarized on as few figures as possible. The choice of meaningful or useful response properties is of course open to individual interpretation. It is evident, however, that in any seakeeping evaluation the response of an ACV must be considered in head and beam seas. In head seas the pitch and heave response of the vehicle may be specified independently from an analysis of the coupled motion. Similarly the roll and heave response of the vehicle are specified in beam seas. Quartering sea response generally exhibits lower response amplitudes in all three variables then those observed in the appropriate responses in head and beam seas. For this reason the quartering sea response may be considered a degree less critical in design seakeeping analysis. Following and stern quartering seas also show generally lower response amplitudes except in surge (and sway and yaw in the case of quartering seas). These responses are horizontal plane (maneuvering) considerations and, without minimizing their importance, are therefore excluded form this presentation.

Seakeeping response is here presented as a transfer function based upon the first harmonic amplitude of the response variable normalized by the first harmonic amplitude of the encountered wave for heave or the corresponding wave slope for pitch and roll. In a model scale experiment these quantities are obtained through regular (sinusoidal) wave excitation. For full scale vehicle response (or corresponding model scale experiments) in irregular waves they may be obtained from the measured sea spectrum and response spectra through either auto- or cross-correlation analysis. The transfer functions presented are shown as functions of the nondimensional encounter frequency μ_e. This representation accounts simultaneously for the speed, scale and heading of the vehicle with respect to the wave field.

The phase relationships between the excitation and response variables are not presented in this review but they are an integral part of a seakeeping data set. The phase relationships are most important in relative motion and slamming analyses, and their effect on seakeeping considerations for structural design may be of major concern.

An important consideration is the degree to which the seakeeping response variables are linear with wave amplitude. The response linearity of an ACV may be determined through four procedures. The magnitude of harmonic components higher and lower than the fundamental in the regular wave response reflect the linearity with respect to the corresponding

analysis of the excitation. Alternatively the similarity of transfer functions derived from irregular wave experiments of differing shape and energy content demonstrate the linearity of ACV seakeeping response. In a similar vein, an irregular sea response may be constructed from the regular wave response operator and the known sea spectrum which excited the irregular sea response. For a linear system these two response curves must be colinear. The fourth procedure for assessing linearity is by direct variation of wave amplitude for a fixed wave encounter frequency in a regular wave investigation. Each of these methods has been employed in investigating linearity for the various air cushion vehicles included in this review. In general it is found that ACV linearity exists for inverse wave slopes greater than 30 ($\lambda/2a > 30$). This finding indicates that regular wave seakeeping analysis is meaningful and that the normal linear seakeeping methods traditionally applied to surface ships are applicable to air cushion vehicles.

A significant potential restriction of the application of model scale experimental or analytic seakeeping response to large scale vehicles is that a general scaling theory has not yet been developed. It is known that the dynamic response of ACV's does not scale to full size by classical methods. Recently proposed scaling methods involving a combination of analysis and experimental data have not shown complete success. This problem is compounded by the small amount of full scale dynamic response data available relative to the abundance of model scale data. The implication of this problem in a seakeeping data base is that the actual length of the vehicle must be included as a classification parameter in the seakeeping data set.

The seakeeping data contained in this presentation is reported as an example of the continued compilation of information which will be of value to the designer. The material should be considered as an accurate but incomplete catalogue of the type of seakeeping information which the ACV designer may continue to collect and classify according to the criteria set in the first section of this presentation and given for the specific vehicles in the table. The data included reflect the variety of skirt and cushion configurations common in contemporary ACVs but many other geometric and operational configurations have been evaluated in recent ACV designs and their inevitable inclusion in the seakeeping data set will increase its future utility. Of special note is the exclusion of surface piercing sidewall sealed air cushion supported vehicles which will be included in a separate presentation.

The following seakeeping data reflects the performance of six air cushion vehicles under a variety of operational conditions. The vehicles are coded and classified in the table according to the standards previously set and with the exclusions previously noted.

The head sea response of vehicle AC is shown in Figures 1, 2 and 3. The seakeeping response of this vehicle may be used to illustrate response linearity through comparison of irregular sea transfer functions measured in different sea states. Figures 1 and 2

demonstrate the result of tripling the excitation significant wave height. Some differences in the responses are obvious. They are, however, small, especially in the subcritical frequency range ($\mu < 3.0$). Increasing Froude number has a greater effect on the head sea response as shown in Figure 3. Increased speed for this vehicle causes increased heave response at higher frequencies, a result which may be of significance to the designer in habitability and vibration analyses.

The effect of peripheral cell skirt design in comparison with bag and finger sealing may be observed by comparing Figures 4 and 5 with the previously discussed results shown in Figures 1, 2, and 3. Vehicle AA shown in these figures exhibits generally higher pitch response but lower heave response than vehicle AC. That is, vehicle AC is less critically damped in pitch but overdamped in heave for the operational conditions designated in the table. The effect of speed on the response of vehicle AA is similar to vehicle AC. Figures 4 and 5 show an increasing response in heave and pitch. The increased pitch response results in a shift of the pitch resonance to a higher frequency.

Recent design trends have been directed toward higher cushion densities. The highest cushion density found in the present data set is shown for vehicle VH in Figures 6 and 7. The major effect of this configuration is a high transfer function in heave. It is interesting to note that the increased cushion density has not resulted in a decrease in the resonant heave period when compared with the other designs. One reason for this is the low cushion length-to-depth ratio employed in the design of vehicle VH. Underdamping in the pitch response is aggravated for this design by a low loop-to-cushion pressure ratio. Response linearity is again demonstrated for air cushion vehicles through the comparison of the two irregular sea states shown in Figures 6 and 7.

Reducing the cushion density while holding other design characteristics nearly constant produces a dramatic reduction in both heave and pitch responses. This is seen by comparing the results for vehicle VL in Figure 8 with vehicle VH in Figure 7 where both vehicles were examined at the same speed in the same sea state. An important consideration in this difference is that the cushion system discharge for model VL was reduced to 0.74 of the cushion discharge of vehicle VH.

A further reduction of cushion density for vehicle BH shown in Figure 9 does not show a corresponding reduction in the amplitude of response. Anomalous behavior of this type will undoubtedly be clarified by the development of a more comprehensive data set. This example points out the need for the collection of seakeeping experimental results and the continued examination of vehicle scale in the data set.

The effect of nonsinusoidal wave excitation on vertical plane response of air cushion vehicles is shown in Figures 10, 11 and 12 where vehicle AB was tested overland. As speed is increased in the succession of Figure 10 through 12 the amplitude of response increases, finally showing a pitch resonant peak at a nondimensional encounter frequency μ_e, equal to 5. Heave response is in all cases overdamped. The effect of the free surface may be seen

by comparing Figures 1 and 2 for vehicle AC with the overland results shown in Figure 10 for vehicle AB.

Beam sea response is portrayed for vehicle AA in Figures 13 and 14. This vehicle exhibits low damping character in roll and the previously noted overdamped response in heave. The effect of speed on the beam seas response for this craft is minimal, showing a slight shift to higher encounter frequency and a minor reduction in amplitude with increased speed. A larger scale vehicle (BH) experiment in irregular beam seas appears to be severely overdamped in roll as seen in Figure 15.

SUMMARY

The intention of this presentation is to review guidelines for and encourage the compilation of a seakeeping data set for air-cushion-supported vehicles. In the absence of fully validated analytic procedures to describe the seakeeping of ACVs the proposed catalogue of pitch, heave and roll transfer functions will provide the ACV designer with basic information with which he can predict the performance in seas of a proposed design.

TABLE : VEHICLE DESCRIPTIONS AND PROPERTIES

Vehicle Code	AA	AB	AC	BH	VH	VL
Side Cushion Seal	B+PC	B+F	B+F	B+F	B+PC	B+PC
Bow Cushion Seal	B+PC	B+F	B+F	B+F	B+PC	B+PC
Stern Cushion Seal	B+SF	B+SF	B+SF	B+SF	B+SF	B+SF
Cushion Compartmentation	No	Yes	Yes	Yes	No	No
Active Cushion Control	No	No	No	No	No	No
Hydrodynamic Motion Control	No	No	No	No	No	No
Cushion Lift Fraction, $\frac{pcA}{m}$	1.08	1.06	1.00	1.02	1.06	1.11
Length-Beam Ratio, A/B_e^2	1.78	2.16	1.94	1.92	1.94	1.94
Length-Depth Ratio, L_e/d	17.0	15.8		11.5	9.5	9.5
Cushion Block Coefficient, A/B_eL_c	.98	.99	1.00	.94		
Cushion Density, $p_c/\rho gL_e$	13.4	18.0	18.3	8.2	23.1	16.2
Loop/Cushion Pressure, p_s/p_c	1.35	1.32			1.10	1.30
Pitch Gyradius/Length Ratio	.30	.29	.27		.27	.28
Roll Gyradius/Length Ratio	.17	.16	.11			
Vehicle Cushion Length, L_c(m)	1.82	2.03	1.94	24.38	2.01	2.01

CUSHION SEAL TYPES

B	Bag
F	Finger
PC	Peripheral cell
SF	Sealed fingers

NOMENCLATURE

a	Wave amplitude, first harmonic
A	Cushion planform area
B_e	Effective cushion beam
d	Cushion depth
F_n	Froude number, $U/\sqrt{L_e g}$
g	Gravitational constant
I	Moment of inertia for a specified rotational axis
k	Wave number, $2\pi/\lambda$
L_c	Maximum cushion length
L_e	Effective cushion length
m	Craft weight
p_c	Cushion pressure
p_s	Seal, bag, or loop pressure
Q	System discharge
T_o	Characteristic decay time, $1/\beta$
U	Craft speed
z	Heave amplitude, first harmonic
β	Exponential decay coefficient
θ	Pitch amplitude, first harmonic
λ	Wave length
μ	Nondimensional frequency, $\omega\sqrt{Le/g}$
μ_e	Nondimensional encounter frequency, $\mu(1+F_n\mu)$
ρ	Density of working cushion fluid
ϕ	Roll amplitude, first harmonic
ω	Frequency

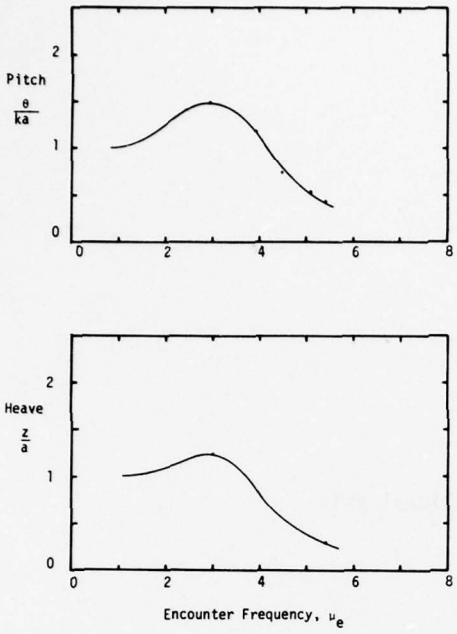

Figure 1 - Vehicle AC: Head sea transfer functions for pitch and heave, irregular sea state 2, F_n = 0.68

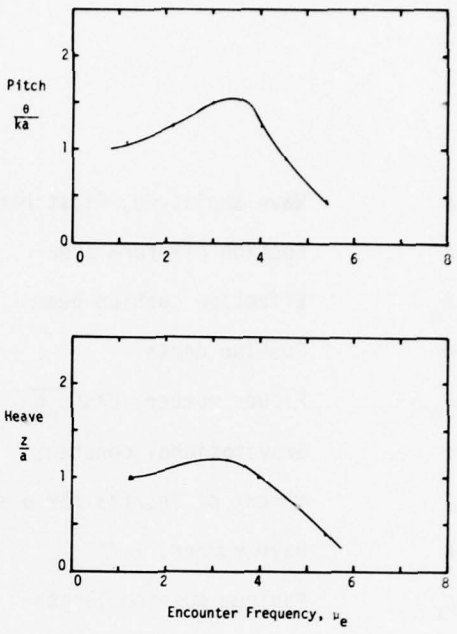

Figure 2 - Vehicle AC: Head sea transfer functions for pitch and heave, irregular sea state 4, F_n = 0.68

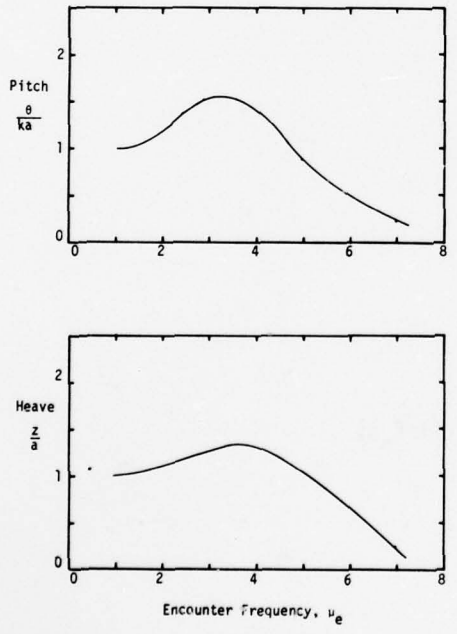

Figure 3 - Vehicle AC: Head sea transfer functions for pitch and heave, irregular sea state 4, F_n = 1.02

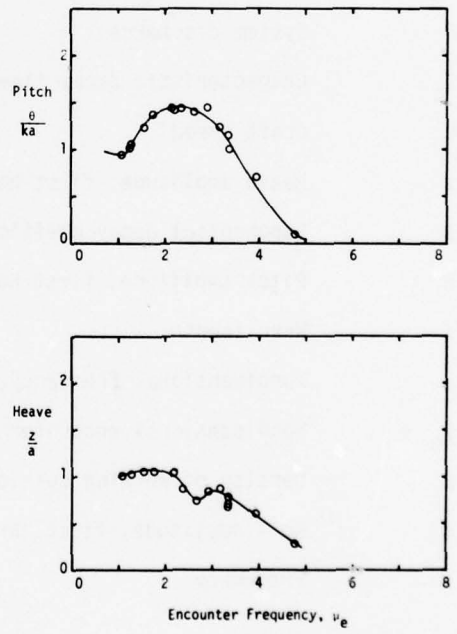

Figure 4 - Vehicle AA: Head sea transfer functions for pitch and heave, regular waves, F_n = 0.48

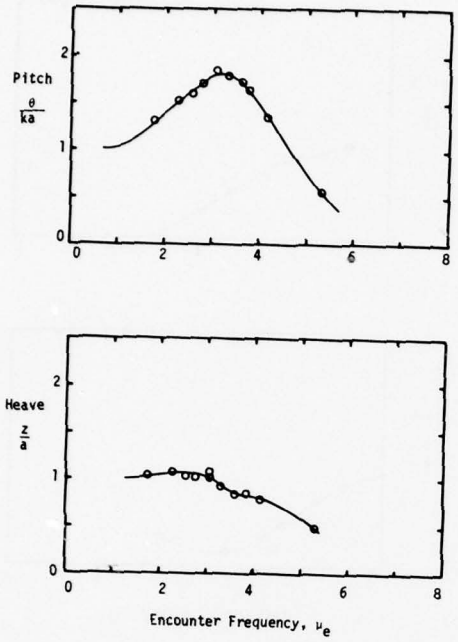

Figure 5 - Vehicle AA: Head sea transfer functions for pitch and heave, regular waves, F_n = 1.13

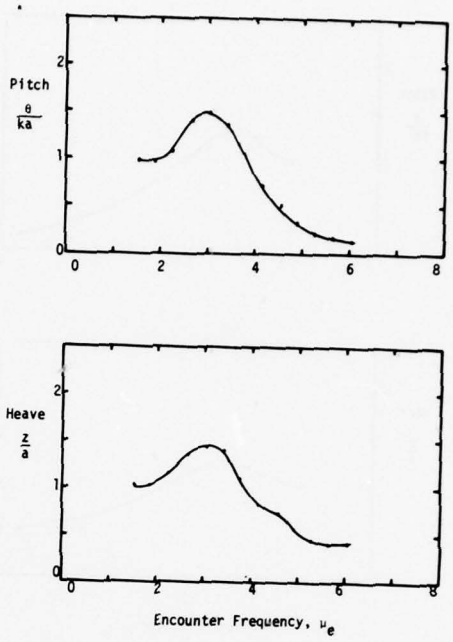

Figure 6 - Vehicle VH: Head sea transfer functions for pitch and heave, irregular sea state 3, F_n = 1.22

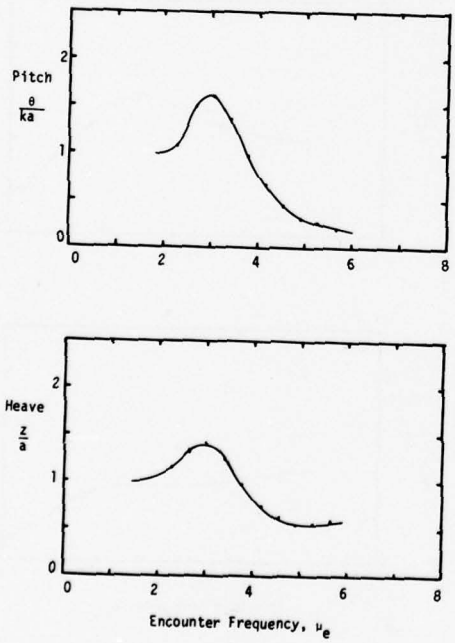

Figure 7 - Vehicle VH: Head sea transfer functions for pitch and heave, irregular sea state 4, F_n = 1.22

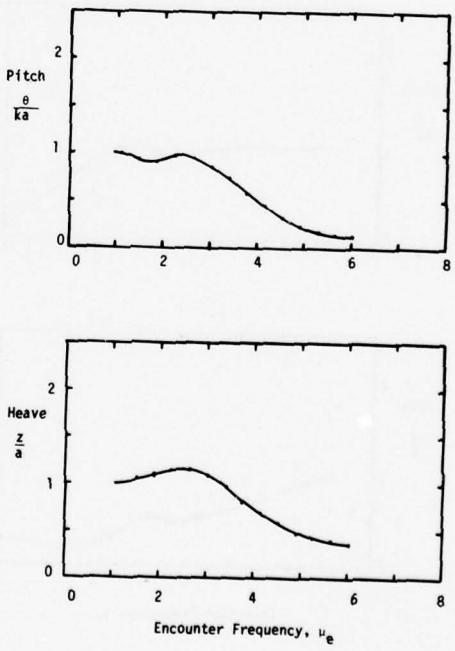

Figure 8 - Vehicle VL: Head sea transfer functions for pitch and heave, irregular sea state 4, F_n = 1.22

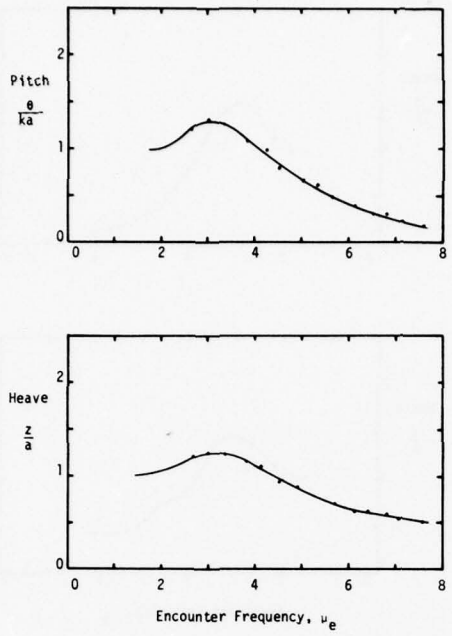

Figure 9 - Vehicle BH: Head sea transfer functions for pitch and heave, irregular sea state 2, F_n = 1.89

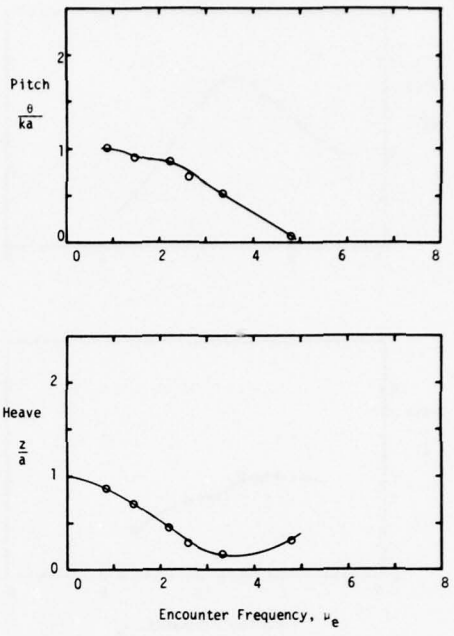

Figure 10. Vehicle AB: Overland transfer functions for pitch and heave, trapezoidal waves, F_n = 0.70

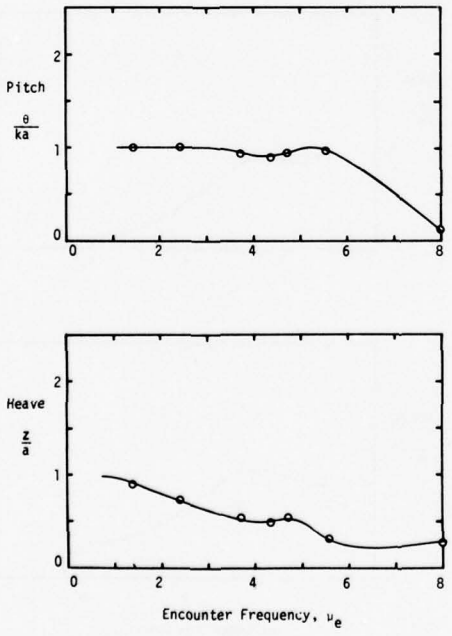

Figure 11 - Vehicle AB: Overland transfer functions for pitch and heave, trapezoidal waves, F_n = 1.16

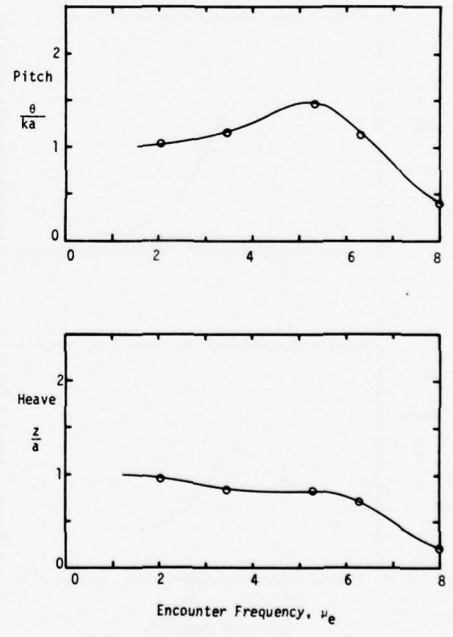

Figure 12 - Vehicle AB: Overland transfer functions for pitch and heave, trapezoidal waves, F_n = 1.67

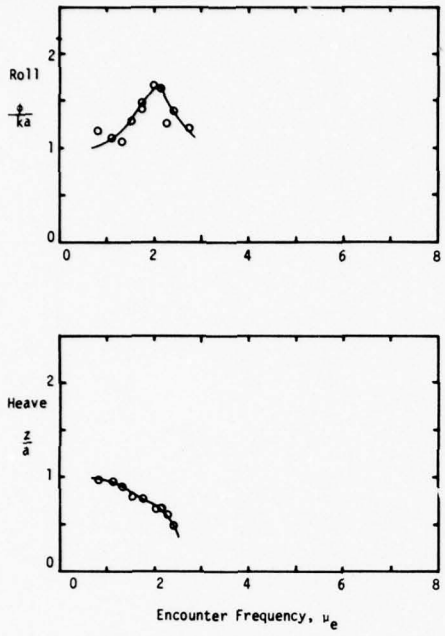

Figure 13 - Vehicle AA: Beam sea transfer functions for roll and heave, regular waves, F_n = 0.48

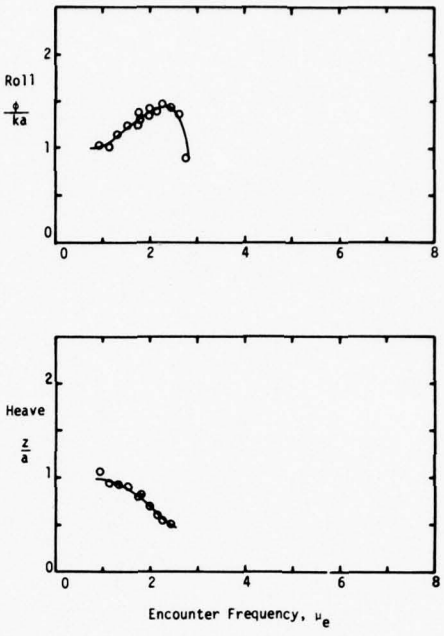

Figure 14 - Vehicle AA: Beam sea transfer functions for roll and heave, regular waves, F_n = 1.13

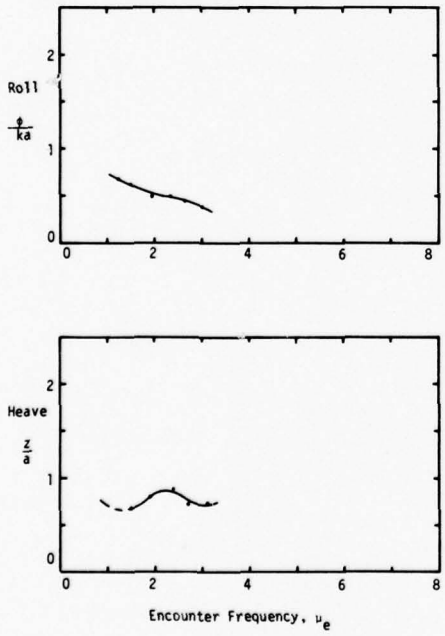

Figure 15 - Vehicle BH: Beam sea transfer functions for roll and heave, irregular sea state 2, F_n = 2.04

DIGITAL SYNTHESIS OF MODELLED IRREGULAR SEAWAY TIME HISTORIES

by

J. Brooks Peters
David W. Taylor Naval Ship Research and Development Center

Although the problem of predicting the responses of a ship to an irregular seaway is a complex one dealing with six degrees of freedom of the vessel's motion, it is now often being solved, at least in part, through the use of computerized simulations. Nevertheless it falls to the experimental naval architect to use model testing to provide the data base on which these simulations depend, to observe and record those nonlinear phenomena such as slamming, extreme motions, and skirt or seal collapse for an air cushion supported vehicle which would be extremely difficult to model successfully within a simulation and to validate analytical solutions to seakeeping problems. Since accurate modelling of the nonlinear responses depends so much on a good representation of the seaway which the prototype will experience, an effort has been undertaken at DTNSRDC to provide the naval architect with as much latitude as possible for the selection of a modelled sea environment. Although this work is continuing, some preliminary results can be shown from an early application and some observations made as to the potential for future development.

WAVE GENERATION EQUIPMENT

Those basins at the Carderock facility designed for seaworthiness testing are equipped with pneumatic wave generation systems capable of producing regular waves with a frequency range of 1.6 to 9.0 rad/sec and single amplitudes of between 0.5 and 12.0 inches. The wavemaking unit consists of a large electrically driven air blower, a partially immersed dome, duct-work connecting the blower and the dome, and a pair of flapper valves which interrupt the ducting between the two major components. In operation, the blower, running at constant speed, moves air between the dome and atmosphere, while the flappers regulate the rate and direction of this flow. The flapper valves are controlled by an externally developed voltage, as in the case of a sinusoid for regular waves or a voltage time history when irregular waves are required. Because the wavemaker is controlled by two independent variables, blower speed and input voltage, it should be understood that although both can regulate wave height, the flapper valve is much more limited and is not generally used to set the significant waveheight.

BASIC APPROACH

The approach used to define the wave generator as a linear system and to use that definition in synthesizing new time histories is much the same as it would be for a model test with a similar purpose. The first step is to assume that the wave generating system is sufficiently linear to apply standard tests for frequency response. In this case measurements were taken of regular wave amplitudes produced at a series of frequencies distributed across the frequency range of the wavemaker. From this, a transfer function of wave amplitude per unit voltage amplitude, as a function of wave frequency, can be produced. Typically these appear as in Figure 1 and show significant dependence, in terms of shape, on the blower speed. Thus it is useful to develop a family of transfer functions, each for a different blower speed. Generally, however, a limited range of blower speeds is used and one centrally located curve should be sufficient for this first step.

This transfer function associates the input voltage to the output waves in a simple fashion. As a result the input can be deduced from examination of the output. For the case here of known, or desired, output fixed by an arbitrary spectral density function, the power spectrum necessary for the input can be found by dividing the output spectral density function by the square of the transfer function.

The problem still exists in the frequency domain and a shift to the time domain will be needed in order to produce the time histories of the control voltage. Two digital programming techniques have been used to accomplish this task. The first is well suited to on-line operations which might be used in the development of a new spectral shape as described later. The second, although available in modified form for on-line use, is much more satisfactory when used off-line in conjunction with a large computer to generate and store the time histories on digital tape.

ON-LINE PROCEDURE

The first technique is the simpler of the two. It subdivides the required input spectrum into a number of arbitrarily spaced regions, evaluates the energy beneath the spectral density function within that region and assigns that energy to a sinusoid with a frequency randomly selected from within that region and with random phase relative to all other components. Thus the voltage at any point in time can be found by summing the contribution from each component at that point in time. The frequencies are randomly assigned so as to avoid a 'system period', that is a repeat period in the time history such that $f(t+Ts) = f(t)$. This problem will show up when the frequencies are regularly spaced or arranged in a simple pattern.

The problems that develop from the employment of this technique stem largely from the fact that rather than having a continuous distribution of energy through the range of frequencies, a large number of sinusoids provide the approximation of it. This can cause difficulty in the model test if the model happens to have a narrow-banded response characteristic which might not be excited or perhaps be overemphasized by the

concentration of energy at resonance. Secondarily, when the model takes on forward speed in head seas, the nonlinear mapping of wave frequency into encounter frequency will tend to spread the sinusoids with this effect accentuated at the higher frequencies.

Spectral analysis, however, will tend to smooth this tendency because it will generally be including several components into the estimate it develops for a single band. This means that the first approach would be successful when applied to an examination of those nonlinear or second order effects which were disregarded earlier.

Because the wavemaker response is most nonlinear on the fringes of its frequency range, it was found necessary to make two or three iterative cycles of wavemaking/transfer function modification when significant amounts of energy were required at these frequencies. This procedure made use of two minicomputers, one at the wavemaker producing the control time history for the wavemaker, and the second mid-length on the basin which monitored the waves and performed spectral analysis on the recorded wave height time history.

Since the control time history being produced on-line was based upon a particular transfer function, modification of that transfer function will cause a corresponding change in the spectral density function of the waves. Thus the mid-basin computer can perform spectral analysis of the waves, the result of which can suggest a change in the transfer function being used to generate the control time history. In this way an iteration could be completed in 20 to 30 minutes.

This procedure seldom required more than two trials except when significant amounts of energy are required at the higher frequencies and the inefficiency of the wavemaker in this region drives the electronics or the hydraulics into saturation. At this point the spectral shape should be judged to be either acceptable or impossible to produce.

RESULTS

Figures 2 and 3 demonstrate the correlation that can be achieved between the desired spectral shape and that measured in the basin. Figure 2 shows the spectral ordinates measured when a Bretschnieder spectrum with a modal period (T_0) of 2.1 seconds and a significant wave height ($H_{1/3}$) of 3.6 inches was requested. The curve shows the spectrum as taken from its mathematical form. Similarly Figure 3 presents nominal versus measured spectral values, this time with T_0 = 2.44 seconds and $H_{1/3}$ = 10.5 inches. Although further iteration may have improved the correlation, these were sufficient for the particular application and were superior to those spectra developed within this range previously.

When a satisfactory spectral shape has been obtained the time history can be recorded on digital or analog tape for future reference and reuse. This time history is still subject to those problems resulting from the discrete sinusoids on which it was built. To reduce or eliminate those effects it would be necessary to spread the energy across the frequency band so that the energy distribution would again be con-

tinuous.

OFF-LINE PROCEDURE

The second program, mentioned earlier, has been used to generate time histories that contain much less of the discrete frequency characteristics of the previous example because each component, rather than being a constant frequency, is a time-varying value that oscillates between the limits of its band thus spreading the energy throughout. Because this numerical oscillation of frequency is more time consuming, the program has been used only in an off-line mode using the Control Data Series 6000 computers at DTNSRDC. An additional advantage in this software comes from its using a larger number of bands which therefore are more closely spaced. This software would generally be used when archive or general purpose time histories are produced.

CONCLUSION

In conclusion the results achieved so far indicate the following:

1. the wave generating system is becoming a more versatile test tool producing a wide variety of seaways;
2. that an arbitrarily selected seaway, once described by a power spectral density function, can be rather easily entered into the system for wave production; and
3. by producing a seaway that more closely models the condition to be encountered by the prototype, the value and effectiveness of the model test is increased.

Suggested improvements for future development include elimination of the costly stage of iterative refinements since a more thorough knowledge of the dynamics of the wavemaker and the interaction of its components will allow their nonlinear effects to be included in the digital programs or excluded from the operating condition of the wavemaker itself.

A NOTE ON THE APPLICATION OF MODERN CONTROL THEORY TO SHIP ROLL STABILIZATION

by

P.H. WHYTE

Defence Research Establishment Atlantic
Dartmouth, Nova Scotia, Canada

ABSTRACT

The techniques of modern control theory are illustrated and employed in the design of several active roll stabilization systems for a sample ship configuration. Both fins and rudders, as well as a combined fin-rudder controller are considered. The results show modern control theory to be a useful tool in the selection of optimal feedback gains for roll stabilizers.

NOTATION

A	system matrix
A_{ij}	added mass coefficient
B	input matrix
B_{ij}	damping coefficient
C_{ij}	stiffness coefficient
E	statistical expectation
F_j	wave excitation
G	feedback gain matrix
I_j	moment of inertia
J	performance index
U	ship speed
g_1	roll angle gain
g_2	roll rate gain
m	ship mass
u	input vector
x	state vector
β	fin deflection
δ	rudder deflection
μ	weighting factor
η_2	sway position
η_4	roll angle
η_6	yaw angle
ζ_β	fin actuator damping ratio
ζ_δ	rudder actuator damping ratio
ω_β	fin actuator natural frequency
ω_δ	rudder actuator natural frequency
$(\dot{})$	time derivative
$(\,)_c$	command input
$(\,)'$	matrix transpose

TABLE OF CONTENTS

1. INTRODUCTION

The need for roll stabilization of a ship in a seaway can be predicted during the early stages of design with recently-developed analytical techniques. If the ship lacks the necessary degree of inherent roll stability, a supplemental means of roll reduction must be provided. A popular technique for attenuating roll involves active feedback control of hydrodynamic surfaces. In this paper, both active fins and active rudders are considered, as well as combined fin-rudder control. The aim is to demonstrate, by means of examples, that modern control theory may be used to select optimal feedback gains for these controllers.

Active devices, as currently implemented, have some disadvantages. The most significant disadvantage, with respect to military applications, is the high level of radiated noise attributable to the operation of an active system. Machinery noise and hydrodynamic flow noise are the major contributors. The high feedback gains typical of present installations force the control surfaces to operate in a 'bang-bang' mode so that they are continuously cavitating. In addition, this high level of activity exposes the mechanism to excessive wear and tear, with a consequent degradation in reliability. For these reasons, a mode of operation is visualized in which the motions of the control surfaces are kept below their cavitation limits. This approach reduces both machinery and flow noise. Such a 'reduced noise mode' would be used when the ship is in a threat situation. At other times, the restrictions on control surface activity would be less severe, so that in peacetime more roll reduction could be obtained than with the reduced noise mode.

Although modern control theory is applicable to both modes of operation, only the reduced noise mode will be considered in this paper. Given a level of control surface activity, the designer must choose his feedback gains to maximize the roll reduction obtained at that level of activity. In other words, the optimum compromise between the conflicting requirements of roll reduction and noise reduction (by restricting control surface motion) must be found. The optimal feedback gains which achieve this goal may be selected using modern control theory.

Control laws for fin, rudder and combined fin-rudder systems are generated below. These designs represent the optimum tradeoff between roll attenuation and excessive control surface deflections which lead to noise. They therefore establish an

upper limit on control system performance. In practice, some sort of suboptimal design would be implemented because fewer feedback signals are required than for the optimal controller. Conventional root locus techniques are used to derive suboptimal fin and fin-rudder controllers which employ only roll angle and roll rate feedbacks. As might be expected, the suboptimal fin controller approaches the optimal design in performance. However, the optimal fin-rudder system is considerably better than the suboptimal design, indicating the power of modern control theory when multiple inputs and outputs are present.

The mathematical model of ship lateral motions used herein was recently developed at DREA[1]. It consists of three linear differential equations for sway, roll and yaw and two linear differential equations which describe the fin and rudder dynamics. Corrections are included for viscous damping due to bilge keels, hull circulatory effects and the effects of hull appendages, i.e., fins, rudders, skeg and propeller shaft brackets. The associated computer program will compute frequency responses and rms motions for any speed and heading to the seaway. This can be done for both stabilized and unstabilized operation.

2. MATHEMATICAL FORMULATION

If nonzero values of sway, roll, yaw, rudder angle and fin angle are treated as small perturbations about the reference condition of rectilinear motion in a seaway at constant speed, the lateral equations of motion are:

Sway:
$$(A_{22} + m)\ddot{\eta}_2 + B_{22}\dot{\eta}_2 + A_{24}\ddot{\eta}_4 + B_{24}\dot{\eta}_4 + A_{26}\ddot{\eta}_6$$
$$+ (B_{26} + mU)\dot{\eta}_6 + A_{2\delta}\ddot{\delta} + B_{2\delta}\dot{\delta} + C_{2\delta}\delta$$
$$+ A_{2\beta}\ddot{\beta} + B_{2\beta}\dot{\beta} + C_{2\beta}\beta = F_2 \qquad (1)$$

Roll: $$A_{42}\ddot{\eta}_2 + B_{42}\dot{\eta}_2 + (A_{44} + I_4)\ddot{\eta}_4 + B_{44}\dot{\eta}_4 + C_{44}\eta_4$$

$$+ A_{46}\ddot{\eta}_6 + B_{46}\dot{\eta}_6 + A_{4\delta}\ddot{\delta} + B_{4\delta}\dot{\delta} + C_{4\delta}\delta$$

$$+ A_{4\beta}\ddot{\beta} + B_{4\beta}\dot{\beta} + C_{4\beta}\beta = F_4 \qquad (2)$$

Yaw: $$A_{62}\ddot{\eta}_2 + B_{62}\dot{\eta}_2 + A_{64}\ddot{\eta}_4 + B_{64}\dot{\eta}_4 + (A_{66} + I_6)\ddot{\eta}_6 + B_{66}\dot{\eta}_6$$

$$+ A_{6\delta}\ddot{\delta} + B_{6\delta}\dot{\delta} + C_{6\delta}\delta$$

$$+ A_{6\beta}\ddot{\beta} + B_{6\beta}\dot{\beta} + C_{6\beta}\beta = F_6 \qquad (3)$$

Rudder $$\ddot{\delta} + 2\zeta_\delta\omega_\delta\dot{\delta} + \omega_\delta^2\delta = \omega_\delta^2\delta_c \qquad (4)$$

Fin: $$\ddot{\beta} + 2\zeta_\beta\omega_\beta\dot{\beta} + \omega_\beta^2\beta = \omega_\beta^2\beta_c \qquad (5)$$

The A_{ij} and B_{ij} are the added mass and damping coefficients, C_{ij} are the stiffness coefficients, and F_j are the exciting forces and moments. These coefficients are frequency dependent and are evaluated for this application at the ship's roll natural frequency. Thus, the controller to be designed will work best at the worst rolling frequencies. Because the coefficients vary rather slowly with frequency, the controller can be expected to be effective over a wide bandwidth. The fin and rudder actuator dynamics, modelled as second order lags, relate the fin or rudder angle commanded by the control system to the actual fin or rudder angle.

The equations of motion in calm seas (i.e., $F_j = 0$) may be expressed in matrix form as

$$\dot{x} = Ax + Bu \tag{6}$$

where x is a vector of system states and u is the control input. In the case of active fin control,

$$x = [\dot{\eta}_2 \ \dot{\eta}_4 \ \eta_4 \ \dot{\eta}_6 \ \dot{\beta} \ \beta]' \tag{7a}$$

$$u = [\beta_c] \tag{7b}$$

whereas for rudder control

$$x = [\dot{\eta}_2 \ \dot{\eta}_4 \ \eta_4 \ \dot{\eta}_6 \ \dot{\delta} \ \delta]' \tag{8a}$$

$$u = [\delta_c] \tag{8b}$$

and for combined fin-rudder control

$$x = [\dot{\eta}_2 \ \dot{\eta}_4 \ \eta_4 \ \dot{\eta}_6 \ \dot{\delta} \ \ \delta \ \dot{\beta} \ \beta]' \tag{9a}$$

$$u = [\delta_c \ \beta_c]' \tag{9b}$$

The prime denotes the vector transpose. The system matrix A and input matrix B are constant. The modes of ship motion are given by the eigenvalues of A.

To reduce rolling, the controller will feed back some or all of the states according to

$$u = -Gx \tag{10}$$

The feedback gains are selected so as to command a given level of fin and/or rudder motion in a specified seaway.

3. DESIGN EXAMPLES

The hull form selected for examination is that of a frigate whose dimensions are given in Table I. The assumed fins, bilge keels and rudders are presented in Table II. The schematic drawing of Fig. 1 shows their arrangement on the hull. The ship is assumed to be moving at 18 kt. through a beam sea of 12 ft. significant wave height. At this speed, the roll, sway and yaw modes of motion are given by the corresponding eigenvalues of A:

roll: $-0.108 \pm 0.570j$

sway: -0.126

yaw: -0.362

The roll mode is lightly damped, so that large roll angles can be expected in the design seaway.

3.1 Optimal Fin Control

Fin motions are to be kept below that required for incipient cavitation. Although this critical angle is a strong function of fin geometry, it is assumed that the data of Fig. 2 applies to the fins of Table II. This relation between cavitation angle and ship speed is derived from another fin stabilization study[2]. The data indicate that the cavitation limit at 18 kt. is reached when the rms fin angle is 6.5^{o}.

In order to apply modern control theory, the designer must specify an index of performance J. Once this is done, the modern control algorithm will automatically select the elements of G which will minimize J. The performance index selected for this application is

$$J = E(\mu\eta_4^2 + \beta_c^2), \quad \mu > 0 \tag{11}$$

where E is the statistical expectation and μ is a weighting factor which is used to trade off roll motion against fin motion. For this problem, modern control theory guarantees that a unique G exists and can be found for all μ given A, B and J[3].

As μ increases, roll angle becomes more heavily penalized. The algorithm responds by selecting large feedback gains so that rms fin motion increases as rms roll angle decreases. The general behaviour is depicted in Fig. 3. The designer chooses the value of μ which, in the design seaway, results in an rms fin angle of 6.5^{o}, the assumed limit. For this example, the optimal control law is found to be

$$\beta_c = - 0.015\dot{\eta}_2 - 2.632\dot{\eta}_4 - 1.499\eta_4 - 0.630\dot{\eta}_6 - 0.007\dot{\beta} - 0.015\beta \qquad (12)$$

The gains shown are expressed in engineering units; i.e., deg./fps, etc. Because of the way J is structured, no other set of constant, linear feedbacks will attenuate roll better than those of equation (12). Therefore this control law is the optimum compromise between the conflicting requirements of roll reduction and cavitation-free operation, subject to the limitations of the linear mathematical model. Equation (12) is a realistic control law, because the roll angle and roll rate feedbacks dominate.

3.2 Optimal Rudder Control

The approach to rudder stabilizer design parallels that for the fin stabilizer except that the allowable rudder motions are more restrictive. Because the rudders must also be used to steer the ship, they cannot be completely dedicated to roll control, as are fins. An arbitrary limit of 5.0^{o} rms in the design sea is chosen. For the performance index

$$J = E(\mu\eta_4^2 + \delta_c^2), \quad \mu > 0 \qquad (13)$$

the corresponding control law is

$$\delta_c = - 0.011\dot{\eta}_2 - 2.880\dot{\eta}_4 - 0.721\eta_4 - 2.395\dot{\eta}_6 - 0.268\dot{\delta} - 0.408\delta \qquad (14)$$

The performances of the optimal fin and rudder controllers are compared in Fig. 4. Mean wave periods from 7 to 11 sec. are shown so that the effect of different excitation frequencies can be assessed. Both feedback systems offer a great improvement over the case in which both fins and rudders operate passively. Even with their relatively slow actuator dynamics (see Table II) and smaller allowable motions,

the rudders attenuate roll almost as well as the fins for high wave periods. Sway and yaw motions are not significantly affected by either fin or rudder control. The rms sway and yaw motions do not exceed 2.7 fps or 0.23 degrees respectively for any of the sea conditions in Fig. 4. The corresponding open loop values are 1.8 fps and 0.19 degrees. Because sway and yaw are low frequency modes compared to roll, they are not excited by control surface motion at common rolling frequencies.

3.3 Suboptimal Fin Control

Suboptimal controllers do not feed back all the elements of x. Although not performing as well as an optimal controller, the suboptimal design may be only marginally inferior and is always easier to implement because there are fewer feedbacks. In this section, a fin controller employing only roll angle and roll rate feedback is compared with the optimal design.

The root locus technique is used to maximize the closed loop roll damping. In Fig. 5, the movement of the roll mode is shown as a function of g_1/g_2 (roll angle gain/roll rate gain). A value of $g_1/g_2 = 0.25$ is best. Then g_2 is selected so that rms fin motion is 6.5°. The resulting control law is

$$\beta_c = -3.26\dot{\eta}_4 - 0.82\eta_4 \tag{15}$$

As Fig. 6 shows, the response of the suboptimal design is only marginally inferior to the optimal control law.

3.4 Combined Fin-Rudder Control

Both an optimal and a suboptimal configuration are considered for the combined fin-rudder controller. They are designed so as to maximize the roll damping. The optimal controller is obtained using the method of Solheim[4]. In this technique, the closed loop eigenvalues may be specified in advance. If critical damping is specified for the roll mode, the control law is

$$\delta_c = -0.027\dot{\eta}_2 - 16.410\dot{\eta}_4 - 2.945\eta_4 - 9.922\dot{\eta}_6 - 1.760\dot{\delta} - 2.663\delta$$
$$- 0.043\dot{\beta} - 0.071\beta \tag{16a}$$

$$\beta_c = -0.037\dot{\eta}_2 - 2.362\dot{\eta}_4 - 2.049\eta_4 + 3.676\dot{\eta}_6 - 0.193\dot{\delta} - 0.414\delta$$

$$- 0.009\dot{\beta} - 0.019\beta \qquad (16b)$$

It should be noted in this case that the performance index J results from the mode specifications and is substantially different from those used in equations (11) and (13). However, the rms fin and rudder motions are 6.5^o and 5.0^o respectively.

Once again the root locus technique is used to select the suboptimal system. The fin loop is given by equation (15). The root locus for the rudder closure is then that of Fig. 7. The maximum roll damping is given by

$$\delta_c = -1.50\dot{\eta}_4 \qquad (17)$$

Although fin motions are at 6.5^o rms in the design sea, rudder motions are only 1.7^o rms. But as the root locus of Fig. 7 indicates, larger rudder gains will destabilise the ship. Thus the classical design does not allow the rudder to be used to full advantage.

The rms rolling motions obtained with these two systems are shown in Fig. 8. The performance gap between optimal and suboptimal control has widened considerably over that of Fig. 6.

4. CONCLUDING REMARKS

The above examples have shown modern control theory to be a powerful tool in the design of feedback control systems. In the case of ship roll stabilization using fins or rudders, the theory has been used to balance the conflicting requirements of roll attenuation and noise reduction. In this way, an upper limit on the performance of the controller is established. Practical, suboptimal designs may then be compared to this standard.

When fins or rudders are used alone to reduce rolling, simple controllers employing roll angle and roll rate feedback can be derived which perform in a near-optimal manner.

The use of the rudders for roll control appears to have no significant effect on sway and yaw motions. Of course, the feasibility of this approach depends upon the ability of conventional rudder servomechanisms to cope with the additional activity.

The use of fins and rudders simultaneously makes the design problem much more complicated. As the number of states and inputs increase, the techniques of modern control theory become more efficient at selecting the optimal feedback scheme than classical techniques, which become unwieldy and time-consuming. The optimal configuration derived using modern control theory is shown in Figure 8 to reduce roll by 49% compared to the use of fins alone. The corresponding reduction with suboptimal fin-rudder control is only 14%. With proper design, a combined fin-rudder system can be very effective, even for the small fin and rudder deflections assumed here.

REFERENCES

1. Schmitke, R. T.: "Prediction of Ship Roll, Sway and Yaw Motions", DREA Report (under review).

2. Jones, H. D. and Cox, G. G.: "Roll Stabilization Investigation for the Guided Missile Frigate (FFG-7)", DTNSRDC Report SPD-495-18, July 1976.

3. Athans, M.: "The Role and Use of the Stochastic Linear - Quadratic - Gaussian Problem in Control System Design", IEEE Transactions on Automatic Control, Vol. AC-16, No. 6, Dec. 1971.

4. Solheim, O. A.: "Design of Optimal Control Systems with Prescribed Eigenvalues", Int. Journal of Control, Vol. 15, 1972.

TABLE I: HULL PARTICULARS

length between perpendiculars	393.7 ft
beam	47.6 ft
draft	14.5 ft
displacement	3711 tons
metacentric height	4.2 ft
longitudinal c.g. location	202.6 ft
height of c.g. above waterplane	7.0 ft

TABLE II: SELECTED APPENDAGES

A.	Fins - one pair, trapezoidal unflapped	
	span	7.5 ft
	root chord	11.8 ft
	taper ratio	0.7
	depression	42 deg
	actuator damping ratio	0.4
	actuator natural frequency	5.0 rps
B.	Bilge Keels - one pair, forward of fins	
	span	2.5 ft
	length	78.8 ft
C.	Rudders - one pair, trapezoidal spade	
	span	12.4 ft
	root chord	9.2 ft
	taper ratio	0.5
	actuator damping ratio	0.8
	actuator natural frequency	1.0 rps

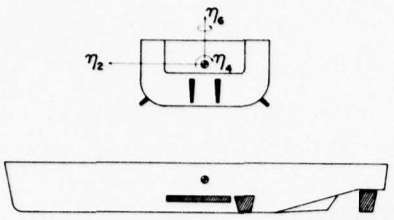

1. FIN, BILGE KEEL AND RUDDER ARRANGEMENT

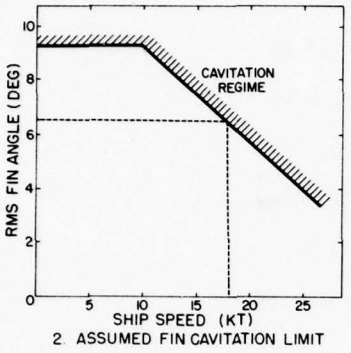

2. ASSUMED FIN CAVITATION LIMIT

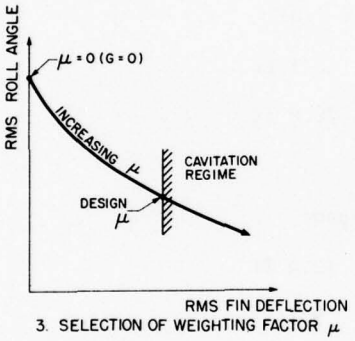

3. SELECTION OF WEIGHTING FACTOR μ

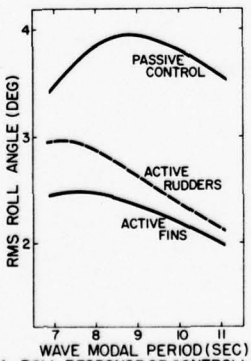

4. ROLL RESPONSE OF CONTROLLERS DESIGNED VIA MODERN CONTROL THEORY

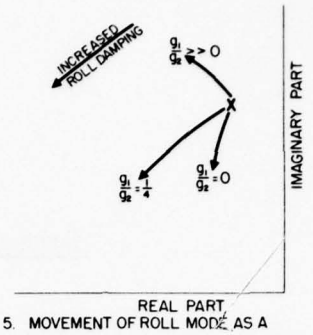

5. MOVEMENT OF ROLL MODE AS A FUNCTION OF g_1/g_2 , $\beta_c = g_1\eta_4 + g_2\dot{\eta}_4$

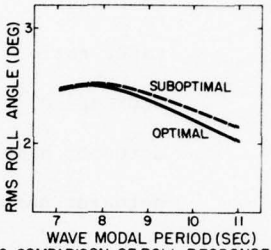

6. COMPARISON OF ROLL RESPONSE OF OPTIMAL AND SUBOPTIMAL ACTIVE FIN CONTROLLERS

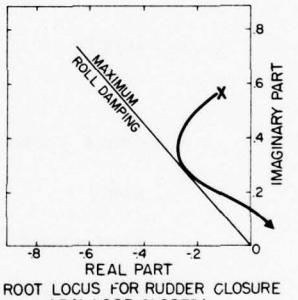

7. ROOT LOCUS FOR RUDDER CLOSURE (FIN LOOP CLOSED)

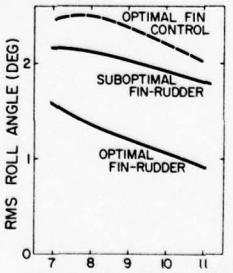

8. ROLL RESPONSE OF COMBINED FIN-RUDDER CONTROL SYSTEMS COMPARED TO OPTIMAL FIN CONTROL

COMPARISONS OF THEORY WITH EXPERIMENT FOR SHIP ROLLING IN OBLIQUE SEAS

by

R. T. SCHMITKE

Defence Research Establishment Atlantic
Dartmouth, Nova Scotia, Canada

ABSTRACT

A computer program to predict ship roll, yaw and sway motions in oblique seas has recently been developed at DREA, based on strip theory with strict account taken of the circulatory and viscous damping effects of hull appendages. Predictions are compared with experimental data from regular wave tests with a fully appended self-propelled frigate model. The effects of varying forward speed, heading to the sea, metacentric height and bilge keel configuration are examined. Agreement between theory and experiment is good.

1. INTRODUCTION

Over the past two decades, considerable success has been achieved in the theoretical prediction of ship heave and pitch motions. Computer programs to perform such predictions are now in common use, and a large number of correlation studies have shown that the accuracy of the absolute motion predictions is generally very satisfactory. For lateral plane motions, however, of which by far the most important is roll, the situation is much different. Although several programs exist which predict roll, sway and yaw by purely theoretical means, for example Reference 1, correlation studies[2] have shown that errors in roll prediction are generally significant, particularly for high speed warship hull forms. As to sway and yaw, correlation studies have been very few and inconclusive.

The fundamental reason for the discrepancies reported in correlation studies is that programs such as Reference 1 generally make inaccurate estimates of roll damping, especially at higher speeds. Experience with these programs has led to the widely held belief that the roll damping prediction problem is so complex and non-linear as to be theoretically intractable. In keeping with this philosophy, certain computer programs[3] require that the roll damping coefficient be input by the user. Model test programs specifically dedicated to the experimental determination of roll damping are fairly common.

The failure of Reference 1 to make accurate predictions of roll damping may be traced to an inadequate treatment of hull appendages, and in particular to the failure to include the effects of dynamic lift on such appendages as rudders, skegs and propeller shaft brackets. The theory used in the present paper includes these effects and consequently produces good estimates of both roll damping and roll response.

2. GENERAL DESCRIPTION OF THEORY

The mathematical model used herein for ship lateral motions in oblique seas has basically four facets:

1) Strip theory for computing hull added mass, wavemaking damping and exciting forces.

2) Lifting surface contributions to damping and exciting forces.

3) Viscous roll damping, principally from bilge keels.

4) Hull circulatory effects.

The equations for coupled sway, roll and yaw response are written in the general form:

$$\sum_k (-\omega^2 A_{jk} + i\omega B_{jk} + C_{jk})\eta_k = F_j \qquad j = 2,4,6$$

where ω is frequency of encounter and the subscripts 2, 4 and 6 refer to sway, roll and yaw, respectively. A_{jk} and B_{jk} are the added mass and damping coefficients, C_{jk} are the restoring coefficients, and F_j are the exciting forces and moments. These coefficients are ascribed the general form:

$$A_{jk} = A^H_{jk} + A^F_{jk}$$

$$B_{jk} = B^H_{jk} + B^F_{jk} + B^C_{jk}$$

$$F_j = F^H_j + F^F_j + F^C_j$$

where superscript H denotes hull coefficients derived from strip theory, superscript F signifies contributions due to appendages (foils) such as rudders and fins, and superscript C denotes hull circulatory terms.

For B_{44}, the roll damping coefficient, there is an additional term, B^V_{44}, the viscous roll damping coefficient. This takes account of the viscous resistance to rolling of bilge keels, skeg, hull, rudder and other appendages.

Detailed expressions for the terms on the right hand side of the above equations are given in Reference 4. Basically, the H-terms are derived from Reference 5, the F-terms from Reference 6, and the C-terms from Reference 7. The viscous

contribution to roll damping is estimated using the data of References 8, 9 and 10.

3. COMPARISON OF THEORY WITH EXPERIMENT

Theoretical predictions are now compared with experimental data from regular wave tests with a fully-appended self-propelled frigate model at the seakeeping basin of the David Taylor Naval Ship Research and Development Center[2]. This was a comprehensive experimental program in which metacentric height, bilge keel configuration, heading and forward speed were systematically varied. Two different bilge keels were used (designated BK_1 and BK_3) and three metacentric heights (GM_1, GM_2 and GM_3). Some details are given below.

Length between perpendiculars	18.182 ft
Beam	2.156 ft
Draft	.716 ft
Block coefficient	.485
Prismatic coefficient	.604

Metacentric height designation	% of beam
GM_1	12.1
GM_2	9.0
GM_3	6.1

Bilge keel designation	Area in % of wetted area	Length in % of LBP
BK_1	2.34	29.6
BK_3	1.00	17.0

Figures 1 and 2 show the effect on roll response of varying sea direction at low and high Froude numbers, respectively. Figures 3, 4 and 5 show the effect of varying metacentric height and bilge keel configuration at low Froude number in bow seas and high Froude number in beam seas. Finally, Figure 6 presents data showing the influence of metacentric height on roll response in quartering seas at low Froude number.

Agreement between theory and experiment is generally good. The following points are especially worthy of mention:

1. The considerable variation in roll response with heading to the sea is resonably well predicted, both at low and high speed.

2. Predictions of peak response are generally good, indicating good estimation of roll damping.

3. Theory correctly predicts a substantial reduction in roll response as speed increases. This decrease is mainly due to the twin rudders, which contribute significantly to roll damping at high speed.

4. The dramatic increase in roll response in quartering seas as metacentric height is reduced is very well predicted. This is of considerable practical importance, since the GM_3 case is representative of the metacentric height/beam ratio at which frigates and destroyers commonly operate.

4. CONCLUSION

Fairly extensive comparisons of predicted and measured roll response for a frigate model show generally good agreement at all headings to the sea. This suggests that the theory of Reference 4 yields predictions of sufficient accuracy for preliminary design purposes.

NOTATION

A_{jk}	added mass coefficient
B_{jk}	damping coefficient
C_{jk}	restoring coefficient
F_j	exciting force or moment
GM	metacentric height
i	$\sqrt{-1}$
β_s	heading angle relative to sea direction (0^o head seas, 180^o following seas)
η_2	sway
η_4	roll
η_6	yaw
ω	frequency of encounter
C	superscript denoting hull circulation
F	superscript denoting foil contribution
H	superscript denoting hull contribution

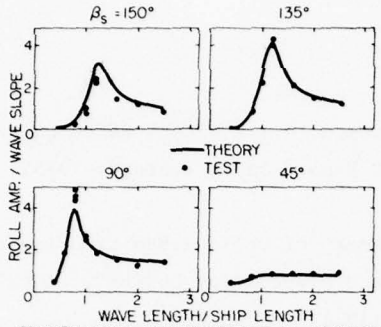

1. FRIGATE MODEL, HEADING EFFECT, F_n = .15, BK_1 GM_1

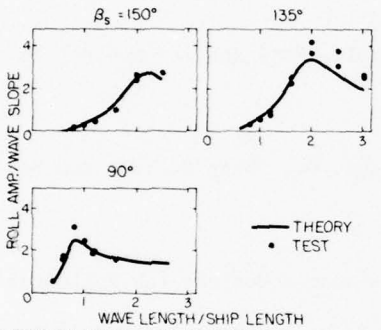

2. FRIGATE MODEL, HEADING EFFECT, F_n = .46, BK_1 GM_1

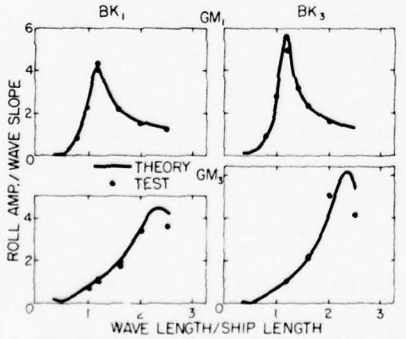

3. FRIGATE MODEL, GM EFFECT, F_n = .15, BOW SEAS

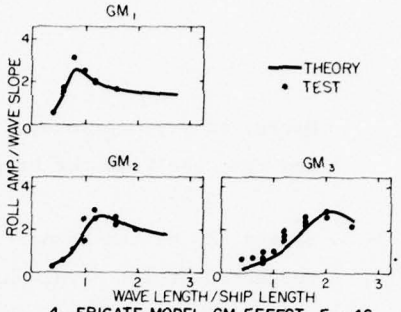

4. FRIGATE MODEL, GM EFFECT, F_n = .46
BEAM SEAS, BK_1

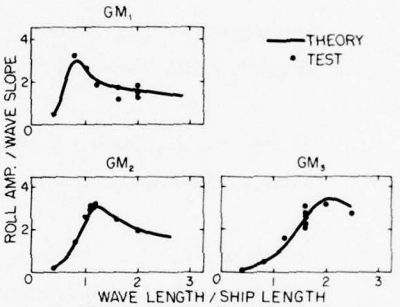

5. FRIGATE MODEL, GM EFFECT, F_n = .46
BEAM SEAS, BK_3

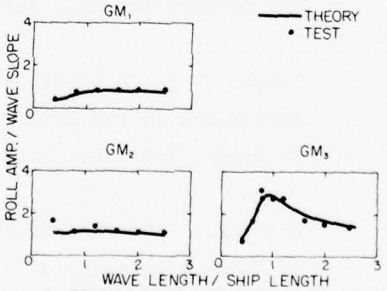

6. FRIGATE MODEL, GM EFFECT, F_n = .15
QUARTERING SEAS

REFERENCES

1. Myers, W. G., Sheridan, D. J. and Salvesen, N.: "Manual NSRDC Ship-Motion and Sea-Load Computer Program". NSRDC Report 3376, February 1975.

2. Baitis, A. E. and Wermter, R.: "A Summary of Oblique Sea Experiments Conducted at the Naval Ship Research and Development Center". 13th International Towing Tank Conference, 1972.

3. Raff, A. I.: "Program SCORES - Ship Structural Response in Waves". Ship Structure Committee Report No. SSC 230-1972.

4. Schmitke, R. T.: "Prediction of Ship Roll, Sway and Yaw Motions in Oblique Waves", DREA Report 77/4, June 1977.

5. Salvesen, N., Tuck, E. O., and Faltinsen, O.: "Ship Motions and Sea Loads". Trans., SNAME, Vol. 78, 1970.

6. Schmitke, R. T.: "Prediction of Wave-Induced Motions for Hullborne Hydrofoils". J. Hydronautics, 1977.

7. Comstrock, J. P. (Ed): "Principles of Naval Architecture". SNAME, 1967.

8. Kato, H.: "Effect of Bilge Keels on the Rolling of Ships:. Memories of the Defence Academy, Japan, Vol. 4, 1966.

9. Tanaka, N.: "A Study on the Bilge Keels (Part 4 - On the Eddy-Making Resistance to the Rolling of a Ship Hull):. Society of Naval Architects of Japan, Vol. 109, 1960.

10. Kato, H.: "On the Frictional Resistance to the Roll of Ships". Society of Naval Architects of Japan, Vol. 102, 1958.

CRITERIA FOR SHIP SPEED IN ROUGH WEATHER

By A R J M Lloyd and R N Andrew

1. INTRODUCTION

The sea is seldom calm and ship responses to waves are an important consideration in the synthesis of a new design. As well as the relatively well defined effects of wave loads on ship structure the behaviour of a ship in a seaway has more abstruse implications in connection with ship design and operation. These latter effects are generally referred to under the heading of 'seakindliness' and various desirable features of ship behaviour have been defined - though not without some obscurity. These include absence of slamming, ride comfort, dry decks and absence of propeller racing.

Evaluation of the merits of a proposed design requires quantification of the way in which features such as those mentioned above influence the ability of a ship to fulfil its function ie provide an adequate return on investment in the case of a merchant ship or an effective military presence in the case of a warship. This is the subject of continuing research both in the UK and elsewhere but results are not yet to hand. Instead it has become usual to measure seakindliness in terms of the ability to maintain speed in rough weather. There is some justification for such an approach in the case of certain types of merchant ships where speed reductions significantly affect earnings potential. Furthermore in this context there are relatively well established techno-economic methods for relating profitability to speed loss thus facilitating value judgements and trade-offs during design.

For warships the ability to maintain speed in rough weather is a less well established measure of seakindliness. The designer's objective rather is a ship which can successfully execute a mission despite adverse environmental conditions. This need not require the ability to maintain high speed for prolonged periods. However at present it is usual to relate the seakindliness of warships to their ability to maintain speed in rough weather and indeed this philosophy is relevant to mission profiles which require rapid response. It has been found convenient to adopt this approach in the work reported herein.

With respect to speed loss in rough weather it is usual to consider the performance in head seas as being representative. In some circumstances the performance at other headings is important but these are not considered in this present paper.

2. REASONS FOR SPEED LOSS

It is generally accepted that the causes of a reduction in speed in rough weather can be broadly divided into two categories:-

1. An increase in the power required to drive the ship at a given speed caused by wind, waves and ship motions. If the available power is limited the speed will be reduced.

2. A reduction of power ordered by the ship's captain to avoid intolerable levels of certain aspects of ship behaviour in rough weather.

The first of these is entirely physical in nature and can, in principle, be deduced from a knowledge of the characteristics of the hull, propulsive equipment and environment. Such speed reductions are generally termed 'involuntary'. The second depends not only on the physical characteristics of the hull, its personnel and equipment but also on the subjective judgement of the captain. Such speed reductions are generally termed 'voluntary' and are more difficult to estimate than involuntary speed reductions which are not considered further in this paper.

In connection with voluntary reductions of power it appears to be generally accepted that the aspects of ship behaviour with which the captain is most concerned are:-

1. Slamming* which can cause damage both to local structure due to high impact pressures, and to the hull girder due to whipping. Whipping can also damage masts and aerials, machinery and delicate electronic equipment.

2. Ship motions which make it difficult for the crew to work effectively, degrade passenger comfort and apply inertial loads to equipment and cargo.

3. Deck wetness which can cause damage to exposed equipment and fittings and restrict access to exposed decks.

4. Propeller emergence which can cause machinery racing and cut-out, particularly if the ship is direct-diesel powered. This problem appears to be mainly confined to ships in ballast.

It is possible that there are other aspects of ship behaviour of concern to the captain but these have not been considered in this paper.

Although the aspects of ship behaviour listed above are of a physical nature the captain cannot detect the level of the ill-effects about which he is concerned - unless crew injury or damage occurs - and instead judges their severity in relation to phenomena he experiences directly. When proposing methods of predicting voluntary speed loss in rough weather it is particularly important to relate criteria to the way in which the captain detects the occurrence and severity of slamming, ship motions, deck wetness and propeller emergence.

3. CRITERIA

In order to predict voluntary speed loss in rough weather methods of estimating the occurrence and severity of the aspects of ship behaviour of concern are required together with limiting values. Several authors have addressed this problem and a selection of their findings is given in Table 1. These criteria and others are important contributions to studies of seakindliness but there are uncertainties associated with

---

* Here and henceforth 'slamming' refers to both bottom and flare impacts.

Table 1

SEAKEEPING CRITERIA

Author	Slamming	Motions	Deck Wetness	Propeller Emergence
Aertssen (References 1-4)	3 or 4 slams[1] per 100 pitch oscillations.	Significant amplitude of acceleration at FP equals. 0.4 g	"Green water"	25 emergences per 100 pitch oscillations.
Conolly (Reference 5)	1 slam[2] at 0.2L abaft FP every 1360 seconds.	± 1.0 g at 0.2L abaft FP every 673 seconds.	1 deck wetness at FP every 110 seconds.	-
Kehoe (Reference 7)	1 slam[3]/minute at 0.15L abaft FP.	-	1 deck wetness at FP every 60 seconds.	-

(1) Slam defined as giving a maximum whipping stress of 5.9 MN/m^2 (in MV JORDAENS).

(2) Slam defined as having an impact velocity greater than $\left(\frac{20.8L}{kH}\right)^{\frac{1}{2}}$.

(3) Slam defined as having an impact velocity greater than $0.093\ \left(\frac{g}{L}\right)^{\frac{1}{2}}$.

their generality, particularly in connection with slamming and ship motions.

Aertssen's criteria are derived from analyses of full-scale trials (References 1-4) and as such represent actual limits on operation in the judgement of the ship's captain of the time. However the measure of slamming is not related to physical realisations of slamming which are detectable by the captain and the motion criterion appears to be irrelevant to the actual environment experienced by the crew.

Conolly derived criteria (Reference 5) by considering the performance of a destroyer which took part in comparative seakeeping trials described in Reference 6. The slamming criterion includes a crude allowance for the effect of hull shape forward on slam severity but nevertheless is not related to sensations experienced by the captain. The motion criterion is subject to the same uncertainty as Aertssen's motion criterion.

Kehoe (Reference 7) adopts Ochi's definition of slamming given in Reference 8. The resulting criterion takes no account of the effect of hull shape on the slamming characteristics of the ship and is not related to events detectable by the captain.

The present authors have therefore sought to establish new methods of predicting voluntary speed loss in rough weather. The following 'rules' have been found useful:

1. Predictions of the occurrence and severity of the aspects of ship behaviour of concern to the captain should be related to physical phenomena actually experienced by the captain, crew and passengers.

2. Limiting values should be derived from the apparent performance of existing ships.

With the first of these in mind a large number of commanding officers and masters of ships of the Royal Navy and Royal Fleet Auxiliary Service have been questioned and extremely informative replies received. Whilst some differences in opinion have been found it has been possible, generally speaking, to establish the ways in which the captain detects some of the aspects of ship behaviour given in section 2. It has been found, for instance, that slamming is generally detected by the resulting whipping vibration of the hull girder and it has been confirmed that estimation of the severity of ship motions is strongly related to the actual environment experienced by personnel throughout the ship. Impressions of deck wetness are related to frequency of occurrence of solid water on deck.

The following measures of ship behaviour are therefore proposed in connection with predictions of voluntary speed loss in rough weather.

1. Slam-induced whipping vibration acceleration at bridge.

2. Subjective motion magnitude weighted according to personnel location and averaged along ship length.

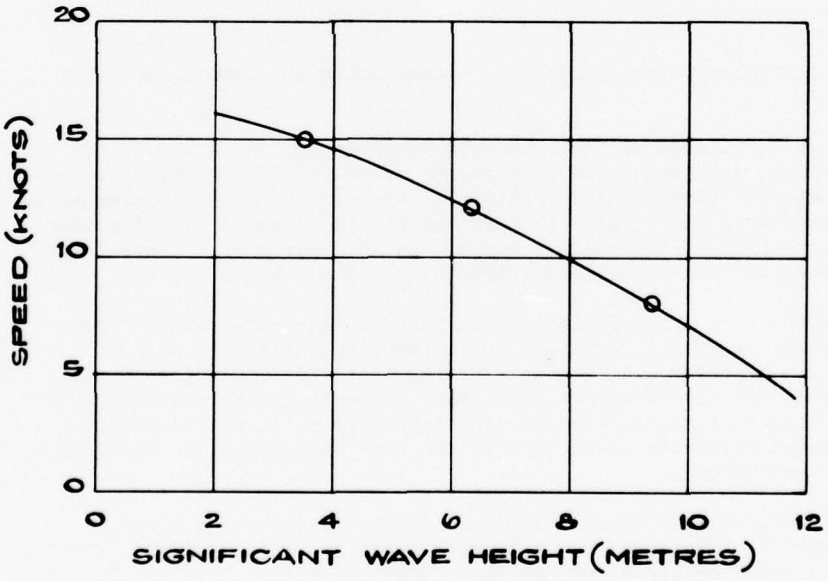

FIG.1. M V JORDAENS 8·5m DRAUGHT SPEED IN HEAD SEAS.

3. Average deck wetness interval at FP.

4. Average propeller emergence interval.

Methods of calculating these aspects of ship behaviour in rough weather are given in Appendices I-VI.

4. MEASUREMENTS OF SHIP SPEED IN ROUGH WEATHER

Aertssen has presented the results of seakeeping trials on several vessels (References 1-4). For present purposes it has been found convenient to consider one of these more closely. Figure 1 shows Aertssen's results for maximum speed in head seas for the MV JORDAENS at deep draught.

Bledsoe et al (Reference 6) presented results of seakeeping trials with three Dutch destroyers. At the end of the trials a special slamming run was carried out. Two of the ships were driven into head seas at a speed of 25 knots. One of the ships, designated ship 'B' in the reference, suffered a succession of heavy slams and took large quantities of green water onto the forecastle and the run was terminated. It appeared that this ship had exceeded the speed considered prudent by the Commanding Officer in those sea conditions. Unfortunately the sea state was not measured during the trials although hindcasts were subsequently

Table 2

WAVEHEIGHTS ESTIMATED FROM SHIP MOTION MEASUREMENTS

(Seakeeping Trials on Three Dutch Destroyers: Reference 6)

Ship	Length (m)	Speed (Knots)	Rms Pitch (Deg)	Estimated Significant Waveheight (m)	Rms Heave Acceleration (g)	Estimated Significant Waveheight (m)	Rms Acceleration Forward (g)	Estimated Significant Waveheight (m)
A	108	12	0.89	2.85	0.045	3.90	0.146	3.30
B	112	12	0.94	3.08	0.037	3.55	0.142	3.58
S	103	12	1.11	3.00	0.045	3.60	0.154	3.10
A	108	17	1.42	3.80	0.077	4.60	0.262	4.85
B	112	17	1.41	4.00	0.075	5.10	-	-
S	103	17	1.66	3.95	0.085	4.73	0.236	3.55

Mean values: 12 knots runs 3.33 m

17 knots runs 4.32 m

attempted. The present authors have found it convenient to represent the sea state by a long crested Pierson-Moskowitz spectrum. The significant waveheight has been estimated from the motion responses measured during the trials using a computer program based on that described in Reference 9. Table 2 gives the results. It has been assumed that the sea state did not change significantly between the end of the runs during which the motion responses were measured and the start of the special slamming run some two hours later.

These estimates of limiting conditions for the two ships have been used to derive maximum acceptable levels of slamming, ship motions, deck wetness and propeller emergence.

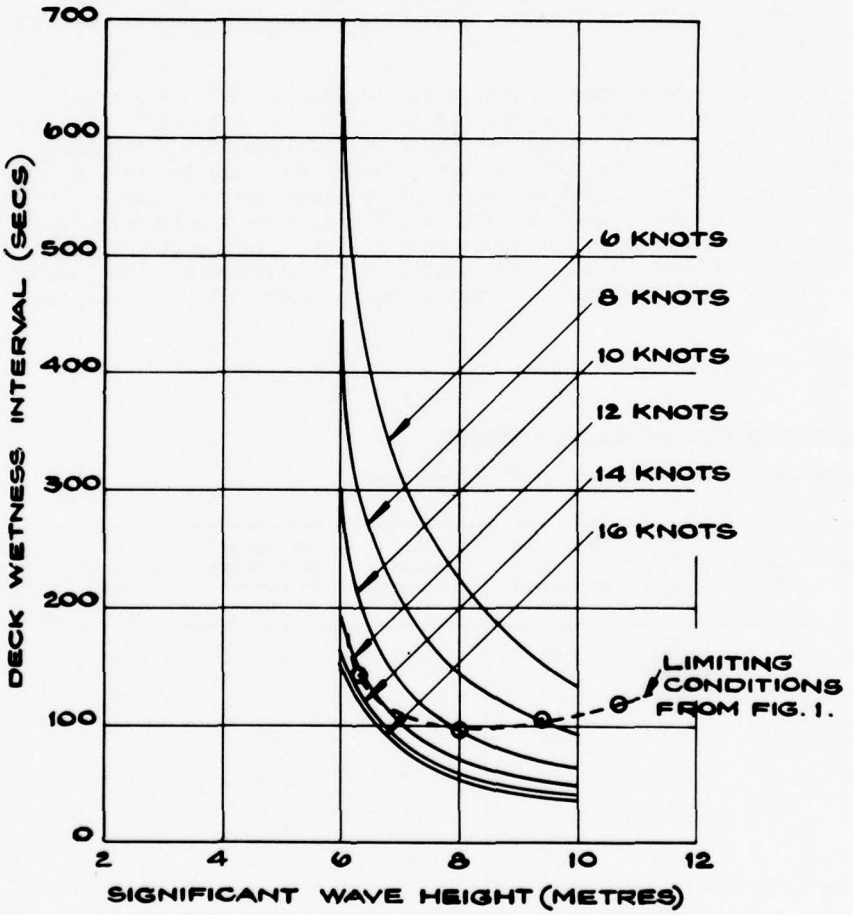

FIG. 2. M V JORDAENS 8·5 m DRAUGHT.
DECK WETNESS AT F. P.

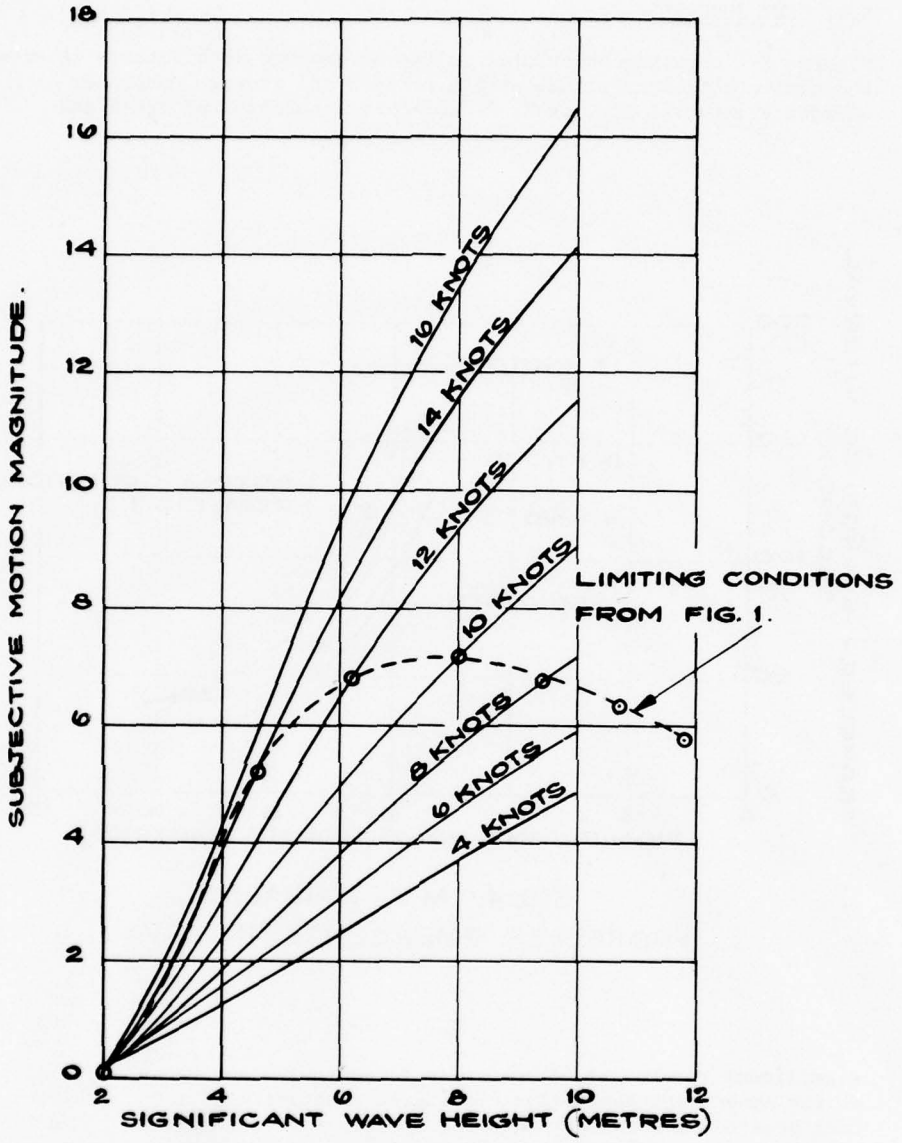

FIG. 3. M.V. JORDAENS 8·5 m DRAUGHT
SUBJECTIVE MOTION MAGNITUDE.

5. SHIP BEHAVIOUR AT LIMITING CONDITIONS

5.1. MV JORDAENS

Figures 2-4 show the calculated values of average deck wetness interval, subjective motion magnitude at the bridge* and average propeller emergence interval for the MV JORDAENS as a function of speed and

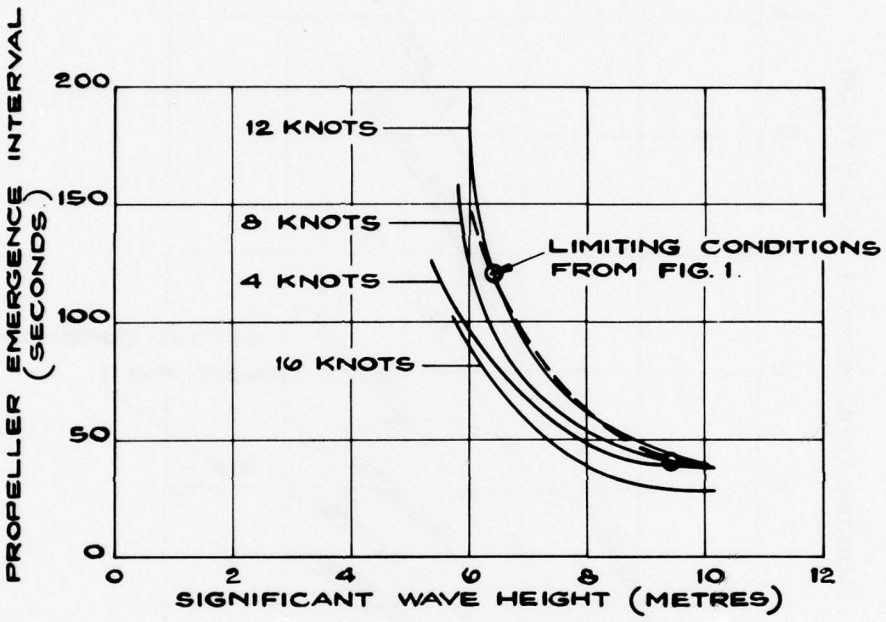

FIG. 4. M V JORDAENS. PROPELLER EMERGENCE INTERVAL.

significant waveheight. It has been found that slamming seldom occurs at the speeds and sea states considered practicable for this ship. Long crested Pierson-Moskowitz sea spectra have been used. In certain circumstances in connection with the design of a new ship more realistic sea spectra are appropriate.

The data of Figure 1 have been superimposed on these results to give the apparent levels of these phenomena at limiting conditions.

---

* In the absence of details of personnel location the subjective motion magnitude has only been evaluated at the bridge.

Aertssen has stated that deck wetness was of most concern and it follows that the curve given in Figure 2 represents the minimum acceptable average deck wetness interval for this ship. It appears that an interval of about 100 seconds represents a criterion in this case.

Since ship motions and propeller emergence were not of particular concern the subjective magnitude of motion and average propeller emergence interval cannot be considered as criteria for these aspects of ship behaviour. All that can be said is that the permissible levels of these phenomena must be worse than the values given in Figures 3 and 4.

5.2. Dutch Destroyer

Figures 5-7 show the calculated values of peak whipping acceleration at the bridge, deck wetness interval and subjective motion magnitude for the Dutch destroyer designated ship 'B' in Reference 6 as a function of significant waveheight at 25 knots. Propeller emergence is known to be of little cause for concern in a ship of this type and has not been calculated. As in the previous example long crested Pierson-Moskowitz sea spectra have been used.

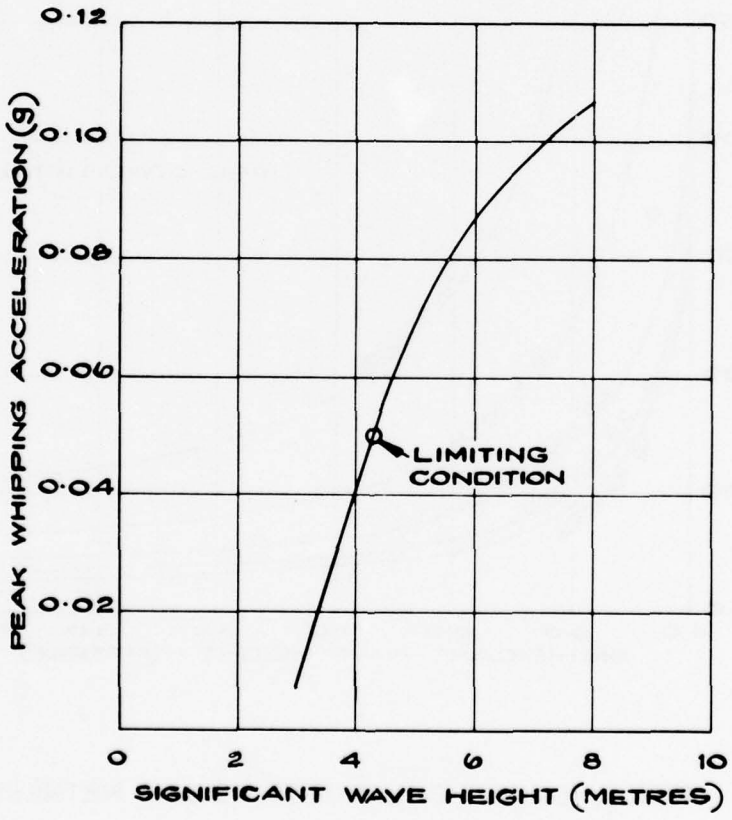

FIG. 5. DUTCH DESTROYER. PEAK WHIPPING ACCELERATION AT BRIDGE AT 25 KNOTS.

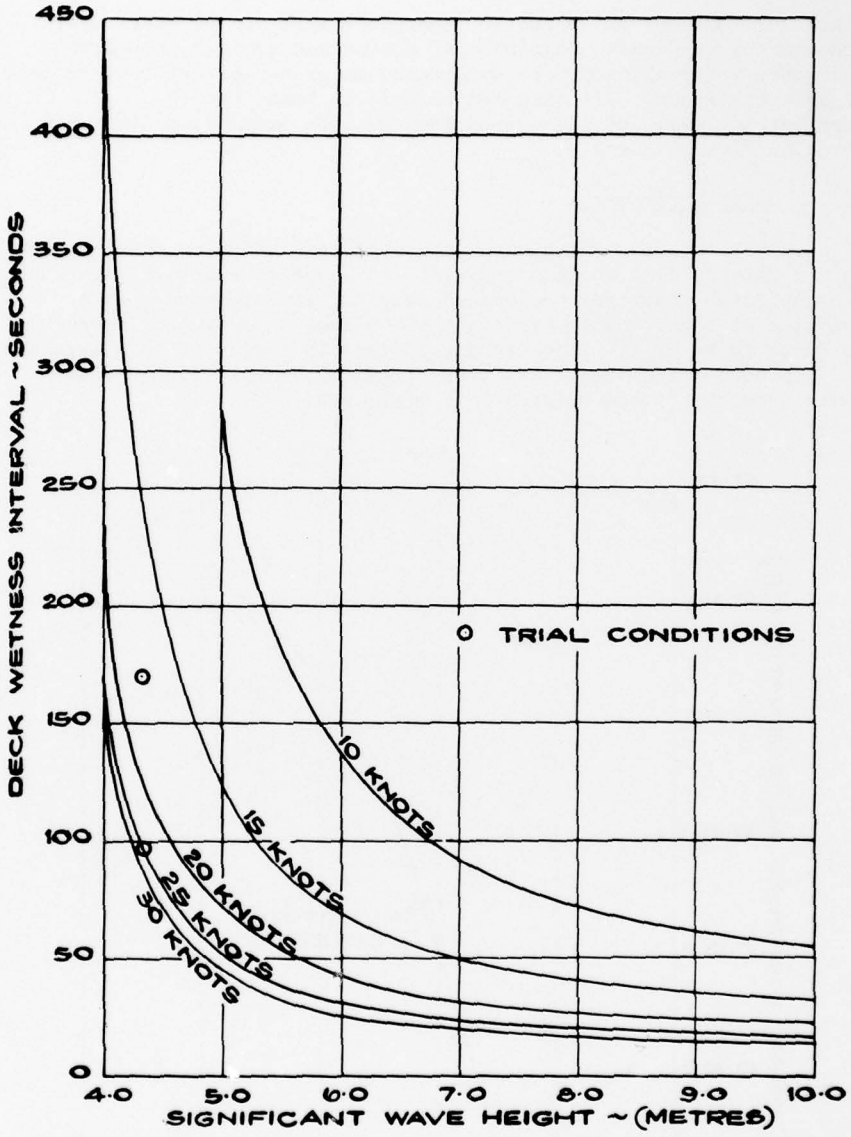

FIG. 6. DUTCH DESTROYER DECK WETNESS.

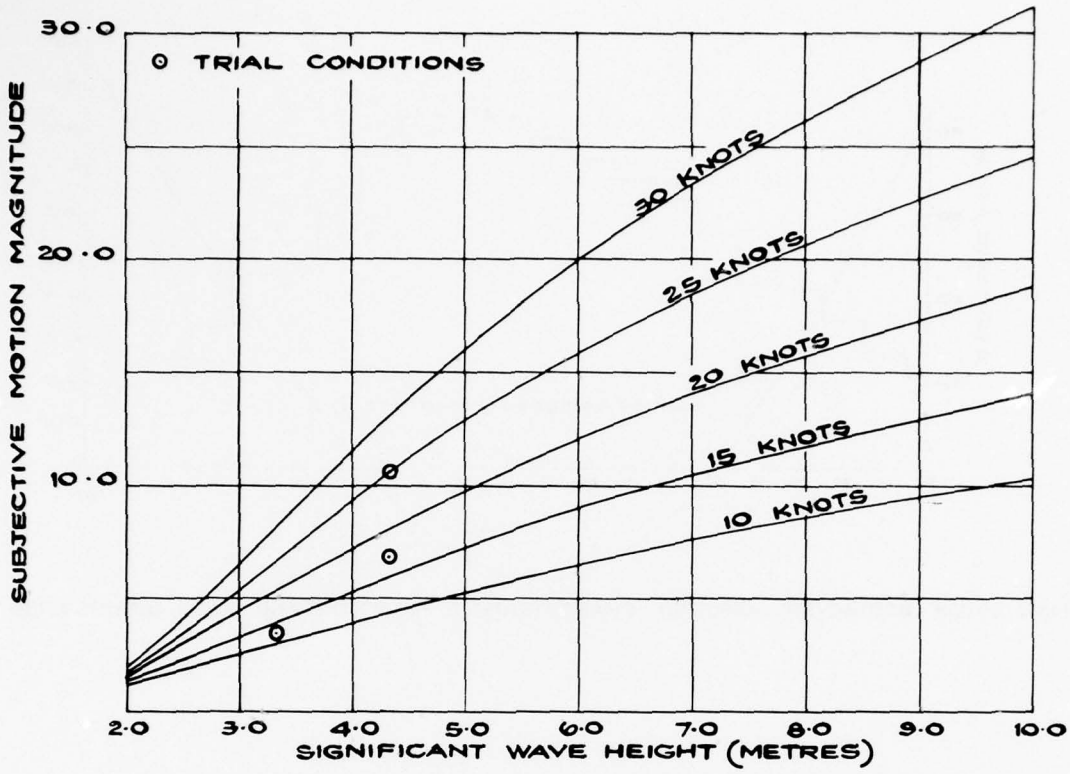

FIG. 7. DUTCH DESTROYER. SUBJECTIVE MOTION MAGNITUDE.

It has been necessary to assume values for certain hull characteristics affecting the whipping vibration calculation. The characteristic function and ship mass distribution shown in Figure 8 have been assumed in place of more accurate data which was unavailable. Hydrodynamic added mass has been estimated using Lewis forms.

In the absence of details of personnel location the weighting function of the form shown in Figure 9 has been used with the breakpoint at the bridge position.

The apparent levels of these phenomena at a limiting condition are given by the values corresponding to the estimated significant wave-height during the special slamming run. It was stated in Reference 6 that slamming was of most concern although deck wetness was judged to be severe. It appears that a whipping acceleration amplitude of 0.05 g represents a criterion for slamming in this case. An average deck wetness interval of about 100 seconds would appear to be near the acceptable minimum for this ship.

Like the JORDAENS, the Dutch destroyer was not limited by ship motions and the highest subjective magnitude of motion experienced in Figure 7 cannot be taken as a criterion for maximum acceptable ship motions. A true criterion would be higher.

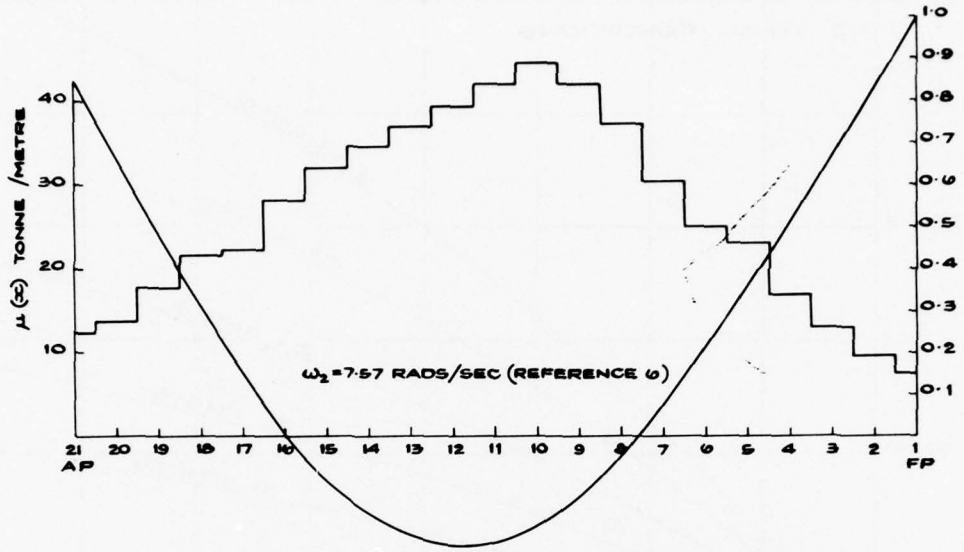

FIG. 8. DUTCH DESTROYER. ASSUMED CHARACTERISTIC FUNCTION AND MASS DISTRIBUTION.

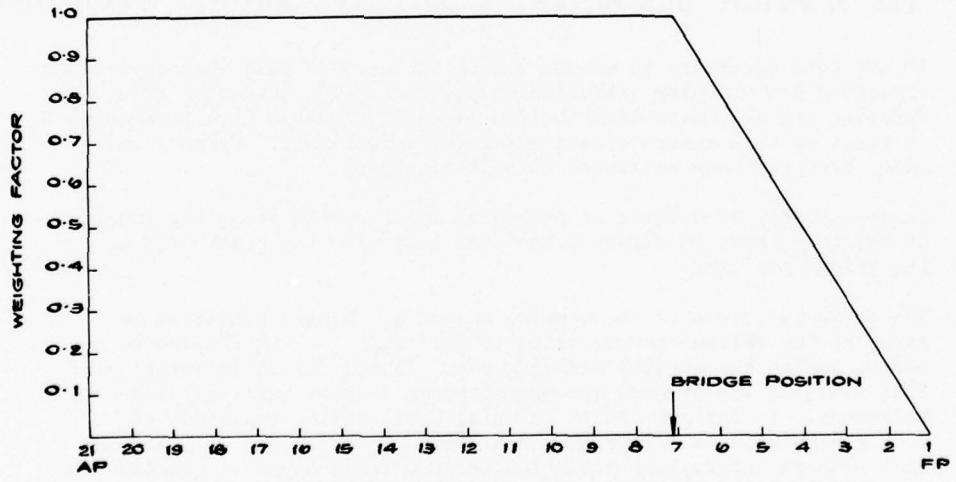

FIG. 9. PROPOSED WEIGHTING FACTOR FOR SUBJECTIVE MAGNITUDE.

6. DISCUSSION AND CONCLUSIONS

Based on the results of the previous section the following criteria are proposed:

a. Slamming

The whipping acceleration at the bridge should not exceed 0.05 g.

b. Wetness

The deck wetness interval should not be less than 100 seconds.

c. Motions

No definite criterion can be proposed but it is clear that subjective magnitudes of 7 (JORDAENS) and 11 (Dutch destroyer) are tolerable. A tentative figure of 15 is suggested as a criterion.

d. Propeller Emergence

No definite criterion can be proposed but it is clear that an average interval of 40 seconds is tolerable (JORDAENS). A tentative figure of 30 seconds is suggested as a criterion.

If this figure seems too permissive it must be remembered that the calculation is not very reliable because of the known difficulties of computing relative motion at the stern.

All of the above criteria depend heavily on the method of calculation. There are many assumptions and uncertainties in the methods used here, particularly in the calculation of the slamming forces. The use of two dimensional drop test data* and the assumption that all stations slam simultaneously are major sources of uncertainty. The simple treatment of deck wetness and propeller emergence which ignores the effects of the ship on the incident wave probably also leads to inaccurate results for these qualities.

Nevertheless the authors feel that they have made an important advance in the study of seakeeping by establishing a rational procedure for predicting voluntary speed loss in rough weather.

In particular the criteria proposed here relate to phenomena which the captain can detect and which are of concern to him. A second important point is that the actual values of the criteria have been obtained by considering the performance of two widely differing ships at sea.

Refinements in the methods of calculation may well change the values of the criteria but these two basic axioms will remain unchanged.

---

* Without correction for forward speed and relative angle between keel and water surface.

The major problem in this work has been the lack of suitably well documented data on the actual performance of ships in rough weather. There is an undeniable need for further trials in order to consolidate the criteria proposed here.

One particular refinement which the authors feel would merit serious consideration is the possibility of combining the separate phenomena discussed here into one single all embracing figure of merit so that a single criterion could be used. It seems likely that the captain does not consider slamming in isolation from deck wetness and ship motions but is concerned about the overall environment and might well accept more slamming in a dry ship than he would in a wet ship. However such a development would require a wide data base which does not at present exist.

7. ACKNOWLEDGEMENT

The authors would like to acknowledge the assistance given by their colleagues at the Admiralty Experiment Works.

References

1. Aertssen, G: "Labouring of Ships in Rough Seas with Special Emphasis on the Fast Ship", SNAME Diamond Jubilee International Meeting, 1968.

2. Aertssen, G: "Service Performance and Seakeeping Trials of MV JORDAENS", Trans RINA, Vol 108, 1966.

3. Aertssen, G: "Service Performance and Seakeeping Trials on MV LUKUGA", Trans RINA, Vol 105, 1963.

4. Aertssen, G and Van Sluys, MF: "Service Performance and Seakeeping Trials on a Large Container Ship", Trans RINA, Vol 114, 1972.

5. Conolly, J E: "Standards of Good Seakeeping for Destroyers and Frigates in Head Seas", Int Symp Dynamics of Marine Vehicles in Waves", Inst Mech Engrs, 1975.

6. Bledsoe, M D, Bussemaker, O and Cummins, W E: "Seakeeping Trials on Three Dutch Destroyers", Trans SNAME, Vol 68, 1960.

7. Kehoe, J W: "Destroyer Seakeeping - Ours and Theirs", Proc US Naval Inst, 1973.

8. Ochi, M K: "Prediction of Occurrence and Severity of Ship Slamming at Sea", 5th ONR Symp Naval Hydrodynamics, Bergen 1964.

9. Raff, A I: "Program SCORES - Ship Structural Response in Waves", Ship Structures Committee Publication SSC-230, 1972.

10. Chuang, S L: "Investigation of Impact of Rigid and Elastic Bodies with Water", NSRDC Report 3248, February 1970.

11. Foxwell, J H and Madden, P E: "Pressure Distribution on a Sphere during Impact with a Water Surface". Unpublished MOD Report.

12. Madden, P E: "Pressure Distribution on a Rigid Ellipsoidal/ Cylindrical Body during Impact with a Water Surface", Unpublished MOD Report.

13. Hagiwara, K and Yuhara, T: "Study of Wave Impact Load on Ship Bow", Japan Shipbuilding and Marine Engineering, Vol 8, No 4, 1974.

14. Chuang, S L and Milne, D T: "Drop Tests of Cones to Investigate the Three-Dimensional Effects of Slamming", NSRDC Report 3543, April 1971.

15. Wagner, H: "Landing of Seaplanes", NACA TN 622, May 1932.

16. Greenspon, J E: "Sea Tests of the USCG UNIMAK. Part 3 - Pressures, Strains and Deflections of the Bottom Plating Incident to Slamming", DTMB Report 978, March 1956.

17. Ochi, M K: "Prediction of Slamming Characteristics and Hull Responses for Ship Design", Trans SNAME, Vol 81, 1973.

18. Bishop, R E D and Price, W G: "On Modal Analysis of Ship Strength", Proc Royal Soc London, A341, 1974.

19. Bishop, R E D and Price, W G: "Allowance for Shear Distortion and Rotary Inertia of Ships Hulls", Jour Sound Vib, Vol 47(3), 1976.

20. Monsour, A and D'Oliveira, J M: "Hull Bending Moment Due to Ship Bottom Slamming in Regular Waves", Jour Ship Research, Vol 19(2) June 1975.

21. Betts, C V, Bishop, R E D and Price, W G: "The Symmetric Generalised Fluid Forces Applied to a Ship in a Seaway", RINA W11, 1976.

22. Betts, C V, Bishop, R E D and Price, W G: "A Survey of Internal Hull Damping", RINA W2, 1976.

23. Leibowitz, R C: "Comparison of Theory and Experiment for Slamming of a Dutch Destroyer", DTMB Report 1511, Nov 1963.

24. Wheaton, J W: "Further Analysis of Slamming Data from the SS WOLVERINE STATE", Ship Struct Committee, SSC-255, Jan 1976.

25. Johnson, A and Ayling, P: "On the Vibration Amplitudes of Ships Hulls", Trans Inst Engnrs Shipbldrs, Scotland, 1961-2.

26. Schoenberger, R W: "Subjective Response to Very Low Frequency Vibration", Aviation, Space and Environmental Medicine, June 1975.

Appendix I

RELATIVE MOTION DURING IMPACT

It is usual to estimate ship motion responses in a seaway on the basis of a spectral analysis in the frequency domain. Whilst this method has been found useful in estimating instantaneous extreme values of relative motion at points along the hull and associated probabilities of occurrence there are significant limitations to its use in connection with predictions of slam-induced whipping. This is because the nature of the whipping vibration following slamming is governed by the space-time distribution of the loads applied to the hull. It would appear therefore that predictions of relative motion - and hence slamming loads - are best undertaken on the basis of a deterministic analysis in the time domain. Such a method is the subject of continuing research but in the meantime it has been found convenient to develop an analysis based on statistical measures of relative motion.

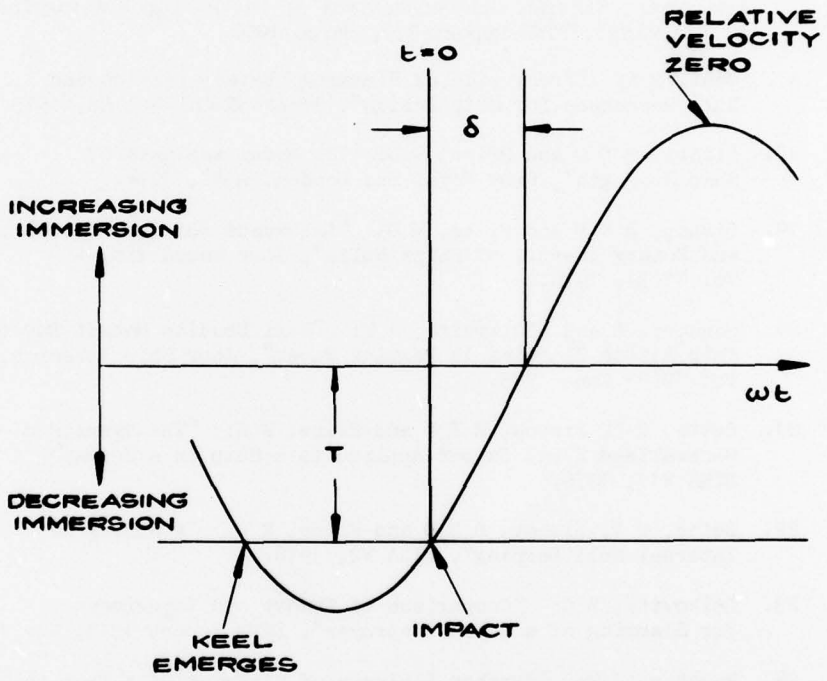

FIG. 10. SKETCH OF RELATIVE MOTION HISTORY INCIDENT TO SLAMMING.

Consider the motion of the hull relative to the water surface at a particular station. It is assumed that the relative motion can be approximated by a sinusoidal waveform during the cycle in which a slam occurs. Hence,

$$r = r_o \sin(\omega t - \delta) \qquad (1)$$

where r_o is the peak relative motion (increasing immersion positive) immediately preceding the slam, ω is the average frequency of oscillation* and δ is a constant defining the phase relationship between the peak relative motion and impact. Figure 10 shows a sketch of the relative motion.

The relative motion at impact (t = 0) is given by:

$$T = - r_o \sin\delta \tag{2}$$

so that

$$\delta = \sin^{-1}\left(- \frac{T}{r_o}\right) \tag{3}$$

where T is the local draught.

The relative velocity during the slam is given by:

$$\dot{r} = \omega r_o \cos(\omega t - \delta) \tag{4}$$

It is generally accepted that the probability of exceeding a peak relative motion of r_o is given by the Rayleigh distribution.

$$\text{ie} \quad P_r\{r \geq r_o\} = \exp\left(- \frac{r_o^2}{2m_o}\right) \tag{5}$$

It is assumed that a peak relative motion very near r_o will be achieved once in N relative motion oscillations where

$$P_r = \frac{1}{N} = \frac{2\pi}{T_s \omega} \tag{6}$$

where T_s is an arbitrary sample period.

Hence

$$r_o = \left[- 2m_o \log_e \left(\frac{2\pi}{T_s \omega}\right)\right]^{\frac{1}{2}} \tag{7}$$

The authors propose a sample period of 900 seconds (ie a quarter of an hour) in connection with predictions of voluntary speed reduction in rough weather.

---

* $\left(= \sqrt{\frac{m_2}{m_o}}\right.$ where m_o and m_2 are the variances of relative motion and velocity respectively)

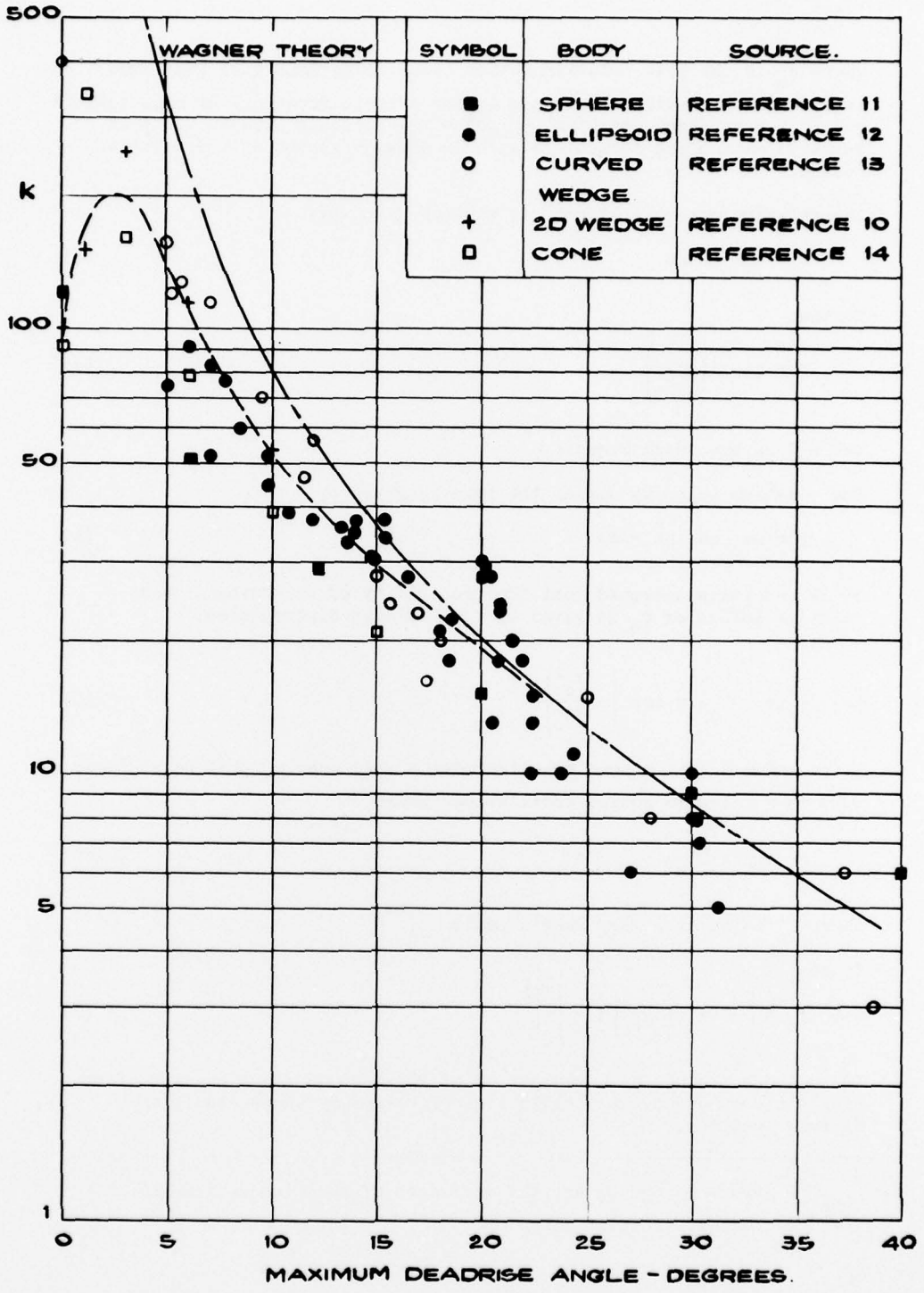

FIG. 11. SLAMMING PRESSURE COEFFICIENT k .

Appendix II

IMPACT PRESSURES AND FORCES

References 10-14 describe slamming drop tests using a variety of body shapes. The results of these tests have been collated and the derived values of the slamming pressure coefficient $k(\beta)$ in the equation

$$p = \tfrac{1}{2}\rho\dot{r}^2 k(\beta) \tag{8}$$

have been plotted as a function of the local deadrise angle in Figure 11. There is considerable scatter but a mean line has been drawn. For values of β greater than about 24 degrees Wagner's formula (Reference 15) seems to hold good.

$$k(\beta) = 1 + \left(\frac{\pi \cot\beta}{2}\right)^2 \tag{9}$$

p is limited to the acoustic pressure $\rho c_w \dot{r}$ where c_w is the velocity of sound in water = 1500 m/sec.

Keel Force

It is assumed that the pressure on the flat of keel rises practically instantaneously to a value p_k and then decays exponentially with a time constant T_k. The pressure at any instant of time is given by

$$p_k = \tfrac{1}{2}\rho\dot{r}^2 k(o) \exp\left(-\frac{t}{T_k}\right) \tag{10}$$

where $\dot{r} = \omega r_o \cos\delta$ (equation 4 with t = 0)

The time history of the vertical force per unit length at a given station is given by

$$F_k(x,t) = \tfrac{1}{2}\rho(\omega r_o \cos\delta)^2 \, k(o) \exp\left(-\frac{t}{T_k}\right) h \tag{11}$$

where h is the local total width of the flat of keel.

Deadrise Force

It is assumed that the pressure in way of the water surface rises practically instantaneously to a value p_D and then decays exponentially with a time constant T_D. The maximum pressure in way of the water surface is given by

$$p_D = \tfrac{1}{2}\rho\dot{r}^2 k(\beta) \tag{12}$$

where $\dot{r}$ and β are the instantaneous local relative velocity and deadrise angle respectively.

Now T_D is small (of order 0.01 second, Reference 16) and so the pressure decays very quickly. It may safely be assumed that only the pressure in way of the water surface contributes to the vertical force. It can be shown that the time history of the vertical force per unit length at a given station is given by:

$$F_D(x,t) = \tfrac{1}{2}\rho(\omega r_o \cos(\omega t - \delta))^3 T_D \cot\beta(t) \qquad (13)$$

Total Force

The time history of the total vertical force per unit length at a given station is given by:

$$F(x,t) = F_k(x,t) + 2F_D(x,t) \qquad (14)$$

Longitudinal Distribution

Little is known concerning the longitudinal distribution of impact loads. Reference 17 has described model experiments in which slamming was observed to start aft and propagate forward, start forward and propagate aft, and to occur simultaneously at a number of stations. In view of these uncertainties it has been found convenient to assume impact occurs simultaneously at all hull sections where keel emergence is predicted to occur in an arbitrary sample period.

Appendix III

WHIPPING VIBRATION OF HULL GIRDER

It has been shown in References 18 and 19 that the vertical plane response of a ship in a seaway may be estimated on the basis of a modal analysis. This method has been used to investigate the distortion of a ship in response to slamming (Reference 20). Recent definitive work (Reference 21) concerning modal analysis of ship responses gives a formulation which has been found to be different from Reference 20 in respect of the generalised hydrodynamic damping. In the work reported herein the formulation described in Reference 21 is preferred.

Modal analysis assumes that the displacement of the hull may be expressed as the sum of displacements in the principal modes of the hull ie

$$z(x,t) = \sum_{i=0}^{\infty} p_i(t)\, w_i(x) \qquad (15)$$

where z is the displacement, p_i is the principal co-ordinate of the displacement in the ith mode and w_i is the characteristic function of the ith mode. The mode number, i, refers to the number of nodes.

A set of coupled differential equations governing the variation of $p_i(t)$ have been given in Reference 21 for the case of continuous

excitation in regular waves. These equations may be considered general and may be used to estimate responses to impact loads. However in this connection it has been found convenient to adopt 'wet' modes (hull supported by water) instead of the 'dry' modes (hull in vacuo) of the Reference. The reasons for this will be seen later.

It has been found that the variation of $p_i(t)$ is governed by the set of coupled differential equations*:-

$$a_{ii}\,\ddot{p}_i(t) + 2a_{ii}\,\omega_i\,\nu_i\,\dot{p}_i(t) + \sum_{j=0}^{\infty} b_{ij}\,p_j(t) + a_{ii}\,\omega_i^2\,p_i(t) + \sum_{j=0}^{\infty} c_{ij}\,p_j(t) = \bar{F}_i(t) \qquad (16)$$

$(i = 0,1,2,....)$

where $$a_{ii} = \int_0^L \left[\mu(x) + m(x)\right]\left[w_i(x)\right]^2 dx$$

$$b_{ij} = -U\int_0^L m(x)\left[w_i(x)\,w_j'(x) - w_i'(x)\,w_j(x)\right]dx - U\left|m(x)\,w_i(x)\,w_j(x)\right|_0^L$$

$$c_{ij} = \int_0^L \left[\rho g\,B(x)\,w_i(x)\,w_j(x) - U^2 m(x)\,w_i'(x)\,w_j'(x)\right]dx + U^2\left|m(x)\,w_i(x)\,w_j'(x)\right|_0^L$$

$$\bar{F}_i(t) = \int_0^L F(x,t)\,w_i(x)\,dx$$

μ and m are the ship mass and added mass distributions, ω_i and ν_i are the natural frequency and structural damping factor of the ith mode, U is the ship speed, B is the local beam and $F(x,t)$ is the space-time distribution of the impact load.

In deriving these equations the formulation for structural damping suggested in Reference 22 has been used.

---

* A dot implies differentiation with respect to time, a prime differentiation with respect to x.

Equation 16 is of considerable generality - far greater than our knowledge of the mechanics of slamming - and its solution requires considerable computation. It would appear to be an attractive alternative to reduce the set of coupled equations to one constant coefficients, second order differential equation in $p_2(t)$ by referring to observations of full-scale behaviour reported in References 23 and 24 in which it is shown that slam induced vibration occurs predominantly in the two-node 'wet' mode. If the displacements in other modes are therefore ignored and c_{22} assumed to be small compared to $a_{22}\ \omega_2{}^2$ as usual the variation of $p_2(t)$ has been found to be governed by the equation

$$a_{22}\ \ddot{p}_2(t) + \left[2a_{22}\ \omega_2\ \nu_2 + b_{22}\right] \dot{p}_2(t) + a_{22}\ \omega_2{}^2\ p(t) = \overline{F}_2(t) \qquad (17)$$

where $\nu_2 = 6.35 \times 10^{-4}\ \omega_2{}^{0.688}$ (Reference 25)

A time history of $p_2(t)$ may be determined from the solution of equation 17 using appropriate numerical methods. The bridge acceleration due to whipping is subsequently determined from the equation:-

$$f(t)^2 = \left[w(x_B)^2 + \left[w'(x_B)\ y_B\right]^2\right] \ddot{p}_2(t)^2 \qquad (18)$$

where f is the acceleration at the bridge, x_B is the longitudinal position of the bridge and y_B is the distance of the bridge above the neutral axis of the hull cross-section.

Appendix IV

DECK WETNESS

It is generally accepted that the probability of deck wetness is the same as the probability of the relative motion exceeding the freeboard. From the Rayleigh distribution

$$P_r = \exp\ -\left(\frac{F^2}{2m_o}\right) \qquad (19)$$

where F is the freeboard and m_o is the variance of the relative motion.

The average time interval between deck wetnesses at a particular station is

$$t_w = \frac{2\pi}{P_r \omega} = \frac{2\pi}{\omega} \exp\left(\frac{F^2}{2m_o}\right) \qquad (20)$$

where ω is the average frequency of the relative motion ($= \sqrt{\frac{m_2}{m_o}}$ where m_2 is the variance of relative velocity).

Appendix V

SHIP MOTIONS

Schoenberger (Reference 26) subjected a number of USAF pilots to vertical sinusoidal motions and found the combinations of frequencies and amplitudes at which they judged the motion to be of equal intensity. He called this intensity a "subjective magnitude" of 10. The results are shown in Table 3. The pilots were then subjected to motions of other amplitudes and frequencies and asked to estimate their subjective magnitudes: thus if a motion was estimated as double the intensity of the "control" motion, it was given a subjective magnitude of 20 and so on.

It was shown that a power law relationship of the form

$$SM = A(f)a^{1.43} \tag{21}$$

seemed to fit the results obtained. Table 3 shows the derived values of the parameter A(f). An empirical equation

$$A(f) = 30 + 13.53\ (\log_e f)^2 \tag{22}$$

fits the results quite well.

Table 3

SUBJECTIVE MAGNITUDE OF VERTICAL SINUSOIDAL MOTION

Acceleration amplitudes for SM = 10
(After Schoenberger; Reference 26)

Frequency Hz	Acceleration Amplitude g	A(f)
.25	.30	55.9
.40	.38	39.9
.63	.46	30.4
1.0	.46	30.4
1.6	.42	34.6
2.5	.38	39.9
4.0	.30	55.9

If we assume that we may apply the sinusoidal results obtained by Schoenberger to the random motions experienced on a ship by putting

$$a = \frac{2}{g}\sqrt{m_{4a}} \tag{23}$$

$$f = \frac{1}{2\pi}\sqrt{\frac{m_{2a}}{m_{oa}}} \tag{24}$$

where m_{oa}, m_{2a} and m_{4a} are the variances of absolute motion, velocity and acceleration respectively we obtain

$$SM = \left[3.087 + 1.392\left[\log_e \frac{1}{2\pi}\sqrt{\frac{m_{2a}}{m_{oa}}}\right]^2\right] m_{4a}^{0.715} \tag{25}$$

(m_{4a} is in SI units: m^2/sec^4)

Hence, knowing the absolute motion variances we can determine the subjective magnitude of the motions at all points in the ship.

Motion Weighting

In general the subjective magnitude of the motion should be determined for those parts of the ship which are occupied by crew and passengers and the result averaged to obtain a mean value for the ship. However this detailed information may not always be available and for warships it is recommended that the simple weighting function shown in Figure 9 is used to obtain a weighted mean value of SM over the whole ship. This avoids the high calculated values of SM at the FP (where there are usually no crew members) dominating the result.

For cargo ships where the crew members are often concentrated in a limited area it may be sufficient to calculate SM at only one station.

Appendix VI

PROPELLER EMERGENCE

The propeller is arbitrarily assumed to have emerged when one quarter of its diameter is exposed above the water surface. With the usual assumption of the Rayleigh distribution the probability of propeller emergence is then given by

$$P_r = \exp\left[-\frac{(T_p - \frac{D}{4})^2}{2m_o}\right] \tag{26}$$

where T_p is the depth of the propeller shaft below the still waterline and D is the propeller diameter. m_o is the variance of the relative motion at the propeller.

The average time interval between propeller emergences is

$$t_p = \frac{2\pi}{P_r \omega} \tag{27}$$

where ω is the average frequency of the relative motion ($= \sqrt{\frac{m_2}{m_o}}$ where m_2 is the variance of the relative velocity).

SIMULATION OF BUOY MOTION IN BREAKING WAVES

by

G.L. Petrie
Hoffman Maritime Consultants Inc.

A time domain simulation of the behavior of a disc buoy in large breaking and non-breaking waves have been developed (1), under contract to the National Data Buoy Office (NDBO). The simulation can be used to determine expected motion amplitudes in extreme conditions, and to predict the occurrence of capsizing in breaking waves. It can also be used for determining time histories of displacements, velocities and accelerations of points on the buoy in moderate and extreme waves.

The three degrees of freedom mathematical model simulates the contour of a wave of any convenient type, such as a Stokes Wave or other, and computes the primarily hydrostatic forces acting on the hull as the wave passes by it. Correction terms are then applied in the equations of motion to account for added mass and damping effects, as well as wind, current and mooring line forces. The equations of motion are then solved to determine the accelerations, velocities and displacements in heave, surge and pitch.

At each time step in the solution, the slope of the wave at the leading edge of the buoy is computed. When this slope exceeds a specified threshold, the wave is assumed to break or "spill." The forces resulting from the impingement of the wave crest on the surface of the buoy are computed, using a quasi-empirical model, which is being introduced into the equations of motion for as long as the wave crest persists.

In order to assess the validity of the mathematical model, a program of scale model tests has been carried out at the OTC tank in Escondido (2). The tests included measurement of buoy displacements and accelerations, along with wave elevation and slope in regular, irregular and breaking waves. In addition, free oscillations resulting from initial displacements in pitch and heave were recorded. Several model tests were then selected for comparison with the mathematical model. Good correlation between the computer predictions and the observed motion has been demonstrated for the breaking wave, large non-breaking wave and free oscillation cases. A comparison for a large non-breaking wave is shown in Figure 1.

The results obtained from the model to date are quite encouraging and demonstrate that an acceptable approximation of rather extreme conditions can be obtained from a relatively simple simulation. Work is presently contemplated to incorporate the simulation with a probability model, to permit a quantitative assessment of capsizing performance. The model could be readily extended to include consideration of roll and stability as well.

REFERENCES

1. Petrie, G. and Walden, D.A. "A Time Domain Analysis of the Motion of a Disc Buoy in Breaking Waves," HMC Report 7643, May 1976.

2. Petrie, G. and Hoffman, D. "Validation of a Time Domain Simulation of Buoy Motion in Breaking Waves," HMC Report 7753, July 1977.

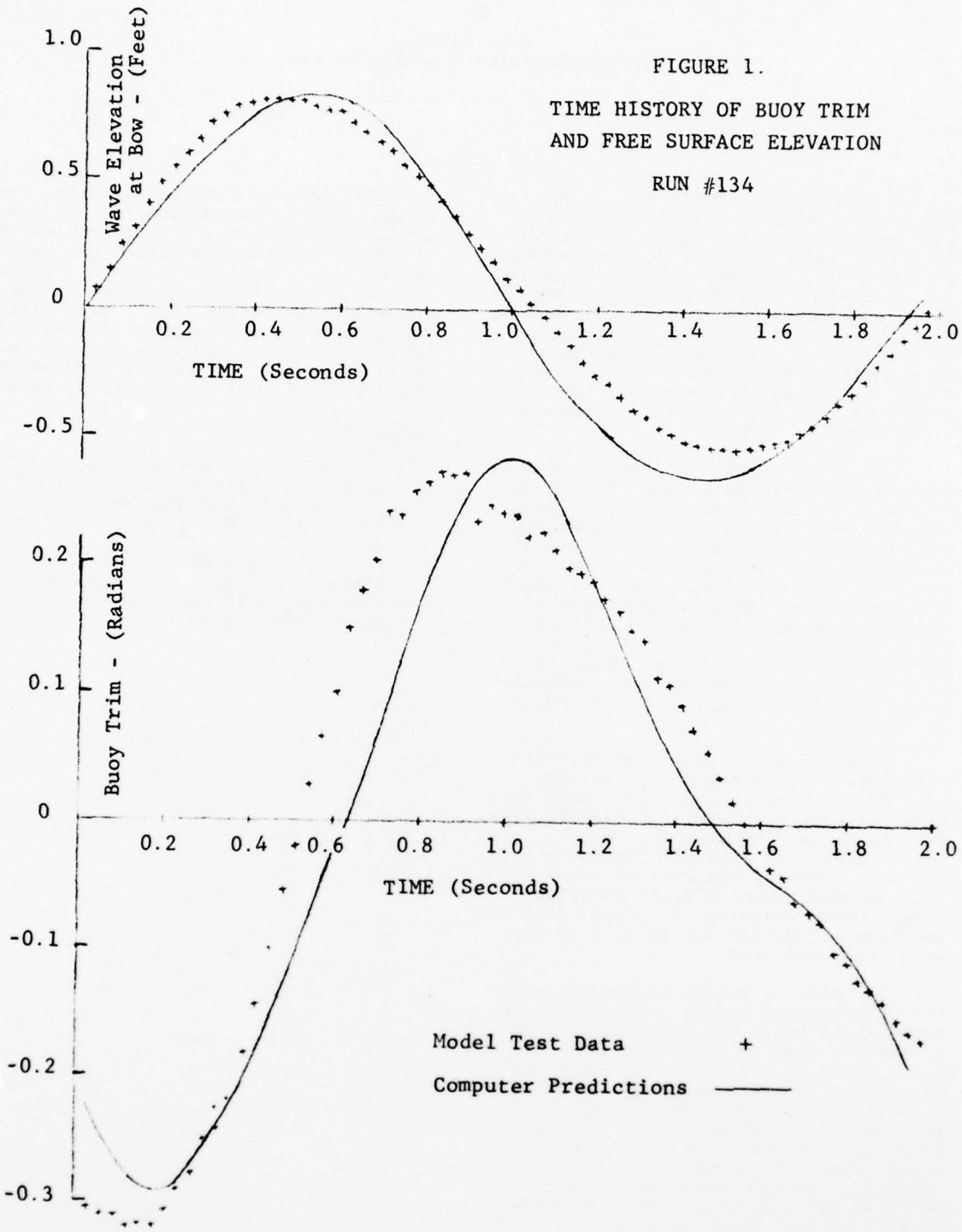

FIGURE 1.

TIME HISTORY OF BUOY TRIM
AND FREE SURFACE ELEVATION

RUN #134

Comment on VII, Dynamic Stability and Capsizing

Seakeeping Committee Report

In the section on the swamping of small recreational boats, it is reported that the model tests duplicated none of the swampings that occured in full scale tests. It was stated that this "may be due to the fairly poor correlation of the model and full scale wave energy spectra." Mathematical simulation had duplicated three of twelve full scale swampings.

Having first hand knowledge of the model test program, I consider a further explanation is in order lest the uninformed accept the above statements as fact. Several spectra where the correlation was not particularly good, were truncated spectra, because it was not possible to produce long period waves, nor was it felt that long period waves had any part in swamping small boats.

The report of the model test, reference (II), provides several thoughts on why there was poor agreement between the model and full scale tests in swamping and shipping of water:

a.) Differences in the character of the waves in the tank and Long Island Sound, since waves in the Sound tend to be more choppy.

b.) Wave directional properties may be important and these are not simulated in the tank with unidirectional waves.

c.) Difficulty in obtaining accurate spectral representation of full scale waves.

d.) Poor matching of the energy content of the waves at resonant periods for heave, pitch, and roll, with the wave spectrum in the tank.

It would appear from studying the report that the fundamental reason for failure to obtain a good correlation between model and full scale results is the inadequate description of the input data.

F. N. Biewer

Comment on VII, Dynamic Stability and Capsizing

Seakeeping Committee Report

In the section on the swamping of small recreational boats, it is reported that the model tests duplicated none of the swampings that occurred in full scale tests. It was stated that this "may be due to the fairly poor correlation of the model and full scale wave energy spectra." Mathematical simulation had duplicated three of twelve full scale swampings.

Having first hand knowledge of the model test program, I consider a further explanation is in order lest the uninformed accept the above statements as fact. Several spectra where the correlation was not particularly good, were truncated spectra, because it was not possible to produce long period waves, nor was it felt that long period waves had any part in swamping small boats.

The report of the model test, reference (II), provides several thoughts on why there was poor agreement between the model and full scale tests in swamping and shipping of water:

a. Differences in the character of the waves in the tank and Long Island Sound, since waves in the Sound tend to be more choppy.

b. Wave directional properties may be important and these are not simulated in the tank with unidirectional waves.

c. Difficulty in obtaining accurate spectral representation of full scale waves.

d. Poor matching of the energy content of the waves at resonant periods for heave, pitch, and roll, with the wave spectrum in the tank.

It would appear from studying the report that the fundamental reason for failure to obtain a good correlation between model and full scale results is the inadequate description of the input data.

F. N. BIEWER